Focus on DNA Repair Replication

Focus op DNA reparatie replicatie

~

Audrey M. Gourdin

ISBN: 978-94-90371-34-0

The work presented in this thesis was performed at the department of Cell Biology and Genetics at the Erasmus MC in Rotterdam.

The studies described in this thesis were supported by the Nederlandse Organisatie voor Wetenschappelijk Onderzoek (NWO)

Cover design: Reprinted by permission from Macmillan Publishers Ltd: NATURE
Morris, M., Uchida, K. and Do, T. *A magnetic torsional wave near the Galactic Centre traced by a 'double helix' nebula.* **440**(7082): 308-10., copyright 2006

The cover was kindly adapted and modified by J.M Gourdin.

Printing: Off Page, Amsterdam

Focus on DNA Repair Replication

Focus op DNA reparatie replicatie

Proefschrift

~

ter verkrijging van de graad van doctor aan de
Erasmus Universiteit Rotterdam
op gezag van de
rector magnificus

Prof.dr. H.G. Schmidt

en volgens besluit van het College voor Promoties

De openbare verdediging zal plaatsvinden op:
vrijdag 1 oktober 2010 om 13:30 uur

door

~

Audrey Marie Gourdin
geboren te Pontoise, Frankrijk

Promotie Commissie:

Promotor:
Prof.dr. J.H.J. Hoeijmakers

Overige Leden:
Prof.dr. L.H.F. Mullenders
Dr. A.B. Houtsmuller
Dr. N. Galjart

Copromotor:
Dr. W. Vermeulen

Contents of the thesis

List of abbreviations

AP	Apurinic/Apyrimidinic
APE-1	AP-Endonuclease-1
AraC	Arabinofuranosyl Cytidine
ATM	Ataxia-Telangectasia Mutated
ATR	Ataxia Telangectasia and Rad3-related
BER	Base Excision Repair
BRCA	Breast Cancer
BrdU	Bromodeoxyuridine
CAMKII	Calmodulin-dependent protein Kinase II
CDK	Cyclin-Dependent Kinase
CDT1	CDC10-Dependent Transcript 1
ChIP	Chromatin ImmunoPrecipitation
CPD	Cyclobutane Pyrimidine Dimer
CS	Cockayne Syndrome
DDB	Damaged DNA-Binding
DDK	Dbf4-Dependent Cdc7 Kinase
DDR	DNA Damage Response
DNA	Deoxyribose Nucleic Acid
DSB	Double-Strand Break
dsDNA	Double-Stranded DNA
DUB	Deubiquitinating (enzyme)
FA	Fanconi Anemia
FEN-1	Flap Endonuclease-1
FLIP	Fluorescence Loss In Photobleaching
FRAP	Fluorescence Recovery After Photobleaching
GFP	Green Fluorescent Protein
GG-NER	Global Genome-NER
HJ	Holliday Junction
HR	Homologous Recombination
HR23	Human Rad 23
HU	Hydroxyurea
ICL	Interstrand Cross-link
IR	Ionizing Radiation
kb	kilobase
MCM	Mini-Chromosome Maintenance
MGMT	O6-MeG-DNA MethylTransferase
MMC	Mitomycin C
MMR	Mismatch Repair
MMS	Methyl Methane Sulfonate

MRN	Mre11-Rad50-Nbs1
NHEJ	Non-Homologous End Joining
NER	Nucleotide Excision Repair
ORC	Origin Recognition Complex
O6-meG	O6-methylguanine
PARP-1	Poly-ADP-Ribose Polymerase-1
PCNA	Proliferating Cell Nuclear Antigen
PI	Phosphoinositide
PIKK	Phosphatidylinositol 3-Kinase-like Kinase
PIP	PCNA Interacting Peptide
PKcs	Protein Kinase catalytic subunit
PNK	Polynucleotide Kinase
Pol	Polymerase
Pre-RC	Pre-Replication Complexes
PRR	Post-Replication Repair
RFC	Replication Factor C
ROS	Reactive Oxygen Species
RPA	Replication Protein A
S.	*Saccharomyces*
SSB	Single-Strand Break
SDSA	Synthesis-dependent Strand Annealing
ssDNA	Single-Stranded DNA
TC-NER	Transcription-Coupled NER
TLS	Translesion Synthesis
TopBP1	Topoisomerase IIβ Binding Protein 1
TOR	Target of Rapamycin
TTD	Trichothiodistrophy
UV	Ultraviolet
XP	Xeroderma Pigmentosum
6-4 PP	6-4 Pyrimidine-Pyrimidone
8-oxoG	8-oxoguanine
9-1-1	Rad9-Hus1-Rad1

Chapter 1

~

Introduction to the DNA damage response

Contents of chapter 1

Scope of this thesis

The crucial factor for the survival of an organism resides in genetic stability. In fact the integrity of the DNA sequence, that carries out and regulates genetic information, can be impaired by inaccurate maintenance processes, endogenous metabolites or exogenous agents. Therefore, a sophisticated network of efficient DNA damage response mechanisms, including DNA repair, checkpoint mechanisms and damage tolerance processes, are dedicated to remove or bypass most of these genomic insults and is known as the DNA Damage Response (DDR). The relevance of this multi-protein DDR response is illustrated by the severe clinical symptoms associated with inherited defects in the DDR factors**.** **Chapter 1** introduces the different DNA lesions, the DDR response and the most appropriate technical approach to study the different DDR factors. The various DDR-associated diseases are also presented in this chapter.

Most of the mechanisms presented in Chapter 1 necessitate a DNA re-synthesis step that is carried out by several replication factors: the tethering of DNA polymerases for further repair synthesis is carried out by PCNA, a sliding ring-shaped clamp that needs to be opened and loaded around the DNA by a clamp loader. In regular DNA replication, the RFCp140 (or RFC1)-containing Replication Factor C complex is responsible for this function, while Replication Protein A (RPA) stabilizes the ss-DNA. Hence in **Chapter 2,** a focus is made on the very accurate process of DNA replication (that is also crucial for genetic stability) as well as on the DDR-associated DNA synthesis mechanisms. The biological properties of the replication factors RFC, RPA and PCNA, as well as their tightly regulated interplay within replication and damage-associated replication, are also extensively described and discussed in this chapter.

An important repair mechanism that allows removal of UV-induced lesions in the cell is Nucleotide Excision Repair (NER). NER is initiated by a lesion recognition step, which is followed by dual incision, leading to a single-stranded DNA patch that is filled in during repair synthesis. In **Chapter 3** the coordination between incision and the start of DNA repair synthesis within NER is described. We propose a "cut-patch-cut-patch" mechanism whereby following 5' cleavage by ERCC1-XPF, the repair synthesis machinery is recruited and repair synthesis is initiated prior to 3' cleavage by XPG. This latter cleavage appears to occur subsequently, may be induced upon stalling of the polymerase and allows the completion of repair synthesis.

Chapter 4 is dedicated to the repair synthesis step of NER. In this chapter, we provide a model where RFC displays other functions in repair replication besides loading of PCNA during NER repair synthesis. Surprisingly, RFC does not seem to be required for recruiting PCNA to NER sites but appears to be crucial for loading PCNA, in order to confer it into a

replication-competent status that allows the recruitment of pol δ and initiation of repair synthesis.

Tagged proteins represent a powerful tool to determine the spatio-temporal distribution of vital processes such as replication, transcription and DNA repair. **In chapter 5**, we keep our focus on the behavior of replication factors in NER. By using tagged versions of these proteins, we show that PCNA, RPA and RFC have a very different kinetic behavior than the other pre-incision NER factors, since they accumulate at prolonged periods at sites of UV repair. This suggests that these factors may have additional functions besides their known functions in repair synthesis. RPA is actually the only factor that is involved both in the pre- and post-incision steps of NER and displays differential dynamic properties.

In **Chapter 6** of this thesis, we have focused on a more quantitative understanding of NER repair complexes assemblies and dynamic interactions in living cells. This analysis is based on kinetic measurements of seven GFP-tagged core NER factors and mathematical modeling and brings about the conclusion that all core NER proteins exchange continuously and rapidly between chromatin-bound and freely diffusing states. Moreover their assembly is not sequential but rather stochastic and reversible. We also highlight the finding that a major component of protein affinity is the state of the DNA substrate.

Besides tagged proteins, many additional tools, like *in vivo* DNA labeling by DNA-stains such as the anthraquinone derivate Draq5, are also important to visualize the interaction of GFP-fused proteins with the target substrate and to determine different chromatin compaction levels. In the technique-orientated **Chapter 7**, the suitability of combining Draq5 staining with protein dynamic measurements is verified and brought to caution, since Draq5 intercalation modifies the localization and dynamic behavior of several chromatin-binding proteins, which results in an inhibition of the corresponding cellular functions of these factors.

When the cell enters S-phase, many UV-induced lesions have not been removed by NER. This leads to a stalling of the classical DNA polymerase, which triggers a bypass mechanism known as Translesion Synthesis (TLS) that requires alternative sets of polymerases. The main TLS polymerase for CPDs bypass in an error-free fashion is pol η, which co-localizes with another TLS polymerase, pol ι, at UV-induced replication foci. In **Chapter 8**, we show that the two polymerases are highly mobile at sites of damage, with pol ι being even more mobile than pol η. Moreover PCNA ubiquitination facilitates but is not essential for accumulation of pol η into the foci. Finally, the polymerases seem to be continuously but transiently probing the DNA/chromatin.

Pol η does not localize to TLS sites exclusively during S phase, but also to UV-induced damage sites in G1 cells in a focal pattern, as shown by an interesting report of 2009 by

Soria et al. in Cell Cycle. Indeed several lines of evidence have shown that the TLS polymerases may have additional functions beyond TLS, such as NER repair synthesis for pol κ or Rev1 and HR for pol η. In **Chapter 9** we try to interpret the meaning of this surprising finding as regards to these reports: indeed pol η might also be implicated in NER or another repair pathway. Alternatively the localization of pol η to foci may support a model known as "be-ready-for", supporting the idea that several DDR factors may accumulate in high local concentrations (foci) near the damage, in order to remain disposable if necessary.

1. DNA damage induction and biological consequences

1.1. Genotoxic insults

The genomic identity of all living organisms is stored in long nucleic acid polymers of four different nucleotides (the basic building blocks of nucleic acids) that are commonly but not exclusively in the form of DNA (Deoxyribose Nucleic Acid). DNA consists of two anti-parallel complementary long polymers folded as a double helical molecule. The main function of DNA is to ensure that the hereditary information, encrypted by the sequence of nucleotides, can be properly read and propagated to the progeny, or daughter cells. The maintenance and faithful transmission of DNA integrity are therefore some of the most crucial parameters for life. Although DNA is a relatively stable molecule, many endogenous and external threats can compromise its stability during the entire lifetime of an organism. Table 1 summarizes the types of lesions than can occur on DNA, as well as the causes and processing of these lesions.

The first type of DNA damaging sources originates from the intrinsic chemical properties of DNA and unavoidable biochemical reactions that are fundamental to life, i.e. respiration and metabolism. (By) products of cellular metabolism, markedly reactive oxygen species (ROS) generated by oxidative respiration and lipid peroxidation, endogenous alkylating agents and others, lead to numerous types of lesions such as oxidative base modifications (8-oxoGuanine) and single-strand breaks [de Bont and van Larebeke, 2004]. The nucleotides are also subjected to spontaneous hydrolysis and to hydrolytic deamination resulting respectively in abasic sites and modified bases like Uracil [Lindahl, 1993]. Finally errors occurring during DNA replication and collapse of the replication fork trigger respectively nucleotide mismatches and the very hazardous double-strand breaks.

Additional to these endogenously produced lesions, all organisms are also exposed to ubiquitous and genotoxic environmental hazards, such as electro-magnetic radiations and contacts with chemical agents. Ultra-violet (UV) light (present in sun light) induces the photoproducts cyclobutane pyrimidine dimers (CPDs) and 6-4 pyrimidine-pyrimidone dimers (6-4 PPs); while ionizing radiation (IR) (gamma- and Röntgen radiations) generate a whole variety of lesions among which oxidative base modifications and single- and double-strand breaks [Hoeijmakers, 2001]. Numerous chemical agents present in our environment are also highly genotoxic since they can form bulky adducts on the DNA (such as benzopyrene, present in cigarette smoke and charred food, or psoralen used in treatment of the skin diseases psoriasis and vitiligo), interstrand cross-links (e.g. nitrogen mustard) and intrastrand crosslinks (the chemotherapy drug cisplatin) [Friedberg et al, DNA Repair and Mutagenesis].

Lesion	Causative agent/process	Repair system
Mismatches	Replication errors	MMR
Modified bases	Cellular metabolism	BER
Abasic sites	Hydrolysis	BER
Single-strand breaks	Cellular metabolism, IR	BER
Double-strand breaks	DNA replication defects, IR	NHEJ and HR
Inter-strand crosslinks	Chemical agents, IR	NHEJ,HR, FA
Intra-strand crosslinks	Cisplatin, IR	NER
CPDs	UV	NER
6-4 PPs	UV	NER
Bulky base adducts	Smoke, food	NER

Table 1: summary of DNA lesions, causative agents and dedicated repair pathways
The dedicated repair pathways with their respective abbreviations are presented throughout this chapter.

1.2. Consequences of DNA lesions on cells and organisms

Several parameters determine the cellular consequences of DNA lesions: the type and the frequency of the lesions, the genomic location and the phase of the cell cycle in which the cell encounters these lesions [Essers et al, 2006]. Lesions directly interfere with the main functions of DNA, i.e. transcription and replication. Lesions disturbing DNA replication and transcription induce cell death (apoptosis) or irreversible cell cycle arrest (senescence), triggering degenerative changes implicated in ageing**.** In addition, some lesions affect the fidelity of replication, causing mutations in the nucleotide sequence and DNA strand breaks induce chromosomal aberrations, both leading to carcinogenesis. Finally, the type, efficiency and fidelity of the pathway(s) implicated in the repair or bypass of the damage are crucial for its further processing (last column of Table 1) [Hoeijmakers, 2001; Garinis et al, 2008].

Indeed, thousands of DNA damages are formed in each cell every hour. As an example, around 600 single-strand breaks (SSBs) and apurinic/apyrimidinic (AP) sites are formed in each cell per hour, while 50 DBSs are formed per cell per cell cycle [Vilenchik and Knudson, 2003]. It has been estimated that each cell is confronted with approximately $1\text{-}5.10^4$ lesions per day [Lindahl et al, 1993]. Hence, an impressive multi-faceted network of genome surveillance mechanisms has evolved in order to counteract the disastrous effects of DNA lesions on the cell and the organism. This network, or DNA Damage Response (DDR), can be subdivided into three interdependent processes: since no single repair process can cope with the whole diversity of damages, several repair pathways act complementarily to remove the different types of lesions (as seen in the last column of Table 1). These pathways

are discussed subsequently in this chapter. Furthermore an integration of these repair pathways with cell cycle control is achieved via the triggering of a damage signaling cascade that temporally pauses cell cycle progression by activating several cell cycle checkpoints. Finally when lesions are not completely removed before replication occurs, damage bypass processes get activated.

The biological importance of DDR on the scale of the organism is demonstrated by the fact that defective genome maintenance processes give rise to different complex human syndromes with a multitude of severe clinical symptoms. Cellular consequences of DNA damage listed above imply that these diseases are all characterized either by abnormally high cancer incidence, by premature ageing features or by a mixed phenotype, in addition to multiple side clinical features. The impact of repair processes, cell cycle regulation and damage bypass on the organism is illustrated in Table 2 [Friedberg et al, DNA Repair and Mutagenesis].

Disease	**Gene mutated**	**Pathway disrupted**	**Symptoms**
Xeroderma Pigmentosum	XPA to -G	GG-NER TC-NER	Cancer, Neurodegeneration
Cockayne Syndrome	CSA, CSB	TC-NER	Progeria, Neurodegeneneration Developmental problems
Trichothiodistrophy	XPB, XPD, TTDA	GG-NER TC-NER	Neurodegeneration Progeria, Immunodeficiency
Ataxia Telangectasia	ATM	Checkpoint signaling DSB Repair	Cancer, Immunodeficiency Neurodegeneration, Progeria Developmental problems
Nijmegen Breakage Syndrome	NBS1	DSB Repair	Cancer, Immunodeficiency Progeria, Developmental problems
Fanconi Anemia	Crosslink Repair genes	Crosslink Repair	Cancer, Progeria Developmental problems
Breast Cancer 1, 2	Brca1 Brca2	DSB Repair Crosslink repair	Cancer
Werner Syndrome	WRN	Recombination Telomere maintenance	Cancer, Progeria Developmental problems
Bloom Syndrome	BLM	Mitotic Recombination	Cancer, Immunodeficiency Progeria, Developmental problems
Xeroderma Pigmentosum Variant	Pol η	Translesion Synthesis	Cancer

Table 2: Clinical impacts of diseases associated with DDR gene mutations

2. The DNA damage response

2.1. DNA Repair pathways

While some lesions are subjected to direct protein-mediated reversal, most DNA insults are repaired by a sequence of catalytic events involving multiple proteins. These pathways all include damage recognition, processing and resolution steps. The most direct way of removing DNA lesions is achieved by a first excision of lesions or mismatches that is followed by DNA synthesis and sealing of the resulting gap. This general cut and patch principle is divided over three main pathways that are dedicated to the different types of DNA aberrations presented earlier in this chapter: base excision repair (BER), nucleotide excision repair (NER) and mismatch repair (MMR). Both BER and MMR will be shortly summarized below, while NER will be discussed in more detail as this process is the main topic of investigation in this thesis. Correct processing of these repair pathways require specific sets of enzymes. Particularly, replication factors implicated in the DNA synthesis steps of these pathways, their recruitment and coordination at these sites of repair replication, with a special focus on NER, and the activation of specialized pathways that are able, at stalled replication forks, to bypass DNA lesions without repairing them are the main object of studies and are discussed in a separate chapter (Chapter 2).

Direct Reversal

Direct reversal is a relatively simple repair system that does not require an incision of the DNA sugar-phosphate backbone or a base excision. Exogenous (such as Methyl Methane Sulfonate, MMS) and endogenous alkylating agents cause a variety of O-alkylated and N-alkylated adducts, such as O6-methylguanine (O6-meG). Part of these lesions can be removed by a specific protein, the O6-meG-DNA methyltransferase (MGMT) that transfers the methyl group to a cysteine residue in an irreversible reaction, thereby destroying its own activity. Obviously this non-enzymatic suicide action has only limited repair capacity and is backed-up mainly by Base Excision Repair (discussed below). Another direct damage reversion is achieved by a group of enzymes referred to as photolyases, which are able to repair UV-induced photoproducts such as CPDs and 6-4 PPs. These flavoproteins bind to the UV-DNA complexes and use photon energy from the visible light spectrum to repair the damage. These photolyases are strongly conserved in evolution and present in all kingdoms of live. However, placental mammals, in contrast to marsupials, do not possess photolyases and have developed more complex mechanisms to cope with UV-induced lesions [Eker et al, 2009].

Repair of base damages and single-strand breaks: BER and SSBR

Base damages triggered by alkylation, oxidation and deamination, are repaired by a more complex pathway known as Base Excision Repair (BER). Recognition of the damaged base is performed by a collection of DNA glycosylases that each have affinity for a specific (group of) lesion(s). These glycosylases remove the damaged base from the sugar-phosphate backbone, thereby creating an abasic or a-purinic/a-pyrimidinic site (AP site) that is incised by AP-endonuclease-1 (APE-1) or the lyase activity of a DNA glycosylase, leading to a single-strand break (SSB). SSBs can also arise directly from reactive oxygen species (ROS), ionizing radiation or incomplete DNA topoisomerase action, in each case SSBs are swiftly recognized by poly-ADP-ribose polymerase 1 (PARP-1). PARP binding further triggers the poly-ADP-ribosylation of different (PAR) targets, including PARP1 and is thought to play an important regulatory role in BER processing [D'Amours et al, 1999]. Different DNA termini may arise from these various processes and need to be restored to the conventional 3'-OH and 5'-P moieties for the further gap filling and ligation steps to occur. Thus, this end processing step requires several enzymes including APE-1, polynucleotide kinase (PNK) or the dRP-lyase activity of DNA polymerase β [reviewed in Caldecott, 2007; Robertson et al, 2009]. Further repair is accomplished via two sub-pathways known as short patch repair (insertion of a single nucleotide) and long patch repair (insertion of 2 to 10 nucleotides). The scaffold protein XRCC1 coordinates short-patch repair which is mainly supported by pol β and DNA-ligase III [Barnes and Lindahl, 2004]. Long patch-repair, on the other hand, is coordinated by PCNA and will be discussed in Chapter 2.

Mismatch Repair (MMR)

Base-base mismatches are produced during normal replication, and from replication of deaminated, alkylated or oxidized nucleotides, such as 8-oxoguanine. In addition, small loops of a few nucleotides (short single-strand deletions or insertions) resulting from replication slippage on highly repetitive genomic sequences, are also a substrate for mismatch repair (MMR). Mismatch Repair is a crucial process that prevents these mismatches from becoming stable mutations and serves to further improve the already high fidelity of replicative DNA synthesis [Kunkel and Erie, 2005; Jiricny, 2006; Li et al, 2008; Hoeijmakers, 2001]. Mismatch recognition is supported by two ATPases, the MutSα dimer (MSH2 and MSH6) for base-base mismatches and MutSβ (MSH2 and MSH3) for insertion/deletion mispairs. Another complex is then recruited, MutLα (MLH1 and PMS1) or MutLβ (PMS2) that searches for strand discontinuity. Discrimination between the parental (correct) and the daughter (incorrect) strands is executed in bacteria via DNA methylation (hypomethylated daughter strand). In eukaryotes it is possibly the nearby replication machinery that plays a role in this strand-discrimination. Degradation past the mismatch (ssDNA fragment of ~150 nucleotides) is supported by the exonuclease Exo I.

Following gap filling synthesis by the replication machinery, sealing is supported by DNA Ligase I.

Nucleotide Excision Repair (NER)

Nucleotide Excision Repair (NER) eliminates in a "cut and patch" mechanism involving more than 30 polypeptides, a broad range of structurally unrelated DNA lesions [Gillet and Scharer, 2006; Friedberg, 2003; de Laat et al, 1999]. These lesions only have in common that they locally impair proper Watson and Crick base pairing, and include on one hand the main UV-induced photoproducts (cyclobutane pyrimidine dimers or CPDs and 6-4 pyrimidine-pyrimidone dimers or 6-4-PPs) and on the other hand, bulky chemical adducts such as those induced by benzopyrene and aflatoxins.
NER can be sub-divided into two pathways that share many similarities but differ by their lesion recognition mechanism. While Global Genome-Nucleotide Excision Repair (GG-NER) detects lesions located anywhere in the genome in order to initiate the NER reaction, Transcription Coupled-Nucleotide Excision Repair (TC-NER) is only active on the transcribed strand of active genes when a lesion obstructs transcription [Venema et al, 1992; Fousteri and Mullenders, 2008; Bohr et al, 1985].

Lesion recognition: two mechanisms

Lesion recognition in GG-NER is achieved by the concerted action of two protein complexes, the XPC-containing complex and the UV-DDB complex. XPC is part of a hetero-trimeric complex further harboring HR23B and Centrin 2 [Araki et al, 2001]. This DNA binding protein complex displays a stronger affinity for damaged DNA and recognizes mainly unpaired short stretches [Sugasawa et al, 1998]. XPC does not bind to lesions directly but rather recognizes the non-damaged DNA opposite the DNA injury [Sugasawa and Hanaoka, 2007]. This recognition is mediated by two aromatic residues that confer to XPC an aversion to damaged strands and a preference for single-stranded DNA [Buterin et al, 2005; Maillard et al, 2007]. This preferential binding to non-damaged DNA opposite a lesion is confirmed by the crystal structure of Rad4, the yeast homologue of XPC [Min and Pavletich, 2007]. Although the exact functions of the HR23B and Centrin2 components in this complex are not known so far, one function of HR23B is to stabilize the XPC protein [Ng et al, 2003] and the distortion-sensing role of XPC is achieved through its binding to HR23B [Sugasawa et al, 1997]. HR23B is one of the two mammalian orthologs of the yeast NER protein Rad23. The other mammalian ortholog, HR23A, is less abundantly expressed than HR23B and only trace amounts are found to co-purify with XPC, though this protein can functionally substitute for HR23B *in vitro* [Sugasawa et al, 2001]. Centrin 2 stabilizes the complex [Araki et al, 2001].
The second complex, the damaged DNA-binding heterodimer UV-DDB, containing DDB1 and DDB2 (p48, mutated in XPE), as its name indicates, has a strong affinity for damaged

DNA, such as 6-4PPs and CPDs [Payne and Chu, 1994]. Since XPC shows very little affinity to CPDs *in vitro* [Hey et al, 2002, Kusumoto et al 2001], the role of UV-DDB might be crucial in damage recognition. And indeed, UV-DDB is stimulating XPC binding [Moser et al, 2005]. One proposed mechanism is that it induces a kink in the DNA which facilitates the recruitment of the XPC complex [Tang and Chu, 2002].

XPC gets polyubiquitinated in a reversible manner following DNA damage [Sugasawa et al, 2005]. However, rather than leading to its degradation, this process increases its affinity for DNA. XPC ubiquitination is dependent on functional UV-DDB activity. Both XPC and DDB2 get polyubiquitinated by the UV-DDB ligase-complex [Sugasawa et al, 2005], though the effect is very different: XPC ubiquitination increases its affinity for damaged and non-damaged DNA, while ubiquitinated DDB2 is targeted for degradation. XPC is also modified by sumoylation in an XPA-dependent manner, which might contribute to its stabilization [Wang et al, 2005].

Lesion recognition in TC-NER is initiated when elongating RNA polymerase II encounters a distorting lesion that blocks its progression [Laine and Egly 2006]. Hyperphosphorylated RNA pol II mediates the recruitment of Cockayne Syndrome B and A (CSB and CSA) proteins which, in brief, allow the recruitment of subsequent repair factors, among which TFIIH [Fousteri et al, 2006; van den Boom et al, 2004].

It is worth noting that since 6-4 PPs are more helix distorting than CPDs, they are recognized and therefore repaired much more efficiently by NER. In mammals, 6-4 PPs are repaired by NER in four to six hours, while CPDs can be present up to twenty-four hours post-irradiation and will therefore play an important role in UV-induced mutagenesis.

Opening of the helix: the transcription factor TFIIH

Following damage recognition, GG-NER and TC-NER channel into a common mechanism which starts with the opening of a the DNA double helix around the lesion by the ten-subunit transcription factor TFIIH [Yokoi et al, 2000; Volker et al, 2001, Fousteri et al, 2006]. TFIIH was originally identified as an essential transcription initiation factor for RNA polymerase I and II transcribed genes [Drapkin et al, 1994; Iben et al, 2002] and turned out to be pivotal for NER as well, with differential kinetic properties [Schaeffer, 1993, Science; Giglia-Mari et al, 2004; Hoogstraten, 2002]. TFIIH consists of a seven-subunit core complex (XPB/p89, XPD/p80, TTDA/p8, p34, p44, p52 and p62) as well as a cyclin-activated kinase (CAK) complex, containing Cdk7, Cyclin H and MAT1. XPB and XPD, together, apply their respective DNA-dependent ATP-ase and helicase activities to open up the DNA helix around the lesion. Open complex formation depends on functional TFIIH and a two-step mechanism is employed in which TFIIH mediates the initial opening (8-10 nucleotides) after which RPA, XPA and XPG bind to obtain full opening of ~ 30 nucleotides around the lesion [Evans et al, 1997; Evans et al, 1997, Mu al, 1997]. During this process, XPA

stimulates specifically the ATPase activity of TFIIH while RPA and XPG stabilize the partially unwound repair intermediate, which allows the full opening around the lesion. The binding of XPA to damaged DNA is greatly enhanced by RPA. Simultaneous binding of RPA to the undamaged strand and of XPA to the kinked DNA duplex allows the detection of base-pair and backbone distortions which contributes to the lesion specificity of NER [Camenisch et al, 2006]. RPA and XPA, together, act therefore as a sensor probe that carries out damage verification before dual incision occurs.

Dual incision and post-incision steps

The presence of RPA on the undamaged strand is also important to properly orient the NER endonucleases that will incise around the lesion on the damaged strand [de Laat et al, 1998]. Dual incision is achieved by the concerted action of two structure-specific endonucleases: the complex ERRCC1/XPF incises 5'to the lesion and XPG 3' to the lesion. In Chapter 3 of this thesis, we have studied the sequential action of these endonucleases that leads to the creation of a 24-32 nucleotide single-stranded DNA gap.
This ss-DNA gap is filled in during a process called DNA repair synthesis. While RPA coats the single-stranded DNA, PCNA is loaded by RFC and allows tethering of the polymerases δ, ε and eventually pol κ. The nick is sealed by Ligase III/Ligase I and chromatin structure is restored upon action of CAF-1. The dual action of RPA as well as DNA repair synthesis and subsequent steps are discussed in Chapter 2.
The different NER factors and their mode of action are illustrated within a schematic representation in Figure 1.

The very broad clinical symptoms associated with inherited NER defects, might in part be derived from the multiple functions (transcription, replication or multiple repair pathways) that several NER factors display. XP patients (who display mutations in the XPA to –G genes) are hypersensitive to sunlight and exhibit an extreme susceptibility for UV-induced skin cancer. Cockayne Syndrome patients (who display mutations in CSA and CSB) are not cancer prone but display other clinical features such as premature ageing. And finally TTD patients, who carry mutations in TFIIH subunits (XPB, XPD, p8/TTDA), present many features similar to CS in addition to specific features such as brittle hair and nails.

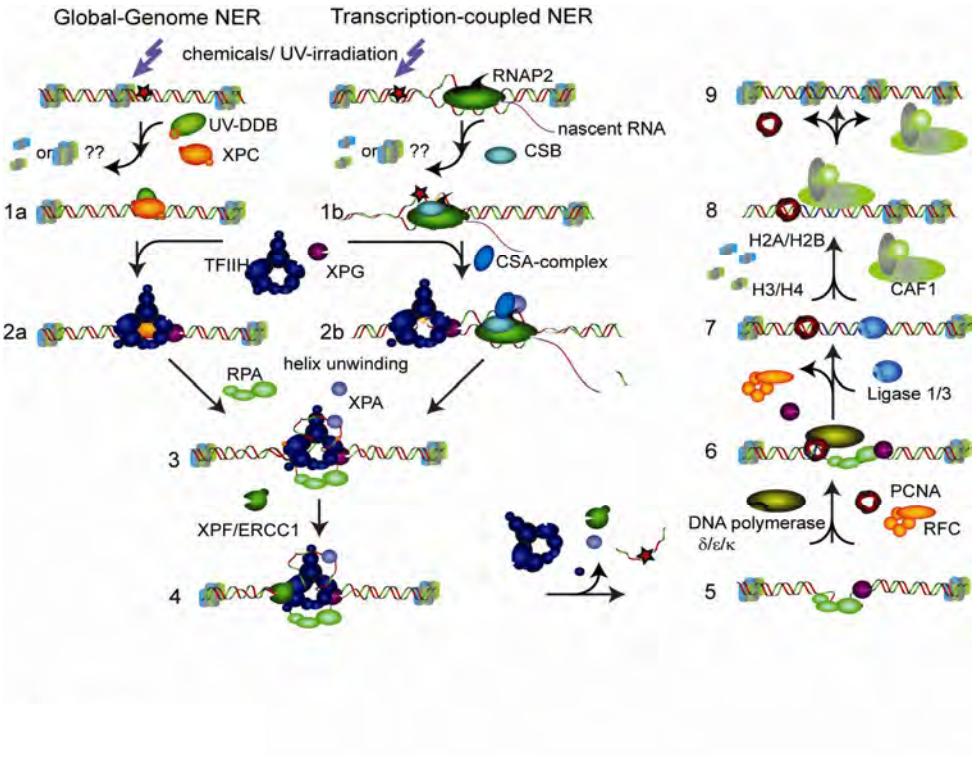

Figure 1: schematic representation of NER.
Adapted from: G. Giglia Mari, A. Zotter and W. Vermeulen, Chapter one DNA damage response, in Cold Spring Harbor; Perspective The Nucleus, 2010.

Choreography of the NER factors

NER is performed by complexes that are assembled from individual components at the lesion site rather than by binding of a pre-assembled complex [Houtsmuller et al, 1999; Hoogstraten et al, 2002]. Hence, the current model is that incorporation of NER components into the pre-incision complex follows a sequential order; however the dynamic interactions between NER components during this assembly are unknown. In Chapter 6 of this thesis, we have used kinetic measurements of seven-GFP tagged NER proteins associated to a mathematical model to develop a quantitative understanding of repair complexes assembly in living cells.

These three excision repair mechanisms (NER, BER, MMR), have in common that they only allow repair of DNA lesions when located in one strand of the double helix, as after excision of the lesions the subsequent resynthesis will use the sequence information of the non-damaged complementary strand. However, DNA lesions involving both strands (i.e.

double strand breaks and interstrand crosslinks) require more complex processes to convert these structures into normal Watson and Crick B-form DNA. Repair processes dealing with these structures will be discussed below.

Repair of Double-Strand Breaks: NHEJ and HR

Double-strand breaks (DSBs) are extremely cytotoxic lesions caused by ionizing radiation and upon replication stress. In addition, they can arise from physiological processes such as V(D)J recombination and class switch recombination in developing lymphocytes or during meiotic recombination. Two different repair processes deal with these DSBs; homologous recombination (HR) and non-homologous end joining (NHEJ). HR is only active in S and G2 phases where a homologous copy of the genome is available that is required for this process (see below) and is thus an important double-strand break processing mechanism in rapidly dividing cells. In G1 and G0 phases of the cell cycle however the only option to seal breaks is by NHEJ [Mahaney et al, 2009].

NHEJ is based on straightforward ligation of DNA ends. Since some processing of DNA ends is required in most cases to create ligatable termini, NHEJ can lead to nucleotide loss, and is potentially an error-prone mechanism. NHEJ is triggered by the binding of the Ku70/80 heterodimer to the extremities of the broken DNA strand [Walker et al, 2001], allowing the recruitment of DNA-PKcs **(**for DNA protein kinase catalytic subunit) [Gottlieb and Jackson, 1993]. DNA-PK belongs to the serine-threonine kinase family of PIKKs (phosphatidylinositol 3-kinase-like kinases), which all share the characteristic catalytic domain of PI-3 (phosphoinositide) kinases and stand out as very large polypeptides that range from 300 to >500 kDa. SMG-a, TOR, ATM and ATR (see below) belong also to this family of PIKKs [Abraham, 2001].
After its recruitment, a key event is the auto-phosphorylation of DNA-PKcs [Chan and Lees-Miller, 1996] and the alignment of the DNA ends in a synaptic complex. Following DNA end processing by Artemis [Ma et al, 2002], ligation of the DNA ends is carried out by the Ligase IV/XRCC4 complex [Grawunder, et al, 1997; Mari et al, 2006]. The XLF/Cernunnos probably stimulates this process [Ahnesorg et al, 2006; Buck et al, 2006]. There is increasing evidence that several other proteins, including MRN (at least in yeast), are involved in NHEJ [Mahaney et al, 2009].

Homologous recombination (HR) requires the presence of a second copy of the sequence, the sister chromatid, since it is based on exchange of genetic information between homologous DNA molecules. HR is initialized by binding of the Mre11-Rad50-Nbs1 complex, which together with CtIP proceeds to the resection of the 5'-ends of the break, creating 3' overhangs [Lee et al, 1998; Tauchi et al, 2002]. The produced single-strand DNA is covered by the single-stranded DNA binding protein RPA. Subsequently, monomers of the Rad51 recombinase assemble into a nucleoprotein filament on the ssDNA ends [Park et

al, 1996]. This assembly is influenced by BRCA2 and several RAD51 paralogs. The RAD51 filament then searches for homology and invades the homologous dsDNA template (a process known as first strand invasion), forming a joint molecule called a displacement loop (D-loop). The 3' end then serves as a primer for DNA synthesis. This step is promoted by the dsDNA-dependent ATPase Rad54. Following the extension of the invading end the reaction can channel into different paths. The second end can invade the homologous template in a Rad51-mediated reaction (second strand invasion), or anneal to the displaced strand of the homologous duplex. The single-strand annealing activity of Rad52 promotes this process. These two pathways can lead to the formation of cross-stranded structures called Holliday Junctions (HJs). Alternatively, the first end extended by a DNA polymerase can be displaced from the joint molecule and re-anneal with the second end of the break in a process called synthesis-dependent strand annealing (SDSA) [Lisby and Rothstein, 2009; Sung and Klein, 2006; Heyer et al, 2006].

Interstrand Cross-link (ICL) repair

Chemical compounds such as the chemotherapeutical cisplatin and Mitomycin C induce interstrand cross-links (ICLs) which, if unrepaired, are highly lethal [Magana-Schwencke et al, 1982]. ICLs are resolved by the Fanconi Anemia pathway. FA patients display twelve complementation groups and the FANC genes products operate in a common pathway that is poorly understood. In brief, the current model indicates that recognition of the ICL is mediated by stalling of the replicative polymerase during replication. The ICL is incised on one side, leading to a DSB. A helicase unwinds around the incised ICL. A second incision on the same strand of the ICL but on its other side, leads to a gap that is later filled in by TLS polymerases. The residual damage in the opposite strand is removed by excision (NER or BER) and the integrity of the DNA template is restored. Finally, the DSB that was created during the first incision is repaired by HR [Niedernhofer et al, 2005]. The endonuclease ERCC1-XPF is required for the multi-step incisions of the ICL. PCNA and RPA are implicated for DNA synthesis during repair of inter-strand crosslink (ICL) caused by chemical agents such as psoralen [Li et al, 2000]. They might also be involved in the incision step of this process [Zhang et al, 2003].

2.2. Cell cycle checkpoints

The DNA Damage Response does not only consist of a subset of different repair pathways but also involves cell cycle checkpoints that delay or temporally arrest the cell cycle progression, which provides more time for the cells to repair the damage. Each cycle comprises two cell growth phases (G1 and G2), one DNA replication phase (S) and a mitosis or M-phase in which the cell splits into two identical daughter cells. A whole array of proteins is dedicated to control or check for correct processing of crucial events throughout every phase of the cell cycle as it is indispensable that each phase gets fully

completed before progression to the next step. When within a certain stage of the cell cycle a problem is encountered, by e.g. the induction of DNA damage that interferes with replication, one or several appropriate repair or bypass mechanism(s) are triggered. On top of this, so-called intra-S-phase checkpoints are activated which temporally arrest cell cycle progression until the insults are removed

In response to genotoxic insults, a signaling cascade is activated that triggers checkpoint activation and subsequently blocks the cell cycle in G1/S or G2/M, or that retards the completion of S-phase (intra-S). Alternatively, apoptosis can be triggered if too many lesions are encountered. This cell cycle signaling pathway is initiated by sensing of damaged or abnormally structured DNA to finally coordinate cell cycle progression with the DNA repair process. Signal transduction that connects damage sensors to effector proteins (which regulate the passage throughout the different phases of the cell cycle) is supported by the two core PI-3 kinases related ATM (Ataxia-Telangectasia Mutated) and ATR (Ataxia Telangectasia and Rad3-related), which have distinctive though partially overlapping functions [Zhou and Elledge, 2000]. These kinases are at the basis of a signaling cascade that resembles standard signal transduction pathways in that signal transmission and amplification are based on an array of differential protein phosphorylation reactions leading to different downstream targets [Matsuoka, et al 2007].

DNA damage–induced signaling

In undamaged cells ATM resides as a catalytically inactive dimer or higher order multimer and gets phosphorylated at Ser^{1981} in response to ionizing radiation [Bakkenist and Kastan, 2003]. Initially, it was thought that the damage itself was sufficient to initiate this process. However, it turned out that the Mre11-Rad50-Nbs1 (MRN) complex is also a key factor for the recruitment and activation of ATM by double strands breaks [Abraham and Tibbetts, 2005; Lee and Paull, 2005]. Next to auto-phosphorylation, ATM acetylation by Tip60 appeared also important for ATM activation, although its exact role and mechanism remain elusive [Sun and Price, 2005].

In human cells ATR resides in a stable complex with ATRIP (ATR-interacting protein) and gets activated in response to different DNA damaging agents (UV, alkylating agents, double strand breaks) and replication stress [Cortez et al, 2001]. ATR-mediated signaling is initiated after binding of ATRIP to a common intermediate, ss-DNA that is covered with Replication Protein A (RPA) [Zou and Elledge, 2003]. RPA is a trimeric replication factor that coats single-stranded DNA and, as such, is also involved in many repair processes. More details on this protein will be discussed in Chapter 2. Next to a role for ATR activation, RPA bound to ss-DNA is involved in the recruitment of another important checkpoint initiator that is in addition also a substrate for ATR: the RAD17 complex, which in turn loads around the DNA the RAD9-HUS1-RAD1 (9-1-1) complex.

During regular DNA replication, a circular sliding clamp, PCNA (Proliferating Cell Nuclear Antigen), acts as a platform that tethers replication factors, among which polymerases, to the DNA. The loading of PCNA around the DNA is performed by the replication complex RFC (Replication Factor C), which contains RFC1 and four other subunits [Tsurimoto and Stillman, 2001].

PCNA and RFC are key replication and repair factors that were extensively studied in this thesis and are being discussed separately in Chapter 2. The 9-1-1 complex is a ring-shape protein complex that resembles the PCNA structure, while the RAD17-RFC like complex presents structural similarity to RFC since the four small subunits of these factors are commonly shared [Caspari et al, 2000; Venclovas and Thelen, 2000; Burtelow et al, 2001]. The RAD17 complex is recruited independently of ATR-ATRIP [Zou et al, 2002], recognizes the junctions between single-and double-stranded DNA and loads the 9-1-1 checkpoint complex onto the DNA. The 9-1-1 complex interacts also with TopBP1 (topoisomerase IIβ binding protein 1), a protein that stimulates the ATR-ATRIP protein kinase activity [Lee et al, 2007; Delacroix et al, 2007]. In addition, a last factor, claspin, is recruited to chromatin in a process independent of ATR and 9-1-1 but that requires ATR-mediated phosphorylation of RAD17 [Lee et al, 2003; Wang et al, 2006]. Claspin is required for the subsequent ATR-mediated activation of CHK1.

Interestingly, the role of RAD17 and the 9-1-1 complex is not limited to checkpoint signaling. Several studies showed that these proteins are also implicated in translesion synthesis (TLS, see below) (in yeast) and different repair pathways, such as HR [Wang et al, Oncogene 2006; Pandita et al, 2006; Budzowska, et al, 2004] and BER [Wang et al, 2004; Friedrich-Heineken et al, 2005].

DNA damage-induced signal transduction

ATM interacts with and phosphorylates a wide range of substrates that eventually control multiple checkpoints throughout the entire cell cycle. The G1/S checkpoint is controlled through p53 phosphorylation [Banin et al, 1998; Canman et al, 1998]. All the different proteins targeted by these processes are too numerous to summarize here and only a few targets will be evaluated. p53 activation is also indirectly controlled by ATM via CHK2 and MDM2 phosphorylation. The intra-S checkpoint is regulated via interaction with several proteins among which NBS1 and SMC1 [Wu et al, 2000; Kim et al, 2002]. BRCA1 gets phosphorylated in S and G2/M transitions [Cortez et al, 1999]. ATM phosphorylates also CHK1 and CHK2.
ATR-phosphorylated Rad 17 interacts with claspin and allows its phosphorylation, which promotes recruitment, phosphorylation and activation of CHK1 [Wang et al, 2006]. Once phosphorylated and activated, CHK1 and CHK2 are able to phosphorylate downstream cell cycle proteins such as CDC25C, WEE1 and CDC25A phosphatase, which in turn can

dephosphorylate and activate some of the cyclin-dependent kinases CDKs [Mailand et al, 2000; Falck et al, 2001].

CDKs, together with cyclins, are the downstream active players of cell cycle progression or arrest. Cyclins are quantitatively and qualitatively specific of each cell cycle phase and bind to the CDKs. The levels of CDK proteins remain stable during normal cell cycle, are regulated by cyclin levels that oscillate through the cell cycle and are responsible for the major transitions throughout the cell cycle. Regulators of cyclin-CDK formation also include CDK inhibitors such as p21. The transcription level of p21 can be regulated by p53. Interestingly, the replication factor PCNA is a downstream target of p53 and interacts with p21 and cyclin D [Xiong et al, 1992; Shivakumar et al, 1995; Morris et al, 1996].

2.3. Replication over damaged DNA

Despite the whole network of efficient DNA repair and checkpoint mechanisms, entirely dedicated to the removal of the different genomic insults, a number of lesions escape direct removal before replication starts. Moreover in some cases the cell is already in S-phase when the lesion is inflicted. Finally, the replication fork itself can collapse and induce hazardous lesions such as DSBs. The price to pay for the stringency of DNA polymerases is that they cannot accommodate these damaged bases. This triggers a block in the progression of the replication fork that may, in the worst case, lead to a definitive arrest of replication and cell death.
Two pathways have evolved in order to avoid the damage and are therefore known as damage tolerance mechanisms or postreplication repair (PRR) processes. The first of these consists of the incorporation of nucleotides opposite the damage (in other words, synthesizing DNA past the lesion or translesion synthesis, TLS). This pathway uses a set of specialized TLS polymerases and appears to be predominant in mammalian cells. The Translesion Synthesis process is illustrated by the gravity of the genetic disorder Xeroderma Pigmentosum Variant (XPV), in which one of these TLS polymerases, polymerase η, is mutated. Despite the fact that these patients have the ability to carry out normal NER, they still show a very high incidence of sunlight-induced skin cancer, caused by a higher UV-induced hypermutability. Another damage avoidance process mainly present in prokaryotes and uni-cellular eukaryotes (such as *Saccharomyces. cerevisiae*) consists of a recombinational mechanism to copy genetic information from the undamaged sister duplex to restore the lost information. This process is considered as error-free. PCNA ubiquitination regulates the transition from regular DNA polymerases to TLS polymerases and guides the cell towards these two different damage tolerance processes. Moreover, RFC and RPA are also involved in these processes. Post-replication repair is described further in Chapter 2.

3. Detection of proteins involved in DNA repair

All the proteins involved in replication, repair and cell cycle control display specific sub-cellular localization and dynamic properties. These characteristics are tightly linked to their intrinsic biochemical properties but also to their biological role(s), i.e. their interactions with other complexes and/or the DNA/chromatin. Genetic and biochemical studies have provided very interesting insights on the structure and function of these proteins. However, to provide more accurate and realistic information, within the context of the complexity of the mammalian cell nucleus, on the spatio-temporal properties and interactions of replication and repair factors, cell biological approaches are necessary. These approaches have been widely used in the studies described in the different chapters of this thesis.

3.1. Chromatin immunoprecipitation

Chromatin immunoprecipitation (ChIP) allows the identification of proteins that associate with specific regions of the genome, by using specific antibodies that recognize a specific protein or a specific modification of a protein [Fousteri et al, 2006]. The initial step of ChIP is the cross-linking of protein-protein and protein-DNA in live cells with formaldehyde. After cross-linking, the cells are lysed and crude extracts are sonicated to shear the DNA. Proteins together with cross-linked DNA are subsequently immunoprecipitated. Cross-linking ChIP uses chromatin fixed with formaldehyde and fragmented by sonication. We have widely used this technique in Chapter 4 of this thesis.

3.2. Fluorescence studies

The mammalian cell is a very complex environment where a huge amount of various proteins are involved in multiple processes. To study a factor or a process in particular, it is necessary to be able to distinguish it clearly and specifically from the cellular environment. As this regard, fluorescence, that displays strong resolution and specific illumining, is a very useful and powerful tool. Fluorescence occurs when a fluorescent molecule absorbs light of a specific wavelength and following this absorption, re-emits light at a higher wavelength.

Immunofluorescence studies

In the case of immunofluorescence, a specific antibody (or secondary antibody) is covalently coupled to a fluorescent molecule. Sub-cellular localization of replication and repair factors can be studied using immuno-fluorescence experiments which require fixation and permeabilization of the cells and lead therefore to an immobilization of the factors at the sites of replication and repair. This can facilitate greatly, for example, the visualization of complexes that are only transiently interacting with the DNA/chromatin or with other partners. Moreover, in the case of ubiquitous proteins that present a diffuse

nuclear pool and a more immobilized chromatin fraction, an additional pre-fixation washing step allows removal of the more diffuse proteins.

These procedures (ChiP and immunofluorescence) are highly powerful and bring very useful information on protein biochemistry, interactions and sub-cellular localization. However they have their limitations since they do not allow any insight into the dynamics of molecular transactions and may reveal artificially enhanced structures as fixation may bias the accumulation of certain reaction intermediates that are frozen by this procedure. To get a global view on replication, repair and damage tolerance mechanisms and to study in-depth the dynamic properties of these factors in these processes, it is therefore necessary to use a more dynamical approach.

Fluorescence coupled to live cell imaging

In order to visualize dynamics in live cells, it is necessary to tag the protein of interest with a fluorescent dye that is not toxic for the cell and that in the same time, does not inhibit the proper functioning, the biochemical and dynamic properties of the protein.

A real breakthrough occurred in the field of biology with the crucial discovery of a 28kDa fluorescent protein, green fluorescent protein (GFP), which fills in all these properties. GFP was originally isolated from the jellyfish *Aequoria Victoria* and emits green light at a wavelength of 508 nm when excited by blue light, with two wavelengths, the major at 395 nm and the minor at 475 nm. Wild type GFP has been modified to several GFP variants with different excitation and emission wavelengths, which can be properly used for live cell studies, as we have done in Chapters 4, 5, 6, 7 and 8 of this thesis [Cubitt et al, 1995; Shimomura et al, 1962; Tsien et al, 1998]. The most important application of this live cell fluorescent marker comes from the possibility to clone the encoding cDNA to the gene encoding the protein of interest. Once fused to the protein of interest, the recombinant protein must be tested for its functionality in living cells. Subsequently, it can be monitored *in situ* in real time thanks to the extensive use of confocal microscopy

Confocal microscopes are more sophisticated than conventional fluorescent microscopes since they are able to block out the “out-of-focus light” which is often encountered with thick samples. With a confocal microscope, point illumination is realized with a laser and fluorescence is detected through a pinhole in front of the detector, which allows sole detection of in-focus fluorescence and results in a better image quality than with a fluorescent microscope.
Confocal microscopy is also a powerful tool to realize photobleaching experiments and determine protein dynamics. Photobleaching is based on the property of fluorescent molecules to become non-fluorescent after a certain number of excitation-emission cycles. Hence, a high intensity laser-pulse induced by a confocal microscope can lead to

photobleaching of a fluorescent molecule. When this fluorophore, such as GFP, is tagged to a protein of interest, several procedures are available to measure the dynamics of this recombinant protein at sites of replication and repair for example.
With FRAP (Fluorescence Recovery After Photobleaching), the recombinant protein is bleached out in a certain area of the cell and the subsequent recovery of fluorescence in the bleached area is monitored over time. FRAP can be combined with FLIP (Fluorescence Loss in Photobleaching), in which the loss of fluorescence is monitored outside of the bleach region (represented in Chapter 5 of this thesis). These two protocols allow a determination of the diffusion and binding times of replication and repair factors and have been extensively used in Chapters 4, 5, 6, 7 and 8 of this thesis. The bleach and monitoring parameters (areas, time…) can be adapted in order to visualize transient binding, such as the "box-frap" protocol designed in Chapter 8.

The development of several systems to locally introduce DNA damage or immobilize DDR factors in cultured living cells in combination with GFP technology has been beneficial in the study of DNA repair: (*i*) irradiation through a filter or mask that partly shield the cells [Nelms et al, 1998; Katsumi et al, 2001; Moné et al, 2001]; (*ii*) micro-beam laser irradiation, with or without photo-sensitizers, at sub-nuclear areas [Cremer et al, 1980; Tashiro et al, 2000; Lukas et al, 2003; Meldrum et al, 2003; Lan et al, 2004; Dinant et al, 2007]; (*iii*) guided α-particle and heavy iron radiation [Jakob et al, 2003; Aten et al, 2004; Hauptner et al, 2004]. ; (*iv*) integration of rare-cutting endonucleases [Lisby et al, 2004; Rodrigue et al, 2006, Soutoglou et al, 2007]; (*v*) DDR protein tethering to specific integrated amplified (arrays) sequences [Soutoglou and Misteli, 2008].

3.3. In vivo-DNA labeling

Spatio-temporal dynamics studies on DNA-related processes such as replication, transcription and DNA repair are greatly facilitated by adequate stains that differentiate chromatin compaction since these processes are tightly regulated by chromatin condensation and DNA conformation. An example is studied in Chapter 7 of this thesis, where we study the cellular consequences and suitability of the anthraquinone-derivate Draq5 that has been utilized in Chapter 8.

3.4. DNA synthesis inhibitors

DNA synthesis inhibitors such as aphidicolin (that inhibits polymerase α by competing for nucleotide incorporation), or HU/AraC (that compete with the polymerase and trigger also a depletion of the nucleotide pool), are very useful to study the interactions between replication and repair proteins and replicating DNA. The impact of HU/AraC on DNA synthesis, especially at repair synthesis sites of NER, is used in Chapters 4, 5 and 6 of this

thesis. Live cells are incubated in the presence of these inhibitors and can then be subjected to the previous techniques or to live cell dynamic studies presented above.

All these techniques combined together represent a very powerful tool to determine the mechanisms that underlie protein interactions and recruitments to sites of replication and repair. For the rest of this thesis, we will focus exclusively on three replication factors, PCNA, RFC and RPA. The role of these replication factors in the different repair pathways listed above is summarized in Table 3. In Chapter 2, we study in details the biochemical properties and the involvement of these proteins in replication, repair (with a focus on NER) and in damage bypass mechanisms.

Protein \ DDR	SSBR	MMR	NER	HR	NHEJ	Checkpoint mechanisms	Damage bypass
PCNA	X	X	X	X			X
RPA	X	X	X	X		X	X
RFC	X	X	X	?			X

Table 3: implications of Replication Factors PCNA, RPA and RFC in the DDR

References chapter 1

Abraham, R.T. (2001). Cell cycle checkpoint signaling through the ATM and ATR kinases. Genes Dev **15**(17): 2177-96.

Abraham, R. T. and Tibbetts, R.S. (2005). *Cell biology. Guiding ATM to broken DNA.* Science **308**(5721): 510-1.

Ahnesorg, P., Smith, P. and Jackson, S.P. (2006). *XLF interacts with the XRCC4-DNA ligase IV complex to promote DNA nonhomologous end-joining*. Cell **124**(2): 301-13

Araki, M., Masutani, C., Takemura, M., Uchida, A., Sugasawa, K., Kondoh, J., Ohkuma, Y. and Hanaoka, F. (2001). *Centrosome protein centrin 2/caltractin 1 is part of the xeroderma pigmentosum group C complex that initiates global genome nucleotide excision repair*. J Biol Chem **276**(22): 18665-72.

Araki, M., Masutani, C., Takemura, M., Uchida, A., Sugasawa, K., Kondoh, J., Ohkuma, Y. and Hanaoka, F. (2001). *Centrosome protein centrin 2/caltractin 1 is part of the xeroderma pigmentosum group C complex that initiates global genome nucleotide excision repair.* J Biol Chem **276**(22): 18665-72.

Aten, J. A., Stap, J., Krawczyk, P.M., van Oven, C.H., Hoebe, R.A., Essers, J. and Kanaar, R.(2004). *Dynamics of DNA double-strand breaks revealed by clustering of damaged chromosome domains*. Science **303**(5654): 92-5.

Bakkenist, C.J. and Kastan, M.B. (2003). *DNA damage activates ATM through intermolecular autophosphorylation and dimer dissociation*. Nature **421**(6922): 499-506.

Banin, S., Moyal, L., Shieh, S., Taya, Y., Anderson, C.W., Chessa, L., Smorodinsky,, N.I., Prives, C., Reiss, Y., Shiloh, Y. and Ziv, Y. (1998). *Enhanced phosphorylation of p53 by ATM in response to DNA damage.* Science **281**(5383): 1674-7.

Barnes, D.E. and Lindahl, T. (2004). *Repair and genetic consequences of endogenous DNA base damage in mammalian cells*. Annu Rev Genet **38**: 445-76.

Bohr, V.A., Smith, C.A., Okumoto, D.S. and Hanawalt, P.C. (1985). *DNA repair in an active gene: removal of pyrimidine dimers from the DHFR gene of CHO cells is much more efficient than in the genome overall.* Cell **40**(2): 359-69.

Buck, D., Malivert, L., de Chasseval, R., Barraud, A., Fondaneche, M.C., Sanal, O., Plebani, A., Stephan, J.L., Hufnagel, M., le Deist, F., Fischer, A., Durandy, A., de Villartay, J.P. and Revy, P. (2006). *Cernunnos, a novel nonhomologous end-joining factor, is mutated in human immunodeficiency with microcephaly*. Cell **124**(2): 287-99.

Budzowska, M., Jaspers, I., Essers, J., de Waard, H., van Drunen, E., Hanada, K., Beverloo, B., Hendriks, R. W., de Klein, A., Kanaar, R., Hoeijmakers, J. H., Maas and A. (2004). *Mutation of the mouse Rad17 gene leads to embryonic lethality and reveals a role in DNA damage-dependent recombination*. Embo J **23**(17): 3548-58.

Burtelow, M.A., Roos-Mattjus, P.M., Rauen, M., Babendure, J.R. and Karnitz, L. M. (2001). *Reconstitution and molecular analysis of the hRad9-hHus1-hRad1 (9-1-1) DNA damage responsive checkpoint complex*. J Biol Chem **276**(28): 25903-9

Buterin, T, Meyer, C., Giese, B., Naegeli, H. (2005). *DNA quality control by conformational readout on the undamaged strand of the double helix.* Chem Biol **12**(8): 913-22.

Canman, C. E., Lim, D. S., Cimprich, K. A., Taya, Y., Tamai, K., Sakaguchi, K., Appella, E., Kastan, M. B. and Siliciano, J. D. (1998). *Activation of the ATM kinase by ionizing radiation and phosphorylation of p53* Science **281**(5383): 1677-9.

Caspari, T., Dahlen, M., Kanter-Smoler, G., Lindsay, H.D., Hofmann, K., Papadimitriou, K., Sunnerhagen, P. and Carr, A,M. (2000). *Characterization of Schizosaccharomyces pombe Hus1: a PCNA-related protein that associates with Rad1 and Rad9.* Mol Cell Biol **20**(4): 1254-62

Cremer, C., Cremer, T., Fukuda, M. and Nakanishi, K. (1980). *Detection of laser--UV microirradiation-induced DNA photolesions by immunofluorescent staining.* Hum Genet **54**(1): 107-10.

De Bont, R. and van Larebeke, N. (2004). *Endogenous DNA damage in humans: a review of quantitative data.* Mutagenesis **19**(3): 169-85.

de Laat, W.L., Appeldoorn, E., Sugasawa, K., Weterings, E., Jaspers, N.G. and Hoeijmakers, J. H. (1998). DNA-binding polarity of human replication protein A positions nucleases in nucleotide excision repair. Genes Dev **12**(16): 2598-609.

de Laat, W. L., Jaspers, N.G. and Hoeijmakers, J.H. (1999). *Molecular mechanism of nucleotide excision repair.* Genes Dev **13**(7): 768-85.

Caldecott, K.W. (2007). *Mammalian single-strand break repair: mechanisms and links with chromatin.* DNA Repair (Amst) **6**(4): 443-53.

Camenisch, U., Dip, R., Schumacher, S. B., Schuler, B. and Naegeli, H. (2006). *Recognition of helical kinks by xeroderma pigmentosum group A protein triggers DNA excision repair.* Nat Struct Mol Biol **13**(3): 278-84.

Chan, D. W. and Lees-Miller, S.P. (1996). *The DNA-dependent protein kinase is inactivated by autophosphorylation of the catalytic subunit.* J Biol Chem **271**(15): 8936-41.

Cortez, D., Wang, Y., Qin, J. and Elledge, S.J. (1999). *Requirement of ATM-dependent phosphorylation of brca1 in the DNA damage response to double-strand breaks.* Science **286**(5442): 1162-6.

Cortez, D., Guntuku, S., Qin, J. and Elledge, S.J. (2001). *ATR and ATRIP: partners in checkpoint signaling.* Science **294**(5547): 1713-6.

Cubitt, A.B., Heim, R., Adams, S.R., Boyd, A.E., Gross, L.A. and Tsien, R.Y. (1995). *Understanding, improving and using green fluorescent proteins.* Trends Biochem Sci **20**(11): 448-55.

D'Amours, D., Desnoyers, S., D'Silva, I. and Poirier, G.G. (1999). *Poly(ADP-ribosyl)ation reactions in the regulation of nuclear functions.* Biochem J **342 (Pt 2)**: 249-68.

Delacroix, S., Wagner, J.M., Kobayashi, M., Yamamoto, K. and Karnitz, L. M. (2007). *The Rad9-Hus1-Rad1 (9-1-1) clamp activates checkpoint signaling via TopBP1.* Genes Dev **21**(12): 1472-7.

Dinant, C., de Jager, M., Essers, J., van Cappellen, W.A., Kanaar, R., Houtsmuller, A.B. and Vermeulen, W. (2007). *Activation of multiple DNA repair pathways by sub-nuclear damage induction methods.* J Cell Sci **120**(Pt 15): 2731-40.

Drapkin, R., Reardon, J.T., Ansari, A., Huang, J.C., Zawel, L., Ahn, K., Sancar, A. and Reinberg, D. (1994). *Dual role of TFIIH in DNA excision repair and in transcription by RNA polymerase II.* Nature **368**(6473): 769-72.

Eker, A.P., Quayle, C., Chaves, I. and van der Horst, G.T. (2009). *DNA repair in mammalian cells: Direct DNA damage reversal: elegant solutions for nasty problems.* Cell Mol Life Sci **66**(6): 968-80.

Essers, J., Vermeulen, W. and Houtsmuller, A.B. (2006). *DNA damage repair: anytime, anywhere?* Curr Opin Cell Biol **18**(3): 240-6.

Evans, E., Fellows, J., Coffer, A. and Wood, R.D. (1997). *Open complex formation around a lesion during nucleotide excision repair provides a structure for cleavage by human XPG protein.* Embo J **16**(3): 625-38.

Evans, E., Moggs, J.G., Hwang, J.R., Egly, J.M. and Wood, R.D. (1997). *Mechanism of open complex and dual incision formation by human nucleotide excision repair factors.* Embo J **16**(21): 6559-73.

Falck, J., Mailand, N., Syljuasen, R.G., Bartek, J. and Lukas, J. (2001). *The ATM-Chk2-Cdc25A checkpoint pathway guards against radioresistant DNA synthesis.* Nature **410**(6830): 842-7.

Fousteri, M. and Mullenders, L.H. (2008). *Transcription-coupled nucleotide excision repair in mammalian cells:molecular mechanisms and biological effects.*Cell Res**18**(1):73-84

Fousteri, M., Vermeulen, W., van Zeeland, A.A. and Mullenders. (2006). *Cockayne syndrome A and B proteins differentially regulate recruitment of chromatin remodeling and repair factors to stalled RNA polymerase II in vivo.* Mol Cell **23**(4): 471-82.

Friedberg, E.C. (2003). *DNA damage and repair.* Nature **421**(6921): 436-40.

Friedrich-Heineken, E., Toueille, M., Tannler, B., Burki, C., Ferrari, E., Hottiger, M. O. and Hubscher, U. (2005). *The two DNA clamps Rad9/Rad1/Hus1 complex and proliferating cell nuclear antigen differentially regulate flap endonuclease 1 activity.* J Mol Biol **353**(5): 980-9.

Garinis, G.A., van der Horst, G.T., Vijg, J. and Hoeijmakers, J.H. (2008). *DNA damage and ageing: new-age ideas for an age-old problem.* Nat Cell Biol **10**(11): 1241-7.

Giglia-Mari, G., Coin, F., Ranish, J.A., Hoogstraten, D., Theil, A., Wijgers, N., Jaspers, N.G., Raams, A., Argentini, M., van der Spek, P.J., Botta, E., Stefanini, M., Egly, J.M., Aebersold, R., Hoeijmakers, J.H. and Vermeulen, W. (2004). *A new, tenth subunit of TFIIH is responsible for the DNA repair syndrome trichothiodystrophy group A.* Nat Genet **36**(7): 714-9.

Gillet, L.C. and Scharer, O.D. (2006). *Molecular mechanisms of mammalian global genome nucleotide excision repair.* Chem Rev **106**(2): 253-76.

Gottlieb, T.M. and Jackson, S.P. (1993). *The DNA-dependent protein kinase: requirement for DNA ends and association with Ku antigen*. Cell **72**(1): 131-42.

Grawunder, U., Wilm, M., Wu, X., Kulesza, P., Wilson, T.E., Mann, M., Lieber, M.R. (1997). *Activity of DNA ligase IV stimulated by complex formation with XRCC4 protein in mammalian cells*. Nature **388**(6641): 492-5.

Hauptner, A., Dietzel, S., Drexler, G.A., Reichart, P., Krucken, R., Cremer, T., Friedl, A.A. and Dollinger, G.(2004). *Microirradiation of cells with energetic heavy ions*. Radiat Environ Biophys **42**(4): 237-45.

Hey, T., Lipps, G., Sugasawa, K., Iwai, S., Hanaoka, F. and Krauss, G. *The XPC-HR23B complex displays high affinity and specificity for damaged DNA in a true-equilibrium fluorescence assay.* Biochemistry **41**(21): 6583-7.

Heyer, W.D., Li, X., Rolfsmeier, M. and Zhang, X.P (2006). *Rad54: the Swiss Army knife of homologous recombination?* Nucleic Acids Res **34**(15): 4115-25.

Hoeijmakers, J.H. (2001). *Genome maintenance mechanisms for preventing cancer.* Nature **411**(6835): 366-74.

Hoogstraten, D., Nigg, A.L., Heath, H., Mullenders, L.H., van Driel, R., Hoeijmakers, J.H., Vermeulen, W. and Houtsmuller, A.B. (2002). *Rapid switching of TFIIH between RNA polymerase I and II transcription and DNA repair in vivo*. Mol Cell **10**(5):1163-74.

Houtsmuller, A.B., Rademakers, S.,Nigg, A L., Hoogstraten, D., Hoeijmakers, J.H. and Vermeulen, W. (1999*). Action of DNA repair endonuclease ERCC1/XPF in living cells.* Science **284**(5416): 958-61.

Iben, S., Tschochner, H., Bier, M., Hoogstraten, D., Hozak, P., Egly, J. M. and Grummt, I. (2002). *TFIIH plays an essential role in RNA polymerase I transcription*. Cell **109**(3): 297-306.

Jakob, B., Scholz, M. and Taucher-Scholz, G. (2003). *Biological imaging of heavy charged-particle tracks.* Radiat Res **159**(5): 676-84.

Jiricny, J. (2006).*The multifaceted mismatch-repair system*. Nat Rev Mol Cell Biol **7**(5): 335-46.

Katsumi, S., Kobayashi, N., Imoto, K., Nakagawa, A., Yamashina, Y., Muramatsu, T., Shirai, T., Miyagawa, S., Sugiura, S., Hanaoka, F., Matsunaga, T., Nikaido, O. and Mori, T. (2001). *In situ visualization of ultraviolet-light-induced DNA damage repair in locally irradiated human fibroblasts*. J Invest Dermatol **117**(5): 1156-61.

Kim, S. T., Xu, B. and Kastan, M.B. (2002). *Involvement of the cohesin protein, Smc1, in Atm-dependent and independent responses to DNA damage*. Genes Dev **16**(5): 560-70.

Kusumoto, R., Masutani, C., Sugasawa, K., Iwai, S., Araki, M., Uchida, A., Mizukoshi, T. and Hanaoka, F. (2001). *Diversity of the damage recognition step in the global genomic nucleotide excision repair in vitro*. Mutat Res **485**(3): 219-27.

Kunkel, T.A. and Erie, D.A. (2005). *DNA mismatch repair.* Annu Rev Biochem **74**: 681-710.

Laine, J. P. and Egly, J.M. (2006*). Initiation of DNA repair mediated by a stalled RNA polymerase II*." Embo J **25**(2): 387-97.

Lan, L., Nakajima, S., Oohata, Y., Takao, M., Okano, S., Masutani, M., Wilson, S.H. and Yasui, A. (2004). *In situ analysis of repair processes for oxidative DNA damage in mammalian cells.* Proc Natl Acad Sci U S A **101**(38): 13738-43.

Lee, S.E., Moore, J.K., Holmes, A., Umezu, K., Kolodner, R.D. and Haber, J.E. (1998). *Saccharomyces Ku70, mre11/rad50 and RPA proteins regulate adaptation to G2/M arrest after DNA damage.* Cell **94**(3): 399-409.

Lee, J., Kumagai, A. and Dunphy W.G. (2003). *Claspin, a Chk1-regulatory protein, monitors DNA replication on chromatin independently of RPA, ATR, and Rad17*. Mol Cell **11**(2): 329-40.

Lee, J. H. and Paull, T.T. (2005). *ATM activation by DNA double-strand breaks through the Mre11-Rad50-Nbs1 complex*. Science **308**(5721): 551-4.

Lee, J., Kumagai, A. and Dunphy, W. G. (2007). *The Rad9-Hus1-Rad1 checkpoint clamp regulates interaction of TopBP1 with ATR*. J Biol Chem **282**(38): 28036-44.

Li, L., Peterson, CA., Zhang, X. And Legerski, R.J. (2000). *Requirement for PCNA and RPA in interstrand crosslink-induced DNA synthesis.* Nucleic Acids Res **28**(6): 1424-7.

Lisby, M., Barlow, J.H., Burgess, R.C. and Rothstein, R. (2004). *Choreography of the DNA damage response: spatiotemporal relationships among checkpoint and repair proteins.*Cell **118**(6): 699-713.

Lisby, M. and Rothstein, R. (2009). *Choreography of recombination proteins during the DNA damage response.* DNA Repair (Amst) **8**(9): 1068-76.

Li, G.M. (2008) *Mechanisms and functions of DNA mismatch repair* Cell Res **18**(1): 85-98.

Lindahl, T. (1993). *Instability and decay of the primary structure of DNA*. Nature **362**(6422): 709-15.

Lukas, C., Falck, J., Bartkova, J., Bartek, J. and Lukas, J. (2003). *Distinct spatiotemporal dynamics of mammalian checkpoint regulators induced by DNA damage*. Nat Cell Biol **5**(3): 255-60.

Ma, Y., Pannicke, U., Schwarz, K., Lieber, M. R. (2002). *Hairpin opening and overhang processing by an Artemis/DNA-dependent protein kinase complex in nonhomologous end joining and V(D)J recombination.* Cell **108**(6): 781-94.

Magana-Schwencke, N., Henriques, J.A., Chanet, R. and Moustacchi, E.(1982). *The fate of 8-methoxypsoralen photoinduced crosslinks in nuclear and mitochondrial yeast DNA: comparison of wild-type and repair-deficient strains.* Proc Natl Acad Sci USA **79**(6): 1722-6.

Mahaney, BL., Meek, K and Lees-Miller,SP (2009)*Repair of ionizing radiation-induced DNA double-strand breaks by non-homologous end-joining* Biochem J **417**(3): 639-50

Mailand, N., Falck, J., Lukas, C., Syljuasen, R.G., Welcker, M., Bartek, J. and Lukas, J. (2000). *Rapid destruction of human Cdc25A in response to DNA damage*. Science **288**(5470): 1425-9.

Maillard, O., Solyom, S., Naegeli, H. (2007). *An aromatic sensor with aversion to damaged strands confers versatility to DNA repair.* PLoS Biol **5**(4): e79.

Mari, P.O., Florea, B.I., Persengiev, S.P., Verkaik, N.S., Bruggenwirth, H.T., Modesti, M., Giglia-Mari, G., Bezstarosti, K., Demmers, J.A., Luider, T.M., Houtsmuller, A. B. and van Gent, D. C. (2006). *Dynamic assembly of end-joining complexes requires interaction between Ku70/80 and XRCC4*. Proc Natl Acad Sci U S A **103**(49): 18597-602.

Matsuoka, S., Ballif, B.A., Smogorzewska, A., McDonald, E.R., 3rd, Hurov, K.E., Luo, J., Bakalarski, C.E., Zhao, Z., Solimini, N., Lerenthal, Y., Shiloh, Y., Gygi, S.P. and Elledge, S.J. (2007). ATM and ATR substrate analysis reveals extensive protein networks responsive to DNA damage. Science **316**(5828): 1160-6.

Min, J.H. and Pavletich, N.P. (2007). *Recognition of DNA damage by the Rad4 nucleotide excision repair protein.* Nature **449**(7162): 570-5.

Meldrum, R.A., Botchway, S.W., Wharton, C.W. and Hirst, G.J (2003). *Nanoscale spatial induction of ultraviolet photoproducts in cellular DNA by three-photon near-infrared absorption..* EMBO Rep **4**(12): 1144-9.

Moné, M.J., Volker, M., Nikaido, O., Mullenders, L.H., van Zeeland, A.A.,Verschure, P.J., Manders, E.M. and van Driel, R. (2001). *Local UV-induced DNA damage in cell nuclei results in local transcription inhibition*. EMBO Rep **2**(11): 1013-7.

Morris, G. F., Bischoff , J.R. and Mathews, M.B. (1996). *Transcriptional activation of the human proliferating-cell nuclear antigen promoter by p53*. Proc Natl Acad Sci U S A **93**(2): 895-9.

Moser, J., Volker, M., Kool, H., Alekseev, S., Vrieling, H., Yasui, A., van Zeeland, A.A. and Mullenders, L.H. (2005). *The UV-damaged DNA binding protein mediates efficient targeting of the nucleotide excision repair complex to UV-induced photo lesions*. DNA Repair (Amst) **4**(5): 571-82.

Mu, D., Wakasugi, M., Hsu, D.S. and Sancar, A. (1997). *Characterization of reaction intermediates of human excision repair nuclease.* J Biol Chem **272**(46): 28971-9.

Nelms, B.E., Maser, R.S., MacKay, J.F., Lagally, M.G. And Petrini, J.H. (1998). *In situ visualization of DNA double-strand break repair in human fibroblasts.* Science **280**(5363): 590-2.

Ng, J. M., Vermeulen, W., van der Horst, G.T., Bergink, S., Sugasawa, K.,Vrieling, H. and Hoeijmakers, J.H. (2003). *A novel regulation mechanism of DNA repair by damage-induced and RAD23-dependent stabilization of xeroderma pigmentosum group C protein.* Genes Dev **17**(13): 1630-45.

Niedernhofer, L.J., Lalai, A.S. AndaHoeijmakers, J.H. (2005). *Fanconi anemia (cross)linked to DNA repair.* Cell **123**(7): 1191-8.

Pandita, R.K., Sharma, G.G., Laszlo, A., Hopkins, K.M., Davey, S., Chakhparonian, M., Gupta, A., Wellinger, R.J., Zhang, J., Powell, S.N., Roti Roti, J.L., Lieberman, H.B. and Pandita, T.K. (2006). *Mammalian Rad9 plays a role in telomere stability, S-and*

G2-phase-specific cell survival, and homologous recombinational repair. Mol Cell Biol **26**(5): 1850-64.

Park, M.S., Ludwig, D.L., Stigger, E. and Lee, S.H. (1996). *Physical interaction between human RAD52 and RPA is required for homologous recombination in mammalian cells.* J Biol Chem **271**(31): 18996-9000.

Payne, A. and Chu, G. (1994). *Xeroderma pigmentosum group E binding factor recognizes a broad spectrum of DNA damage*. Mutat Res **310**(1): 89-102.

Robertson, A.B., Klungland, A., Rognes, T. and Leiros, I. (2009). *DNA repair in mammalian cells: Base excision repair: the long and short of it.* Cell Mol Life Sci **66**(6): 981-93.

Rodrigue, A., Lafrance, M., Gauthier, M.C., McDonald, D., Hendzel, M., West, S.C., Jasin, M. and Masson, J.Y. (2006). *Interplay between human DNA repair proteins at a unique double-strand break in vivo*. Embo J **25**(1): 222-31.

Schaeffer, L., Roy, R., Humbert, S., Moncollin, V., Vermeulen, W., Hoeijmakers, J.H., Chambon, P. and Egly, J.M. (1993). *DNA repair helicase: a component of BTF2 (TFIIH) basic transcription factor*. Science **260**(5104): 58-63.

Shivakumar, C.V., Brown, D.R., Deb, S. and Deb, S.P. (1995). *Wild-type human p53 transactivates the human proliferating cell nuclear antigen promoter.* Mol Cell Biol **15**(12): 6785-93.

Shimomura, O., Johnson, F.H. and Saiga, Y.1962). *Extraction, purification and properties of aequorin, a bioluminescent protein from the luminous hydromedusan, Aequorea.* J Cell Comp Physiol **59**: 223-39.

Soutoglou, E., Dorn, J.F. Sengupta, K., Jasin, M., Nussenzweig, A., Ried, T., Danuser, G. and Misteli, T. (2007). *Positional stability of single double-strand breaks in mammalian cells.* Nat Cell Biol **9**(6): 675-82.

Soutoglou, E. and Misteli, T. (2008*). Activation of the cellular DNA damage response in the absence of DNA lesions.* Science **320**(5882): 1507-10.

Sugasawa, K., Ng, J.M., Masutani, C., Maekawa, T., Uchida, A., van der Spek, P.J., Eker, A.P., Rademakers, S., Visser, C., Aboussekhra, A., Wood, R.D., Hanaoka, F., Bootsma, D. and Hoeijmakers, J. H. (1997). *Two human homologs of Rad23 are functionally interchangeable in complex formation and stimulation of XPC repair activity.* Mol Cell Biol **17**(12): 6924-31.

Sugasawa, K., Ng, J.M., Masutani, C., Iwai, S., van der Spek, P.J., Eker, A.P., Hanaoka, F., Bootsma, D. and Hoeijmakers, J.H. (1998). *Xeroderma pigmentosum group C protein complex is the initiator of global genome nucleotide excision repair*. Mol Cell **2**(2): 223-32.

Sugasawa, K., Okamoto, T., Shimizu, Y., Masutani, C., Iwai, S. and Hanaoka, F. (2001). *A multistep damage recognition mechanism for global genomic nucleotide excision repair.* Genes Dev **15**(5): 507-21.

Sugasawa, K., Okuda, Y., Saijo, M., Nishi, R., Matsuda, N., Chu, G., Mori, T., Iwai, S., Tanaka, K.,Tanaka, K. and Hanaoka, F. (2005). *UV-induced ubiquitylation of XPC protein mediated by UV-DDB-ubiquitin ligase complex.* Cell **121**(3): 387-400.

Sugasawa, K. and Hanaoka, F. (2007). *Sensing of DNA damage by XPC/Rad4: one protein for many lesions.* Nat Struct Mol Biol **14**(10): 887-8.

Sun, Y., Jiang, X., Chen, S., Fernandes, N. and Price, B.D. (2005). *A role for the Tip60 histone acetyltransferase in the acetylation and activation of ATM*. Proc Natl Acad Sci U S A **102**(37): 13182-7.

Sung, P. and Klein, H. (2006). *Mechanism of homologous recombination: mediators and helicases take on regulatory functions*. Nat Rev Mol Cell Biol **7**(10): 739-50.

Tang, J. and Chu, G. (2002). *Xeroderma pigmentosum complementation group E and UV-damaged DNA-binding protein*. DNA Repair (Amst) **1**(8): 601-16.

Tashiro, S., Walter, J., Shinohara, A., Kamada, N. and Cremer, T. (2000). *Rad51 accumulation at sites of DNA damage and in postreplicative chromatin*. J Cell Biol **150**(2): 283-91.

Tauchi, H., Kobayashi, J., Morishima, K., van Gent, D.C., Shiraishi, T., Verkaik, N.S., vanHeems, D., Ito, E., Nakamura, A., Sonoda, E., Takata, M., Takeda, S., Matsuura, S. and Komatsu, K. (2002). *Nbs1 is essential for DNA repair by homologous recombination in higher vertebrate cells.* Nature **420**(6911): 93-8.

Tsien, R. Y. and Miyawaki, A. (1998). *Seeing the machinery of live cells.* Science **280**(5371): 1954-5.

Tsurimoto, T. and B. Stillman (1991). *Replication factors required for SV40 DNA replication in vitro. I. DNA structure-specific recognition of a primer-template junction by eukaryotic DNA polymerases and their accessory proteins.* J Biol Chem **266**(3): 1950-60.

van den Boom, V., Citterio, E., Hoogstraten, D., Zotter, A., Egly, J.M., van Cappellen, W.A., Hoeijmakers, J.H., Houtsmuller, A.B. and Vermeulen, W. (2004). *DNA damage stabilizes interaction of CSB with the transcription elongation machinery*. J Cell Biol **166**(1): 27-36.

Venclovas, C. and Thelen, M.P. (2000). *Structure-based predictions of Rad1, Rad9, Hus1 and Rad17 participation in sliding clamp and clamp-loading complexes*. Nucleic Acids Res **28**(13): 2481-93.

Venema, Bartosova, Z., Natarajan, A.T., van Zeeland, A.A., Mullenders, L.H. (1992). *Transcription affects the rate but not the extent of repair of cyclobutane pyrimidine dimers in the human adenosine deaminase gene*. J Biol Chem **267**(13): 8852-6.

Vilenchik, M.M. and Knudson, A.G. (2003). *Endogenous DNA double-strand breaks: production, fidelity of repair, and induction of cancer*. Proc Natl Acad Sci U S A **100**(22): 12871-6.

Villartay, J.P. and Revy, P. (2006). *Cernunnos, a novel nonhomologous end-joining factor, is mutated in human immunodeficiency with microcephaly*. Cell **124**(2): 287-99.

Volker, M., Moné, M.J., Karmakar, P., van Hoffen, A., Schul, W., Vermeulen, W., Hoeijmakers, J.H., van Driel, R., van Zeeland, A.A. and Mullenders, L. H. (2001*). Sequential assembly of the nucleotide excision repair factors in vivo.* Mol Cell **8**(1): 213-24.

Walker, J.R., Corpina, R.A. and Goldberg, J (2001) *Structure of the Ku heterodimer bound to DNA and its implications for double-strand break repair*. Nature **412**(6847): 607-14

Wang, W., Brandt, P., Rossi, M.L., Lindsey-Boltz, L., Podust, V., Fanning, E., Sancar, A. and Bambara, R.A. (2004). *The human Rad9-Rad1-Hus1 checkpoint complex stimulates flap endonuclease 1.* Proc Natl Acad Sci U S A **101**(48): 16762-7

Wang, Q.E., Zhu, Q., Wani, G., El-Mahdy, M.A., Li, J.and Wani, A.A. (2005). *DNA repair factor XPC is modified by SUMO-1 and ubiquitin following UV irradiation.* Nucleic Acids Res **33**(13): 4023-34.

Wang, X., Hu, B., Weiss, R.S. and Wang, Y. (2006). *The effect of Hus1 on ionizing radiation sensitivity is associated with homologous recombination repair but is independent of nonhomologous end-joining.* Oncogene **25**(13): 1980-3.

Wang, X., Zou, L., Lu, T., Bao, S., Hurov, K.E., Hittelman, W.N., Elledge, S.J. and Li, L. (2006). *Rad17 phosphorylation is required for claspin recruitment and Chk1 activation in response to replication stress.* Mol Cell **23**(3): 331-41.

Wu, X., Ranganathan, V., Weisman, D.S., Heine, W.F., Ciccone, D.N., O'Neill, T.B., Crick, K.E., Pierce, K.A., Lane, W.S., Rathbun, G., Livingston, D.M. and Weaver, D.T. (2000). *ATM phosphorylation of Nijmegen breakage syndrome protein is required in a DNA damage response*. Nature **405** (6785): 477-82.

Xiong, Y., Zhang, H. and Beach, D. (1992*). D type cyclins associate with multiple protein kinases and the DNA replication and repair factor PCNA*. Cell **71**(3): 505-14.

Yokoi, M., Masutani, C., Maekawa, T., Sugasawa, K.. Ohkuma, Y. and Hanaoka, F. *The xeroderma pigmentosum group C protein complex XPC-HR23B plays an important role in the recruitment of transcription factor IIH to damaged DNA*. J Biol Chem **275**(13): 9870-5.

Zhang, N., Lu, X. and Legerski, R.J.(2003). *Partial reconstitution of human interstrand cross-link repair in vitro: characterization of the roles of RPA and PCNA*. Biochem Biophys Res Commun **309**(1): 71-8.

Zhou, B. B. and Elledge, S.J. (2000). The DNA damage response: putting checkpoints in perspective. Nature **408**(6811): 433-9.

Zou, L., Cortez, D. and Elledge, S.J. (2002). *Regulation of ATR substrate selection by Rad17-dependent loading of Rad9 complexes onto chromatin*. Genes Dev **16**(2): 198-208

Zou, L. and Elledge, S.J. (2003). *Sensing DNA damage through ATRIP recognition of RPA-ssDNA complexes.* Science **300**(5625): 1542-8.

Friedberg , E.C, Walker, G.C. Siede, W. , Wood, R.D., Schultz, R.A. and Ellenberger, G. DNA Repair and Mutagenesis, Second Edition, ASM Press 2005

Chapter 2

~

Replication

of undamaged

and damaged DNA

Contents of chapter 2

3. Replication over damaged DNA

3.1. Triggering post-replication repair processes: the role of PCNA ubiquitination

3.2. Translesion Synthesis

Family of specialized Translesion Synthesis DNA polymerases.
Switching from the replicative to the TLS polymerase
TLS polymerase choice
Regulation of PCNA ubiquitination

3.3. Recombination-associated processes

Homologous recombination during S-phase, an error-free pathway
Recombinational events and PCNA poly-ubiquitination

4. Discussion and future perspectives

Interplay between TLS, HR, NER and the cell cycle checkpoints

Focus on the repair synthesis step of NER

1. Replication of undamaged DNA

1.1. Basic principles of the replication process

DNA replication requires extreme precision and specificity; hence, its timing and frequency must be tightly controlled by regulatory factors. In bacteria, the whole genome is replicated from a single replication point or replication origin. By contrast, eukaryotic chromosomes contain multiple origins that must fire once during each cell division, thus demanding a tight coordination. DNA replication is initiated by the formation of a pre-replication complex at the origins during G1. Subsequently, activation of the origin by at least two kinases triggers the transition to actual DNA replication during S phase, which involves the ordered assembly of replication factors that allow DNA unwinding and loading of several DNA polymerases for the further elongation step.

Replication initiation

Origin activation starts with origin licensing, i.e. the assembly, on replication origins, of initiator proteins, forming the pre-replication complexes (pre-RC) [Diffley et al, 1994]. Origin licensing occurs during late mitosis and early G1 while the CDKs, the downstream players of cell cycle progression, are still inactive. The first initiator which selects the sites for subsequent initiation of replication is the six-subunit ATPase complex ORC (Origin Recognition Complex) [reviewed in Bell and Stillman, 1992; Bell and Dutta, 2002]. Two other factors, CDC6 and Cdt1 (CDC10-dependent transcript 1), are then required for the key step in pre-RC assembly, i.e. the loading of the six MCM2-7 (Mini-Chromosome Maintenance) proteins. Once the MCM proteins have been loaded, ORC and CDC6 are removed from the chromatin without preventing subsequent replication. Displacement of Cdt1 from MCM2-7 may be triggered by MCM10 (see below). The current hypothesis is that the MCM2-7 complex serves as DNA helicase to open the DNA ahead of the replication machinery [as reviewed in Bell and Dutta, 2002].

All origins are licensed approximately synchronously, but origin firing (the conversion of pre-RC into replication forks) occurs in a temporally regulated manner during S phase, which makes it possible to distinguish early- and late-firing origins [Zou and Stillman 1998]. This replication timing correlates with the local chromatin environment: early replicating origins tend to be associated with transcriptionally active euchromatic regions, while late replicating origins associate with transcriptionally repressed genes in heterochromatin [Diller et al, 1994; Friedman et al, 1996].

The further assembly of MCM10 and Cdc45 requires the control of the CDK and DDK (Dbf4-dependent Cdc7 kinase) kinases. Subsequent origin unwinding requires both the presence of Cdc45 and of MCM2-7, as well as stabilization of the created ssDNA by RPA

[Walter and Newport, 2000]. Cdc45, as well as *S. cerevisiae* Dpb11 (mammalian TOPBP1) are at last required for further recruitment of the DNA polymerases [Masumoto et al, 2000].

Importantly, each part of the genome needs to be replicated once and only once. Control of a sole and unique replicating event is achieved via several mechanisms. CDKs have a dual role, including a regulatory one: elevated levels of CDKs allow the activation of origins upon entry into S phase but they also ensure that origin licensing cannot occur again during the S, G2 and M phases. Moreover, together with geminin, CDKs regulate the DNA binding and degradation of the different pre-RC components, ensuring that origin activation does not occur twice. Soon after initiation the replication-licensing factor Cdt1 is degraded, which also prevents re-initiation of replication. This degradation occurs via poly-ubiquitination by the Cul40-DDB1-Roc1 complex. Although Cdt1 binds DDB1 directly, poly-ubiquitination is initiated by the binding of Cdt to PCNA [Arias and Walter, 2006; Senga et al, 2006]. Cdt1 is also a target of geminin.

The actual *de novo* synthesis of DNA catalyzed by the DNA polymerases (see below) first requires the synthesis of an RNA primer, as DNA polymerases need base-pared duplex DNA to start synthesis. The initial RNA primer production is catalyzed by the DNA polymerase α/primase complex that consists of four subunits: p180 is responsible for the DNA polymerase activity, p70 may tether the complex to Cdc45 and the RNA-primase activity is achieved by the p48 and p58 proteins [Lehman and Kaguni, 1989]. It synthesizes short RNA/DNA primers of ~12 RNA nucleotides and ~ 20 DNA nucleotides [Conaway and Lehman, 1982]. The ssDNA binding protein RPA represents an auxiliary factor that stabilizes this polα/primase complex and enhances fidelity [Maga et al, 2001].

Replication elongation

After unwinding, initiation occurs at the junction between ds- and ssDNA, at the so-called replication fork. DNA synthesis can only occur in the 5' to 3' direction, however both DNA strands should be duplicated, but after unwinding this can only happen on one strand. This strand, referred to as leading strand, is replicated continuously over about 5-10 kb, until the polymerase encounters the previously replicated DNA fragment. The lagging strand on the other hand is replicated in a discontinuous manner, via the formation of small DNA pieces called Okazaki fragments that are about 180-200 bp in size and are ligated. Okazaki fragments are initiated by DNA polymerase α/primase. DNA elongation is executed by the DNA polymerases δ and ε (Pol δ and Pol ε). Therefore, a so-called polymerase switch from pol α to either pol δ or pol ε is required. Recruitment and tethering of the polymerases during elongation is facilitated by the sliding clamp protein PCNA, which on its turn is loaded by the RFC complex (both PCNA and RFC are detailed below) in an ATP-dependent manner. The loading of PCNA at the 3'-OH end of the nascent DNA triggers the

displacement of pol α by one of the two elongating polymerases [Maga et al, 2000; Tsurimoto et al, 1990; Tsurimoto and Stillman, 1991].

RFC dissociates after PCNA has been loaded [Podust et al, 1998]. PCNA, together with pol δ or pol ε, forms a highly processive holoenzyme that extends the RNA-DNA primer without dissociating from the template. The presence of PCNA increases the activity and processivity of pol δ up to ~100 fold [Prelich et al, 1987]. Mammalian pol δ consists of four subunits, p12, p50, p66 and p125 that is the catalytic subunit and harbors the proofreading 3'-5' exonuclease activity [Hughes et al, 1999; Liu et al, 2000]. The human pol ε also comprises four subunits, a large catalytic one (p261) and three associated subunits (p12, p17 and p59) [Li et al, 2000]. It is also loaded by PCNA, but its processivity is not dramatically stimulated by PCNA [Eissenberg, et al, 1997].
The division of tasks between pol δ and pol ε is not clearly identified, though they do not display redundant functions, as pol δ cannot be substituted by pol ε and *vice versa* [Fukui et al, 2004; Waga and Stillman, 1998]. Additionally Pol ε interacts with proteins of the checkpoint machinery [Post et al, 2003] and could therefore be involved, on top of its function in replication, in checkpoint controlling of the replicated DNA. Similarly, DNA replication can restart downstream of a lesion at a stalled fork and this activity, dependent on PCNA, pol δ and pol ε, contributes to the phosphorylation of CHK1 and therefore to checkpoint activation [Lopes et al, 2006; Heller and Marians, 2006; Van et al, 2010].

When during lagging strand synthesis pol δ or pol ε encounters the 5'end of the RNA strand of the previously synthesized Okazaki fragment, this fragment will be displaced, forming a flap structure. RPA binds to this structure and triggers dissociation of pol δ from PCNA. Subsequently the FEN-1 endonuclease and the helicase/nuclease DNA2 are recruited to PCNA and this complex catalyzes the removal of the flap structure [Bae et al, 2000]. The resulting nick is sealed by DNA Ligase I [Hubscher and Seo, 2001]. DNA LigaseI has been shown to interact with PCNA through its PCNA Interacting Peptide (PIP) motif [Montecucco et al, 1998], as well as with RFC [Levin et al, 2004].

The multiple interactions of PCNA are regulated by CDK-mediated phosphorylation of proteins, among which are RPA, RFC, FEN-1, Ligase I and possibly also pol δ. Hence, phosphorylation appears very important in controlling DNA replication by sequentially disrupting the interactions between PCNA and replication proteins: (*i*) CDKs inhibit the activity of pol α; (*ii*) the calmodulin-dependent protein kinase II (CAMKII) and CDKs act together to dissociate the pol δ holoenzyme from DNA; (*iii*) CAMKII and the CDKs disrupt the interactions between FEN1, Ligase 1 and PCNA, which ends the lagging strand processing; (*iv*) RPA phosphorylation triggers its dissociation from DNA [Henneke et al, 2003; Xiong et al, 1992].

DNA replication and chromatin assembly

During DNA replication, parental nucleosomes ahead of the replication fork are transiently disrupted and the corresponding histones redistributed onto daughter DNA behind the fork [Gruss et al, 1993]. On top of this, newly synthesized histones must be deposited to obtain the full nucleosome complement on the nascent DNA [Verreault, 2000]. This process occurs in two steps, with a first deposition of H3-H4 that is followed by H2A-H2B. Histones are escorted by chaperones from their sites of synthesis up to their delivery sites for nucleosome assembly [Mello et al, 2001]. The heterotrimeric complex CAF-1 is one of these chaperones and delivers histones H3 and H4 to replicating DNA during S phase [Smith and Stillman, 1989]. This complex contains three subunits (p150, p60 and p48). CAF-1 is targeted to replication sites through the interaction of the large subunit with PCNA, via its two PIP domains [Rolef Ben-Shahar et al, 2009; Zhang et al, 2000]. More specifically, the kinase Cdc7-Dbf4 promotes the interaction of the p150 subunit of CAF-1 with PCNA [Gerard et al, 2006]. Interestingly, one histone chaperone that has the potential to remove H3/H4 from replicating chromatin, Asf1 (anti-silencing function), has been shown to interact in yeast with RFC [Franco et al, 2005].

Replication foci

Eukaryotic chromosomal DNA replication is divided into hundreds to thousands of independent subunits of replication called replicons. Moreover, adjacent origins of replication throughout a chromosomal region are activated synchronously during the S phase of the cell cycle [Hand, 1978]. Immunofluorescence microscopy experiments using incorporated biotin-labeled dUTP or BrdU showed that in mammalian cells, newly synthesized DNA localizes to discrete and numerous subnuclear sites known as replication foci [Nakayasu and Berezney, 1989; Nakamura et al, 1986; O'Keefe et al, 1992]. These studies altogether have revealed that replication occurs within replication foci which represent clusters of replicons that are co-ordinately processed. These structures are found in species ranging from mammals to plants [Philimonenko et al, 2004].

The location, number and size of the replication foci vary throughout S-phase. The number of foci can rise up to ~ 1000 [Jackson and Pombo, 1998]. Three distinct replication patterns are distinguished, that correspond to DNA synthesis in early to mid-S phase, mid to late S-phase and very late S-phase (Nakayasu and Berezney, 1989]. Early small and discrete S-phase foci are located over the extranucleolar euchromatic regions and correspond to the replication of transcribed genes. Mid-S phase foci are concentrated over the perinucleolar and perinuclear heterochromatic regions. Late S-phase foci, larger and less numerous, coincide also with the replication of the silent heterochromatic regions [O'Keefe et al, 1992]. It has been estimated that in early S-phase in a human cell, the average number of replication forks in a focus ranges from five to forty [Jackson and Pombo, 1998; Newport

and Yan, 1996; Hozak et al, 1993], while late S-phase foci may cluster hundreds of replicons [Frouin, et al, 2003].

Replication foci or replisomes are "mega-complexes" that contain large amounts of DNA polymerases and other replication factors (PCNA, RPA, DNA polymerases α and ε, DNA Ligase I, CAF 1) as well as a growing list of cell cycle control factors (Cdk2/cyclinA, MRE11 etc) and TLS polymerases (DNA polymerases η and ι) [Tubo and Berezney, 1987; Cook, 1999; Frouin et al, 2003]. Early and late foci do not only differ in size but also in protein composition.

A fundamental issue concerning replication foci is whether the DNA synthesis results from motion of the replication machinery along the DNA, or from spooling of the DNA through replication factories. First, it was suggested that the newly replicated DNA moves away from the replication sites [Manders et al, 1992] and evidence was provided, which suggests that DNA polymerases are immobile, in favor of the spooling hypothesis (Kitamura et al, 2006 and reviewed in Cook, 1999). Additional studies using GFP-tagged PCNA as a marker for replication factories, lead to the model that replication factories are stably anchored in the nucleus and that changes in the focal pattern throughout S-phase occur via a gradual and coordinated assembly and disassembly of these factories in an asynchronous manner [Leonhardt et al, 2000]. Hence, larger late S-phase replication factories may not originate from a coalescence of several small factories, but are assembled *de novo.* The transition from earlier to later replicons occurs by the dissociation of PCNA into a nucleoplasmic pool, followed by a reassembly at newly activated sites [Sporbert et al, 2002; Essers et al, 2005]. The finding that new replication foci assemble *de novo* at sites that are located next to the previous cluster of origins rejects a sliding or jumping of the replication machinery to the next origins cluster and argues for an indirect mechanism of origin activation, known as "domino model". This model is in opposition with the "clock model" that suggests that origins are activated according to a specific program [Goren and Cedar, 2003].

Currently the actual trigger for the formation of the replication focus is unknown. It is possible that foci formation triggers the assembly of replication factories. Early studies on *Xenopus* extracts have revealed that the clustered organization of DNA into foci may be an early replication event which occurs prior to the activation of the kinase activity of Cdk2 at the G1-S transition, also suggesting that this focal formation may correspond to a stable, higher order chromatin state [Newport and Yan, 1996].
It is probably more likely, however, that the activation of the replication process itself at certain loci is fundamental for the formation of these structures. Depositions of proteins at replication initiation sites that have an intrinsic affinity for a number of replication-associated factors are, in this scenario, likely candidates to be fundamental for focus formation. One of these proteins could be PCNA, since a short sequence of homology, called the Replication Factory Targeting Sequence (RFTS), that targets proteins to

replication factories, is for a lot of replication factors the binding site for PCNA [Frouin et al, 2003; Chuang et al, 1997; Montecucco et al, 2001]. Besides, Foci-Forming Activity-1 (FFA-1), a 170 kDa protein and orthologue of the human WRN protein (Werner Syndrome), was reported to have a role in foci formation through its interaction with RPA [Yan et al, 1998; Yan and Newport, 1995].

Sub-cellular localization of replication factors during DNA replication

Immunofluorescence studies associated with live cell studies have shown that the replication factors PCNA, RFC and RPA accumulate at replication foci. Immunofluorescence staining of PCNA has revealed the very typical early, mid and late S-phase patterns [Celis and Celis, 1985] that were further confirmed by live cell studies using a GFP-tagged version of the protein [Chapter 5, this thesis; Leonhardt et al 2000; Somanathan et al, 2001; Essers et al, 2005]. Live cell imaging of GFP-tagged Replication Factor C showed that this protein also presents these characteristic S-phase focal patterns [Chapter 5, this thesis]. Interestingly, RPA also accumulates in replication foci, but this accumulation is only visible using immunofluorescence of fixed cells [Murti et al, 1996] or upon addition of replication inhibitors such as HU/AraC [Chapter 5] or aphidicolin. Treatment of cells by aphidicolin specifically inhibits DNA pol α and DNA pol δ; in these conditions, the accumulation of RPA34 increased at replication foci, suggesting an inhibition of replication fork progression, thereby creating long patches of ssDNA covered with RPA34 [Görisch et al, 2008]. These results confirm that while RPA is certainly present in replication foci, its interactions with the DNA and/or various replication factors are very transient [see below and Chapters 5 and 6].

Dynamics of replication factors at sites of replication

The dynamics of replication factors at replication foci was studied using tagged versions of the proteins. Several reports showed altogether that there is a turn-over of PCNA at sites of replication, even if the protein remains associated with the replication factory for around three minutes [Chapter 5, this thesis; Solomon et al, 2004; Essers et al, 2005; Sporbert et al, 2002]. This has led to the model that the clamp is being re-used for consecutive rounds of Okazaki fragment synthesis [Essers et al, 2005; Sporbert et al 2002]. Besides, a model has been proposed, that favors two pools of PCNA within a single focus, one directly engaged in DNA replication, and another recruiting a reserve of replication factors within the vicinity of active replicons [Frouin et al, 2003]. In this case, it is plausible that many replication factors may be recruited via their interaction with PCNA, but may not be actively involved in replication processes; in this model referred to as “be ready-for” the factors are in close proximity and are incorporated into functional units only when required.

On the contrary, studies on the dynamics of RFC have shown that the clamp loader RFC interacts very transiently with sites of DNA replication [Chapter 4]. This can be explained by the fact that dissociation of RFC from PCNA is necessary for interaction of PCNA with the DNA polymerase [Podust et al, 1998]. Hence, the clamp loader continuously associates and dissociates to and from replication sites. The localization of replication factors into the vicinity of replication factories, however, may ensure that the protein could be recruited easily for subsequent loading and/or unloading of PCNA.

A transient binding of RPA (that exchanges in seconds and completely redistributes in 1 minute) at sites of DNA replication was observed [Chapter 5, this thesis; Görisch et al, 2008; Sporbert et al, 2002]. It can be explained by the fact that RPA must rapidly coat ssDNA but is also displaced by the DNA polymerase [Hübscher and Seo, 2001]. Hence, RPA is continuously binding and dissociating from ssDNA patches.

1.2. Properties of the replication factors PCNA, RFC and RPA

Clamps and clamp loaders

Functional and structural analyses show that the architecture and mechanisms of clamps and clamp loaders are conserved across the three domains of life. All sliding clamps are circular structures with a sixfold symmetry that are wide enough to accommodate double-stranded DNA [Kong et al, 1992; Moarefi et al, 2000; Gulbis et al, 1996; Krishna et al, 1994]. Clamp loaders are multiprotein complexes of which the different subunits share high levels of sequence similarities [Miyata et al, 2005; Bowman et al, 2004; Cullman et al, 1995].

The eukaryotic sliding clamp PCNA

PCNA is involved in multiple processes, such as DNA replication, repair, cell cycle control and chromatin remodeling [reviewed in Maga and Hubscher, 2003; Warbrick, 2000; Moldovan et al, 2007]. Protein levels of PCNA fluctuate during the cell cycle with an obvious peak in S phase. It has been proposed that PCNA acts as a loading dock or scaffolding station for the more than 60 proteins implicated in these processes [Maga, Hubscher, 2003]. Most PCNA-binding proteins contain a conserved PCNA-interacting peptide or PIP box. Since this motif is generally found in the amino or carboxy termini of these proteins, it is predicted to protrude from their surface and directly make a contact with PCNA [Warbrick,, 1998; Warbrick, 2000]. A novel PCNA binding motif, termed the KA box and a conserved PCNA binding fold, dubbed APIM have also been identified [Xu et al, 2001; Gilljam et al, 2009].

Regulation of PCNA binding and activity with its numerous partners is achieved via posttranslational modifications, such as acetylation [Naryzhny and Lee, 2004], mono- or

poly-ubiquitination or sumoylation. PCNA ubiquitination on lysine 164 directs the cell towards damage tolerance mechanisms [Hoege et al, 2002; Pfander et al, 2005; Matunis, 2002], whereas sumoylation on residues K164 and K127 (in yeast *S. cerevisiae*) is supposed to suppress unwanted recombination by recruiting the helicase Srs2 that disrupts Rad51 filaments necessary for recombination [reviewed in Moldovan et al, 2007]. It is worth noting that PCNA modifications affect its binding affinities in both a positive and a negative manner: ubiquitination increases the affinity of PCNA for TLS polymerases, but on the contrary K127-dependent sumoylation exhibits repressive effects on the association with PIP-box proteins such as EXO1 [Moldovan et al, 2006].

Eukaryotic PCNA is a homotrimeric, doughnut-shaped molecule with an inner diameter of around 35Å, which is big enough to let double-stranded DNA pass through, and an external diameter of around 80Å [Ellison et al, 2001; Krishna et al, 1994]. Although the surface of the PCNA ring is very acidic, the inner surface is positively charged due to the presence of several lysine and arginine residues, which implies that the negatively charged DNA can pass through the ring without any electrostatic repulsion.

PCNA presents two distinct sides, a "front" side (C'-terminus side or outer surface) and a "back" side. Most PCNA-binding proteins associate with PCNA through the center loop and the inter-domain connecting loop located on the front side. Intriguingly, a recent study has shown that ubiquitin moieties are located on the back face of ubiquitinated PCNA [Freudenthal et al, 2010]. This raises a very interesting issue: do proteins assemble simultaneously or in a sequential manner to the three PCNA subunits? The answer to this question is crucial in understanding the regulation of Translesion Synthesis and will be discussed in the section dedicated to this process.

The eukaryotic clamp loader Replication Factor C

The PCNA homo-trimer is a closed ring in solution. To get loaded around the DNA, PCNA needs to be opened, a task achieved by RFC (Replication Factor C) or RFC-like complexes. RFC is a five subunit complex containing RFCp140, RFCp36, RFCp37, RFC p38 and RFCp40 (representing the protein sizes) and belongs to the AAA^+ family of ATPases that contains characteristic ATP-binding/hydrolysis motifs and converts the chemical energy derived from ATP binding and hydrolysis to mechanic force that is required for clamp loading [Cullman et al, 1995]. RFC can bind at a template-primer junction by covering fifteen bases of the primer DNA from the 3' end and twenty bases of the template [Tsurimoto et al, 1990] and load PCNA onto the DNA in an absolute ATP-dependent fashion.

The small subunits share strikingly conserved sequence similarities defined as seven regions (boxes II-VIII) that are also found in the large RFC subunit. Box II, IV and VI contain an

ATP/GTP binding region, while Box III contains the most conserved motif, a phosphate-binding loop [Mossi and Hubscher, 1998].

The C-terminus of RFCp140 contains a region essential for DNA binding at the 3' terminus of a primer-template junction [Uhlmann et al, 1997]. Box I, at the N-terminus of RFCp140 harbors a "BRCT"-domain, this motif is present in a superfamily of proteins mainly involved in DNA damage-response [Cullman et al, 1995; Bork et al, 1997]. This BRCT domain displays a clear DNA-binding activity with an unusual specificity for 5'-phosphorylated double-stranded DNA termini [Uhlmann et al, 1997; Allen, et al 1998]. Recruitment of RFCp140 to RFC only occurs after the formation of the core-complex between the four smaller subunits [Podust et al, 1997; Uhlmann et al, 1996]. Phosphorylation of RFCp1 [Koundrioukoff et al, 2000; Salles-Passador et al, 2003; Munshi et al, 2003] leads to its dissociation from this core complex and might play a regulatory role in destabilizing the replicative RFC-complex and facilitating the replacement of RFCp140 by one of its related proteins.

Three RFC1-related proteins are present in eukaryotes: Rad17, Ctf18 and Elg1 [Majka and Burgers 2004], which can replace RFC1 in the heteropentameric complex. Rad17-RFC acts concomitantly with the 9-1-1 complex in checkpoint signaling [chapter 1]. Ctf18-RFC is able to load PCNA in an ATP-dependent manner *in vitro* [Shiomi et al, 2004]. It associates with two additional subunits, Ddc1 and Ctf8, to form a heptameric complex that stimulates pol δ activity on a circular template [Bermudez et al, 2003; Shiomi et al, 2007]. This complex is also essential for sister chromatid cohesion in yeast, together with another protein, Ctf7 [Mayer et al, 2001; Skibbens et al, 1999]. Very recent studies have shown as well that Ctf18 may be involved in recruiting pol ε at sites of NER [Ogi et al, 2010].
Elg1-RFC also interacts with PCNA and is involved in genome maintenance [Bellaoui et al, 2003; Ben-Aroya et al, 2003; Kanellis et al, 2003]. Several studies have revealed possible roles of Elg1-RFC in the stabilization or restart of stalled replication forks, in lagging strand DNA synthesis and/or Okazaki fragment processing [reviewed in Kim and MacNeill, 2003], in sister chromatid cohesion [Maradeo et al, 2009; Parnas et al, 2009], in telomere maintenance [Smolikov et al, 2004] and in double strand break repair [Ogiwara et al, 2006].

Interactions between RFC and PCNA

Two PCNA-interacting domains have been identified on RFCp140, one in a domain that is also conserved between the smaller subunits [Fotedar et al, 1996 and Uhlmann et al, 1996] and another PIP domain located at the N-terminus [Mossi and Hubscher, 1998].
The structure of the RFC/PCNA complex has revealed that interactions between RFC and PCNA occur via the p38 and p140 RFC subunits [Bowman et al, 2004]. However further studies showed that RFC displays more associations with PCNA. The RFCp140 subunit makes a major contact with PCNA but is not required for clamp opening [Yao et al, 2006]. In the absence of ATP, RFC has a closed two-finger structure also called U-form that is able

to hold PCNA. Upon addition of ATP, RFC opens up to a C-form. This triggers the opening of PCNA that can then encircle the DNA [Shiomi et al, 2000].

RFC induction of the polymerase switch is phosphorylation dependent: CAMKII phosphorylates the PCNA binding region of RFC p140 *in vitro*, thus blocking the PCNA-RFC interaction [Maga and Hubscher, 1997].

A key feature that is still under debate concerns the unloading of PCNA from DNA. In model loading/unloading systems, human RFC is able to unload PCNA from template-primer DNA in an ATP-dependent reaction [Cai et al, 1996; Yao et al, 1996; Yao et al, 2006]. However, several RFC-like complexes could also support this function in replication and repair. Both Ctf18-RFC and Rad17-RFC are able to remove PCNA from DNA [Bylund and Burgers, 2005; Yao et al, 2006]. Ctf18 is involved in cohesion and may therefore be able to unload PCNA from cohesion proteins. In addition, the recently identified Ctf18 recruitment to NER-sites suggests a role in PCNA unloading after the DNA synthesis step has been completed [Ogi et al, 2010]. By contrast, yeast genetic data link Elg1 to replication, implying that Elg1-RFC might be involved in PCNA unloading during replication or repair.

Replication Protein A, an essential ss-DNA binding protein

Single-stranded DNA (ssDNA) is a ubiquitous and important reaction intermediate in different DNA-transacting processes to allow the assembly of the multiprotein complexes. However, it is also a very vulnerable structure, since it can then be degraded or disrupted in many fashions by chemicals, metabolic reactions and endonucleases. Replication Protein A is a crucial factor in maintaining and protecting the integrity of ss-DNA and is therefore involved in DNA replication, DNA repair, DNA recombination, cell cycle control and telomere maintenance processes. This eukaryotic heterotrimer comprises three subunits RPA70, RPA32 and RPA14 (that represent the respective protein sizes).

RPA binds ssDNA, with a 5' to 3' polarity and has around three times higher affinity for ssDNA than for dsDNA [Wold, 1997; de Laat et al, 1998; Kim et al, 1992].
The central structural and functional element of RPA is the oligosaccharide/oligonucleotide binding fold (OB-fold). RPA70 contains four OB-folds called DBD-A, DBD-B, DBD-C and DBD-F (for DNA-binding domain), while RPA32 and RPA14 contain DBD-D and DBD-E, respectively [Gomes et al, 1996]. The major ssDNA binding affinity is localized in the tandem DBD-A/DBD-B of RPA70. RPA presents two modes of binding that may underlie its ability to unwind DNA [Blackwell et al, 1994]. First, the binding is initiated by an interaction of DBD-A and DBD-B with 8-10 nucleotide at the 5'side of ssDNA [Bochkarev et al, 1997]. The additional participation of DBD-C leads to a more stable intermediate binding of a 13-22 nucleotide strand [Brill, et al, 1998]. Finally, the involvement of DBD-D brings RPA to cover a region of around 30 nucleotides [Kim et al, 1992; Blackwell et al,

1994]. The role of RPA14 is linked to stable formation of the trimer rather than to ssDNA binding [Wold, 1997].

RPA gets phosphorylated in a cell-cyle dependent manner on two sites at the N-terminus of RPA32. A first CDK2-kinase dependent phosphorylation event occurs at the G1/S transition [Din et al, 1990; Dutta and Stillman, 1992]. This leads to inhibition of Simian virus 40 DNA replication *in vitro* [Pan et al, 1995]. RPA32 is also phosphorylated by CDK1-cyclinA and CDK1-cyclinB in late S phase, which leads to dissociation of the RPA trimer [Treuner et al, 1999].

RPA32 also undergoes hyperphosphorylation in response to different damaging agents such as UV [Carty et al, 1994], IR [Liu et al, 1993] or hydroxyurea in a much more extensive fashion since nine phosphorylation sites have been discovered so far [reviewed in Zou et al, 2006]. Several lines of evidence have shown that RPA gets hyperphosphorylated by different members of the PIKKS family such as DNA-PK [Boubnov et al, 1995] and ATM [Oakley et al, 2001; Cruet-Hennequart et al, 2006]. It is known that hyperphosphorylation diminishes the role of RPA in replication by preventing its association with replication centers [Vassin et al, 2004]. Since these kinases are involved in initiation of DNA damage checkpoints, RPA hyperphosphorylation might represent a mechanism to direct RPA towards the cellular activities controlled by these checkpoints proteins in response to different genetic stresses.

2. Replication factors in DNA damage response

2.1. Replication factors and repair processes

Base Excision Repair

Base Excision DNA synthesis and ligation in BER can be achieved by XRCC1-mediated short-patch repair (as described in Chapter 1) or by long-patch repair. Long-patch repair is carried out by PCNA, pol β or pol δ/ε and is followed by cleavage of the displaced strand by the Flap-Endonuclease 1 (FEN-1) and a final nick-sealing step by DNA Ligase I. It is worth noting that in short-patch BER, ligation is performed by XRCC1-LigIII. PCNA coordinates the enzymatic activities of pol δ/ε, FEN-1 and DNA Ligase I [Dianov et al, 1999; Gary et al, 1999; Tom et al, 2000; Levin et al, 2000; Tom et al, 2001]. Recently RFC was found to stimulate FEN-1 [Cho et al, 2009].
Interestingly, PCNA is involved in different stages of the BER process, starting before DNA synthesis where it interacts with APE-1 [Dianova et al, 2001], DNA glycosylases such as UNG2 [Krokan et al, 2001] and NEIL-1 [Theriot et al, 2010], as well as with XRCC1 [Fan et al, 2004; Lan et al, 2004].
Live-cell studies using GFP-tagged proteins have showed that both RFC and PCNA accumulate upon UV-A dependent damage induction, however this technique does not

create specifically SSBs and oxidative damage and interpretation of these data should therefore be considered with caution [Hashiguchi et al, 2007].

Mismatch Repair

As one of the main functions of mismatch repair (MMR) is to correct replication inaccuracies such as mis-incorporation or nucleotide slippages, a direct connection to the replication machinery is expected. Indeed, *in vitro* reactions confirmed that PCNA, RPA, RFC, pol δ, Ligase 1 and EXO 1 are involved in the DNA synthesis step of MMR [Zhang et al, 2005]. Several other studies established a role of PCNA in early events of MMR, i.e. mismatch recognition, through its interactions with MSH2, MSH3 and MSH6, MLH1 and EXO1 via their PIP domains [Umar et al, Cell 1996; Clark et al, 2000; Flores-Rozas et al, 2000; Kleczkowska et al, 2001]. MMR is only functional when it corrects lesion in the newly transcribed strand so selectivity is an important issue. In eukaryotes, this strand selection likely occurs by the presence of nicks in the lagging strand, as these nicks may be identified by the MMR recognition factors in conjunction with PCNA. Alternatively, PCNA could bind to a pre-formed MSH/MLH complex and acts as a scaffold for consecutive protein-protein interactions necessary for the re-synthesis step of MMR [Bowers et al, 2001; Lee et al, 2006]. RFC, that recognizes the 3'-OH terminus of a break, loads PCNA. The subsequent displacement of RFC by the MutS-MutL dimer is followed by recruitment of EXO1 that degrades the defective strand in the 5' to 3' direction. The ssDNA is further stabilized by RPA [Jiricny et al, 2006] and EXO1 is inhibited when the mismatch is removed. At last pol δ is recruited by PCNA, proceeds to DNA synthesis and DNA Ligase I seals the gap [Guo et al, 2004; Nielsen et al, 2004; Surtees et al, 2004; Dzantiev et al, 2004]. On the leading strand, the endonucleolytic activity of MMS2 is required to create nicks 5' of the mispairs, which can be further processed by EXO1. PCNA and RFC are required to activate MMS2 [Kadyrov et al, 2006].

Double-Strand Break Repair

A role of PCNA in NHEJ has been proposed since an increased interaction between PCNA and Ku70/80 was observed after γ-irradiation in human cells [Balajee and Geard, 2001]. However no other data support these findings and no clear biological function for such an interaction has been found, which is in line with the notion that for this process replication is likely not involved.

However, in HR-directed DSB repair replication is very important and a role of replication factors in this process has been established [Lisby and Rothstein, 2009]. In HR, RPA is pivotal for the nucleo-protein filament formation after end-resection [Chapter 1]. PCNA also interacts with the Werner Syndrome Helicase WRN [Lebel et al, 1999; Franchitto et al, 2004] and might be involved in the resolution of crossed DNA strands or holliday junctions [Wyman et al, 2006]. Finally, PCNA poly-ubiquitination is implicated in the damage bypass

of stalled replication forks via homologous-recombination associated processes [see below]. A role for RFC in HR has not been shown, but studies in yeast suggest that the RFC-like complex Elg1 has a role in HR [Ogiwara et al, 2007], besides its other roles including sister chromatid cohesion [Parnas et al, 2009].

2.2. Replication factors and Nucleotide Excision Repair

Recruitment of PCNA and RFC to NER

Gap-filling synthesis in NER, likewise to regular DNA replication, necessitates that PCNA tether the polymerases δ and ε to the DNA [Maga and Hubscher, 2003; Podust et al, 1998]. The involvement of PCNA in the DNA synthesis step of NER, has been shown *in vitro* [Nichols and Sancar, 1992; Shivji et al, 1992; Aboussekhra et al, 1995; Araujo et al, 2000] and *in vivo* [Green et al, 2003; Essers et al, 2005].

Loading of PCNA to NER-induced short single-strand gaps requires the incision of the ERCC1-XPF structure-specific endonuclease that incises 5' to the lesion thereby creating a 3'-OH end, which is a substrate for PCNA [Miura, et al, 1996 and chapter 3]. PCNA recruitment and loading has always been considered to depend on RFC, similar as in replicative DNA synthesis. Indeed, in *in vitro* reconstituted NER reactions, addition of RFC appears to induce DNA repair synthesis [Araujo et al, 2000; Mocquet et al, 2008]. This is however not a proof that also *in vivo* RFC is the clamp-loader in NER, as there exists other clamp loaders and alternative routes for PCNA recruitment. For example, evidence is accumulating that PCNA is recruited to NER via its interaction with XPG. The endonuclease XPG binds to PCNA [Gary et al, 1997] and was shown to recruit PCNA in *in vitro* reactions [Mocquet et al, 2008]. XPG contains a PIP motif that is required for its interaction with PCNA and for efficient NER reconstitution *in vitro* [Roberts et al, 2003]. *In vivo* studies showed that PCNA recruitment is impaired in XPG deficient cells [Miura et al, 1996; Essers et al, 2005]. Very recently, we confirmed this finding and showed that a catalytic-dead mutant of XPG is sufficient to recruit PCNA [Chapter 3]. Based on these finding we propose a model in which following ERCC1-XPF 5'-mediated incision, PCNA is recruited to the DNA in an XPG dependent manner but does not require RFC. This model is supported by live cell studies on PCNA recruitment that appeared to be independent of RFC [Hashiguchi et al, 2007]. However this analysis was not made with UV-C irradiation (that directs the cell into NER), but upon UV-A irradiation, which creates SSBs, DSBs and oxidative damage.

Although RFC seems dispensable for PCNA recruitment, this does not necessarily mean that PCNA loading does not require RFC, as the clamp must be opened and loaded in an energy-dependent mechanism around the DNA. In Chapter 4, we demonstrate that indeed Replication Factor C is required for proper loading of PCNA at sites of *in vivo* NER

reactions. In the absence of RFC PCNA was shown to be recruited to local UV-damaged sites but does not support pol δ recruitment and DNA repair synthesis. These findings favor a model in which PCNA is recruited to NER sites. After the ERCC1-XPF incision, RFC opens and loads PCNA, which then allows loading and activation of pol δ [Figure 7, Chapter 4]. However RFC may not be the sole clamp loader implicated in this process, since Ctf18 has also been found to localize to sites of *in vivo* NER [Ogi et al, 2010]

Similarly to DNA replication, it remains unclear how the clamp is unloaded. Also in Chapter 4, we describe the notion that RFC accumulation at sites of DNA synthesis lasts much longer than the actual induction of this synthesis step. These findings brought us to speculate about the possible role of RFC as an unloader of the PCNA ring.

The dual role of RPA in NER

RPA displays a dual involvement in NER since it is implicated both in the pre-incision and the post-incisions steps of NER. RPA binds to the undamaged DNA strand and is indispensable for open complex formation. It interacts with several NER proteins (XPA, XPG, ERCC1-XPF) and stimulates the incision activity of both endonucleases [de Laat et al, 1998; He et al, 1995; Matsunaga et al, 1996]. First of all, it covers on the 5'-side of the lesion a partially unwound structure of 8-10 nucleotides. After this, it elongates towards the 3' direction and binds ssDNA with a region of around 30 nucleotides, which is highly correlated to its biochemical property (two binding modes) [Hermanson-Miller and Turchi, 2002; Kolpashchikov et al, 2001]. It also plays a crucial role in DNA synthesis [Shivji et al, 1995]. In Chapter 5 of this thesis, more insights are provided on the differential behavior of RPA at sites of NER pre- and post-incision.

DNA synthesis, ligation and chromatin remodeling in NER

Addition of pol δ and ε supports DNA repair synthesis in *in vitro* NER assays [Shivji et al, 1995; Aboussekhra et al, 1995], but this does not mean that these two polymerases are the sole factors implicated *in vivo* in DNA polymerization at sites of NER. Recent studies showed that the TLS polymerase pol κ (see paragraph on TLS below) is also implicated in this process [Ogi et al, 2010]. Recruitment of these polymerases seems to be differentially regulated. Pol δ is recruited by the classical RFCp140-containing RFC complex and PCNA. Similarly, pol κ is recruited by the same factors but requires the ubiquitinated form of PCNA in conjunction with XRCC1. On the other hand, pol ε is recruited by the Ctf18-factor [Ogi et al, 2010]. Recruitment of pol η at the sites of NER synthesis was not observed. However pol η appeared to accumulate in a focal pattern at local UV-damaged sites in non-S-phase cells [Soria et al, 2009]. The exact function of TLS polymerases at sites of UV-induced damage outside S-phase has not been elucidated yet but several hypotheses have been proposed [Chapter 9; Ogi et al, 2010]. A possible reason for the recruitment of TLS

polymerases to sites of NER is that the very close proximity of two lesions would necessitate the recruitment of a TLS polymerase, but estimations on the incidence of this event indicated that it certainly cannot explain such an intensive recruitment of TLS polymerases. In addition to alternative polymerases, differential PCNA modifications and possibly also distinct clamp-loaders, different enzymes, i.e. DNA Ligase I and the XRCC1-Ligase III complex appear to be implicated in the final nick-sealing step of NER [Moser et al, 2007]. Finally, re-establishment of the chromatin structure occurs via the recruitment of the histone-chaperone CAF-1 in a PCNA-dependent manner [Gaillard et al, 1996]. The process is very similar to that during DNA replication: PCNA recruits CAF-1 to the sites of DNA repair and Asf1 hands the histones to CAF-1 for deposition onto the DNA [Green et al, 2003].

Localization of replication factors to NER sites

Sub-cellular localization studies of replication factors at sites of UV-induced damage using tagged versions of the proteins have revealed the surprising, yet not explained, finding that replication factors accumulate in a focal pattern [Chapter 5]. Various studies on early NER factors have shown that the proteins involved in the pre-incision and dual incision steps of NER accumulate in a diffuse fashion following overall cellular induction of UV damage. Similarly, these factors accumulate homogeneously within a localized area of UV damage, as was shown for example with XPA or XPG [Luijsterburg et al, 2010; Zotter et al, 2006; Rademakers et al, 2003]. Hence, once more, RPA, RFC and PCNA display a specific behavior that might be tightly connected to their intrinsic properties as replication factors. In Chapter 5 of this thesis, we extensively discuss this finding and attempt to find a rationale for it by proposing several models.

Dynamics of replication factors at sites of NER

The dynamics of replication factors at sites of NER are extensively studied in this thesis using tagged versions of PCNA, RFC and RPA. While PCNA shows little turnover similarly to DNA replication, both RFC and RPA interact transiently with repair synthesis sites. However this transient kinetics is coupled to a persistent localization of these factors at sites of repair, hence suggesting novel functions of these proteins in NER [Chapter 4 and Chapter 5]. Similarly, RPA is very transiently immobilized at sites of repair following different kinds of DNA damaging treatments [Solomon, Cardoso, 2004], but these data should be taken with caution since in these studies no distinction between S-phase and non-S-phase cells was made, so the observed RPA action can simply reflect its functioning in replication.

3. Replication over damaged DNA

All organisms must duplicate their genome accurately prior to every cell division in order to distribute complete and intact DNA copies to each of the daughter cells. As discussed above, a complex 'replication machinery' is dedicated to the execution of this process. DNA polymerases must incorporate the right nucleotide and should thus be extremely accurate, which is (in part) achieved through their proofreading activity. Moreover, since this tremendous task of duplicating $3x10^9$ base pairs (i.e. the entire mammalian genome) must be achieved within a few hours, DNA replication occurs at a polymerization rate of about 50 nucleotides per second in mammals. Hence DNA polymerases also have to be tremendously fast. Indeed these polymerases accommodate perfectly in their active sites the four complementary DNA bases with respect to the template strand in order to incorporate these in the growing chain. Besides a whole battery of additional replication factors (see above) enhances the processivity of replication. This complete replication machinery is delicately tuned for undamaged templates; but difficulties start when these polymerases encounter damaged bases during DNA replication. As mentioned in Chapter 1, two pathways act coordinately to bypass lesions that block the passage of replication forks: Translesion Synthesis and Homologous-Recombination processes. The triggering and regulation of these pathways is achieved via PCNA ubiquitination.

3.1 Triggering post-replication repair processes: the role of PCNA ubiquitination

Replication of damaged DNA is controlled by members of the Rad6 epistasis group of *S. cerevisiae*. Within this group, several proteins are involved in ubiquitination. Ubiquitin-dependent post-translational protein modifications occur via a multi-step enzymatic reaction involving the ubiquitin-activating (E1) enzyme, a group of ubiquitin conjugating (E2) activities and an even larger group of ubiquitin-ligases (E3 enzymes). This leads to ligation of the C-terminal glycine of ubiquitin to a lysine residue in the target protein [Glickman and Ciechanover, 2002]. Target selection is performed by the combination of E2 and E3 enzymes. Different ubiquitination modifications (mono and poly-ubiquitination) may occur, with differential effects to their target proteins. When several ubiquitin molecules are added via lysine-48 of ubiquitin, usually proteins are targeted for degradation. Poly-ubiquitination on lysine 63 may induce a change in the sub-cellular distribution or the activity of the target protein.
Rad6 is an E2 ubiquitin conjugating enzyme, which acts with Rad 18, an E3 ubiquitin ligase to ubiquitinate PCNA at lysine-164 in response to DNA damaging agents (UV-light, MMS) and replication inhibitors such as hydroxyureum [Jentsch et al, 1987; Bailly et al, 1997; Hoege et al, 2002; Torres-Ramos et al, 1996; Niimi et al, 2008]. Mono-ubiquitinated PCNA directs the cell towards the error-prone translesion synthesis pathway, by enhanced affinity of the TLS polymerases for this modified PCNA. The *S. cerevisiae* proteins Ubc13 and Mms2 E2 conjugator complex, together with the E3-ligase Rad5, poly-ubiquitinate mono-

ubiquitinated PCNA via lysine-63 of ubiquitin, which activates a recombination-directed error-free pathway of damage avoidance [Hofmann et al, 1999; Stelter et al, 2003].

3.2. Translesion synthesis

Family of specialized Translesion Synthesis DNA polymerases

Translesion Synthesis requires the recruitment of specialized polymerases that, contrary to classical DNA polymerases, can accommodate the damage in their active site and bypass it. PCNA, as a consequence of replication fork stalling at DNA lesions, recruits these different and specialized DNA polymerases, referred to as Translesion synthesis (TLS) polymerases. This group of polymerases is less stringent for selection of the incoming template nucleotide by having a more open active site than the replicative polymerases, allowing them to accommodate the lesion [Ling et al, 2003]. Additionally, TLS polymerases have a significant lower processivity than the elongating polymerases. Importantly, they do not display a 3'-5' exonuclease activity [Yang, 2003]. Together with the reduced selectivity of the active site this causes a severely reduced fidelity of TLS polymerase when compared to the processive ones, hence the error-prone TLS enzymes cause mutations. Indeed, an intrinsic compromise resides in the process of translesion synthesis: the fact that these proteins allow a bypass of the lesion and therefore avoid a complete and very hazardous blockage of replication may certainly represent an advantage for the cell and/or the organism; but on the other hand, these polymerases frequently introduce mutations by incorporating incorrect nucleotides. Interestingly, the less error-prone recombinational type of damage bypass is not very prominent in mammals [Daigaku et al, 2010].

In humans, five polymerases are involved in TLS: Pol η, pol ι, pol κ, Rev1 and pol ξ. The first four belong to the Y family of polymerases and have a much more open structure than the class B superfamily polymerases that contains, among others, pol ξ [Yang and Woodgate, 2007]. Each of these polymerases has specificity for one or several substrates, but their exact functions, as well as their potential interactions and their differential recruitment to a specific lesion, are far from being understood.

Polymerase η can accommodate both bases of a CPD in its active site and is able to replicate past a CPD with similar efficiency to an undamaged base [Mc Culloch et al, 2004]. It is considered mainly error-free since in most cases it will insert the correct nucleotides opposite the CPD [Masutani et al, 2000]. Pol η localizes to replication foci during S phase [Kannouche et al, 2001; Kannouche et al, 2003]. After treatment with e.g. UV or HU the number of cells containing pol η foci increases dramatically, indicating the recruitment of the protein to stalled replication forks [Kannouche, et al, 2001]. In Chapter 8 of this thesis, we have used a GFP-tagged version of this protein to study its dynamics. We show that polymerase η is only transiently interacting with the chromatin and propose a model to explain its two-step recruitment to stalled replication forks

Polymerase ι shares a high homology with pol η and colocalizes with it after UV and HU treatment, although it is not efficient at bypassing TT-CPD, but is able to insert bases opposite 6-4 PP and abasic sites [Johnson et al, 2000; Tissier et al, 2000; Zhang et al, 2001; Johnson et al, 2001; Kannouche et al, 2003]. Pol ι cannot extend from the nucleotide inserted opposite a damaged base and therefore needs to act together with another extender polymerase such as pol ξ. *In vitro* pol ι displays also a 5'-Deoxyribose Phosphate Lyase activity, therefore it has been suggested that it could use its dRP lyase enzymatic activity together with its polymerase activity in Base Excision Repair (BER) [Bebenek et al, 2001]. The exact function of this polymerase remains elusive and it has been suggested that it may serve as a back-up for pol η. At least pol ι is not a vital gene in mammals as the mouse 129 strain that carries a nonsense mutation in exon 2 of pol ι gene is viable and does not exhibit a clear DDR-deficient phenotype as in the case of pol η deficiency [Mc Donald et al, 2003]. In Chapter 8 of this thesis, using a GFP-tagged version of pol ι, we show however that the two proteins act independently and that pol ι displays an even faster dynamics of interaction with the chromatin than pol η. Finally, recent evidence is provided that pol iota may play a role in oxidative-induced DNA damage defense [Petta et al, 2008].

The other Y-family polymerase, polymerase κ, is able to extend terminal mismatches on undamaged templates and bypass benzo(a)pyrene adducts *in vitro* and *in vivo* [Ogi et al, 2002; Avkin et al, 2004]. It has also been proposed to act as an extender polymerase in bypass of UV-induced lesions [Prakash and Prakash, 2002]. Pol κ localizes also to replication factories in S-phase cells and upon treatment with UV, HU or benzo(a)pyrene, but this localization is only limited and does not correlate with PCNA accumulation [Ogi et al, 2005]. Very recently, it was also shown that this polymerase is involved in gap-filling synthesis in NER [Ogi et al, 2006; Ogi et al, 2010].

Structurally, Rev1 is a member of the Y family of polymerases, but it is actually a deoxicytidyl transferase that can insert dCMPs opposite either guanines or abasic sites [Nelson et al, 1996]. Rev1 can support the mutagenic bypass of a wide variety of lesions, including 6-4 PPs and abasic sites [Gibbs et al, PNAS 2000]. In addition to its catalytic domain, it is able via its C-terminal domain to interact with other Y-family polymerases and with Rev7 [Ohashi et al 2004; Tissier et al, 2004]. Therefore, it has been proposed to act as a scaffold protein that facilitates switching between polymerases when the bypass involves two TLS polymerases [Guo et al, 2003; Kannouche and Stary, 2003]. Rev1 localizes to replication foci following UV irradiation [Tissier et al, 2000]

Pol ξ belongs to the B family of polymerases and is a heterodimer of Rev3 and Rev7, respectively its catalytic and regulatory subunits [Nelson et al, 1996]. In yeast, pol ξ is responsible for damage-induced mutagenesis [Lawrence et al, 1985] and for bypass of 6-4 PPs and abasic sites. hRev3 is responsible for UV induced mutagenesis [Li et al, 2002] but the role of hRev7 in this process, as well as the role of pol ξ, still remain unclear. However, it

is clear that pol ξ acts as an extender of terminally mismatched primers and primer termini opposite lesions [Prakash and Prakash, 2002]. Mouse studies suggest that this complex is implicated in a late step of the post-replication gap-filling, i.e. filling in gaps that are produced as a consequence of new replication starts behind lesions [Jansen et al, 2009].

Switching from the replicative to the TLS polymerase

The switch from the replicative polymerase to the TLS polymerase is triggered by PCNA mono-ubiquitination. It was first demonstrated that PCNA mono-ubiquitination increases PCNA affinity for pol η [Kannouche et al, 2004; Watanabe et al, 2004]. Indeed the four Y-family polymerases contain ubiquitin-binding domains known as UBM for pol ι and Rev 1 and the zinc finger motifs UBZ for pol η and pol κ [Bienko et al, 2005], which together with their PCNA-binding motifs (PIP boxes for pol η and pol ι and BRCT domain for Rev1) generate their increased affinity for ubiquitinated PCNA.
It is not known whether the three monomers of the homotrimeric ring are ubiquitinated concomitantly, even if this hypothesis is likely [Niimi et al, 2008]. Similarly, the dynamic properties of the polymerase switch are unknown.

TLS polymerase choice

A key issue in TLS is to understand how the different polymerases that all display different functions are recruited to the stalled replication forks. Two models have emerged. In the first one it was suggested that all these polymerases are associated at the same time to moving replication forks. This so-called 'tool-belt' model [Maga and Hubscher, 2003], in which all the equipment is around to act on demand, is based on the notion that ubiquitin moieties bind to the back side of PCNA and thus allows docking of pol η while pol δ is still attached to the front region of the ubi-PCNA ring [Indiani et al, 2005; Freudenthal et al 2010]. This model is supported by sub-cellular localization studies showing that several TLS polymerases localize to S-phase replication foci. However, these microscopic studies were not suited to reveal interactions at the molecular level and thus do not provide further support for simultaneous binding of multiple polymerases to the same PCNA trimer. An opposing model is that the TLS polymerases move freely through the nucleus and constantly probe DNA/chromatin for fork stalling. They would therefore assemble upon ubiquitinated-PCNA to fulfill their function. Our live cell studies described in Chapter 8 showed that pol η and pol ι interact with replication foci in a highly dynamic fashion and thus favor this latter model. Accordingly to this model, it was shown that Fen-1 and Ligase I cannot bind PCNA simultaneously during Okazaki fragment maturation and that Fen-1 needs to be dislodged from PCNA to allow association of the clamp with DNA Ligase I [Pascal et al, 2004; Johnson et al, 2005; Sakurai et al, 2005]. Similarly RFC needs to dissociate from PCNA to allow the loading of pol δ or pol ε [Podust et al, 1998] and binding of pol δ and DNA ligase I is mutually exclusive [Riva et al, 2004].

Another challenging issue in TLS deals with the sequential recruitment and specific choice of the TLS polymerases involved in the lesion bypass. Interestingly, pol η, pol ι and Rev1 can also become monoubiquitinated [Bienko et al, 2005; Guo et al 2006]. Since it has been proposed that TLS polymerases may act in concert (an inserter followed by an extender), this suggests a model in which monoubiquitination might facilitate the sequential action of TLS polymerases by a kind of hand-over mechanism. The current model of "trial and error" suggests that the polymerases compete for binding to ubiquitinated PCNA and either succeed in their task, or fall off, leaving the spot for another polymerase [Pages and Fuchs, 2002]. Moreover PCNA-triggered monoubiquitination of the TLS polymerases might also prevent the enzyme from rebinding to ubiquitinated-PCNA if it failed to replicate across the lesion. Such a mechanism would facilitate the efficient pairing of PCNA with the optimal TLS polymerases (or at least would ensure that a non-adapted polymerase would not bind twice). It is clear that although several mechanisms are proposed, the current insight into the molecular transactions is too limited to design an over-arching model.

Regulation of PCNA ubiquitination

PCNA ubiquitination is triggered in response to UV and different chemicals, which all cause stalling of the replication fork. As a result of fork stalling, the replicative helicase might dissociate from the replication machinery, leading to exposure of ssDNA ahead of the replication fork. Alternatively, synthesis of the leading and lagging strands get uncoupled, exposing also ssDNA on the leading strand [Lopes et al, 2006]. This ssDNA binds Rad18 which carries out the ubiquitination process together with Rad6.
Ubiquitination of PCNA is also regulated by the deubiquitinating (DUB) enzyme USP1, which is able to remove ubiquitin from Ub-PCNA [Huang et al, 2006]. This process might explain how the action of the TLS polymerase is terminated and allows again access of the regular, high-fidelity polymerase to the replication fork. However, it is not known yet whether the affinity of regular DNA polymerases for PCNA is modified by PCNA ubiquitination. Remarkably, a fraction of ubiquitinated PCNA persists for up to 24 hours [Niimi et al, 2008; Kannouche et al, 2004].

The function of this persistent PCNA modification, which lasts beyond replication and is even detected in G1 and G2 cells, remains unknown [Soria et al, 2006, Ogi et al, 2010]. A possible explanation for the persistence of Ub-PCNA could rely in the regulation of TLS with respect to fork progression. In other words, two models have emerged, that raise the question whether lesion bypass is immediately followed by replication restart, or whether the two processes are independent of each other. Hence, the first model assumes that TLS occurs at the stalled forks and is coordinated with fork progression. The second model suggests that the bypass past the lesion is independent of fork progression. In that case, a new replication apparatus would be assembled beyond the lesion, leaving out a gap at the proximity of the lesion. This gap could be sealed later by the TLS polymerase or a recombination-mediated mechanism [Lopes et al, 2006; Hellers et al, 2006; Waters et al,

2006; Niimi et al, 2008]. Consequently, ubiquitinated PCNA would represent a signal for the gap to be processed. Ub-PCNA could be disassembled at the next round of replication or, in the case of UV damage, de-ubiquitinated concomitantly with restoration of normal USP1 levels.

3.3. Recombination-associated process(es)

Homologous recombination during S-phase, an error-free pathway

The gap that is left upon restart of the replication fork can be repaired either by action of one or several TLS polymerases or by recombination-based mechanisms.
Moreover, the replication fork stalled at the lesion can also regress to form a four-way junction called "chicken foot" [Lopes et al, 2006]. This puts back the lesion in the dsDNA area; hence the homologous DNA strand can serve as a template for damage repair. When the damage is removed, the nascent strand re-anneals with the original template strand and fork progression may occur. It is also possible that the nascent DNA strand synthesized using the undamaged DNA strand, is used as an alternative template for the strand that was blocked by the lesion, a mechanism referred to as template switching. Finally, this chicken-foot may also be cut upon by the action of an endonuclease, generating a one-ended DSB that can invade the homologous DNA molecule. The interplay between these mechanisms is poorly understood.

Recombinational events and PCNA poly-ubiquitination

In Escherichia Coli, PRR consists predominantly of recombination-driven events [Pham et al, PNAS 2001]. In eukaryotes however, TLS or recombinational events are employed differentially, depending on the type of lesion, the structure that is created at the fork and the organism. It is clear however that in (some) eukaryotes PCNA ubiquitination mediates the switch of the replication machinery to one or the other processes. While mono-ubiquitination promotes TLS, poly-ubiquitination promotes error-free, recombination-mediated rescue of stalled replication forks. [Hoege et al, 2002; Lehmann, 2006]. The presence of this recombination directed bypass is however poorly described in mammals and poly-ubiquitinated PCNA species are difficult to reveal in contrast to the more abundant detection in yeast [Chiu et al, 2006; Langie et al, 2007]. The E2 enzymes responsible for PCNA poly-ubiquitination in yeast, i.e. Ubc13-Mms2 genes are conserved in mammals [Li et al, 2002], though the functional Rad5 (the corresponding E3) ortholog remains to be detected. In conclusion, it seems that poly-ubiquitination associated to recombination-directed damage bypass is not a prominent option in mammals.

4. Discussion and future perspectives

The DNA Damage Response is a complex process that is crucial to maintain DNA integrity and consists of several interdependent and highly regulated pathways. Various specific repair mechanisms, post-replication repair pathways and cell cycle checkpoint processes act together in order to provide the cell with the most efficient DNA damage processing throughout the cell cycle. However, the exact regulation and interplay between these pathways still remains to be understood, as illustrated by the interplay between TLS and other DDR processes.

Interplay between TLS, HR, NER and the cell cycle checkpoints

More and more lines of evidence show that TLS polymerases are not exclusively dedicated to the TLS process [Lehmann, 2006], as many of the alternative polymerases appear to function in other DDR pathways.

Within the post-replication repair process itself, the crosstalk between TLS and HR is very complex. While in bacteria, RecA-mediated HR is employed predominantly to deal with stalled replication forks, it also became clear that RecA plays a crucial role in inducing a global damage response (SOS response) that is also involved in regulating TLS mediated-mutagenesis and stimulates NER via the induced selfdestruction of the LexA repressor [Pages et al, 2003; Lopes et al, 2006]. Similarly, there might exist such an interdependency between TLS and HR in mammals. Evidence supporting this interplay is provided by the finding that polymerase η is involved in the extension of the invading strand of the D-loop structure within HR [McIllwraith et al, 2005; Kawamoto et al, 2005]. In addition, Pol ξ and Rev 1 are also involved in HR-mediated DSB repair [Okada et al, 2005]. Altogether it seems that recombination-directed PRR is not a major strategy used in mammals to deal with the lesion. It is surprising to note that mammals would favour an error-prone mechanism such as TLS while an error-free mechanism (HR) is available. It should be noted however, that a choice for HR, when not regulated properly, can induce very hazardous reaction intermediates such as double-strand breaks that may result in chromosomal deletions, duplications and translocations.
Recently, it has become clear that there is direct interplay between TLS and NER. In Chapter 9 of this thesis, we have discussed the localization of pol η to sites of UV repair in G1 cells and propose an additional role of this protein in the main pathway involved in the removal of these lesions, NER. Recent evidence shows that pol η is also involved in GG-NER, though exclusively in S phase cells [Auclair et al, 2010], which further extends the multiple functions of the TLS polymerases. Moreover, DNA polymerase κ (that acts as a putative extender polymerase in bypass of UV-induced lesions), is implicated in the repair synthesis step of NER [Prakash and Prakash, 2002; Ogi et al, 2010, Ogi et al, 2006].

Furthermore, there is a tight connection between TLS and the cell cycle checkpoint machinery, as illustrated by the fact that the pol κ homolog in *S. pombe*, DinB, is recruited to the replication fork by the 9-1-1 and Rad 17 complexes [Kai et al, 2003]. Similarly, in *S. cerevisiae,* there is a correlation between the binding of the 9-1-1 complex, checkpoint activation, and recruitment of specific TLS polymerases (pol κ and the Rev1/pol ξ complex) with repriming of DNA synthesis downstream of a fork stalled at a template lesion [Jansen et al, 2007].

Although these reports show interdependency between TLS polymerases, repair systems and the cell cycle checkpoint machinery, the regulation of this intricate interplay is not elucidated yet. Differential PCNA modifications play at least an important role in this regulation.
The unexpected finding that some TLS polymerases are recruited to sites of NER [Sorial et al, 2009; Ogi et al, 2010; Auclair et al, 2010] also sheds light on the interplay between NER, replication and replication-associated processes, and raises several issues.

Focus on the repair synthesis step of NER

Most of the DNA repair processes require a DNA synthesis step that is carried out by various replication factors including PCNA, RPA, RFC, different ligases and DNA polymerases. Several studies of this thesis have brought about intriguing results.
Replication factors appear to behave in a manner different from early NER factors at sites of NER. Indeed, studies on their kinetics of accumulation have revealed that they do remain at sites of damage far longer than it is needed for the removal and subsequent gap filling synthesis of 6-4 PPs (the main UV-induced target for NER). The replication factors do remain at sites of damage and likely have additional roles beyond the sole DNA synthesis step of NER. Indeed, they are involved in DNA replication as well as in post-replication repair processes. They might even have a function in post DNA repair restoration of the chromatin surrounding the lesions. Hence, the specific behaviour of replication factors at sites of repair reveals the tight interconnection between NER and replication-associated processes.
Moreover, surprisingly, replication factors implicated in the DNA synthesis step of NER also seem to accumulate at local UV damage nuclear areas in a focal manner, similarly to DNA replication. In regular S phase DNA replication, it has not been elucidated yet whether replication foci formation arises from the accidental clustering of replication origins, or from an intrinsic property of replication factories. The focal formation of replication factors during NER replication also raises the question whether this pattern is derived from a structural requirement of replication, which only can happen in clusters. In this case, the formation of replication factories could trigger a clustering of NER sites and it has indeed been observed that incorporation of nucleotides within sites of NER repair

synthesis occurs in a focal fashion [Jackson et al, 1994; Jackson et al, 1994; Svetlova et al, 1999; Svetlova et al, 2002]. The surprising finding that some TLS polymerases are also recruited to NER repair synthesis (and in a focal fashion) while their role at these sites is not clearly defined yet, could support the hypothesis that the replication factories formed at sites of NER would attract in their vicinity several replication factors. In this case, these factors would not obligatorily be actively implicated in the repair replication process, but rather remain disposable if necessary. This also implies that the signaling pathway for this recruitment still has to be determined.

Another plausible hypothesis comes from the fact that the various UV-damage inducing systems used for these studies do trigger a very high amount of lesions within a very condensed area, which could lead to a very close proximity of lesions on the DNA. This could trigger an artificial repair response or a collapse of repair or replication processes when NER is activated simultaneously at proximal lesions. Calculations have been carried out in order to determine the number of lesions induced by UV-irradiation (i.e. a UV dose of $20J/m^2$ induces 4 photolesions per 10kb of double stranded-DNA) and the probability that two lesions may be inflicted within the same or very proximal repair patches (less than 0.5 % of the total amount of lesions) [van Hoffen et la, 1995; Ogi et al, 010]. It is not likely that this sole hypothesis could explain the observed focal localization of replication factors at sites of NER, however these results should still be taken with a certain caution.

Nevertheless, it is certain that once assembled at site of NER repair synthesis, the various replication factors do remain at these challenging places in order to fulfil their functions in replication and replication-associated lesion bypass, highlighting the very tight interplay between the different replication and repair replication mechanisms.

References chapter 2

Aboussekhra, A., Biggerstaff, M., Shivji, M.K., Vilpo, J.A., Moncollin, V., Podust, V.N., Protic, M., Hubscher, U., Egly, J.M.,and Wood, R.D. (1995). *Mammalian DNA nucleotide excision repair reconstituted with purified protein components.* Cell **80**(6): 859-68.

Allen, B.L., Uhlmann, F., Gaur, L.K., Mulder, B.A., Posey, K.L., Jones, L.B. and Hardin, S.H. (1998). *DNA recognition properties of the N-terminal DNA binding domain within the large subunit of replication factor C*. Nucleic Acids Res **26**(17): 3877-82.

Araujo, S.J.,Tirode, F., Coin, F., Pospiech, H., Syvaoja, J.E., Stucki, M., Hubscher, U., Egly, J.M. and Wood, R.D.(2000). *Nucleotide excision repair of DNA with recombinant human proteins: definition of the minimal set of factors, active forms of TFIIH, and modulation by CAK.* Genes Dev **14**(3): 349-59.

Arias, E.E. and Walter, J.C. (2006). *PCNA functions as a molecular platform to trigger Cdt1 destruction and prevent re-replication*. Nat Cell Biol **8**(1): 84-90.

Auclair, Y., Rouget, R., Belisle, J.M., Costantino, S. and Drobetsky, E.A. (2010) *Requirement for functional DNA polymerase eta in genome-wide repair of UV-induced DNA damage during S phase.* DNA Repair (Amst) **9**(7): 754-64.

Avkin, S., Goldsmith, M., Velasco-Miguel, S., Geacintov, N., Friedberg, E.C. And Livneh, Z. (2004). *Quantitative analysis of translesion DNA synthesis across a benzo[a]pyrene-guanine adduct in mammalian cells: the role of DNA polymerase kappa*. J Biol Chem **279**(51): 53298-305.

Bae, S. H. and Seo, Y.S. (2000). *Characterization of the enzymatic properties of the yeast dna2 Helicase/endonuclease suggests a new model for Okazaki fragment processing*. J Biol Chem **275**(48): 38022-31.

Bailly, V., Lauder, S., Prakash S. and Prakash, L.(1997). *Yeast DNA repair proteins Rad6 and Rad18 form a heterodimer that has ubiquitin conjugating, DNA binding, and ATP hydrolytic activities.* J Biol Chem **272**(37): 23360-5.

Balajee, A. S. and Geard, C.R. (2001). *Chromatin-bound PCNA complex formation triggered by DNA damage occurs independent of the ATM gene product in human cells.* Nucleic Acids Res **29**(6): 1341-51.

Bebenek, K., Tissier, A., Frank, E.G., McDonald, J.P., Prasad, R., Wilson, S.H., Woodgate, R. and Kunkel, T.A. (2001*). 5'-Deoxyribose phosphate lyase activity of human DNA polymerase iota in vitro.* Science **291**(5511): 2156-9.

Bell, S. P. and Stillman, B. (1992). *ATP-dependent recognition of eukaryotic origins of DNA replication by a multiprotein complex*. Nature **357**(6374): 128-34.

Bell, S. P. and Dutta, A. (2002). *DNA replication in eukaryotic cells*. Annu Rev Biochem **71**: 333-74.

Bellaoui, M., Chang, M., Ou, J., Xu, H., Boone, C. and Brown, G.W. (2003). *Elg1 forms an alternative RFC complex important for DNA replication and genome integrity.* Embo J **22**(16): 4304-13.

Ben-Aroya, S., Koren, A., Liefshitz, B., Steinlauf, R. And Kupiec, M. (2003). *ELG1, a yeast gene required for genome stability, forms a complex related to replication factor C*. Proc Natl Acad Sci U S A **100**(17): 9906-11.

Bermudez, V.P., Maniwa, Y., Tappin, I., Ozato, K., Yokomori, K. and Hurwitz, J. (2003). *The alternative Ctf18-Dcc1-Ctf8-replication factor C complex required for sister chromatid cohesion loads proliferating cell nuclear antigen onto DNA*. Proc Natl Acad Sci U S A **100**(18): 10237-42.

Bienko, M., Green, C. M., Crosetto, N., Rudolf, F., Zapart, G., Coull, B., Kannouche, P., Wider, G., Peter, M., Lehmann, A.R., Hofmann, K. and Dikic, I. (2005). *Ubiquitin-binding domains in Y-family polymerases regulate translesion synthesis*. Science **310**(5755): 1821-4.

Blackwell, L.J. and Borowiec, J.A. (1994). *Human replication protein A binds single-stranded DNA in two distinct complexes.* Mol Cell Biol **14**(6): 3993-4001.

Bochkarev, A., Pfuetzner, R.A., Edwards, A. M. and Frappier, L. (1997). *Structure of the single-stranded-DNA-binding domain of replication protein A bound to DNA*. Nature **385**(6612): 176-81.

Bork, P., Hofmann, K., Bucher, P., Neuwald, A.F., Altschul, S.F. and Koonin, E.V. (1997). *A superfamily of conserved domains in DNA damage-responsive cell cycle checkpoint proteins*. Faseb J **11**(1): 68-76.

Bowman, G.D., O'Donnell, M. and Kuriyan, J. (2004). *Structural analysis of a eukaryotic sliding DNA clamp-clamp loader complex.* Nature **429**(6993): 724-30.

Bowers, J., Tran, P.T., Joshi, A., Liskay, R.M. and Alani, E. (2001). *MSH-MLH complexes formed at a DNA mismatch are disrupted by the PCNA sliding clamp.* J Mol Biol **306**(5): 957-68.

Boubnov, N.V. and Weaver, D.T. (1995). *scid cells are deficient in Ku and replication protein A phosphorylation by the DNA-dependent protein kinase*. Mol Cell Biol **15**(10): 5700-6.

Brill, S.J. and Bastin-Shanower, S. (1998). *Identification and characterization of the fourth single-stranded-DNA binding domain of replication protein A*. Mol Cell Biol **18**(12): 7225-34.

Bylund, G.O. and Burgers, P.M. (2005). *Replication protein A-directed unloading of PCNA by the Ctf18 cohesion establishment complex*. Mol Cell Biol **25**(13): 5445-55.

Cai, J., Uhlmann, F., Gibbs, E., Flores-Rozas, H., Lee, C.G., Phillips, B., Finkelstein, J., Yao, N., O'Donnell, M. and Hurwitz, J. (1996). *Reconstitution of human replication factor C from its five subunits in baculovirus-infected insect cells*. Proc Natl Acad Sci USA **93**(23): 12896-901.

Carty, M.P., Zernik-Kobak, M., McGrath, S. and Dixon, K. (1994). *UV light-induced DNA synthesis arrest in HeLa cells is associated with changes in phosphorylation of human single-stranded DNA-binding protein.* Embo J **13**(9): 2114-23.

Celis, J.E. and Celis, A. (1985). *Cell cycle-dependent variations in the distribution of the nuclear protein cyclin proliferating cell nuclear antigen in cultured cells: subdivision of S phase.* Proc Natl Acad Sci U S A **82**(10): 3262-6.

Chiu, R.K., Brun, J., Ramaekers, C., Theys, J., Weng, L., Lambin, P., Gray, D.A. and Wouters, B.G. (2006). *Lysine 63-polyubiquitination guards against translesion synthesis-induced mutations.* PLoS Genet **2**(7): e116.

Chuang, L.S., Ian, H.I., Koh, T.W., Ng, H.H., Xu, G. and Li, B.F. (1997). *Human DNA-(cytosine-5) methyltransferase-PCNA complex as a target for p21WAF1*. Science **277**(5334): 1996-2000.

Cho, I.T., Kim, D.H., Kang, Y.H., Lee, C.H., Amangyelid, T., Nguyen, T.A., Hurwitz, J. and Seo, Y.S. (2009). *Human replication factor C stimulates flap endonuclease 1.* J Biol Chem **284**(16): 10387-99.

Clark, A.B., Valle, F., Drotschmann, K., Gary, R.K. and Kunkel, T.A. (2000). *Functional interaction of proliferating cell nuclear antigen with MSH2-MSH6 and MSH2-MSH3 complexes.* J Biol Chem **275**(47): 36498-501.

Conaway, R.C. and Lehman, I.R. (1982). *Synthesis by the DNA primase of Drosophila melanogaster of a primer with a unique chain length*. Proc Natl Acad Sci U S A **79**(15): 4585-8.

Cook, P.R. (1999). *The organization of replication and transcription*. Science **284**(5421): 1790-5.

Cruet-Hennequart, S., Coyne, S., Glynn, M. T., Oakley, G.G. And Carty, M.P. (2006). *UV-induced RPA phosphorylation is increased in the absence of DNA polymerase eta and requires DNA-PK.* DNA Repair (Amst) **5**(4): 491-504.

Cullmann, G., Fien, K., Kobayashi, R. and Stillman, B (1995). *Characterization of the five replication factor C genes of Saccharomyces cerevisiae.*Mol Cell Biol**15**(9):4661-71

de Laat, W.L., Appeldoorn, E., Sugasawa, K., Weterings, E., Jaspers, N.G. and Hoeijmakers, J.H. (1998). *DNA-binding polarity of human replication protein A positions nucleases in nucleotide excision repair*. Genes Dev **12**(16): 2598-609.

Dianov, G.L., Jensen, B.R., Kenny, M.K. and Bohr, V.A.(1999). *Replication protein A stimulates proliferating cell nuclear antigen-dependent repair of abasic sites in DNA by human cell extracts.* Biochemistry **38**(34): 11021-5.

Dianova, II, Bohr, V.A. and Dianov, G.L. (2001). *Interaction of human AP endonuclease 1 with flap endonuclease 1 and proliferating cell nuclear antigen involved in long-patch base excision repair*. Biochemistry **40**(42): 12639-44.

Diffley, J.F., Cocker, J.H., Dowell, S.J. and Rowley, A. (1994*). Two steps in the assembly of complexes at yeast replication origins in vivo.* Cell **78**(2): 303-16.

Diller, J. D. and Raghuraman, M.K. (1994). *Eukaryotic replication origins: control in space and time.* Trends Biochem Sci **19**(8): 320-5.

Din, S., Brill, S.J., Fairman, M.P., Stillma, B. (1990). *Cell-cycle-regulated phosphorylation of DNA replication factor A from human and yeast cells.* Genes Dev **4**(6): 968-77.

Dutta, A. and Stillman, B. (1992). *cdc2 family kinases phosphorylate a human cell DNA replication factor, RPA, and activate DNA replication*. Embo J **11**(6): 2189-99.

Dzantiev, L., Constantin, N., Genschel, J., Iyer, R.R., Burgers, P.M. and Modrich, P. (2004). *A defined human system that supports bidirectional mismatch-provoked excision*. Mol Cell **15**(1): 31-41.

Eissenberg, J.C., Ayyagari, R., Gomes, X.V. and Burgers, P.M. (1997). *Mutations in yeast proliferating cell nuclear antigen define distinct sites for interaction with DNA polymerase delta and DNA polymerase epsilon*. Mol Cell Biol **17**(11): 6367-78.

Ellison, V. and Stillman, B. (2001*). Opening of the clamp: an intimate view of an ATP-driven biological machine.* Cell **106**(6): 655-60.

Essers, J., Theil, A.F., Baldeyron, C., van Cappellen, W.A., Houtsmuller, A.B., Kanaar, R. and Vermeulen, W. (2005). *Nuclear dynamics of PCNA in DNA replication and repair.* Mol Cell Biol **25**(21): 9350-9.

Fan, J., Otterlei, M., Wong, H.K., Tomkinson, A.E. and Wilson, D.M., 3rd (2004). *XRCC1 co-localizes and physically interacts with PCNA.* Nucleic Acids Res **32**(7): 2193-201.

Flores-Rozas, H., Clark, D. and Kolodner, R.D. (2000). *Proliferating cell nuclear antigen and Msh2p-Msh6p interact to form an active mispair recognition complex*. Nat Genet **26**(3): 375-8.

Fotedar, R., Mossi, R., Fitzgerald, P., Rousselle, T., Maga, G., Brickner, Messier, H., Kasibhatla, S., Hubscher, U. and Fotedar, A. (1996). *A conserved domain of the large subunit of replication factor C binds PCNA and acts like a dominant negative inhibitor of DNA replication in mammalian cells.* Embo J **15**(16): 4423-33.

Franchitto, A. and Pichierri, P. (2004). *Werner syndrome protein and the MRE11 complex are involved in a common pathway of replication fork recovery*. Cell Cycle **3**(10): 1331-9.

Franco, A.A., Lam, W.M., Burgers, P.M. and Kaufman, P.D. (2005). *Histone deposition protein Asf1 maintains DNA replisome integrity and interacts with replication factor C*. Genes Dev **19**(11): 1365-75.

Freudenthal, B.D., Gakhar, L., Ramaswamy, S. and Washington, M.T. *Structure of monoubiquitinated PCNA and implications for translesion synthesis and DNA polymerase exchange*. Nat Struct Mol Biol **17**(4): 479-84.

Friedman, K.L., Diller, J.D., Ferguson, B.M., Nyland, S.V., Brewer, B.J. and Fangman, W.L. (1996). *Multiple determinants controlling activation of yeast replication origins late in S phase*. Genes Dev **10**(13): 1595-607.

Frouin, I., Montecucco, A., Spadari, S. and Maga, G (2003). *DNA replication: a complex matter*. EMBO Rep **4**(7): 666-70.

Fukui, T., Yamauchi, K., Muroya, T., Akiyama, M., Maki, H., Sugino, A. and Waga, S. (2004). *Distinct roles of DNA polymerases delta and epsilon at the replication fork in Xenopus egg extracts*. Genes Cells **9**(3): 179-91.

Gaillard, P.H., Martini, E.M., Kaufman, P.D., Stillman, B., Moustacchi, E. and Almouzni, G. (1996). *Chromatin assembly coupled to DNA repair: a new role for chromatin assembly factor I.* Cell **86**(6): 887-96.

Gary, R., Ludwig, D.L., Cornelius, H.L., MacInnes, M.A. and Park, M.S. (1997). *The DNA repair endonuclease XPG binds to proliferating cell nuclear antigen (PCNA) and shares sequence elements with the PCNA-binding regions of FEN-1 and cyclin-dependent kinase inhibitor p21*. J Biol Chem **272**(39): 24522-9.

Gary, R., Kim, K., Cornelius, H.L., Park, M.S. and Matsumoto, Y. (1999). *Proliferating cell nuclear antigen facilitates excision in long-patch base excision repair.* J Biol Chem **274**(7): 4354-63.

Gerard, A., Koundrioukoff, S. Ramillon, V., Sergere, J.C., Mailand, N., Quivy, J.P. and Almouzni, G. (2006). *The replication kinase Cdc7-Dbf4 promotes the interaction of the p150 subunit of chromatin assembly factor 1 with proliferating cell nuclear antigen.* EMBO Rep **7**(8): 817-23.

Gibbs, P.E., Wang, X.D., Li, Z., McManus, T.P., McGregor, W.G., Lawrence, C.W. and Maher, V.M. (2000). *The function of the human homolog of Saccharomyces cerevisiae REV1 is required for mutagenesis induced by UV light*. Proc Natl Acad Sci USA **97**(8): 4186-91.

Gilljam, K.M., Feyzi, E., Aas, P.A., Sousa, M.M., Muller, R., Vagbo, C.B., Catterall, T.C., Liabakk, N.B., Slupphaug, G., Drablos, F., Krokan, H.E. and Otterlei, M. (2009). *Identification of a novel, widespread, and functionally important PCNA-binding motif.* J Cell Biol **186**(5): 645-54

Glickman, M.H. and Ciechanover, A. (2002). *The ubiquitin-proteasome proteolytic pathway: destruction for the sake of construction*. Physiol Rev **82**(2): 373-428.

Gomes, X.V., Henricksen, L.A. and Wold, M.S. (1996). *Proteolytic mapping of human replication protein A:evidence for multiple structural domains and a conformational change upon interaction with single-stranded DNA.* Biochemistry **35**(17): 5586-95.

Goren, A. and Cedar, H. (2003). *Replicating by the clock.* Nat Rev Mol Cell Biol **4**(1):25-32

Görisch, S.M., Sporbert, A., Stear, J.H., Grunewald, I., Nowak, D., Warbrick, E., Leonhardt, H. and Cardoso, M.C. (2008). *Uncoupling the replication machinery: replication fork progression in the absence of processive DNA synthesis* Cell Cycle **7**(13):1983-90

Green, C. M. and Almouzni, G. (2003). *Local action of the chromatin assembly factor CAF-1 at sites of nucleotide excision repair in vivo*. Embo J **22**(19): 5163-74.

Gruss, C., Wu, J., Koller, T. and Sogo, J.M. (1993). *Disruption of the nucleosomes at the replication fork.* Embo J **12**(12): 4533-45.

Gulbis, J.M., Kelman, Z., Hurwitz, J., O'Donnell, M. and Kuriyan, J. (1996). *Structure of the C-terminal region of p21(WAF1/CIP1) complexed with human PCNA*. Cell **87**(2): 297-306.

Guo, C., Fischhaber, P.L., Luk-Paszyc, M.J., Masuda, Y., Zhou, J., Kamiya, K., Kisker, C. and Friedberg, E.C. (2003). *Mouse Rev1 protein interacts with multiple DNA polymerases involved in translesion DNA synthesis*. Embo J **22**(24): 6621-30.

Guo, S., Presnell, S.R., Yuan, F., Zhang, Y., Gu, L. and Li, G.M. (2004). *Differential requirement for proliferating cell nuclear antigen in 5' and 3' nick-directed excision in human mismatch repair.* J Biol Chem **279**(17): 16912-7.

Guo, C., Tang, T.S., Bienko, M., Parker, J.L., Bielen, AB., Sonoda, E., Takeda, S., Ulrich, H.D., Dikic, I. and Friedberg, E.C. Guo (2006). *Ubiquitin-binding motifs in REV1 protein are required for its role in the tolerance of DNA damage*. Mol Cell Biol **26**(23): 8892-900.

Hand, R. (1978). *Eukaryotic DNA: organization of the genome for replication.* Cell **15**(2): 317-25.

Hashiguchi, K., Matsumoto, Y. and Yasui, A. (2007). *Recruitment of DNA repair synthesis machinery to sites of DNA damage/repair in living human cells*. Nucleic Acids Res **35**(9): 2913-23.

He, Z., Henricksen, L.A. Wold, M.S. and Ingles, C.J.(1995). *RPA involvement in the damage-recognition and incision steps of nucleotide excision repair*. Nature **374**(6522): 566-9

Heller, R.C. and Marians, K.J. (2006). *Replication fork reactivation downstream of a blocked nascent leading strand*. Nature **439**(7076): 557-62.

Henneke, G., Koundrioukoff, S. and Hubscher, U. (2003). *Multiple roles for kinases in DNA replication.* EMBO Rep **4**(3): 252-6.

Hermanson-Miller, I. L. and Turchi, J.J. (2002). *Strand-specific binding of RPA and XPA to damaged duplex DNA.* Biochemistry **41**(7): 2402-8.

Hoege, C., Pfander, B., Moldovan, G.L., Pyrowolakis, G. and Jentsch, S. (2002). *RAD6-dependent DNA repair is linked to modification of PCNA by ubiquitin and SUMO*. Nature **419**(6903): 135-41.

Hofmann, R.M. and Pickart, C.M. (2001). *In vitro assembly and recognition of Lys-63 polyubiquitin chains.* J Biol Chem **276**(30): 27936-43.

Hozak, P., Hassan, A.B., Jackson, D.A. and Cook, P.R. (1993). *Visualization of replication factories attached to nucleoskeleton*. Cell **73**(2): 361-73.

Huang, T.T., Nijman, S.M., Mirchandani, K.D., Galardy, P.J., Cohn, M.A., Haas, W., Gygi, S.P., Ploegh, H.L., Bernards, R. and D'Andrea, A.D.(2006). *Regulation of monoubiquitinated PCNA by DUB autocleavage.* Nat Cell Biol **8**(4): 339-47.

Hübscher, U. and Seo, Y.S. (2001). *Replication of the lagging strand: a concert of at least 23 polypeptides.* Mol Cells **12**(2): 149-57.

Hughes, P., Tratner, I., Ducoux, M., Piard, K. and Baldacci, G. (1999). *Isolation and identification of the third subunit of mammalian DNA polymerase delta by PCNA-affinity chromatography of mouse FM3A cell extracts.* Nucleic Acids Res **27**(10): 2108-14.

Indiani, C., McInerney, P., Georgescu, R., Goodman, M.F. and O'Donnell, M. (2005). *A sliding-clamp toolbelt binds high- and low-fidelity DNA polymerases simultaneously.* Mol Cell **19**(6): 805-15.

Jackson, D.A., Hassan, A.B., Errington, R.J and Cook, P.R. (1994). *Sites in human nuclei damage induced by ultraviolet light is repaired: localization relative to transcription*

sites and concentrations of proliferating cell nuclear antigen and the tumour suppressor protein, p53. J Cell Sci **107 (Pt 7)**: 1753-60.

Jackson, D.A., Balajee, A.S., Mullenders, L. and Cook, P.R. (1994*). Sites in human nuclei where DNA damaged by ultraviolet light is repaired: visualization and localization relative to the nucleoskeleton.* J Cell Sci **107 (Pt 7)**: 1745-52.

Jackson, D. A. and Pombo, A. (1998). *Replicon clusters are stable units of chromosome structure: evidence that nuclear organization contributes to the efficient activation and propagation of S phase in human cells*. J Cell Biol **140**(6): 1285-95.

Jansen, J.G., Fousteri, M.I. and de Wind, N. (2007). *Send in the clamps: control of DNA synthesis in eukaryotes.* Mol Cell **28(**4**):**522-9

Jansen, J.G., Tsaalbi-Shtylik, A., Hendriks, G., Verspuy, J., Gali, H., Haracska, L. and de Wind, N. (2009). *Mammalian polymerase zeta is essential for post-replication repair of UV-induced DNA lesions*. DNA Repair (Amst) **8**(12): 1444-51.

Jentsch, S., McGrath, J.P. and Varshavsky, A. (1987). *The yeast DNA repair gene RAD6 encodes a ubiquitin-conjugating enzyme.* Nature **329**(6135): 131-4.

Johnson, R.E., Washington, MT., Haracska, L., Prakash, S. and Prakash, L.(2000). *Eukaryotic polymerases iota and zeta act sequentially to bypass DNA lesions*. Nature **406**(6799): 1015-9.

Johnson, R. E., Haracska, L. Prakash, S. and Prakash, L (2001). *Role of DNA polymerase zeta in the bypass of a (6-4) TT photoproduct.* Mol Cell Biol **21**(10): 3558-63.

Johnson, A. and O'Donnell, M. (2005). *DNA ligase: getting a grip to seal the deal.* Curr Biol **15**(3): R90-2.

Kadyrov, F.A., Dzantiev, L., Constantin, N. and Modrich, P. (2006). *Endonucleolytic function of MutLalpha in human mismatch repair.* Cell **126**(2): 297-308.

Kai, M. and Wang, T.S. (2003). *Checkpoint activation regulates mutagenic translesion synthesis.* Genes Dev **17**(1): 64-76.

Kanellis, P., Agyei, R. and Durocher, D. (2003). *Elg1 forms an alternative PCNA-interacting RFC complex required to maintain genome stability*. Curr Biol **13**(18): 1583-95.

Kannouche, P., Broughton, B.C., Volker, M., Hanaoka, F., Mullenders, L.H. and Lehmann, A.R. (2001). *Domain structure, localization, and function of DNA polymerase eta, defective in xeroderma pigmentosum variant cells*. Genes Dev **15**(2): 158-72.

Kannouche, P., Fernandez de Henestrosa, A.R., Coull, B., Vidal, A.E., Gray, C., Zicha, D., Woodgate, R. and Lehmann, A.R. (2003). *Localization of DNA polymerases eta and iota to the replication machinery is tightly co-ordinated in human cells*. Embo J **22**(5): 1223-33.

Kannouche, P. and Stary, A. (2003). *Xeroderma pigmentosum variant and error-prone DNA polymerases.* Biochimie **85**(11): 1123-32.

Kannouche, P. L., Wing, J. and Lehmann, A.R. (2004). *Interaction of human DNA polymerase eta with monoubiquitinated PCNA: a possible mechanism for the polymerase switch in response to DNA damage*. Mol Cell **14**(4): 491-500.

Kawamoto, T., Araki, K., Sonoda, E., Yamashita, Y.M., Harada, K., Kikuchi, K., Masutani, C., Hanaoka, F., Nozaki, K., Hashimoto, N. and Takeda, S. (2005). *Dual roles for DNA polymerase eta in homologous DNA recombination and translesion DNA synthesis*. Mol Cell **20**(5): 793-9.

Kim, C., Snyder, R.O. and Wold, M.S. (1992). *Binding properties of replication protein A from human and yeast cells.* Mol Cell Biol **12**(7): 3050-9.

Kim, J. and MacNeill, S.A. (2003). *Genome stability: a new member of the RFC family*. Curr Biol **13**(22): R873-5.

Kitamura, E., Blow, J.J. and Tanaka, T.U. (2006). *Live-cell imaging reveals replication of individual replicons in eukaryotic replication factories*. Cell **125**(7): 1297-308.

Kleczkowska, H. E., Marra, G., Lettieri, T. and Jiricny, J. (2001). *hMSH3 and hMSH6 interact with PCNA and colocalize with it to replication foci* Genes Dev**15**(6):724-36

Kong, X. P., Onrust, R., O'Donnell, M. and Kuriyan, J.(1992). *Three-dimensional structure of the beta subunit of E. coli DNA polymerase III holoenzyme: a sliding DNA clamp*. Cell **69**(3): 425-37.

Kolpashchikov, D.M., Khodyreva, S.N., Khlimankov, D.Y., Wold, M.S., Favre, A. and Lavrik, O.I. (2001). *Polarity of human replication protein A binding to DNA.* Nucleic Acids Res **29**(2): 373-9.

Koundrioukoff, S., Jonsson, Z.O., Hasan, S., de Jong, R.N., van der Vliet, P.C., Hottiger, M.O. And Hubscher, U.(2000). *A direct interaction between proliferating cell nuclear antigen (PCNA) and Cdk2 targets PCNA-interacting proteins for phosphorylation.* J Biol Chem **275**(30): 22882-7.

Krishna, T.S., Kong, X.P., Gary, S., Burgers, P.M. and Kuriyan, J.(1994). *Crystal structure of the eukaryotic DNA polymerase processivity factor PCNA.* Cell **79**(7): 1233-43.

Krokan, H.E., Otterlei, M., Nilsen, H., Kavli, B., Skorpen, F., Andersen, S., Skjelbred, C., Akbari, M., Aas, P.A. and Slupphaug, G. (2001). *Properties and functions of human uracil-DNA glycosylase from the UNG gene.* Prog Nucleic Acid Res Mol Biol **68**: 365-86.

Lan, L., Nakajima, S., Oohata, Y., Takao, M., Okano, S., Masutani, M., Wilson, S. H. and Yasui, A. (2004). *In situ analysis of repair processes for oxidative DNA damage in mammalian cells.* Proc Natl Acad Sci U S A **101**(38): 13738-43.

Langie, S.A., Knaapen, A.M., Ramaekers, C.H., Theys, J., Brun, J., Godschalk, R.W., van Schooten, F.J., Lambin, P., Gray, D.A., Wouters, B.G. and Chiu, R.K. (2007). *Formation of lysine 63-linked poly-ubiquitin chains protects human lung cells against benzo[a]pyrene-diol-epoxide-induced mutagenicity*. DNA Repair (Amst) **6**(6): 852-62.

Lawrence, C.W., Das, G. and Christensen, R.B. (1985). *REV7, a new gene concerned with UV mutagenesis in yeast*. Mol Gen Genet **200**(1): 80-5.

Lebel, M., Spillare, E.E., Harris, C.C and Leder, P.(1999). *The Werner syndrome gene product co-purifies with the DNA replication complex and interacts with PCNA and topoisomerase I*. J Biol Chem **274**(53): 37795-9.

Lee, S. D. and Alani, E. (2006). *Analysis of interactions between mismatch repair initiation factors and the replication processivity factor PCNA*. J Mol Biol **355**(2): 175-84.

Lehman, I. R. and Kaguni, L.S. (1989).*DNA polymerase alpha*. J Biol Chem **264**(8):4265-8

Lehmann, A.R. (2006). *New functions for Y family polymerases.* Mol Cell **24**(4): 493-5

Lehmann, A. R. (2006). *Translesion synthesis in mammalian cells. Exp* Cell Res **312**(14): 2673-6.

Leonhardt, H., Rahn, H.P., Weinzierl, P., Sporbert, A., Cremer, T., Zink, D. and Cardoso, M.C. (2000). *Dynamics of DNA replication factories in living cells.* J Cell Biol **149**(2): 271-80.

Levin, D.S., McKenna, A.E., Motycka, T.A., Matsumoto, Y. and Tomkinson, A.E. (2000). *Interaction between PCNA and DNA ligase I is critical for joining of Okazaki fragments and long-patch base-excision repair.* Curr Biol **10**(15): 919-22.

Levin, D.S., Vijayakumar, S., Liu, X., Bermudez, V.P., Hurwitz, J. and Tomkinson, A.E. (2004). *A conserved interaction between the replicative clamp loader and DNA ligase in eukaryotes: implications for Okazaki fragment joining.* J Biol Chem **279**(53): 55196-201.

Li, Z., Zhang, H., McManus, T.P., McCormick, J.J., Lawrence, C.W. and Maher, V.M.(2002) *hREV3 is essential for error-prone translesion synthesis past UV or benzo[a]pyrene diol epoxide-induced DNA lesions in human fibroblasts*. Mutat Res **510**(1-2): 71-80.

Li, Y., Z. Pursell, F. and Linn, S. (2000). *Identification and cloning of two histone fold motif- containing subunits of HeLa DNA polymerase epsilon*. J Biol Chem **275**(40): 31554.

Li, Z., Xiao, W., McCormick, J.J. and Maher, V.M. (2002). *Identification of a protein essential for a major pathway used by human cells to avoid UV- induced DNA damage.* Proc Natl Acad Sci U S A **99**(7): 4459-64.

Ling, H., Boudsocq, F., Plosky, B.S., Woodgate, R. and Yang, W. (2003). *Replication of a cis-syn thymine dimer at atomic resolution*. Nature **424**(6952): 1083-7.

Lisby, M. and Rothstein, R. (2009). *Choreography of recombination proteins during the DNA damage response.* DNA Repair (Amst) **8**(9): 1068-76.

Liu, V.F. and Weaver, D.T. (1993). *The ionizing radiation-induced replication protein A phosphorylation response differs between ataxia telangiectasia and normal human cells*. Mol Cell Biol **13**(12): 7222-31.

Liu, L., Mo, J., Rodriguez-Belmonte, E.M. and Lee, M.Y. (2000). *Identification of a four* subunit of mammalian DNA polymerase delta. J Biol Chem **275**(25): 18739-44.

Lopes, M., Foiani, M. and Sogo, J.M. (2006). *Multiple mechanisms control chromosome integrity after replication fork uncoupling and restart at irreparable UV lesions*. Mol Cell **21**(1): 15-27.

Luijsterburg, M.S., von Bornstaedt, G**.,** Gourdin, A.M., Politi, A.Z., Moné, M.J., Warmerdam, D.O., Goedhart, J., Vermeulen, W., van Driel, R., and Höfer, T. (2010). *Stochastic and reversible assembly of a multiprotein DNA repair complex ensures accurate target site recognition and efficient repair.*J Cell Biol**189**(3): 445-63

Maga, G., Mossi, R., Fischer, R., Berchtold, M. W. and Hubscher, U. (1997).*Phosphorylation of the PCNA binding domain of the large subunit of replication factor C by Ca2+/calmodulin-dependent protein kinase II inhibits DNA synthesis.* Biochemistry **36**(18): 5300-10.

Maga, G., Stucki, M. Spadari, S. and Hübscher, U. (2000). *DNA polymerase switching: I. Replication factor C displaces DNA polymerase alpha prior to PCNA loading*. J Mol Biol **295**(4): 791-801.

Maga, G., Frouin, I., Spadari, S. and Hubscher, U. (2001). *Replication protein A as a "fidelity clamp" for DNA polymerase alpha.* J Biol Chem **276**(21): 18235-42.

Maga, G. and Hubscher, U. (2003). *Proliferating cell nuclear antigen (PCNA): a dancer with many partners.* J Cell Sci **116**(Pt 15): 3051-60.

Majka, J. and Burgers, P.M (2004). *The PCNA-RFC families of DNA clamps and clamp loaders*. Prog Nucleic Acid Res Mol Biol **78**: 227-60.

Manders, E.M., J. Stap, Brakenhoff, G.J., van Driel, R. and Aten, J.A.(1992). *Dynamics of three-dimensional replication patterns during the S-phase, analysed by double labelling of DNA and confocal microscopy.* J Cell Sci **103 (Pt 3)**: 857-62.

Maradeo, M. E. and Skibbens, R.V. (2009). *The Elg1-RFC clamp-loading complex performs a role in sister chromatid cohesion*. PLoS One **4**(3): e4707.

Masumoto, H., Sugino, A. and Araki, H. (2000). *Dpb11 controls the association between DNA polymerases alpha and epsilon and the autonomously replicating sequence region of budding yeast.* Mol Cell Biol **20**(8): 2809-17.

Masutani, C., Kusumoto, R., Iwai, S. and Hanaoka, F. (2000). *Mechanisms of accurate translesion synthesis by human DNA polymerase eta.* Embo J **19**(12): 3100-9.

Matunis, M.J. (2002). *On the road to repair: PCNA encounters SUMO and ubiquitin modifications.* Mol Cell **10**(3): 441-2.

Matsunaga, T., Park, C. H., Bessho, T., Mu, D. and Sancar, A.(1996). *Replication protein A confers structure-specific endonuclease activities to the XPF-ERCC1 and XPG subunits of human DNA repair excision nuclease.* J Biol Chem **271**(19): 11047-50.

Mayer, M. L., Gygi, S.P., Aebersold, R. and Hieter, P. (2001). *Identification of RFC(Ctf18p, Ctf8p, Dcc1p): an alternative RFC complex required for sister chromatid cohesion in S. cerevisiae.* Mol Cell **7**(5): 959-70.

McCulloch, S.D., Kokoska, R.J., Masutani, C., Iwai, S., Hanaoka, F. and Kunkel, T.A. (2004). *Preferential cis-syn thymine dimer bypass by DNA polymerase eta occurs with biased fidelity.* Nature **428**(6978): 97-100.

McDonald, J.P.,Frank, E.G., Plosky, B.S., Rogozin, I.B., Masutani, C., Hanaoka, F., Woodgate, R. and Gearhart, P.J. (2003). *129-derived strains of mice are deficient in DNA polymerase iota and have normal immunoglobulin hypermutation*. J Exp Med **198**(4): 635-43.

McIlwraith, M.J., Vaisman, A., Liu, Y., Fanning, E., Woodgate, R. and West, S.C. (2005). *Human DNA polymerase eta promotes DNA synthesis from strand invasion intermediates of homologous recombination*. Mol Cell **20**(5): 783-92.

Mello, J. A. and Almouzni, G. (2001). *The ins and outs of nucleosome assembly.* Curr Opin Genet Dev **11**(2): 136-41.

Miura, M., Nakamura, S., Sasaki, T., Takasaki, Y., Shiomi, T. and Yamaizumi, M. (1996). *Roles of XPG and XPF/ERCC1 endonucleases in UV-induced immunostaining of PCNA in fibroblasts.* Exp Cell Res **226**(1): 126-32.

Miyata, T., Suzuki, H., Oyama, T., Mayanagi, K., Ishino, Y. and Morikawa, K. (2005). *Open clamp structure in the clamp-loading complex visualized by electron microscopic image analysis.* Proc Natl Acad Sci U S A **102**(39): 13795-800.

Moldovan, G. L., B. Pfander and Jentsch, S. (2006). *PCNA controls establishment of sister chromatid cohesion during S phase.* Mol Cell **23**(5): 723-32.

Moldovan, G. L., Pfander, B. and Jentsch, S. (2007). *PCNA, the maestro of the replication fork.* Cell **129**(4): 665-79.

Moarefi, I., Jeruzalmi, D., Turner, J., O'Donnell, M. and Kuriyan, J. (2000). *Crystal structure of the DNA polymerase processivity factor of T4 bacteriophage.* J Mol Biol **296**(5): 1215-23.

Mocquet, V., Laine, J. P., Riedl, T., Yajin, Z., Lee, M. Y. and Egly, J. M. (2008). *Sequential recruitment of the repair factors during NER: the role of XPG in initiating the resynthesis step.* Embo J **27**(1): 155-67.

Montecucco, A., Rossi, R., Levin, D.S., Gary, R., Park, M.S., Motycka, T.A., Ciarrocchi, G., Villa, A., Biamonti, G. and Tomkinson, A.E. (1998). *DNA ligase I is recruited to sites of DNA replication by an interaction with proliferating cell nuclear antigen: identification of a common targeting mechanism for the assembly of replication factories.* Embo J **17**(13): 3786-95.

Montecucco, A., Rossi, R., Ferrari, G., Scovassi, A. I., Prosperi, E. and Biamonti, G. (2001). *Etoposide induces the dispersal of DNA ligase I from replication factories.* Mol Biol Cell **12**(7): 2109-18.

Moser, J., Kool, H., Giakzidis, I., Caldecott, K., Mullenders, L.H. and Fousteri, M.I. (2007). *Sealing of chromosomal DNA nicks during nucleotide excision repair requires XRCC1 and DNA ligase III alpha in a cell-cycle-specific manner.* Mol Cell **27**(2): 311-23.

Mossi, R. and Hubscher, U. (1998). *Clamping down on clamps and clamp loaders--the eukaryotic replication factor C.* Eur J Biochem **254**(2): 209-16.

Munshi, A., Cannella, D., Brickner, H., Salles-Passador, I., Podust, V., Fotedar, R. and Fotedar, A. (2003). *Cell cycle-dependent phosphorylation of the large subunit of replication factor C (RF-C) leads to its dissociation from the RF-C complex.* J Biol Chem **278**(48): 48467-73.

Murti, K.G., He, D.C., Brinkley, B.R., Scott, R. And Lee, S.H.(1996). *Dynamics of human replication protein A subunit distribution and partitioning in the cell cycle.* Exp Cell Res **223**(2): 279-89.

Nakamura, H., Morita, T. and Sato, C. (1986). *Structural organizations of replicon domains during DNA synthetic phase in the mammalian nucleus.* Exp Cell Res **165**(2): 291-7.

Nakayasu, H. and Berezney, R. (1989). *Mapping replicational sites in the eucaryotic cell nucleus.* J Cell Biol **108**(1): 1-11.

Naryzhny, S.N. and Lee, H. (2004). *The post-translational modifications of proliferating cell nuclear antigen: acetylation, not phosphorylation, plays an important role in the regulation of its function*. J Biol Chem **279**(19): 20194-9.

Nelson, J.R., Lawrence, C.W. and Hinkle, D.C. (1996). *Deoxycytidyl transferase activity of yeast REV1 protein.* Nature **382**(6593): 729-31.

Nelson, J.R., Lawrence, C.W. and Hinkle, D.C. (1996). *Thymine-thymine dimer bypass by yeast DNA polymerase zeta.* Science **272**(5268): 1646-9.

Newport, J. and Yan, H. (1996). *Organization of DNA into foci during replication.* Curr Opin Cell Biol **8**(3): 365-8.

Nichols, A.F. and Sancar, A. (1992). *Purification of PCNA as a nucleotide excision repair protein.* Nucleic Acids Res **20**(13): 2441-6.

Nielsen, F.C., Jager, A.C., Lutzen, A., Bundgaard, J.R. and Rasmussen, L.J. (2004). *Characterization of human exonuclease 1 in complex with mismatch repair proteins, subcellular localization and association with PCNA.* Oncogene **23**(7): 1457-68.

Niimi, A., Brown, S., Sabbioneda, S., Kannouche, P.L., Scott, A., Yasui, A., Green, C.M. and Lehmann, A.R. (2008). *Regulation of proliferating cell nuclear antigen ubiquitination in mammalian cells*. Proc Natl Acad Sci U S A **105**(42): 16125-30.

Oakley, G.G., Loberg, L.I., Yao, J., Risinger, M.A., Yunker, R.L., Zernik-Kobak, M., Khanna, K.K., Lavin, M.F., Carty, M.P. and Dixon, K. (2001). *UV-induced hyperphosphorylation of replication protein a depends on DNA replication and expression of ATM protein.* Mol Biol Cell **12**(5): 1199-213.

O'Keefe, R.T., Henderson, S.C. and Spector, D.L. (1992). *Dynamic organization of DNA replication in mammalian cell nuclei: spatially and temporally defined replication of chromosome-specific alpha-satellite DNA sequences.* J Cell Biol **116**(5): 1095-110.

Ogi, T., Shinkai, Y., Tanaka, K and Ohmori, H. (2002). *Polkappa protects mammalian cells against the lethal and mutagenic effects of benzo[a]pyrene*. Proc Natl Acad Sci USA **99**(24): 15548-53.

Ogi, T., Kannouche, P. and Lehmann, A.R. (2005). *Localisation of human Y-family DNA polymerase kappa: relationship to PCNA foci.* J Cell Sci **118**(Pt 1): 129-36.

Ogi, T. and Lehmann, A.R. (2006). *The Y-family DNA polymerase kappa (pol kappa) functions in mammalian nucleotide-excision repair*. Nat Cell Biol **8**(6): 640-2.

Ogi, T., Limsirichaikul, S., Overmeer, R.M., Volker, M., Takenaka, K., Cloney, R., Nakazawa, Y., Niimi, A., Miki, Y., Jaspers, N. G., Mullenders, L.H., Yamashita, S., Fousteri, M.I. and Lehmann, A.R. (2010) *Three DNA polymerases, recruited by different mechanisms, carry out NER repair synthesis in human cells*. Mol Cell **37**(5): 714-27.

Ogiwara, H., Ui, A., Onoda, F., Tada, S., Enomoto, T. and Seki, M. (2006). *Dpb11, the budding yeast homolog of TopBP1, functions with the checkpoint clamp in recombination repair.* Nucleic Acids Res **34**(11): 3389-98.

Ogiwara, H., Ohuchi, T., Ui, A., Tada, S., Enomoto, T. and Seki, M. (2007). *Ctf18 is required for homologous recombination-mediated double-strand break repair.* Nucleic Acids Res **35**(15): 4989-5000.

Ohashi, E., Murakumo, Y., Kanjo, N., Akagi, J., Masutani, C., Hanaoka, F. and Ohmori, H. (2004). *Interaction of hREV1 with three human Y-family DNA polymerases.* Genes Cells **9**(6): 523-31.

Okada, T., Sonoda, E., Yoshimura, M., Kawano, Y., Saya, H., Kohzaki, M. and Takeda, S. (2005). *Multiple roles of vertebrate REV genes in DNA repair and recombination*. Mol Cell Biol **25**(14): 6103-11.

Pages, V. and Fuchs, R.P. (2002). *How DNA lesions are turned into mutations within cells?* Oncogene **21**(58): 8957-66.

Pages, V. and Fuchs, R.P. (2003). *Uncoupling of leading- and lagging-strand DNA replication during lesion bypass in vivo.* Science **300**(5623): 1300-3.

Pan, Z Q., Park, C.H., Amin, A.A., Hurwitz, J. and Sancar, A. (1995). *Phosphorylated and unphosphorylated forms of human single-stranded DNA-binding protein are equally active in simian virus 40 DNA replication and in nucleotide excision repair*. Proc Natl Acad Sci U S A **92**(10): 4636-40.

Parnas, O., Zipin-Roitman, A., Mazor, Y., Liefshitz, B., Ben-Aroya, S. and Kupiec, M. (2009). *The ELG1 clamp loader plays a role in sister chromatid cohesion*. PLoS One **4**(5): e5497.

Pascal, J. M., O'Brien, P.J., Tomkinson, A.E. and Ellenberger, T. (2004). *Human DNA ligase I completely encircles and partially unwinds nicked DNA.* Nature **432**(7016): 473-8.

Petta, T. B., Nakajima, S., Zlatanou, A., Despras, E., Couve-Privat, S., Ishchenko, A., Sarasin, A., Yasui, A. and Kannouche, P. (2008). *Human DNA polymerase iota protects cells against oxidative stress*. Embo J **27**(21): 2883-95.

Pfander, B., Moldovan, G.L. and Sacher, M., Hoege, C. and Jentsch, S. (2005). *SUMO-modified PCNA recruits Srs2 to prevent recombination during S phase.* Nature **436**(7049): 428-33.

Pham, P., Rangarajan, S., Woodgate, R. and Goodman, M.F. (2001). *Roles of DNA polymerases V and II in SOS-induced error-prone and error-free repair in Escherichia coli*. Proc Natl Acad Sci U S A **98**(15): 8350-4.

Philimonenko, A.A., Jackson, D.A., Hodny, Z., Janacek, J., Cook, P.R. and Hozak, P. (2004). *Dynamics of DNA replication: an ultrastructural study*. J Struct Biol **148**(3): 279-89.

Podust, V.N. and Fanning, E. (1997). *Assembly of functional replication factor C expressed using recombinant baculoviruses.* J Biol Chem **272**(10): 6303-10.

Podust, V.N., Tiwari, N., Stephan, S. and Fanning, E. (1998). *Replication factor C disengages from proliferating cell nuclear antigen (PCNA) upon sliding clamp formation, and PCNA itself tethers DNA polymerase delta to DNA.* J Biol Chem **273**(48): 31992-9.

Post, S.M., A. Tomkinson, E. and Lee, E.Y. (2003). *The human checkpoint Rad protein Rad17 is chromatin-associated throughout the cell cycle, localizes to DNA*

replication sites and interacts with DNA polymerase epsilon.Nucleic Acids Res **31**(19):5568-75

Prakash, S. and Prakash, L. (2002). *Translesion DNA synthesis in eukaryotes: a one- or two-polymerase affair.* Genes Dev **16**(15): 1872-83.

Prelich, G., Tan, C.K., Kostura, M., Mathews, M.B., So, A.G., Downey, K.M. and Stillman, B. (1987). *Functional identity of proliferating cell nuclear antigen and a DNA polymerase-delta auxiliary protein*. Nature **326**(6112): 517-20

Rademakers, S., Volker, M., Hoogstraten, D., Nigg, A.L., Mone, M.J., Van Zeeland, A.A., Hoeijmakers, J.H., Houtsmuller, A.B. and Vermeulen, W. (2003). *Xeroderma pigmentosum group A protein loads as a separate factor onto DNA lesions*. Mol Cell Biol. **23**:5755-67.

Riva, F., Savio, M., Cazzalini, O., Stivala, L. A., Scovassi, I. A., Cox, L.S., Ducommun, B. and Prosperi, E. (2004). *Distinct pools of proliferating cell nuclear antigen associated to DNA replication sites interact with the p125 subunit of DNA polymerase delta or DNA ligase I.* Exp Cell Res **293**(2): 357-67.

Roberts, J.A., Bell, S.D. and White, M.F. (2003). *An archaeal XPF repair endonuclease dependent on a heterotrimeric PCNA.* Mol Microbiol **48**(2): 361-71.

Rolef Ben-Shahar, T., Castillo, A.G., Osborne, M.J., Borden, K.L., Kornblatt, J. and Verreault, A. (2009). *Two fundamentally distinct PCNA interaction peptides contribute to chromatin assembly factor 1 function* Mol Cell Biol **29**(24): 6353-65

Sakurai, S., Kitano, K., Yamaguchi, H., Hamada, K., Okada, K., Fukuda, K., Uchida, M., Ohtsuka, E., Morioka, H. and Hakoshima, T. (2005). *Structural basis for recruitment of human flap endonuclease 1 to PCNA*. Embo J **24**(4): 683-93.

Salles-Passador, I., Munshi, A., Cannella, D., Pennaneach, V., Koundrioukoff, S.,Jaquinod, M., Forest, E., Podust, V., Fotedar, A. and Fotedar, R. (2003*). Phosphorylation of the PCNA binding domain of the large subunit of replication factor C on Thr506 by cyclin-dependent kinases regulates binding to PCNA.* Nucleic Acids Res **31**(17): 5202-11.

Senga, T., Sivaprasad, U., Zhu, W., Park, J.H., Arias, E.E., Walter, J.C. and Dutta, A. (2006). *PCNA is a cofactor for Cdt1 degradation by CUL4/DDB1-mediated N-terminal ubiquitination*. J Biol Chem **281**(10): 6246-52.

Shiomi, Y., Usukura, J., Masamura, Y., Takeyasu, K., Nakayama, Y., Obuse, C., Yoshikawa, H. and Tsurimoto, T. (2000). *ATP-dependent structural change of the eukaryotic clamp-loader protein, replication factor C* Proc Natl Acad Sci USA**97**(26): 14127-32

Shiomi, Y., Masutani, C., Hanaoka, F., Kimura, H. and Tsurimoto, T. (2007). *A second proliferating cell nuclear antigen loader complex, Ctf18-replication factor C, stimulates DNA polymerase eta activity*. J Biol Chem **282**(29): 20906-14.

Shivji, K. K., Kenny, M.K and Wood, R.D. (1992). *Proliferating cell nuclear antigen is required for DNA excision repair.* Cell **69**(2): 367-74.

Skibbens, R.V., Corson, L.B., Koshland, D. and Hieter, P. (1999). *Ctf7p is essential for sister chromatid cohesion and links mitotic chromosome structure to the DNA replication machinery*. Genes Dev **13**(3): 307-19.

Smith, S. and Stillman, B. (1989). *Purification and characterization of CAF-I, a human cell factor required for chromatin assembly during DNA replication in vitro*. Cell **58**(1): 15-25.

Smolikov, S., Mazor, Y. and Krauskopf, A. (2004). *ELG1, a regulator of genome stability, has a role in telomere length regulation and in silencing*. Proc Natl Acad Sci U S A **101**(6): 1656-61.

Solomon, D.A., Cardoso, M.C and Knudsen, E.S. (2004). *Dynamic targeting of the replication machinery to sites of DNA damage.* J Cell Biol **166**(4): 455-63.

Somanathan, S., Suchyna, T.M., Siegel, A.J. and Berezney, R. (2001). *Targeting of PCNA to sites of DNA replication in the mammalian cell nucleus.* J Cell Biochem **81**(1):56-67

Soria, G., Podhajcer, O., Prives, C. and Gottifredi, V. (2006). *P21Cip1/WAF1 downregulation is required for efficient PCNA ubiquitination after UV irradiation.* Oncogene **25**(20): 2829-38.

Soria, G., Belluscio, L., van Cappellen, W.A., Kanaar, R., Essers, J. And Gottifredi, V. (2009). *DNA damage induced Pol eta recruitment takes place independently of the cell cycle phase.* Cell Cycle **8**(20): 3340-8.

Spadari, S. and Hubscher, U. (2000). *DNA polymerase switching: I. Replication factor C displaces DNA polymerase alpha prior to PCNA loading.* J Mol Biol **295**(4): 791-801.

Sporbert, A., Gahl, A., Ankerhold, R., Leonhardt, H. and Cardoso, M.C. (2002). *DNA polymerase clamp shows little turnover at established replication sites but sequential de novo assembly at adjacent origin clusters.* Mol Cell **10**(6): 1355-65.

Stelter, P. and Ulrich, H.D. (2003). *Control of spontaneous and damage-induced mutagenesis by SUMO and ubiquitin conjugation.* Nature **425**(6954): 188-91.

Surtees, J.A. and Alani, E. (2004). *Replication factors license exonuclease I in mismatch repair.* Mol Cell **15**(2): 164-6.

Svetlova, M.P., Solovjeva, L.V., Pleskach, N.A. and Tomilin, N.V.(1999). *Focal sites of DNA repair synthesis in human chromosomes*Biochem Biophys Res Commun **257**(2):378-83

Svetlova, M., Solovjeva, L., Pleskach, N., Yartseva, N., Yakovleva, T., Tomilin, N. and Hanawalt, P. (2002). *Clustered sites of DNA repair synthesis during early nucleotide excision repair in ultraviolet light-irradiated quiescent human fibroblasts*. Exp Cell Res **276**(2): 284-95.

Theriot, C.A., Hegde, M.L., Hazra, T.K. and Mitra, S. *RPA physically interacts with the human DNA glycosylase NEIL1 to regulate excision of oxidative DNA base damage in primer-template structures.* DNA Repair (Amst) **9**(6): 643-52.

Tissier, A., Frank, E.G., McDonald, J.P., Iwai, S., Hanaoka, F. and Woodgate, R. (2000). *Misinsertion and bypass of thymine-thymine dimers by human DNA polymerase iota*. Embo J **19**(19): 5259-66.

Tissier, A., Kannouche, P., Reck, M.P., Lehmann, A.R., Fuchs, R.P. and Cordonnier, A. (2004). *Co-localization in replication foci and interaction of human Y-family members, DNA polymerase pol eta and REVl protein*. DNA Repair (Amst) **3**(11): 1503-14.

Tom, S., Henricksen, L.A. and Bambara, R.A. (2000). *Mechanism whereby proliferating cell nuclear antigen stimulates flap endonuclease 1.* J Biol Chem **275**(14): 10498-505.

Tom, S., Henricksen, L.A., Park, M.S. and Bambara, R.A. (2001). *DNA ligase I and proliferating cell nuclear antigen form a functional complex.* J Biol Chem **276**(27): 24817-25.

Torres-Ramos, C.A., Yoder, B.L., Burgers, P.M., Prakash, S. and Prakash, L. (1996). *Requirement of proliferating cell nuclear antigen in RAD6-dependent postreplicational DNA repair.* Proc Natl Acad Sci U S A **93**(18): 9676-81.

Treuner, K., Findeisen, M., Strausfeld, U. And Knippers, R. (1999). *Phosphorylation of replication protein A middle subunit (RPA32) leads to a disassembly of the RPA heterotrimer*. J Biol Chem **274**(22): 15556-61.

Tsurimoto, T., Melendy, T. and Stillman, B. (1990). *Sequential initiation of lagging and leading strand synthesis by two different polymerase complexes at the SV40 DNA replication origin.* Nature **346**(6284): 534-9.

Tsurimoto, T. and B. Stillman (1991). Replication factors required for SV40 DNA replication in vitro. I. *DNA structure-specific recognition of a primer-template junction by eukaryotic DNA polymerases and their accessory proteins*. J Biol Chem **266**(3): 1950-60.

Tubo, R.A. and Berezney, R. (1987). *Pre-replicative association of multiple replicative enzyme activities with the nuclear matrix during rat liver regeneration.* J Biol Chem **262**(3): 1148-54.

Uhlmann, F., Cai, J. Flores-Rozas, H., Dean, F.B., Finkelstein, J., O'Donnell, M. and Hurwitz, J. (1996). *In vitro reconstitution of human replication factor C from its five subunits*. Proc Natl Acad Sci U S A **93**(13): 6521-6.

Uhlmann, F., Cai, J., Gibbs, E., O'Donnell, M. and Hurwitz, J. (1997). *Deletion analysis of the large subunit p140 in human replication factor C reveals regions required for complex formation and replication activities.* J Biol Chem **272**(15): 10058-64.

Umar, A., Buermeyer, A.B., Simon, J.A., Thomas, D.C., Clark, A.B., Liskay, R.M. and Kunkel, T.A. (1996). *Requirement for PCNA in DNA mismatch repair at a step preceding DNA resynthesis.* Cell **87**(1): 65-73.

Van, C., Yan, S., Michael, W.M., Waga, S. and Cimprich, K.A. (2010). *Continued primer synthesis at stalled replication forks contributes to checkpoint activation*. J Cell Biol **189**(2): 233-46.

van Hoffen, J. Venema, R. Meschini, A.A. van Zeeland and Mullenders, L.H.F. (1995) *Transcription-coupled repair removes both cyclobutane pyrimidine dimers and 6-4-photoproducts with equal efficiency and in a sequential way from transcribed DNA in xeroderma-pigmentosum group-C fibroblasts. EMBO J.* **14** (1995), pp. 360–367

Vassin, V.M., Wold, M.S. and Borowiec, J.A. (2004). *Replication protein A (RPA) phosphorylation prevents RPA association with replication centers*. Mol Cell Biol **24**(5): 1930-43.

Verreault, A. (2000). *De novo nucleosome assembly: new pieces in an old puzzle.* Genes Dev **14**(12): 1430-8.

Waga, S. and Stillman, B. (1998). *The DNA replication fork in eukaryotic cells.* Annu Rev Biochem **67**: 721-51.

Walter, J. and Newport, J. (2000). *Initiation of eukaryotic DNA replication: origin unwinding and sequential chromatin association of Cdc45, RPA, and DNA polymerase alpha*. Mol Cell **5**(4): 617-27.

Warbrick, E. (2000). *The puzzle of PCNA's many partners*. Bioessays **22**(11): 997-1006.

Warbrick, E. (1998). *PCNA binding through a conserved motif*. Bioessays **20**(3): 195-9.

Watanabe, K., Tateishi, S., Kawasuji, M., Tsurimoto, T., Inoue, H. and Yamaizumi, M. (2004). *Rad18 guides poleta to replication stalling sites through physical interaction and PCNA monoubiquitination*. Embo J **23**(19): 3886-96.

Waters, L.S. and Walker, G.C. (2006). *The critical mutagenic translesion DNA polymerase Rev1 is highly expressed during G(2)/M phase rather than S phase*. Proc Natl Acad Sci USA **103**(24): 8971-6.

Wold, M.S. (1997). *Replication protein A: a heterotrimeric, single-stranded DNA-binding protein required for eukaryotic DNA metabolism*. Annu Rev Biochem **66**: 61-92.

Wyman, C. and Kanaar, R. (2006). *DNA double-strand break repair: all's well that ends well.* Annu Rev Genet **40**: 363-83.

Xiong, Y., Zhang, H. and Beach, D. (1992*). D type cyclins associate with multiple protein kinases and the DNA replication and repair factor PCNA*. Cell **71**(3): 505-14.

Xu, H., Zhang, P., Liu, L and Lee, M.Y. (2001). *A novel PCNA-binding motif identified by the panning of a random peptide display library.* Biochemistry **40**(14): 4512-20.

Yan, H., Chen,C.Y., Kobayashi, R. and Newport, J. (1998). *Replication focus-forming activity 1 and the Werner syndrome gene product.* Nat Genet **19**(4): 375-8.

Yan, H. and Newport, J. (1995). *FFA-1, a protein that promotes the formation of replication centers within nuclei.* Science **269**(5232): 1883-5.

Yang, W. (2003). *Damage repair DNA polymerases*. Y.Curr Opin Struct Biol **13**(1): 23-30.

Yang, W. and Woodgate, R. (2007). *What a difference a decade makes: insights into translesion DNA synthesis.* Proc Natl Acad Sci U S A **104**(40): 15591-8.

Yao, N., Turner, J., Kelman, Z., Stukenberg, P.T., Dean, F., Shechter, D., Pan, Z.Q., Hurwitz, J. and O'Donnell, M. (1996). *Clamp loading, unloading and intrinsic stability of the PCNA, beta and gp45 sliding clamps of human, E. coli and T4 replicases*. Genes Cells **1**(1): 101-13.

Yao, N.Y., Johnson, A., Bowman, G.D., Kuriyan, J. and O'Donnell, M. (2006). *Mechanism of proliferating cell nuclear antigen clamp opening by replication factor C*. J Biol Chem **281**(25): 17528-39.

Zhang, Z., Shibahara, K. and Stillman, B.(2000). *PCNA connects DNA replication to epigenetic inheritance in yeast.* Nature **408**(6809): 221-5.

Zhang, Y., Yuan, F., Wu, X., Taylor, J.S. and Wang, Z. (2001). *Response of human DNA polymerase iota to DNA lesions.* Nucleic Acids Res **29**(4): 928-35.

Zhang, Y., Yuan, F., Presnell, S.R., Tian, K., Gao, Y., Tomkinson, A.E., Gu, L. and Li, G.M. (2005). *Reconstitution of 5'-directed human mismatch repair in a purified system.* Cell **122**(5): 693-705.

Zotter, A., Luijsterburg, M.S., Warmerdam, D.O., Ibrahim, S., Nigg, A., van, Cappellen, W.A., Hoeijmakers, J.H., van Driel, R., Vermeulen, W. and Houtsmuller, A.B. (2006). *Recruitment of the nucleotide excision repair endonuclease XPG to sites of UV-induced dna damage depends on functional TFIIH*. Mol Cell Biol **26**(23): 8868-79.

Zou, L. and Stillman, B. (1998). *Formation of a preinitiation complex by S-phase cyclin CDK-dependent loading of Cdc45p onto chromatin.* Science **280**(5363): 593-6.

Zou, Y., Liu, Y., Wu, X., and Shell, S.M. (2006). *Functions of human replication protein A (RPA): from DNA replication to DNA damage and stress responses*. J Cell Physiol **208**(2): 267-73.

Chapter 3

~

Coordination of dual incision and repair synthesis in human nucleotide excision repair

EMBO Journal (2009), **28** (8)**:** 1111-1120

The EMBO Journal (2009) 28, 1111–1120 | © 2009 European Molecular Biology Organization | All Rights Reserved 0261-4189/09
www.embojournal.org

THE EMBO JOURNAL

Coordination of dual incision and repair synthesis in human nucleotide excision repair

Lidija Staresincic[1], Adebanke F Fagbemi[1], Jacqueline H Enzlin[2,5], Audrey M Gourdin[3], Nils Wijgers[3], Isabelle Dunand-Sauthier[4,6], Giuseppina Giglia-Mari[3,7], Stuart G Clarkson[4,8], Wim Vermeulen[3] and Orlando D Schärer[1,2,*]

[1]Departments of Pharmacological Sciences and Chemistry, Stony Brook University, Stony Brook, NY, USA, [2]Institute of Molecular Cancer Research, University of Zurich, Zurich, Switzerland, [3]Department of Cell Biology and Genetics, Erasmus Medical Center, Rotterdam, The Netherlands and [4]Department of Microbiology and Molecular Medicine, University Medical Centre, Geneva, Switzerland

Nucleotide excision repair (NER) requires the coordinated sequential assembly and actions of the involved proteins at sites of DNA damage. Following damage recognition, dual incision 5′ to the lesion by ERCC1-XPF and 3′ to the lesion by XPG leads to the removal of a lesion-containing oligonucleotide of about 30 nucleotides. The resulting single-stranded DNA (ssDNA) gap on the undamaged strand is filled in by DNA repair synthesis. Here, we have asked how dual incision and repair synthesis are coordinated in human cells to avoid the exposure of potentially harmful ssDNA intermediates. Using catalytically inactive mutants of ERCC1-XPF and XPG, we show that the 5′ incision by ERCC1-XPF precedes the 3′ incision by XPG and that the initiation of repair synthesis does not require the catalytic activity of XPG. We propose that a defined order of dual incision and repair synthesis exists in human cells in the form of a 'cut-patch-cut-patch' mechanism. This mechanism may aid the smooth progression through the NER pathway and contribute to genome integrity.

The EMBO Journal (2009) **28,** 1111–1120. doi:10.1038/emboj.2009.49; Published online 12 March 2009
Subject Categories: genome stability & dynamics
Keywords: DNA repair synthesis; ERCC1-XPF; nucleotide excision repair; xeroderma pigmentosum; XPG

*Corresponding author. Departments of Pharmacological Sciences and Chemistry, Stony Brook University, Chemistry 619, Stony Brook, NY 11794-3400, USA. Tel.: +1 631 632 7545; Fax: +1 631 632 7546; E-mail: orlando@pharm.stonybrook.edu
[5]Present address: Cancer Research UK, Weatherall Institute of Molecular Medicine, John Radcliffe Hospital, University of Oxford, Oxford OX3 9DS, UK
[6]Present address: Department of Pathology and Immunology, University Medical Centre, Geneva, Switzerland
[7]Present address: CNRS and Université du Toulouse; IPBS, 205 route de Narbonne, F-31077 Toulouse, France
[8]Present address: Rivadavia 350, Colonia del Sacramento, Colonia 70000, Uruguay

Received: 27 May 2008; accepted: 30 January 2009; published online: 12 March 2009

Introduction

Nucleotide excision repair (NER) is a versatile DNA repair pathway that enables cells to eliminate a plethora of helix-distorting lesions caused by different environmental agents. Versatility and specificity in NER are achieved through the sequential and highly coordinated actions of at least 30 polypeptides that detect the lesion and excise a damage-containing oligonucleotide, carry out repair synthesis and ligation events to restore the DNA sequence to its original state (de Laat *et al*, 1999; Friedberg *et al*, 2005; Gillet and Schärer, 2006). A subpathway of NER, transcription-coupled NER, preferentially removes damage from the transcribed strand of active genes and is initiated through stalling of an elongating RNA polymerase at DNA lesions (Hanawalt, 2002; Svejstrup, 2002). In bulk DNA, XPC-RAD23B appears to be the initial sensor of DNA damage and is essential for the assembly of all subsequent NER factors in the process known as global genome NER (GG-NER) (Sugasawa *et al*, 1998, 2001; Volker *et al*, 2001; Min and Pavletich, 2007). TFIIH, the next factor to be recruited, is responsible for strand separation around the lesion (Evans *et al*, 1997b; Wakasugi and Sancar, 1998; Tirode *et al*, 1999), enabling XPA, RPA and XPG to join the complex. ERCC1-XPF is then engaged (Mu *et al*, 1997; Tapias *et al*, 2004; Tsodikov *et al*, 2007) to perform the incision 5′ to the damage (Bardwell *et al*, 1994; Sijbers *et al*, 1996), whereas XPG cleaves 3′ to the lesion (O'Donovan *et al*, 1994). An oligonucleotide of 24–32 nucleotides in length containing the lesion is then released, and the resulting gap is filled by DNA polymerase δ/ε (and/or possibly κ (Ogi and Lehmann, 2006)), replication factor C (RFC), PCNA, RPA and the nick is sealed by DNA ligase I or DNA ligase III/XRCC1 (Shivji *et al*, 1995; Moser *et al*, 2007) to restore the original DNA sequence. At a higher level of organization, chromatin assembly factor 1 (CAF-1) has been implicated in the restoration of chromatin after the repair reaction (Green and Almouzni, 2003).

Although many recent studies have been concerned with the mechanisms of damage recognition (Schärer, 2007), less is known about the coordination of the two incision and the repair synthesis steps. For repair synthesis to occur, the 5′ incision by ERCC1-XPF is required to generate a free 3′-OH group, the substrate for the DNA polymerase. By contrast, the 3′ incision by XPG may not necessarily be needed to initiate polymerization. If both incisions occurred without any DNA repair synthesis, simple release of the oligonucleotide containing the damaged residue could result in the formation of a single-stranded DNA (ssDNA) gap, another deleterious DNA lesion with a key role in activating DNA damage signalling pathways (Shechter *et al*, 2004). Furthermore, the occurrence of aberrant DNA breaks is associated with inadvertent NER activity at nondamaged sites in XP/CS cells, underscoring the importance of avoiding the formation of unwanted NER incision reactions (Berneburg *et al*, 2000; Theron *et al*, 2005). Therefore, it

appears likely that a mechanism ensuring the smooth transition between the dual incision and repair synthesis steps would have evolved.

The similar kinetics of the damage removal and repair synthesis indeed suggests a coordination of these two events (Riedl *et al*, 2003). Analysis of the literature, however, reveals that there is no consensus concerning the order of the two incisions. Although there is agreement that the 5′ and 3′ incisions are made in a near-synchronous manner (Moggs *et al*, 1996), both 5′ uncoupled (Matsunaga *et al*, 1995; Moggs *et al*, 1996) and 3′ uncoupled (Mu *et al*, 1996; Evans *et al*, 1997a, 1997b) incisions have been observed in different experimental contexts *in vitro*. Using catalytically inactive forms of XPG, it has been shown that the presence of XPG, but not its catalytic activity, is required for the generation of the 5′ incision by ERCC1-XPF (Wakasugi *et al*, 1997; Constantinou *et al*, 1999). Another study showed that the efficient 3′ incision by XPG required the presence and catalytic activity of ERCC1-XPF (Tapias *et al*, 2004).

Here we report the use of catalytically inactive mutants of XPF and XPG to establish the relative temporal order of the two incision reactions and DNA repair synthesis in human cell-free extracts and cells. The results suggest a novel 'cut-patch-cut-patch' mechanism whereby the dual incision and repair synthesis events of NER are highly coordinated. In turn, this mechanism can explain how the potentially dangerous effects of ssDNA intermediates are minimized or even prevented.

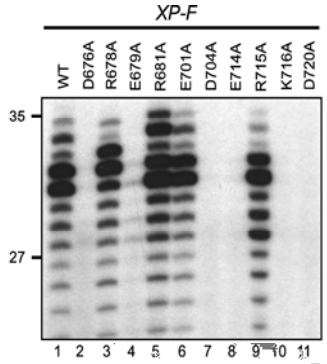

Figure 1 XPF active site mutants deficient in NER *in vitro*. Cell extracts prepared from XPF-deficient XPF-1EO cells were incubated with a plasmid containing a single 1,3 cisplatin intrastrand crosslink in the presence of 200 fmol purified recombinant wild-type ERCC1-XPF (lane 1) or ERCC1-XPF proteins with different point mutations in XPF (lanes 2–11). The excision products containing the cisplatin adduct were labelled by the annealing of an oligonucleotide complementary to the excised oligonucleotides with a G_4 overhang and filling in with Sequenase 2.0 and [α-^{32}P] dCTP. The products were separated on a 14% denaturing polyacrylamide gel and visualized by autoradiography. The positions of size markers are indicated on the left.

Results

Active site mutants of XPG and XPF do not support dual incision

To try to determine whether there is a strict temporal order to the 5′ and 3′ incisions in human NER, we made use of mutants of ERCC1-XPF and XPG that are catalytically inactive, but retain full DNA binding ability, with the hope of trapping NER intermediates. Three useful active site mutants of XPG have been reported earlier. These D77A, E791A and D812A proteins do not display 3′ nuclease activity and prevent dual incision in NER *in vitro* but allow 5′ incision by ERCC1-XPF to occur (Wakasugi *et al*, 1997; Constantinou *et al*, 1999). We have recently characterized the active site of human XPF and constructed several mutants with severely impaired endonuclease activity that retain full DNA binding activity (Enzlin and Schärer, 2002). Here, we further characterized these mutants to select a catalytically inactive mutant devoid of NER dual incision activity analogous to the previously characterized XPG mutants. Hence, we tested the ability of these purified recombinant proteins, expressed as heterodimers with ERCC1, to restore NER activity in XP-F deficient cell extracts (Moggs *et al*, 1996).

The wild-type, R678A, R681A, E701A and R715A XPF proteins fully restored the excision of a lesion-oligonucleotide from a plasmid containing a site-specific 1,3-intrastrand d(GpTpG) cisplatin DNA crosslink (Figure 1, lanes 1, 3, 5, 6 and 9, respectively), whereas E679A displayed residual activity (Figure 1, lane 4). By contrast, the D676A, D704A, E714A, K716A and D720A XPF mutants (Figure 1, lanes 2, 7, 8, 10 and 11, respectively) failed to restore any NER activity. An earlier study using a fully reconstituted system showed that XPF-D676A was devoid of any NER activity, whereas D720A had some residual activity (Tapias *et al*, 2004).

Efficient 3′ incision by XPG is dependent on prior 5′ incision by ERCC1-XPF

We used ERCC1-XPF-D676A and XPG-E791A for further studies to discern any possible interdependency of the 5′ and 3′ incision steps. Covalently closed circular DNA containing a single 1,3-intrastrand cisplatin DNA crosslink was incubated with an XPF- or XPG-deficient cell-free extract complemented with wild-type or nuclease-deficient ERCC1-XPF and XPG proteins. The reaction products were purified and cleaved with *Bss*HII to excise a 190-bp fragment from the plasmid DNA. Incision products were detected by annealing an oligonucleotide complementary to the *Bss*HII incision site 3′ to the lesion followed by a fill-in reaction to generate a fragment of approximately 130 nt for the 5′ uncoupled incision by XPF and a 100-nt fragment for incision by XPG, in the presence or absence of the 5′ incision (Figure 2A).

Incubation of the plasmid with XP-G or XP-F cell extract did not yield any incision products (Figure 2B, lanes 2 and 5, respectively). When the extracts were complemented with wild type XPG or XPF proteins (lanes 3 and 6, respectively), products specific for 3′ incision by XPG (three bands around 100 nt) were visible. Addition of XPF-D676A to the XP-F cell extract only yielded marginal amounts of 3′ incision products (lane 7), suggesting that 3′ uncoupled incision by XPG does not occur efficiently in the presence of catalytically inactive XPF. By contrast, addition of XPG-E791A to the XP-G cell extract resulted in the appearance of two intense specific bands (of around 130 nt in length) corresponding to the product of XPF 5′-uncoupled incision (lane 4). These results indicate that efficient 3′ incision by XPG is dependent on the presence and catalytic activity of ERCC1-XPF, whereas the presence, but not the catalytic activity of XPG is required for

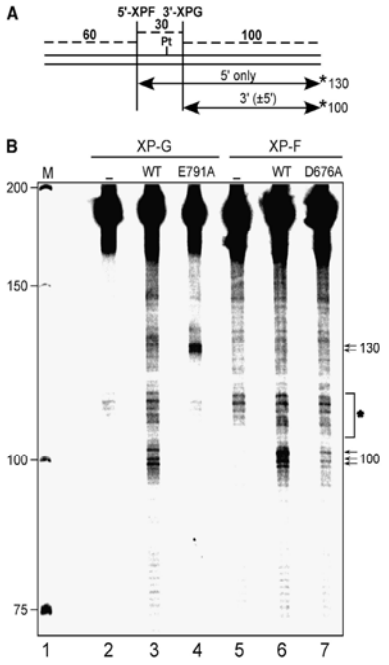

Figure 2 Efficient XPG cleavage is dependent on the catalytic activity of XPF. (**A**) Schematic representation of a 190-bp *Bss*HII fragment with a single defined cisplatin lesion. Incision sites by ERCC1-XPF and XPG are indicated. Incisions were detected using fill-in reactions with Sequenase 2.0 and [α-^{32}P] dCTP by annealing an oligonucleotide complementary to a *Bss*HII cleavage site containing a G_4 overhang allowing for the visualization of the 130 and 100 mer products for 5′ and 3′ incision, respectively. Possible excision products are indicated by arrows and the position of the [α-^{32}P] label is indicated with an asterisk. (**B**) cccDNA with a single defined cisplatin lesion was incubated with cell extracts lacking XPG- (XPCS1RO, lanes 2–4) or XPF-deficient (XP2YO, lanes 5–7), either alone (lanes 2 and 5) or complemented with wild-type XPG (lane 3), XPG E791A (lane 4), wild-type XPF (lane 6), XPF D676A (lane 7), purified, digested with *Bss*HII, radioactively labelled and analysed on a denaturing PAGE gel. The positions of size markers are indicated on the left, and the position of the reaction products on the right of the gel. Unspecific bands present in all the lanes are marked with an asterisk.

the 5′ incision by ERCC1-XPF. Hence, the 5′ incision might precede the 3′ incision.

DNA Repair Synthesis can be initiated in vitro without the 3′ incision by XPG

To determine whether both 5′ and 3′ incisions need to occur before DNA repair synthesis can be initiated, we investigated the nature of the repair synthesis products in XP-G cell extracts complemented with wild-type XPG and XPG-E791A, by incubating a plasmid containing a single defined cisplatin lesion in the extracts together with [α-^{32}P]-dCTP and [α-^{32}P]-TTP.

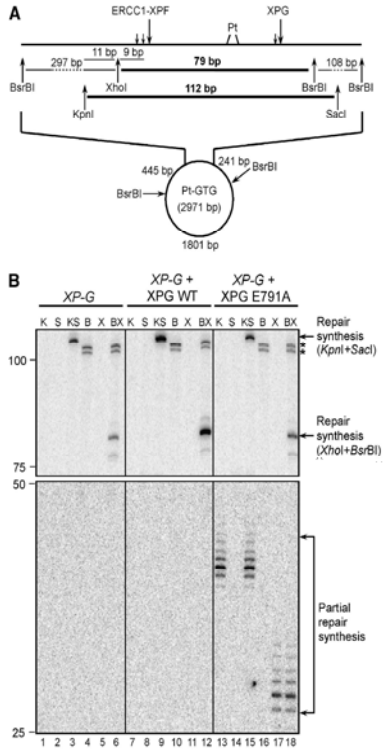

Figure 3 XPG E791A supports partial DNA repair synthesis *in vitro*. (**A**) Schematic representation of the lesion-containing plasmid used in the assay. Incision sites by ERCC1-XPF and XPG and the sizes of restriction fragments are indicated. The fragments containing the repair synthesis products are shown in bold (79 and 112 bp). (**B**) cccDNA with a single defined cisplatin lesion was incubated with a XP-G cell extract, either alone (lanes 1–6) or in the presence of 600 fmol of wild-type XPG (lanes 7–12) or XPG E791A (lanes 13–18) as well as 10 μCi of [α-^{32}P]dCTP and 10 μCi [α-^{32}P]TTP. DNA was further purified, digested with *Kpn*I (lanes 1, 7, 13), *Sac*I (lanes 2, 8, 14), *Kpn*I + *Sac*I (lanes 3, 9, 15), *Bsr*BI (lanes 4, 10, 16), *Xho*I (lanes 5, 11, 17), *Bsr*BI + *Xho*I (lanes 6, 12, 18) and analysed on a denaturing PAGE gel. The positions of size markers are indicated on the left, the nature of the observed products on the right of the gel. Two unspecific bands are marked with an asterisk. Abbreviations: K, *Kpn*I; S, *Sac*I; KS, *Kpn*I + *Sac*I; B, *Bsr*BII X, *Xho*I; BX, *Bsr*BI + *Xho*I.

After the reaction, DNA was purified and digested with *Kpn*I and/or *Sac*I or *Xho*I and/or *Bsr*BI (Figure 3A).

When DNA was incubated with the XP-G cell extract alone, products of nonspecific DNA synthesis were observed with signal intensities roughly proportional to the length of the DNA fragments (Figure 3B, lanes 1–6). These signals are likely due to random nicks produced by topoisomerases and/or nucleases present in the cell-free extracts (Hansson *et al*, 1989). Addition of wild-type XPG to the mixture led to a significant increase in the intensity of the bands of 112 nt

(*Kpn*I and *Sac*I) and 79 nt (*Bsr*BI and *Xho*I), corresponding to newly synthesized and ligated DNA at the site of the cisplatin lesion (lanes 9 and 12, respectively). Note that the 79 nt signal of the *Bsr*BI/*Xho*I digestion in lane 12 is much more intense than the nonspecific signal at 108 nt, strongly suggesting that the 79-bp band results from XPG-induced repair synthesis. The specificity of the signal for repair synthesis was further supported by the observation that no increase of the specific band at 79 bp was seen if the reaction was carried out with the parental nondamaged plasmid (data not shown). Addition of nuclease deficient XPG-E791A, which permits incision by ERCC1-XPF, to the XP-G cell extracts, did not result in a change in the intensity of the full-length repair synthesis products of 112 and 79 bp. However, two new products with the most intensive bands of 39 nt (*Kpn*I and *Sac*I) and 28 nt (*Bsr*BI and *Xho*I) were visible after a longer exposure of the gel (lanes 15 and 18, respectively). These bands were also present after the cleavage with only one restriction enzyme 5′ to the damaged site (lanes 13 and 17), while no products were visible after cutting with restriction enzymes 3′ to the incision sites (lanes 14 and 16). The appearance of these bands is, therefore, consistent with their being partial repair synthesis products, in which the polymerase extended the 3′-OH group generated by ERCC1-XPF about 18–20 nt in the absence of XPG incision. These observations indicate that initiation of repair synthesis is dependent on cleavage by ERCC1-XPF and that it can occur before 3′ cleavage by XPG. No partial repair synthesis products were observed when an extract made from XP-F cells was complemented with wild-type XPF or XPF-D676A (data not shown). These results demonstrate that repair synthesis can be initiated *in vitro* before the 3′ incision by XPG.

Catalytically inactive XPF persists at sites of UV damage

Having observed partial repair synthesis without XPG cleavage *in vitro*, we wished to test whether repair synthesis could also be initiated *in vivo* before 3′ incision by XPG. For repair synthesis to take place, the DNA replication machinery has to be recruited to the sites of DNA damage. Therefore, we examined the localization of PCNA, a component of the DNA replication machinery, after local UV irradiation of a XP-G cell line expressing wild-type XPG or XPG-E791A and a XP-F cell line expressing wild-type XPF or XPF-D676A. We have described earlier the generation and characterization of XP-G cell lines expressing wild-type XPG and XPG-E791A using lentiviral transduction. Both XPG proteins were localized to UV-damaged spots in cell nuclei shortly after damage infliction, but only XPG-E791A persisted in these spots, suggesting that completion of NER is required for the dissociation of XPG (Thorel *et al*, 2004). XP-F cell lines expressing wild-type XPF and XPF-D676A were generated in an analogous fashion by transducing XPF-deficient XP2YO cells with lentiviral recombinants encoding HA-tagged wild-type XPF and XPF-D676A. The resulting cells were subjected to local UV irradiation and the recruitment of XPC, the initial damage recognition factor, and XPF to sites of UV damage was analysed (Volker *et al*, 2001).

At 0.5 h after irradiation, we observed colocalization of XPC with both HA-tagged wild-type XPF and XPF-D676A (Figure 4A). At 3 h after local UV irradiation, XPC and XPF were no longer present at the damaged sites in the cells expressing wild-type XPF. However, in the mutant XPF transductants, XPC remained colocalized with the catalytically deficient XPF-D676A (Figure 4B). Hence, cleavage by ERCC1-XPF and XPG is needed for both nucleases to dissociate from the damaged site and for the completion of NER.

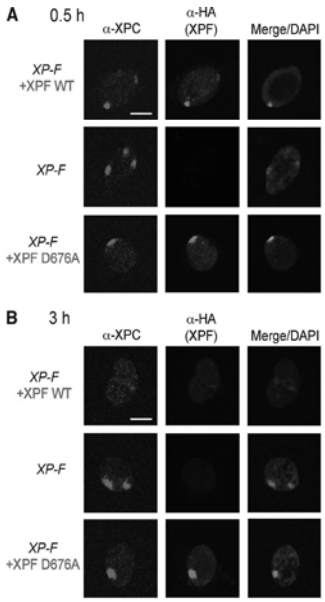

Figure 4 Recruitment of XPF to sites of local UV damage in different XP-F cell lines. XP2YO (XP-F) cells, untransduced or transduced with XPF-WT or XPF-D676A, were grown on coverslips and locally irradiated with a UV dose of 150 J/m^2 through filters with 5 μm pores and fixed 0.5 h (**A**) or 3 h (**B**) after irradiation. The cells were immunolabelled with antibodies against XPC (red) or the HA tag present on the C-terminus of XPF (green). Merged images indicate the overlay of XPC, XPF and DAPI staining. Scale bars, 10 μm.

Recruitment of PCNA, and CAF-1 to sites of local UV damage depends on the presence, but not the catalytic activity of XPG

Using the transduced XP-G and XP-F cell lines, we studied how the catalytic activity of the two nucleases correlates with the recruitment of repair synthesis factors to NER sites. It has been shown before that recruitment of PCNA to the sites of local UV damage is severely affected in XPG-deficient cells (Essers *et al*, 2005). In agreement with this report, we did not observe any colocalization of PCNA with XPC in XP-G cells 0.5 h after UV irradiation (Figure 5A, middle row). However, as expected, XPC and PCNA colocalized at sites of UV damage in XP-G cells expressing wild-type XPG (Figure 5A, top row). PCNA also colocalized with XPC in the XPG-E791A transductants (Figure 5A, bottom row). In principle, the recruitment of PCNA to sites of UV damage in the presence of catalytically inactive XPG could reflect partial DNA repair synthesis or be due to the recruitment of PCNA before

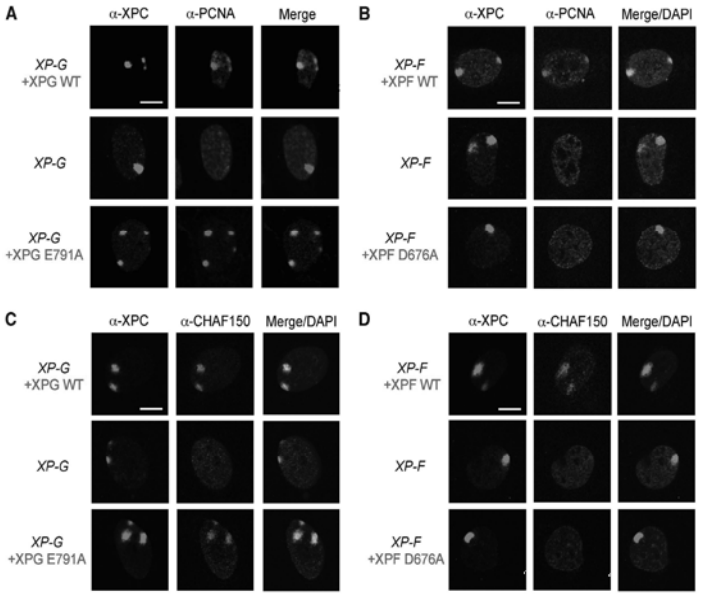

Figure 5 XPF- and XPG-dependent colocalization of PCNA and CAF-1 with XPC. XPCS1RO (XP-G) cells, untransduced or transduced with XPG-WT or XPG-E791A (**A**, **C**) and XP2YO (XP-F) cells, untransduced or transduced with XPF-WT or XPF-D676A (**B**, **D**), were grown on coverslips and locally irradiated with a UV dose of 150 J/m^2 through filters with 5 μm pores and fixed 0.5 h after irradiation. The cells were immunolabelled with antibodies against XPC (green), PCNA (red) and CHAF150, the largest subunit of CAF-1 (red). Merged images indicate the overlay of XPC, PCNA or CHAF150 and DAPI staining. Scale bars, 10 μm.

incision, possibly by direct interaction with XPG (Gary *et al*, 1997). To distinguish between these possibilities, we investigated the recruitment of PCNA in various XP-F cells. Although PCNA was found at sites of UV damage in XP-F cells expressing wild-type XPF, PCNA did not colocalize with XPC in untransduced XP-F cells or in the XPF-D676A transductants (Figure 5B). These observations demonstrate that the recruitment of PCNA to sites of UV damage is dependent on the catalytic activity of XPF and, therefore, likely on active DNA repair synthesis. Consistent with this notion, the presence of Polδ at sites of UV damage also required catalytically active XPF (Supplementary Figure 1).

Having established that the recruitment of the replication machinery required the catalytic activity of XPF, but not that of XPG, we asked whether factors acting even later in NER could be recruited to sites of UV damage in the absence of XPG incision. We examined the recruitment of CHAF150, a subunit of the CAF-1 that is involved in the restoration of chromatin after an NER reaction (Green and Almouzni, 2003). CHAF150 behaved like PCNA in that its recruitment was dependent on the catalytic activity of XPF, but not on that of XPG (Figure 5D and C). These results are consistent with an earlier observation that CAF-1 is recruited to the sites of DNA damage in a PCNA-dependent manner (Green and Almouzni, 2003). The important novel conclusion is that even factors acting downstream of DNA repair synthesis can be recruited to sites of UV damage before the second incision 3′ to the lesion has occurred.

Partial unscheduled DNA synthesis occurs in the absence of 3′ incision by XPG

To test whether loading of PCNA to NER sites is able to stimulate DNA repair synthesis in the absence of 3′ incision *in vivo*, we examined DNA repair by unscheduled DNA synthesis (UDS) after UV irradiation of XP-G transductants expressing wild-type XPG or XPG-E791A. Wild-type XPG complemented the severe UDS defect of untransduced XP-G cells (102 versus 7%, with NER-proficient cells assayed in parallel set at 100%, Figure 6A). In line with the observed partial DNA repair synthesis *in vitro* and recruitment of PCNA, the very low UDS level of untransduced XP-G cells was significantly increased upon expression of the catalytically inactive XPG (from 7 to 49% UDS, Figure 6A). To try to ensure that this UV-induced DNA synthesis occurs at sites of NER rather than being a nonspecific artifact, we monitored repair synthesis at locally UV-damaged areas (Figure 6B). Although quantification is difficult, significant numbers of autoradiographic grains were found clustered together over non-S phase nuclei in NER-proficient cells and XP-G transductants expressing wild-type XPG (Figure 6B, upper panels). Very few grains were found over comparable nuclear areas of untransduced XP-G cells but the nuclei of

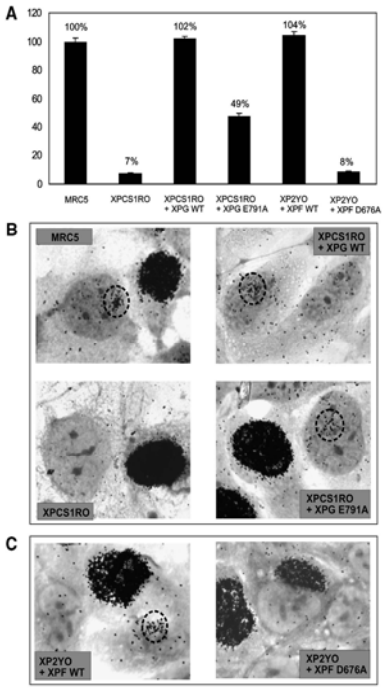

Figure 6 UDS in XP-F and XP-G cells transduced with wild-type and mutant *XPF* and *XPG*, respectively. (**A**). DNA repair synthesis or UV-induced UDS levels of different, as indicated, XP-F and XP-G cells, expressed as percentage of the UDS of an NER-proficient cell line (MRC5) assayed in parallel. (**B**, **C**) UDS in cells locally irradiated through a 5-μm microporous filter (60 J/m^2). NER-proficient MRC, XPCS1RO, XPCS1RO transduced with wild-type XPG and XPG-E791A (B) and XP2YO transduced with wild-type XPF or XPF-D676A (C). Heavily labelled cells were those in S-phase, incorporating large amounts of tritiated thymidine by replicative DNA synthesis. Dotted circles indicate the position of pores in which UV damage has been induced and UDS has been observed.

the XPG-E791A transductants exhibited a significant amount of grain clustering, roughly mid-way between the wild-type and XP-G levels (Figure 6B, lower panels). In contrast, the levels of UDS in XP-F cells expressing XPF-D676A (8% of wild type, Figure 6A) was at the same background level as untransduced XP-F cells, whereas UDS was restored to normal levels in cells expressing wild-type XPF (104%, Figure 6A). Local UDS experiments confirmed these findings; although UDS sites were clearly observed for XP-F transductants expressing wild-type XPF, they were not evident in XPF-D676A transductants (Figure 6C). Together, these results strongly suggest that the observed UDS is linked to sites of local UV damage, and that partial repair synthesis can occur in living cells in the absence of the catalytic activity of XPG, whereas it does require the catalytic activity of XPF.

Discussion

An unresolved longstanding issue for human NER is whether the 5′ and 3′ incisions, by ERCC1-XPF and XPG, respectively, occur in a strict temporal order and, if so, which one occurs first. A related issue is how these incisions are coordinated with DNA repair synthesis to prevent the exposure of potentially extremely damaging ssDNA gaps. We believe that the following observations described here provide novel and important insight into these issues.

First, the 5′ incision by ERCC1-XPF depends on the presence, but not catalytic activity, of XPG whereas efficient 3′ incision by XPG requires the catalytic activity of ERCC1-XPF (Figure 2), extending previous findings (Wakasugi *et al*, 1997; Constantinou *et al*, 1999; Tapias *et al*, 2004). Second, and most important, partial DNA synthesis is detectable *in vitro* in the presence of catalytically inactive XPG (Figure 3), thereby demonstrating that the incision 5′ to the lesion by ERCC1-XPF is both necessary and sufficient for the initiation of repair synthesis, whereas 3′ incision by XPG is needed for the completion, but not the initiation of repair synthesis. Third, some late NER factors, including the replication factors PCNA and Polymerase δ as well as the CAF-1, are recruited to sites of local UV damage in cells expressing catalytically inactive XPG, but not in cells expressing catalytically inactive XPF (Figure 5). Fourth, cells expressing catalytically inactive XPG, but not those expressing catalytically inactive XPF, are capable of undergoing intermediate levels of unscheduled DNA repair synthesis (Figure 6).

A defined temporal order for human NER incision and DNA repair synthesis events

Based on these observations we suggest that the human NER pathway does indeed have a defined temporal order for the 5′ and 3′ incisions and for DNA repair synthesis. Specifically, we propose the following model for the coordination of the dual incision and repair synthesis steps (Figure 7). After assembly of all the factors of the preincision complex, 5′ cleavage by ERCC1-XPF takes place, generating a free 3′-OH group. The repair synthesis machinery consisting minimally of polymerase δ, the clamp loader RFC and the processivity factor PCNA are recruited and repair synthesis is initiated. Which factors and interactions may facilitate this recruitment remains to be established, but it is possible that RPA has an important role in this transition (Riedl *et al*, 2003). DNA synthesis is then initiated and proceeds about half way through the repair patch. The stalling of the polymerase at this point might trigger the XPG endonuclease activity, allowing the repair synthesis to be completed. We have shown earlier that XPG has distinct requirements for binding and cleaving DNA (Hohl *et al*, 2003) raising the possibility that a conformational change in the NER complex brought about by the polymerase activity triggers the catalytic activity of XPG.

Due to the near simultaneous occurrence of the two incision reactions, we have not yet been able to prove that this reaction sequence is also favoured in a situation where wild-type XPF and XPG proteins are present. However, indirect support for our model comes from a recent study that considered the sequence of arrival and release of various NER factors during the dual incision and repair synthesis steps in NER using a fully reconstituted system (Mocquet *et al*, 2008). This study showed that ERCC1-XPF is released from repair

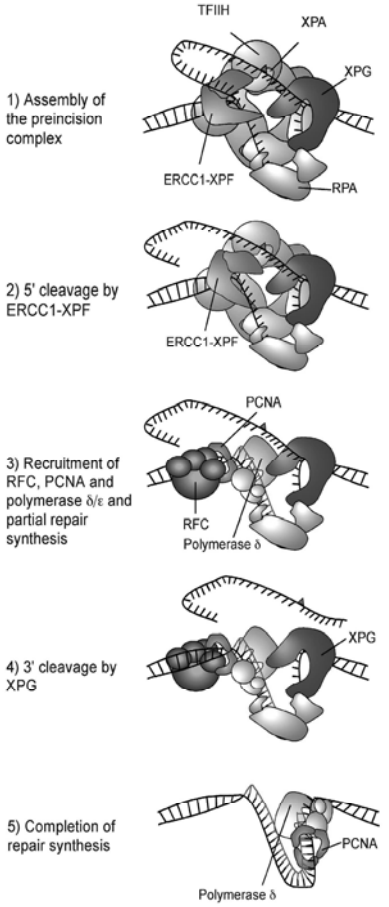

Figure 7 Model for the coordination of dual incision and repair synthesis steps in NER. Schematic representation of the proposed sequence of events following the assembly of the preincision complex. The red triangle stands for the DNA lesion. Individual proteins involved in each step are indicated.

complexes with the arrival of RFC, whereas XPG (and RPA) are only fully displaced once the entire repair synthesis machinery (RFC, PCNA and Polδ) has been recruited.

One prediction of our model is that the addition of DNA polymerase inhibitors might inhibit 3′ incision by XPG. We observed that addition of the Polδ inhibitor aphidicolin to an *in vitro* NER reaction did not show a significant inhibition of the 5′ or 3′ incision (data not shown), consistent with an earlier study (Moggs *et al*, 1996). Although further studies will be necessary to fully delineate the biochemical relationship of repair synthesis and the 3′ incision by XPG, it is interesting to note that a recent study found that treatment of cells with HU and AraC inhibited the removal of 6-4PPs (Moser *et al*, 2007). Although the molecular basis for this observation is currently unknown, it is consistent with our model and the notion that inhibition of repair synthesis blocks at least one of the incisions (presumably by XPG).

The model proposed here does not exclude an involvement of additional protein-protein interactions or protein modifications in the various steps. For example, it is known that XPG has a PIP box and that it can interact with PCNA (Gary *et al*, 1997). Although it has not yet been shown convincingly that the interaction between PCNA and XPG is required for NER, an interaction between the two proteins may contribute to the activation of the XPG incision. A recent study has implicated polκ in the repair synthesis step of NER (Ogi and Lehmann, 2006). It is possible that two polymerases, polδ and polκ, act at different steps of repair synthesis, for example before and after incision by XPG has taken place. Further studies will be required to determine how the various phases of repair synthesis in NER are regulated by protein-protein interactions and possibly post-translational modifications.

Apparent contradictions

One set of experimental observations appears to be in contrast with our results. Under very similar experimental conditions and using a variety of substrates either 5′ uncoupled (Matsunaga *et al*, 1995; Moggs *et al*, 1996) or 3′ uncoupled (Matsunaga *et al*, 1995; Mu *et al*, 1996; Evans *et al*, 1997a, b) incisions have been observed. Our model would predict that 3′ uncoupled incision by XPG should not occur at any appreciable frequency. One possible explanation is that ERCC1-XPF and XPG, can incise NER intermediates under certain conditions *in vitro* that would be disfavoured *in vivo*. It is known, for example, that the intrinsic structure-specific endonuclease activity of both ERCC1-XPF and XPG can be readily detected *in vitro* without the need for additional proteins (O'Donovan *et al*, 1994; Sijbers *et al*, 1996). Similarly, high relative concentration of XPG or the absence of ERCC1-XPF in a cell extract or reconstituted system may allow incision by XPG 3′ to the lesion in the absence of a properly assembled NER complex. We have shown earlier that XPG has distinct requirements for binding and cleaving DNA substrates and that the XPG spacer region has a critical role in mediating this substrate preference (Hohl *et al*, 2003, 2007; Dunand-Sauthier *et al*, 2005). We suggest that XPG is present in a catalytically inactive conformation before 5′ incision and partial repair synthesis and that its catalytic activity is revealed by a change in the complex brought about by partial repair synthesis. The barrier for XPG to cleave certain substrates does not occur at the level of substrate binding, but likely involves a subsequent rearrangement of an XPG-substrate complex (Hohl *et al*, 2003). We propose that a lowering of this activation barrier under certain experimental conditions leads to 3′ uncoupled incisions.

A 'cut-patch-cut-patch' mechanism

Early investigations of excision repair in bacteria focused on the discrimination between two models: 'patch and cut', involving a first incision close to the damage, followed by repair synthesis and second incision, and 'cut and patch', invoking excision of the damaged base/s before repair synthesis (Hanawalt, 1966; Hanawalt and Haynes, 1967). Subsequently, in particular with the ability to reconstitute

NER *in vitro*, and the ability to observe dual incision on NER substrates in the absence of repair synthesis, the 'cut and patch' model became accepted as the way by which NER operates (Aboussekhra *et al*, 1995; Mu *et al*, 1995; Moggs *et al*, 1996; Araujo *et al*, 2000).

The present work suggests that the human NER machinery operates via a 'cut-patch-cut-patch' mechanism that includes features of both previous models. Interestingly, long-patch base excision repair (BER) has been shown to proceed in a similar way. In long-patch BER, polymerase δ/ε, supported by the replication accessory factors RFC and PCNA or polymerase β, carries out repair synthesis past the abasic site and introduces 2–6 nucleotides. The short oligonucleotide overhang generated in this way is excised by the Flap endonuclease FEN-1, and the nick is sealed by DNA ligase I (Matsumoto *et al*, 1999; Pascucci *et al*, 1999). In line with this model, it was demonstrated that PCNA facilitates excision in long-patch BER (Gary *et al*, 1999). Stimulation of the dual incision by PCNA has also been observed in NER, leading to the proposal that PCNA may promote the turnover of the early NER factors (Nichols and Sancar, 1992) linking the excision and repair synthesis steps. Although many aspects of these important DNA repair processes remain to be discovered, it is interesting and unexpected that both NER and long-patch BER have operational similarities.

Materials and methods

Protein purification

Wild-type XPF, XPF D676A, XPF R678A, XPF E679A, XPF 681A, XPF E701A, XPF D704A, XPF E714A, XPF R715A, XPF K716A, XPF D720A, wild-type XPG and XPG E791A proteins were expressed in Sf9 insect cells and purified, as described earlier (Enzlin and Schärer, 2002; Hohl *et al*, 2003). The purity of the enzyme preparations was very similar to the ones reported earlier and 0.2–0.5 mg of proteins were obtained at concentrations of 0.2–0.3 mg/ml.

In vitro NER dual incision assay

Covalently closed circular DNA (pBluescript) containing a single 1,3-intrastrand d(GpTpG) cisplatin-DNA crosslink was prepared, as described earlier (Moggs *et al*, 1996) and additionally purified over two consecutive sucrose gradients. Reactions were carried out in a buffer containing 40 mM HEPES-KOH (pH 7.8), 70 mM KCl, 5 mM $MgCl_2$, 0.5 mM DTT, 2 mM ATP, 0.36 mg/ml BSA, 22 mM phosphocreatine (di-Tris salt) and 50 ng/μl creatine phosphokinase. Each reaction contained 200 ng DNA and 30 μg of cell-free extract prepared from XPG- or XPF-deficient fibroblast cells (XPCS1RO and XP2YO, respectively). Complementation was assayed upon addition of 730 fmol wild-type or mutant protein (XPG or XPF). Reactions were incubated at 30°C for 45 min. 50 nM of an oligonucleotide complementary to the excision product with a G_4 5′-overhang (5′-GGGGGAAGAGTGCACAGAAGAAGACCTGGTCGACC) was added, followed by heat inactivation at 95°C for 5 min. For detection of individual incisions, the incision reaction was inactivated by addition of 1 M EDTA, pH 8.0, 3% SDS and 12 μg proteinase K. DNA was extracted with phenol:chloroform and ethanol precipitated, as described earlier (Shivji *et al*, 1999), then 50 nM of an oligonucleotide complementary to the BssHII restriction site with a G_5 5′-overhang was added (5′-GGGGGCAATTAACCCTCACTAAAGGGAACAAAAGCTGG) followed by heat inactivation at 95°C for 5 min. After cooling down the reactions for 15 min at room temperature, 0.5 units of Sequenase and 3.5 μCi of [α-^{32}P]-dCTP (both from Amersham-Pharmacia, diluted in Sequenase dilution buffer) were added. Reactions were incubated for 3 min at 37°C prior the addition of 1.2 μl dNTP mix (100 μM of each dATP, dGTP, TTP and 50 μM dCTP) and incubation for another 12 min at 37°C. This fill-in reaction labelled the product using the G_4 overhang provided by the respective complementary oligonucleotides as a template. Reactions were stopped by addition of formamide loading buffer, heated at 95°C for 5 min and analysed on a 12 or 8% denaturing polyacrylamide sequencing gel. The gel was exposed on a phosphor screen and scanned on a PhosphorImager.

In vitro NER repair synthesis assay

The assay was performed using the same substrate, cell extracts and proteins as described for the excision assay. The reaction mixtures additionally contained 10 μM dATP, 10 μM dGTP, 5 μM dCTP, 5 μM TTP, 10 μCi of [α-^{32}P]-dCTP and 10 μCi [α-^{32}P]-TTP. Complementation was assayed upon addition of 600 fmol of wild-type or mutant protein (XPG or XPF). Reactions were incubated at 30°C for 3 h. DNA was purified using MinElute PCR Purification Kit (Qiagen), cleaved with *Kpn*I and *Sac*I or *Bsr*BI and *Xho*I and analysed on a 10% denaturing polyacrylamide sequencing gel.

Cell culture conditions and preparation of whole cell extracts

For the generation of whole cell extracts, SV40-transformed fibroblast cells XPCS1RO (XPG-deficient (Ellison *et al*, 1998) and XP2YO (XPF-deficient, GM08437) were cultured in Dulbecco's Modified Eagle's Medium (DMEM, Invitrogen) supplemented with 10% fetal calf serum and 2 mM L-glutamine, 100 U/ml penicillin, and 0.1 mg/ml streptomycin at 37°C in the presence of 5% CO_2. Cells were grown to near confluency, and whole cell extract was prepared accordingly to a published procedure (Biggerstaff and Wood, 1999).

Cell transduction with lentiviral recombinants

XPG wild-type cDNA, XPG-E791A cDNA were cloned into the pLOX/EWGFP lentiviral vector and XPF wild type (with a C-terminal HA tag) and XPF-D676A (with a C-terminal HA tag) cDNAs were cloned into the pWPXL lentiviral vector by replacing the GFP cDNA. Lentiviruses containing the different constructs under the control of the EF1α promoter were produced by co-transfecting 293T cells with the following three plasmids: the packaging plasmid pMD2G, the envelop plasmid psPAX2 and the lentiviral vector containing the different XPG and XPF cDNAs. Details of the vectors and protocols are described on the following Web site http://www.lentiweb.com. XP-G/CS (94RD27, patient XPCS1RO) and XP-F (XP2YO) SV40 immortalized fibroblasts at 50% confluency were infected with viral particles containing the different XPG and XPF recombinants. Transduced cells were then cultured in DMEM supplemented with 10% FCS, 2 mM L-glutamine, 100 U/ml penicillin and 0.1 mg/ml streptomycin in a 5% CO_2 humidified incubator. The transduction efficiency was further assessed by immunofluorescence.

Local UV irradiation and immunofluorescence

Local DNA damage infliction within cultured cells was performed, as described earlier (Mone *et al*, 2001). Briefly, cells cultured on coverslips were rinsed with PBS and covered with a micro-porous polycarbonate filter containing 5 μm pores (Millipore). Cells were irradiated through the filter with a Philips TUV lamp (254 nm) with a dose of 150 J/m^2. After UV −irradiation, cells were cultured for 0.5 h, washed first with PBS and then with PBS containing 0.05% Triton X-100 for 30 s before fixation with 3% paraformaldehyde for 15 min at room temperature or with ice-cold methanol for 20 min (for PCNA staining). Subsequently, cells were permeabilized by a 2 times 10 min incubation in PBS containing 0.1% Triton X-100, and washed with PBS$^+$ (PBS containing 0.15% glycine and 0.5% bovine serum albumin). For the experiments with Polδ, cells were incubated with Hu-AraC (10 mM HU, 0.1 mM AraC) from 30 min before irradiation until fixation and cells were fixed with MeOH rather than formaldehyde. Cells were incubated at room temperature with the primary antibody (diluted in PBS$^+$) for 2 h in a moist chamber. Subsequently cells were washed 5 times for 10 min. with PBS Triton X-100, washed with PBS$^+$, and incubated at room temperature with the secondary antibody (diluted in PBS$^+$) for 1 h in a moist chamber. Cells were washed 5 times for 10 min in PBS Triton X-100, washed in PBS, and embedded in Vectashield mounting medium (Vector) containing 0.1 mg of DAPI (4′-6′-diamidino-2-phenylindole)/ml.

Primary antibodies were as follows: mouse monoclonal anti-PCNA (Dako, clone PC10), 1:1000, rabbit polyclonal affinity purified anti-XPC (Ng *et al*, 2003), 1:300, rabbit polyclonal anti-XPB (TFIIH p89, S-19m Santa Cruz), 1:1000, mouse monoclonal anti-Polδ (A-9, Santa Cruz), 1:25, mouse monoclonal anti-CHAF150 (CAF-1) (abcam, ab7655), 1:2000, and mouse monoclonal FITC-conjugated

anti-HA (Roche, clone 3F10) Secondary antibodies were as follows: Cy3-conjugated goat anti-mouse (Jackson ImmunoResearch Laboratories), 1:1000, Cy3-conjugated goat anti-rabbit (Jackson ImmunoResearch Laboratories), 1:1000, and Alexa-488 conjugated goat anti-rabbit (Molecular Probes), 1:800.

Confocal microscopy

Confocal images of the cells were obtained using a Zeiss LSM 510 microscope equipped with a 25 mW Ar laser at 488 nm, a He/Ne 543 nm laser, and a 40 × 1.3 NA oil immersion lens. Alexa-488 was detected using a dichroic beam splitter (HFT 488), and an additional 505- to 530-nm bandpass emission filter. Cy3 was detected using a dichroic beam splitter (HFT 488/543) and a 560- to 615-nm bandpass emission filter.

Unscheduled DNA synthesis

To determine GG-NER activity in cultured cells, UV-induced DNA repair synthesis or UDS was measured. Coverslip cultures were rinsed with PBS, UV-irradiated (16 J/m^2, Philips 254 nm TUV lamp) and subsequently incubated for 2 h in culture medium supplemented with 20 μCi/ml [^{3}H-1′,2′]-thymidine (120 Ci/mmol, Amersham TRK565). After fixation coverslips were dipped in Ilford K2 photographic emulsion, exposed for three days an after development stained with Giemsa. Autoradiographic grains above the nuclei of 50 cells were counted and compared to the number of grains above nuclei of NER-proficient fibroblasts (MRC5, set at 100% UDS), assayed in parallel. UDS in locally damaged cells (local UDS) with 60 J/m^2 was performed in a similar fashion with the exception of an extended exposure time to six days.

Supplementary data

Supplementary data are available at *The EMBO Journal* Online (http://www.embojournal.org).

Acknowledgements

We acknowledge Philip C Hanawalt for insightful discussions regarding early models of NER. This work was supported by the Swiss National Science Foundation grants No. 3100A0-00744 and 3130-054873 to ODS and grant No. 3100A0-100487 and the 'Frontiers in Genetics' NCCR program to SGC, the New York State Office of Science and Technology and Academic Research (NYSTAR) grant No. C040069 and NIH grants No. GM080454 and CA092584 to ODS, the Human Frontier Science Organization grant RGP7/2004 to ODS and WV, ZonMW (Dutch Science Organization, NWO) grants No 912-03-012 and 917-46-364 to WV, NWO grant 805-47-193 to AMG and WV and EU grant MRTN-CT-2003-503618 to WV and AMG. LS was supported in part by EMBO short-term fellowship ASTF191.00-05.

References

Aboussekhra A, Biggerstaff M, Shivji MK, Vilpo JA, Moncollin V, Podust VN, Protic M, Hübscher U, Egly JM, Wood RD (1995) Mammalian DNA nucleotide excision repair reconstituted with purified protein components. *Cell* **80:** 859–868

Araujo SJ, Tirode F, Coin F, Pospiech H, Syvaoja JE, Stucki M, Hübscher U, Egly JM, Wood RD (2000) Nucleotide excision repair of DNA with recombinant human proteins: definition of the minimal set of factors, active forms of TFIIH, and modulation by CAK. *Genes Dev* **14:** 349–359

Bardwell AJ, Bardwell L, Tomkinson AE, Friedberg EC (1994) Specific cleavage of model recombination and repair intermediates by the yeast Rad1-Rad10 DNA endonuclease. *Science* **265:** 2082–2085

Berneburg M, Lowe JE, Nardo T, Araujo S, Fousteri MI, Green MH, Krutmann J, Wood RD, Stefanini M, Lehmann AR (2000) UV damage causes uncontrolled DNA breakage in cells from patients with combined features of XP-D and Cockayne syndrome. *EMBO J* **19:** 1157–1166

Biggerstaff M, Wood RD (1999) Assay for nucleotide excision repair protein activity using fractionated cell extracts and UV-damaged plasmid DNA. *Methods Mol Biol* **113:** 357–372

Constantinou A, Gunz D, Evans E, Lalle P, Bates PA, Wood RD, Clarkson SG (1999) Conserved residues of human XPG protein important for nuclease activity and function in nucleotide excision repair. *J Biol Chem* **274:** 5637–5648

de Laat WL, Jaspers NG, Hoeijmakers JHJ (1999) Molecular mechanism of nucleotide excision repair. *Genes Dev* **13:** 768–785

Dunand-Sauthier I, Hohl M, Thorel F, Jaquier-Gubler P, Clarkson SG, Schärer OD (2005) The spacer region of XPG mediates recruitment to nucleotide excision repair complexes and determines substrate specificity. *J Biol Chem* **280:** 7030–7037

Ellison AR, Nouspikel T, Jaspers NG, Clarkson SG, Gruenert DC (1998) Complementation of transformed fibroblasts from patients with combined xeroderma pigmentosum-Cockayne syndrome. *Exp Cell Res* **243:** 22–28

Enzlin JH, Schärer OD (2002) The active site of XPF-ERCC1 forms a highly conserved nuclease motif. *EMBO J* **21:** 2045–2053

Essers J, Theil AF, Baldeyron C, van Cappellen WA, Houtsmuller AB, Kanaar R, Vermeulen W (2005) Nuclear dynamics of PCNA in DNA replication and repair. *Mol Cell Biol* **25:** 9350–9359

Evans E, Fellows J, Coffer A, Wood RD (1997a) Open complex formation around a lesion during nucleotide excision repair provides a structure for cleavage by human XPG protein. *EMBO J* **16:** 625–638

Evans E, Moggs JG, Hwang JR, Egly JM, Wood RD (1997b) Mechanism of open complex and dual incision formation by human nucleotide excision repair factors. *EMBO J* **16:** 6559–6573

Friedberg EC, Walker GC, Siede W, Wood RD, Schultz RA, Ellenberger T (2005) *DNA Repair and Mutagenesis*, 2nd edn. Washington DC: ASM Press

Gary R, Dale LL, Cornelius HL, MacInnes MA, Park MS (1997) The DNA repair endonuclease XPG binds to Proliferating Cell Nuclear Antigen (PCNA) and shares sequence elements with the PCNA-binding regions of FEN-1 and cyclin-dependent kinase inhibitor p21. *J Biol Chem* **272:** 24522–24529

Gary R, Kim K, Cornelius HL, Park MS, Matsumoto Y (1999) Proliferating cell nuclear antigen facilitates excision in long-patch base excision repair. *J Biol Chem* **274:** 4354–4363

Gillet LC, Schärer OD (2006) Molecular mechanisms of mammalian global genome nucleotide excision repair. *Chem Rev* **106:** 253–276

Green CM, Almouzni G (2003) Local action of the chromatin assembly factor CAF-1 at sites of nucleotide excision repair *in vivo*. *EMBO J* **22:** 5163–5174

Hanawalt PC (1966) Repair replication in the bacterial genome. In *Genetical Aspects of Radiosensitivity: Mechanisms of Repair* Vol. 24, pp 97–104. Vienna: International atomic energy agency

Hanawalt PC (2002) Subpathways of nucleotide excision repair and their regulation. *Oncogene* **21:** 8949–8956

Hanawalt PC, Haynes RH (1967) The repair of DNA. *Sci Am* **216:** 36–43

Hansson J, Munn M, Rupp WD, Kahn R, Wood RD (1989) Localization of DNA repair synthesis by human cell extracts to a short region at the site of a lesion. *J Biol Chem* **264:** 21788–21792

Hohl M, Dunand-Sauthier I, Staresincic L, Jaquier-Gubler P, Thorel F, Modesti M, Clarkson SG, Schärer OD (2007) Domain swapping between FEN-1 and XPG defines regions in XPG that mediate nucleotide excision repair activity and substrate specificity. *Nucleic Acids Res* **35:** 3053–3063

Hohl M, Thorel F, Clarkson SG, Schärer OD (2003) Structural determinants for substrate binding and catalysis by the structure-specific endonuclease XPG. *J Biol Chem* **278:** 19500–19508

Matsumoto Y, Kim K, Hurwitz J, Gary R, Levin DS, Tomkinson AE, Park MS (1999) Reconstitution of proliferating cell nuclear antigen-dependent repair of apurinic/apyrimidinic sites with purified human proteins. *J Biol Chem* **274:** 33703–33708

Matsunaga T, Mu D, Park CH, Reardon JT, Sancar A (1995) Human DNA repair excision nuclease. Analysis of the roles of the subunits involved in dual incisions by using anti-XPG and anti-ERCC1 antibodies. *J Biol Chem* **270:** 20862–20869

Min JH, Pavletich NP (2007) Recognition of DNA damage by the Rad4 nucleotide excision repair protein. *Nature* **449:** 570–575

Mocquet V, Laine JP, Riedl T, Yajin Z, Lee MY, Egly JM (2008) Sequential recruitment of the repair factors during NER: the role of XPG in initiating the resynthesis step. *EMBO J* **27:** 155–167

Moggs JG, Yarema KJ, Essigmann JM, Wood RD (1996) Analysis of incision sites produced by human cell extracts and purified proteins during nucleotide excision repair of a 1,3-intrastrand d(GpTpG)-cisplatin adduct. *J Biol Chem* **271:** 7177–7186

Mone MJ, Volker M, Nikaido O, Mullenders LH, van Zeeland AA, Verschure PJ, Manders EM, van Driel R (2001) Local UV-induced DNA damage in cell nuclei results in local transcription inhibition. *EMBO Rep* **2:** 1013–1017

Moser J, Kool H, Giakzidis I, Caldecott K, Mullenders LH, Fousteri MI (2007) Sealing of chromosomal DNA nicks during nucleotide excision repair requires XRCC1 and DNA ligase III alpha in a cell-cycle-specific manner. *Mol Cell* **27:** 311–323

Mu D, Hsu DS, Sancar A (1996) Reaction mechanism of human DNA repair excision nuclease. *J Biol Chem* **271:** 8285–8294

Mu D, Park CH, Matsunaga T, Hsu DS, Reardon JT, Sancar A (1995) Reconstitution of human DNA repair excision nuclease in a highly defined system. *J Biol Chem* **270:** 2415–2418

Mu D, Wakasugi M, Hsu DS, Sancar A (1997) Characterization of reaction intermediates of human excision repair nuclease. *J Biol Chem* **272:** 28971–28979

Ng JMY, Vermeulen W, van der Horst GTJ, Bergink S, Sugasawa K, Vrieling H, Hoeijmakers JHJ (2003) A novel regulation mechanism of DNA repair damage-induced and RAD23-dependent stabilization of xeroderma pigmentosum group C protein. *Genes Dev* **17:** 1630–1645

Nichols AF, Sancar A (1992) Purification of PCNA as a nucleotide excision repair protein. *Nucleic Acids Res* **20:** 2441–2446

O'Donovan A, Davies AA, Moggs JG, West SC, Wood RD (1994) XPG endonuclease makes the 3′ incision in human DNA nucleotide excision repair. *Nature* **371:** 432–435

Ogi T, Lehmann AR (2006) The Y-family DNA polymerase kappa (pol kappa) functions in mammalian nucleotide-excision repair. *Nat Cell Biol* **8:** 640–642

Pascucci B, Stucki M, Jonsson ZO, Dogliotti E, Hübscher U (1999) Long patch base excision repair with purified human proteins. DNA ligase I as patch size mediator for DNA polymerases delta and epsilon. *J Biol Chem* **274:** 33696–33702

Riedl T, Hanaoka F, Egly JM (2003) The comings and goings of nucleotide excision repair factors on damaged DNA. *EMBO J* **22:** 5293–5303

Schärer OD (2007) Achieving broad substrate specificity in damage recognition by binding accessible nondamaged DNA. *Mol Cell* **28:** 184–186

Shechter D, Costanzo V, Gautier J (2004) Regulation of DNA replication by ATR: signaling in response to DNA intermediates. *DNA Repair (Amst)* **3:** 901–908

Shivji MK, Moggs JG, Kuraoka I, Wood RD (1999) Dual-Incision Assays for Nucleotide Excision Repair Using DNA with a Lesion at a Specific Site. *Methods Mol Biol* **113:** 373–392

Shivji MK, Podust VN, Hübscher U, Wood RD (1995) Nucleotide excision repair DNA synthesis by DNA polymerase epsilon in the presence of PCNA, RFC, and RPA. *Biochemistry* **34:** 5011–5017

Sijbers AM, de Laat WL, Ariza RR, Biggerstaff M, Wei YF, Moggs JG, Carter KC, Shell BK, Evans E, de Jong MC, Rademakers S, de Rooij J, Jaspers NG, Hoeijmakers JH, Wood RD (1996) Xeroderma pigmentosum group F caused by a defect in a structure-specific DNA repair endonuclease. *Cell* **86:** 811–822

Sugasawa K, Ng JMY, Masutani C, Iwai S, van der Spek PJ, Eker APM, Hanaoka F, Bootsma D, Hoeijmakers JHJ (1998) Xeroderma pigmentosum group C protein complex is the initiator of global genome nucleotide excision repair. *Mol Cell* **2:** 223–232

Sugasawa K, Okamoto T, Shimizu Y, Masutani C, Iwai S, Hanaoka F (2001) A multistep damage recognition mechanism for global genomic nucleotide excision repair. *Genes Dev* **15:** 507–521

Svejstrup JQ (2002) Mechanisms of Transcription-Coupled DNA Repair. *Mol Cell Biol* **3:** 21–29

Tapias A, Auriol J, Forget D, Enzlin JH, Schärer OD, Coin F, Coulombe B, Egly JM (2004) Ordered conformational changes in damaged DNA induced by nucleotide excision repair factors. *J Biol Chem* **279:** 19074–19083

Theron T, Fousteri MI, Volker M, Harries LW, Botta E, Stefanini M, Fujimoto M, Andressoo JO, Mitchell J, Jaspers NG, McDaniel LD, Mullenders LH, Lehmann AR (2005) Transcription-associated breaks in xeroderma pigmentosum group D cells from patients with combined features of xeroderma pigmentosum and Cockayne syndrome. *Mol Cell Biol* **25:** 8368–8378

Thorel F, Constantinou A, Dunand-Sauthier I, Nouspikel T, Lalle P, Raams A, Jaspers NG, Vermeulen W, Shivji MK, Wood RD, Clarkson SG (2004) Definition of a short region of XPG necessary for TFIIH interaction and stable recruitment to sites of UV damage. *Mol Cell Biol* **24:** 10670–10680

Tirode F, Busso D, Coin F, Egly JM (1999) Reconstitution of the transcription factor TFIIH: assignment of functions for the three enzymatic subunits, XPB, XPD, and cdk7. *Mol Cell* **3:** 87–95

Tsodikov OV, Ivanov D, Orelli B, Staresincic L, Shoshani I, Oberman R, Schärer OD, Wagner G, Ellenberger T (2007) Structural basis for the recruitment of ERCC1-XPF to nucleotide excision repair complexes by XPA. *EMBO J* **26:** 4768–4776

Volker M, Mone MJ, Karmakar P, van Hoffen A, Schul W, Vermeulen W, Hoeijmakers JH, van Driel R, van Zeeland AA, Mullenders LH (2001) Sequential assembly of the nucleotide excision repair factors *in vivo*. *Mol Cell* **8:** 213–224

Wakasugi M, Reardon JT, Sancar A (1997) The non-catalytic function of XPG protein human nucleotide excision repair. *J Biol Chem* **272:** 16030–16034

Wakasugi M, Sancar A (1998) Assembly, subunit composition, and footprint of human DNA repair excision nuclease. *Proc Natl Acad Sci USA* **95:** 6669–6674

Chapter 4

~

RFC recruits DNA polymerase δ to sites of NER but is not required for PCNA recruitment

Mol Cell Biol, in press

MOLECULAR AND CELLULAR BIOLOGY , Oct. 2010, p. 000 Vol. 30, No. 20
0270-7306/10/$12.00 doi:10.1128/MCB.00285-10

Replication Factor C Recruits DNA Polymerase δ to Sites of Nucleotide Excision Repair but Is Not Required for PCNA Recruitment ▽

René M . Overmeer,[2]† Audrey M. Gourdin,[1]† Ambra Giglia-Mari,[1,5] Hanneke Kool,[2] Adriaan B. Houtsmuller,[3] Gregg Siegal,[4] Maria I. Fousteri,[2,6] Leon H. F. Mullenders,[2]* and Wim Vermeulen[1]*

Department of Genetics, Erasmus MC, Dr. Molewaterplein 50, 3015 GE Rotterdam, Netherlands[1]; Department of Toxicogenetics, Leiden University Medical Center, 2333 RC Leiden, Netherlands[2]; Department of Pathology, Erasmus MC, Dr. Molewaterplein 50, 3015 GE Rotterdam, Netherlands[3]; Leiden Institute of Chemistry, Leiden University, Einsteinweg 55 2300 RA Leiden, Netherlands[4]; CNRS, Institut de Pharmacologie et de Biologie Structurale, 205 route de Narbonne, F-31077 Toulouse, France[5]; and Biomedical Sciences Research Center Alexander Fleming, Vari 166-72, Greece[6]

Received 15 March 2010/Returned for modification 20 April 2010/Accepted 28 July 2010

Nucleotide excision repair (NER) operates through coordinated assembly of repair factors into pre- and postincision complexes. The postincision step of NER includes gap-filling DNA synthesis and ligation. However, the exact composition of this NER-associated DNA synthesis complex in vivo and the dynamic interactions of the factors involved are not well understood. Using immunofluorescence, chromatin immunoprecipitation, and live-cell protein dynamic studies, we show that replication factor C (RFC) is implicated in postincision NER in mammalian cells. Small interfering RNA-mediated knockdown of RFC impairs upstream removal of UV lesions and abrogates the downstream recruitment of DNA polymerase delta. Unexpectedly, RFC appears dispensable for PCNA recruitment yet is required for the subsequent recruitment of DNA polymerases to PCNA, indicating that RFC is essential to stably load the polymerase clamp to start DNA repair synthesis at 3′ termini. The kinetic studies are consistent with a model in which RFC exchanges dynamically at sites of repair. However, its persistent localization at stalled NER complexes suggests that RFC remains targeted to the repair complex even after loading of PCNA. We speculate that RFC associates with the downstream 5′ phosphate after loading; such interaction would prevent possible signaling events initiated by the RFC-like Rad17 and may assist in unloading of PCNA.

A multitude of endogenous and exogenous genotoxic agents induce damage to DNA. When not repaired properly, these DNA lesions can interfere with replication and transcription and thereby induce deleterious events (i.e., cell death, mutations, and genomic instability) that affect the fate of organisms (18). To ensure the maintenance of the DNA helix integrity, a network of defense mechanisms has evolved including accurate and efficient DNA repair processes. One of these processes is the nucleotide excision repair (NER) pathway that removes a wide range of DNA helix-distorting lesions, such as sunlight-induced photodimers, for example, cyclobutane pyrimidine dimers (CPD) and pyrimidine 6-4 pyrimidone photoproducts (6-4PP). Within NER, more than 30 polypeptides act coordinately, starting from the detection and removal of the lesion up to the restoration of the DNA sequence and chromatin structure. The importance of NER is underlined by the severe clinical consequences associated with inherited NER defects, causing UV-hypersensitive autosomal recessive syndromes: the cancer-predisposing xeroderma pigmentosum (XP) and the premature ageing and neurodegenerative disorders Cockayne syndrome (CS) and trichothiodystrophy (TTD) (27).

The initial DNA damage recognition step in NER involves two subpathways: transcription-coupled repair (TC-NER) and global genome repair (GG-NER). TC-NER is responsible for the rapid removal of transcription-blocking DNA lesions and is initiated when elongating RNA polymerase II stalls at a DNA lesion on the transcribed strand (16). In GG-NER, which removes lesions throughout the genome, damage recognition is facilitated by the concerted action of the heterodimeric XP group C (XPC)-HR23B protein complex and by the UV-damaged DNA-binding protein (UV-DDB) complex (10, 33). Subsequently, the 10-subunit TFIIH complex unwinds the DNA around the lesion. This partially unwound structure is stabilized by the single-strand binding protein replication protein A (RPA) and the damage-verifying protein XPA. Collectively, these proteins load and properly orient the structure-specific endonucleases XPF-ERCC1 and XPG that incise 5′ and 3′ of the damage, respectively, creating a single-strand gap of approximately 30 nucleotides (nt) (14, 40). The postincision stage of NER consists of gap-filling DNA synthesis (repair replication), ligation, and restoration of chromatin structure. These steps involve various factors that are also implicated in replicative DNA synthesis. For gap-filling synthesis the proliferating cell nuclear antigen (PCNA) is recruited and loaded onto the 3′ double-stranded DNA (dsDNA)–single-strand junction.

* Corresponding author. Mailing address for Leon H. F. Mullenders: Department of Toxicogenetics, Leiden University Medical Center, 2333 RC Leiden, Netherlands. Phone: [illegible]. Fax: [illegible]. E-mail: [illegible]. Mailing address for Wim Vermeulen: Department of Genetics, Erasmus MC, Dr. Molewaterplein 50, 3015 GE Rotterdam, Netherlands. Phone: 31 10 4087194. Fax: 31 10 4089468. E-mail: w.vermeulen@erasmusmc.nl.

† R.M.O. and A.M.G. contributed equally.

▽ Published ahead of print on 16 August 2010.

This facilitates DNA synthesis by several DNA polymerases including polymerase epsilon (Pol ε) and polymerase delta (Pol δ), the latter of which has been shown to require polymerase kappa (Pol κ) for efficient repair synthesis (35). The resulting nick is sealed by either DNA ligase III/XRCC1 in quiescent cells or by both DNA ligase III/XRCC1 and DNA ligase I in dividing cells (32). Finally, chromatin assembly factor 1 (CAF-1) facilitates the restoration of the chromatin (15).

PCNA is a mobile platform for a large number of proteins involved in DNA replication and repair. In eukaryotes, PCNA forms a very stable homotrimeric ring, which must be opened to be loaded around dsDNA. During nuclear DNA replication this task is performed by replication factor C (RFC) at a primer-template junction in an ATP-dependent reaction (41, 48). RFC consists of five subunits, RFC1 to RFC5 (RFC1-5) (140, 40, 37, 38, and 36 kDa), which share a large extent of homology (46). In in vitro reconstituted NER assays, purified RFC was able to perform the loading of PCNA (4, 30) in a manner similar to that observed for in vitro replicative DNA synthesis. However, the role of RFC as the responsible clamp-loader in NER has not been proven in vivo. Moreover, XPG possesses PCNA binding capacity and has been implicated in the recruitment of PCNA to incised DNA (12, 30, 40). Nevertheless, the involvement of RFC in other DNA repair pathways is supported by a recent study in living cells showing that both green fluorescent protein (GFP)-tagged RFC and PCNA accumulate rapidly at sites of single- and double-strand breaks induced by UVA laser irradiation (17).

The uncertainty concerning the role of RFC in loading PCNA during NER is even further extended by the presence of other RFC-like complexes with largely unknown functions in which the four smaller subunits of RFC are associated with other proteins. First, the heteropentameric complex of Ctf18 and RFC2-5 was shown to associate with two other factors, Dcc1 and Ctf8, and is implicated in sister chromatid cohesion during mitosis (24). Interestingly, in vitro data show that the Ctf18 complex is able, though in an inefficient manner, to perform the loading/unloading of PCNA (38). PCNA has also been shown to interact with Elg1-RFC, another RFC-like complex (23). Little is known about this complex except that it is involved in genome stability (25). The most studied RFC-like complex in eukaryotes is the Rad17-RFC protein complex that plays an important role in the DNA damage response. In vitro studies reported that Rad17-RFC does not load PCNA itself but a PCNA-like sliding clamp formed by Rad9-Rad1-Hus1 (also known as 9-1-1) at 5′ termini of double- and single-stranded DNA junctions (5, 7). This loading leads to the activation of an ATR-dependent DNA damage signaling pathway and subsequent activation of cell cycle checkpoints (36).

In order to separate replication factor C from these alternative RFC-like complexes and to study its role and behavior in repair, we focused our study on the unique component, i.e., the largest subunit, or RFCp140 (RFC1). The data show that RFCp140 dynamically interacts with other NER postincision factors in a UV-dependent fashion but unexpectedly associates with the repair site even after loading PCNA, suggestingadditional roles of RFC in the postincision step of NER.

MATERIALS AND METHODS

Cell lines and culture conditions. All cells were grown under standard conditions at 37°C and 5% CO_2: simian virus 40 (SV40)-immortalized fibroblasts, MRC5 (wild type), C5ROhtert-GFP-hPCNA cells (9), and XPCS2BA (XPB) cells transfected with pEGFP were grown in a 1:1 mixture of Ham's F-10 medium and Dulbecco's modified Eagle's medium (DMEM) supplemented with 10% fetal calf serum (FCS) and 1% penicillin-streptomycin (PS). Human diploid primary fibroblasts or human telomerase reverse transcriptase (hTERT)-immortalized fibroblasts derived from a healthy individual (VH10 cells) or from NER patients (XP25RO, XP21RO, XP51RO and XPCS1RO, corresponding to XP group A, C, F, and G cells, respectively), and human quasi-diploid bladder carcinoma cells (EJ30) were grown on DMEM with 10% FCS and 1% PS. G418 (600 μg/ml) was added as a selection marker where appropriate. To study quiescent cells, the cells were grown to confluence and subsequently incubated for 5 days with medium containing 0.2% FCS.

Global and local UV irradiation. Prior to (confocal) microscopy and immunofluorescence experiments, cells were seeded on 24-mm coverslips (Menzol), coated with Alcian blue (Fluka), rinsed with phosphate-buffered saline (PBS), and irradiated with a Philips TUV lamp (predominantly 254 nm). After irradiation cells were incubated with their original medium before being processed for microscopy experiments or immunofluorescence. For local irradiation cells were covered with a microporous polycarbonate filter containing 3-, 5-, or 8-μm pores (Millipore, Bradford, MA) as previously described (31, 45). For living-cell studies, the UV doses were as follows: for cells irradiated with a lamp through the filter, the UV dose induced was 120 J/m^2; for cells treated with hydroxyurea/cytosine-β-arabinofuranoside (HU/Ara-C), the irradiation dose was 30 J/m^2; for the UVC laser, the scanning time was 500 ms.

Immunofluorescence. Experiments were performed as described previously (32). All immunofluorescence experiments were performed using hTERT-immortalized cells, with the exception of XPF cells, which were primary. Prior to fixation cells were kept on ice and washed with PBS. If required, PBS–0.2% Triton X-100 (Triton wash) was added to the cells for 5 min. Cells were fixed and permeabilized by adding PBS containing 2% paraformaldehyde for 10 min, followed by a 5-min incubation in 0.2% Triton X-100. After fixation and permeabilization, slides were washed with PBS and blocked with 3% BSA in PBS for 30 min. Slides were incubated with primary and secondary antibodies diluted in PBS containing 0.5% BSA–0.05% Tween 20 for 2 h and 1 h at room temperature, respectively, with 1.5 μg/ml 4′,6′-diamidino-2-phenylindole (DAPI) added to the secondary antibody solution. After each antibody the slides were washed three times with PBS–0.05% Tween 20. Slides were then mounted with Polymount (Polysciences Inc., Warrington, PA). For the competition experiments, hydroxyurea (Fluka) and cytosine-β-arabinofuranoside were added to the medium 30 min prior to the first irradiation, with final concentrations of 10 mM and 100 μM, respectively.

6-4PP repair analysis. To measure 6-4PP repair, cells were treated as described above and irradiated with 15 J/m^2 of UVC. After 1, 2, 4, or 8 h of repair, cells were fixed and stained for the presence of 6-4PP using 6-4PP-recognizing antibodies (see below). Microscopy settings used for quantification of fluorescent signal have been described previously (33). In short, images were taken with equal exposure times, and the total fluorescence per nuclei was measured for 50 to 100 nuclei per point per experiment (Axiovision software). Graphs represent the average of four independent experiments.

Quantitative spot analysis. To quantify spot incidence and intensity, cells were locally irradiated (8 μm) with 30 J/m^2 and stained for XPA and PCNA or XPA and Polδ. Spot incidence was measured by manually scoring >100 cells containing XPA local UVC damage (LUD) for colocalization of PCNA or Polδ. Spot intensity was measured by making images with identical exposure settings. Subsequently, the XPA LUD was used to define the spot area and the XPA, PCNA, or Polδ average signal intensity within the spot was measured (Axiovision software). Cells scored negative for PCNA or Polδ spot incidences were excluded from further analysis. The average spot intensities of >100 cells were measured for each point.

Antibodies. Primary antibodies were rabbit polyclonal anti-PCNA (Ab2426; Abcam), mouse monoclonal anti-PCNA (PC10 Ab29; Abcam and Dako), anti-GFP (clone 7.1 and 13.1, Roche), anti-DNA Polδ (Abcam), anti-RPA (Abcam), anti-XRCC1 (Santa Cruz), anti-6-4PP dimer (clone 64 M-2; Cosmo Bio), rabbit polyclonal anti-p89 (Santa Cruz), anti-RFC5 (Abcam), anti-Ki67 (Ab16667; Abcam), anti-DNA Polδ (Santa Cruz), and goat polyclonal anti-RFC1 (Ab3566; Abcam). Mouse monoclonal anti-RFC1 was a kind gift of B. Stillman, Cold Spring Harbor Laboratory, and rabbit polyclonal anti-Lig1 was a gift from A. E. Tomkinson, University of Baltimore, Baltimore, MD. Whereas mouse monoclo-

nal anti-RFC1 was used for immunofluorescence, goat polyclonal anti-RFC1 was used for Western analysis.

Secondary antibodies for immunofluorescence staining were Cy3-conjugated goat anti-mouse, Cy3-conjugated goat anti-rabbit IgG and fluorescein isothiocyanate (FITC)-conjugated donkey anti-mouse (Jackson ImmunoResearch Laboratories), Alexa Fluor 488-conjugated goat anti-mouse IgG, Alexa Fluor 488-conjugated goat anti-rabbit (references), and Alexa Fluor 555-conjugated goat anti-rabbit (Molecular Probes). For Western blotting, the following were used: horseradish peroxidase (HRP)-coupled polyclonal rabbit anti-mouse and polyclonal donkey anti-rabbit (DakoCytomation), IR700-coupled donkey anti-goat and donkey anti-rabbit, and IR800-coupled donkey anti-mouse. All secondary antibodies were used according to the manufacturer's instructions.

Subcellular fractionation and immunoprecipitation. For coimmunoprecipitation (co-IP) studies, non-cross-linked cells were fractionated by adaptation of an Abcam protocol (1). After trypsinization and a PBS wash, cells were resuspended in 10 mM HEPES (pH 7.9), 1.5 mM $MgCl_2$, 10 mM KCl, 0.5 mM dithiothreitol (DTT), and 0.05% NP-40 (or Igepal) and left on ice for 10 min and centrifuged at 3,000 rpm for 10 min at 4°C. The pellet was resuspended in 5 mM HEPES (pH 7.9), 1.5 mM $MgCl_2$, 0.2 mM EDTA, 0.5 mM DTT, and 26% glycerol (vol/vol) and supplemented with 5 M NaCl to a final concentration of 400 mM. The solution was homogenized by pipetting 20 times through a 200-μl fine tip and kept for 1 h on ice. The supernatant (soluble fraction) was aliquoted after being spun for 60 min at 13,200 rpm at 4°C. The pellet (chromatin fraction) was dissolved in SDS sample buffer.

Co-IP reactions were performed in binding buffer (20 mM HEPES-KOH [pH 7.8], 1 mM EDTA, 0.5 mM EGTA, 0.15 M NaCl, 10% glycerol, 0.1% Triton X-100, 1 mM phenylmethylsulfonyl fluoride [PMSF], and a mixture of protease/phosphatase inhibitors) overnight at 4°C. For each reaction, 400 mg of nuclear extract was immunoprecipitated with 0.5 to 3 μg of antibody. Immunocomplexes were then collected by adsorption for 1 h at 4°C to precleared protein A or G beads (Upstate). The beads/immunocomplexes were subsequently washed five times with 20 bed volumes of binding buffer containing 300 mM NaCl and 0.5% Triton X-100. Finally, they were resuspended in 1 bed volume of SDS sample buffer, incubated for 10 min at 95°C, and analyzed by Western blotting.

ChIP. In vivo cross-linking and chromatin immunoprecipitation (ChIP) were performed as described previously (11). Briefly, human quasi-diploid bladder carcinoma cells (EJ30 cells) were incubated for 40 min after UV irradiation (time corresponding to a maximal amount of NER complexes). Cells were cross-linked at 4°C with 1% formaldehyde buffer and lysed, and chromatin was purified and fractionated. For each ChIP reaction, an equal amount of cross-linked chromatin extract was added to the mixture and incubated overnight in 1× radioimmunoprecipitation assay (RIPA) buffer with 0.5 to 3 μg of a specific antibody. Antibody complexes were bound by adding precleared protein A or G beads (Upstate). The supernatant (unbound fraction) was kept, and the beads were washed for a total of six times with increasing stringency. Antibody and bound complexes were then eluted by boiling the beads in 1 bed volume of 2× Laemmli SDS sample buffer for 30 min to 1 h at 95°C, which reversed the cross-linking, and analyzed by SDS-PAGE. Coprecipitating proteins were analyzed by Western blotting.

Knockdown of RFCp140. A total of 10^6 of hTERT-immortalized fibroblasts were seeded per p90 dish, followed by three rounds of transfection with HiPerfect and control RNA (small interfering RNA [siRNA] directed against GFP [siGPF] or siRFC; Smartpool, Dharmacon) (see reference 35 for details) at 24 h, 48 h, and 96 h after seeding. Experiments were done 72 h after the last transfection.

Confocal microscopy. (i) Live-cell microscopy. Confocal images of the cells were obtained using a Zeiss LSM 510 microscope equipped with a 25-mW Ar laser at 488 nm and a 40×, 1.3-numerical aperture (NA) oil immersion lens. GFP fluorescence was detected using a dichroic beam splitter (HFT 488), a beam splitter (NFT 490), and an additional 505- to 550-nm band-pass emission filter.

(ii) Fixed cells. For images of cells after immunofluorescence, the 25-mW Ar laser at 488 nm together with a He/Ne 543-nm laser, and a 40×, 1.3-NA oil immersion lens were used. Alexa Fluor 488 was detected using a dichroic beam splitter (HFT 488) and an additional 505- to 530-nm band-pass emission filter. Cy3 was detected using a dichroic beam splitter (HFT 488/543) and a 560- to 615-nm band-pass emission filter.

Photobleaching procedures. (i) Half-nucleus bleaching combined with FLIP-FRAP. Data analysis was performed in the following way (schematically illustrated in Fig. 5): the fluorescence recovery (FRAP) in the bleached area was subtracted from the fluorescence loss (FLIP) in the nonbleached part of the nucleus. The difference in fluorescence signal between the FLIP and FRAP areas before bleaching was set at 0, and the difference in fluorescence between the FLIP and FRAP areas after bleaching was normalized to 1 and plotted against the time after bleaching. The mobility of the protein was determined as the time necessary for FLIP-FRAP to return to 0 (i.e., the time required to reach full redistribution of bleached and nonbleached molecules).

(ii) FRAP in local damage. The entire local damage was bleached in 1.2 s by two bleaching pulses, and the recovery of fluorescence was monitored for 60 s by scanning the whole cell every 5 s. To overcome the variability in the size and intensity of the damage (i.e., the number of proteins immobilized), the curve was normalized to the overall fluorescence in the cell (including the local damage itself).

RESULTS

Involvement of replication factor C in nucleotide excision repair in vivo. To investigate the involvement of RFC in NER, we assessed the subcellular distribution of endogenous mammalian RFC in quiescent human fibroblasts following induction of local UVC damage (LUD) through a microporous filter (31, 45). As RFC also plays a role in replication and likely in other replication-associated strategies to overcome DNA damage-induced replication blockage (such as translesion synthesis or recombination), the analysis in quiescent cells is crucial to investigate its possible function in NER. Immunofluorescence analysis using an antibody against RFCp140 revealed that RFC is recruited to the LUD and colocalizes with other NER core factors, such as the TFIIH complex subunit p89 (Fig. 1A) and replication-associated postincision NER factors such as PCNA (Fig. 1C). The recruitment of RFC to LUD is dependent on active NER as RFC binding is severely impaired in NER-deficient cell strains carrying mutations in upstream factors such as XPA, XPF, or XPG (Fig. 1A).

Previously, we found that ligation of the repair patch in NER involves different DNA ligases depending on the proliferative status of the cell, i.e., ligase III/XRCC1 in quiescent cells and both ligase I and ligase III/XRCC1 in proliferating cells (32). Since RFC is also an essential replication factor differentially regulated in proliferating cells (43), we investigated whether RFC loading to LUD depends on the proliferation status of the cell. As shown in the top panel of Fig. 1B, RFCp140 is bound to LUD in both proliferating (Ki67 marker positive) and in quiescent cells. This proliferation-independent RFC recruitment is confirmed by costaining with ligase I; i.e., RFCp140 accumulates at LUD in cells lacking ligase I and in cells having ligase I present at LUD.

Surprisingly, in virtually all cells both PCNA and RFCp140 were already visible at LUD shortly (<5 min) after damage infliction, similar to the preincision factor TFIIH (p89) (Fig. 1C). Please note that this does not imply that the postincision factors are loaded simultaneously with preincision factors as this analysis is not suited to determine actual assembly kinetics. In previous work we showed that the assembly of preincision precedes the loading of the postincision factors (29). Four hours post-UV TFIIH localization to LUD is significantly reduced and almost undetectable 8 h after UV-exposure, following the kinetics of 6-4PP removal (44). In contrast, RFC and PCNA remain clearly visible at LUD up to 8 h after exposure. These data suggest that the release of factors involved in the postincision stage of NER is much slower than the actual damage removal and gap-filling synthesis step. Strikingly, although RFC is supposed to function as PCNA loader, these data argue for a role beyond simply loading of PCNA.

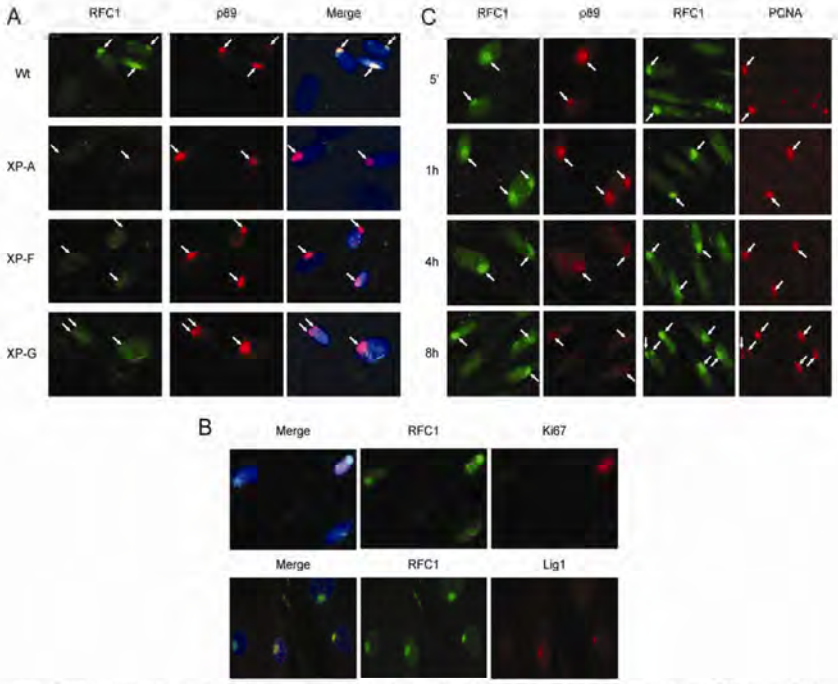

FIG. 1. RFCp140 localizes to sites of damage in an NER-dependent and cell cycle-independent manner. Primary and hTERT-immortalized cells were grown to confluence prior to UV irradiation. (A) Immunofluorescent staining of RFCp140 (RFC1) and TFIIH subunit p89 in normal and NER-deficient human fibroblasts. Wt, wild type. (B) Costaining of RFCp140 and proliferation marker Ki67 (top panel) or ligase I (lower panel) in normal human fibroblasts. (C) Kinetics of RFCp140 localization at sites of damage over time compared to preincision factor p89 (left) and postincision factor PCNA (right). Arrows point to position of the LUD.

UV-induced binding of RFC to chromatin and NER postincision factors. To further investigate the involvement of RFC in NER-induced repair replication, we isolated NER complexes actively engaged in the repair process by in vivo formaldehyde cross-linking of UV-irradiated cells, isolation of chromatin fragments (300 to 600 bp), and chromatin immunoprecipitation (ChIP) (11). Subsequently, candidate NER proteins that were expected to be coprecipitated were analyzed by Western blotting. For this purpose, confluent cells were irradiated with 20 J/m^2 of UVC, creating an average of 1 photolesion (CPD or 6-4PP) every 2.5 kb of dsDNA (11), ensuring that the vast majority of the purified chromatin fragments contained no more than a single repair complex. RFCp140-specific ChIP revealed a UV-induced coprecipitation of RPA, PCNA, and Polδ (Fig. 2A). Strikingly, no increase of the preincision factor p89 was observed, further corroborating that the pre- and postincision NER stages are temporally separable events. A reciprocal experiment using ChIP against

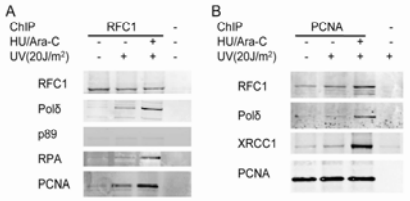

FIG. 2. UV-dependent association of RFCp140 (RFC1) with postincision complexes. Serum-starved EJ30 cells were irradiated with 20 J/m^2 1 h prior to formaldehyde cross-linking. Subsequent ChIP was performed with goat anti-RFCp140 (A) and mouse anti-PCNA (B). In both panels, no antibody was added to the far-right lanes. Precipitated proteins were analyzed by Western blotting as indicated.

PCNA revealed a clear UV-dependent increase of the postincision NER factors XRCC1 and RFCp140 (Fig. 2B). Inhibition of gap-filling synthesis significantly increased the amount of coprecipitating replication factors, including Polδ. In particular, coprecipitation of RPA was only marginally increased after UV irradiation but significantly increased after synthesis inhibition. Such an increase in interaction is likely due to the accumulation of incomplete gap-filling complexes (R. M. Overmeer, unpublished data). These data confirm the role of RFC in repair of UV lesions and suggest that RFC remains involved in the postincision complex after loading PCNA.

The accumulation of both p89 and RFCp140 at LUD shortly after local UV exposure (5 min) (Fig. 1C) seems to contradict the two temporally separable complexes identified by ChIP (Fig. 2). However, a single LUD site contains numerous photolesions with various repair complexes in different phases of the repair process; as such, immunofluorescence studies reveal an ensemble of multiple dynamic repair complexes and are not suited to dissect temporal stages of NER. In contrast, ChIP analysis deals with chromatin fragments that encompass, on average, a single repair complex, thereby allowing accurate determination of the composition of RFCp140-containing complexes.

RFC1 is required for loading but not for recruitment of PCNA to NER sites. Having shown that RFCp140 is involved in NER-associated repair replication, we further analyzed the consequences of depleting RFCp140 for the different stages of the NER reaction. To that aim we performed siRNA-mediated knockdown of RFCp140 in high-density seeded cells, resulting in approximately 90% knockdown when cells reached confluence (Fig. 3A).

Knockdown of RFCp140 resulted in inhibition of DNA damage removal in a fashion reminiscent of that seen when repair synthesis is inhibited by HU and Ara-C, thereby confirming the requirement for RFCp140 for efficient NER (Fig. 3C) (32; also Overmeer, unpublished). Interestingly, when we analyzed the colocalization of Polδ with XPA at LUD in cells treated with siRNA against RFCp140, approximately half of the cells showed no Polδ at sites of damage marked by XPA accumulation (Fig. 3D and F), whereas control siRNA-treated cells displayed >99% colocalization. This reduced colocalization was not due to a spurious remaining fraction of RFCp140 bound to chromatin after the siRNA as cellular fractionation showed that RFCp140 was depleted from both the soluble and chromatin-bound pools (Fig. 3B). In contrast, knockdown of RFCp140 had no significant effect on the recruitment of PCNA to sites of UV damage (Fig. 3E and F). This surprising result suggests that RFCp140 is not required for the recruitment of PCNA to NER sites but is needed to recruit and/or stably load Polδ.

Semiquantitative measurement of the average spot intensity of proteins at LUD sites in cells treated with siRNA against RFCp140 revealed enhanced intensities of accumulation for XPA (Fig. 3D, E, and F), compared to cells treated with control siRNA. Impaired gap filling in cells treated with siRNA against RFCp140 might underlie the enhanced XPA intensity as similarly enhanced XPA intensity at LUD sites was observed in cells when gap filling was abolished by treatment with the DNA synthesis inhibitors HU and Ara-C (39) (Fig. 3F).

The reduced amount of Polδ, together with a reduced spot incidence of Polδ (relative to XPA) at LUD after knockdown of RFCp140 (Fig. 3E and F), further corroborates the suggestion that in the absence of RFC, Polδ is not efficiently recruited to repair sites. In contrast to repair inhibition by RFCp140 knockdown, inhibition of repair synthesis by HU and Ara-C caused increased signals of PCNA and Polδ (confirming the ChIP data shown in Fig. 2). This is expected as all postincision NER factors are properly loaded in the presence of chemical inhibitors (Overmeer, unpublished), and repair synthesis (or UV-induced unscheduled DNA synthesis [UDS]) is initiated but not finished (34, 39), thereby generating substrate for these factors to bind. The slight decrease in PCNA spot intensity at LUD after RFCp140 knockdown might imply that although PCNA is recruited, it is improperly loaded and might easily dissociate, resulting in a decreased signal. Thus, although RFC is not required for recruitment of PCNA, it is necessary for stable association to 3′ termini and subsequent loading of Polδ.

The data demonstrate that both depletion of RFCp140 and chemical interference with replication affect the postincision NER step, although with variable consequences for the resulting accumulation of repair intermediates. However, the consequences for repair synthesis were similar as we recently found that RFCp140 depletion caused a 50% reduction of UDS (35). Previously, we showed that inhibition of repair patch ligation led to a surprising concomitant reduction in actual damage removal (32). Similarly, we observed reduced damage removal both after depletion of RFCp140 and after HU/Ara-C treatment (Fig. 3B).

Association of RFCp140-GFP with sites of replication and repair. The extended accumulation of RFC (Fig. 1C) and other postincision factors at LUD sites compared to preincision factors (e.g., p89 of TFIIH) (Fig. 1C) reflects either slow dissociation kinetics of postincision factors or additional functions of these factors beyond repair replication. To investigate the dynamics of RFC association with sites of repair, a human cell line (SV40-transformed MRC5 fibroblasts) that stably expresses RFCp140 tagged with green fluorescent protein (GFP) was generated. To prevent disturbed population growth features due to overexpression of RFCp140-GFP (13, 21, 43), we carefully checked the expression level of RFCp140-GFP and cellular growth. Immunoblot analysis of cells expressing RFCp140-GFP with an anti-RFCp140 antibody showed that endogenous RFCp140 and RFCp140-GFP were expressed at similar levels (Fig. 4D). Hybridization with anti-GFP antibodies revealed no RFCp140-GFP breakdown products, indicating that the majority of fluorescence observed in the cells is derived from the full-length fusion protein (data not shown). Moreover, the presence of RFCp140-GFP in the cells did not affect cellular growth, nor did it interfere with DNA replication, as revealed by fluorescence-activated cell sorting (FACS) analysis; UV-induced cytotoxicity (UV survival) was not enhanced, suggesting efficient repair of UV photolesions (data not shown). Immunoprecipitation of nuclear extracts with an antibody directed against one of the other RFC subunits (RFCp36) precipitated similar amounts of endogenous RFCp140 and RFCp140-GFP (Fig. 4E). These findings demonstrate that the GFP tag does not disrupt the ability of RFCp140-GFP to form a complex with the smaller RFC subunits, which is necessary for the protein to fulfill its function in replication and repair.

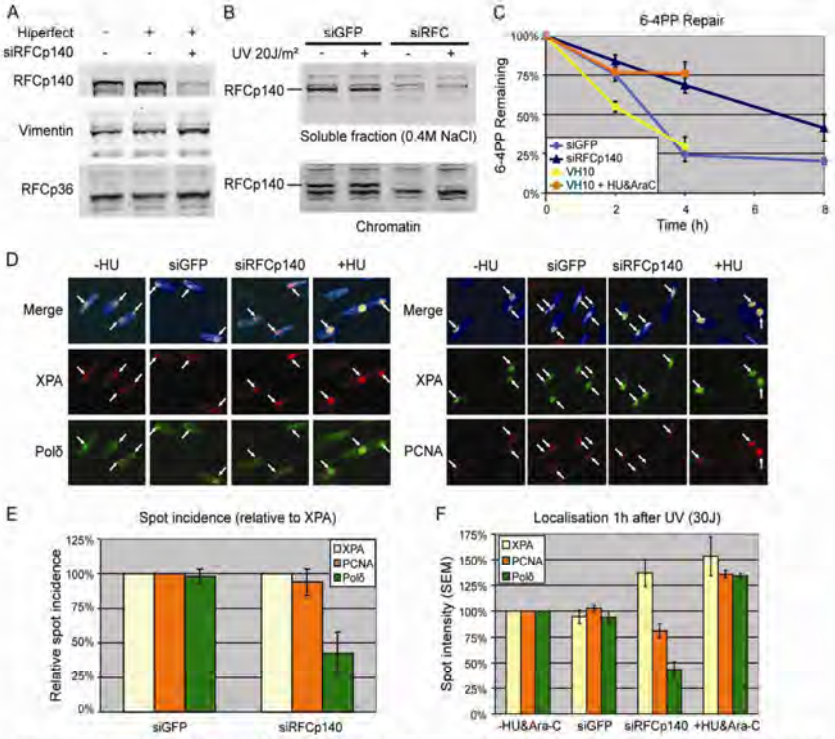

FIG. 3. Knockdown (KD) of RFCp140 inhibits efficient NER through impaired Polδ recruitment. (A) Western blot analysis of RFCp140 KD in hTERT-immortalized VH10 cells, with vimentin as a loading control. Specific KD of RFC was confirmed by staining with an RFC5-specific antibody. (B) Subcellular fractionation and subsequent Western blot analysis show that RFCp140 is depleted from both the nuclear soluble fraction and from the chromatin fraction. (C) Immunohistochemical analysis of 6-4PP repair in cells treated with siRNAs against GFP or RFCp140. Graph represents the average of four independent experiments. (D) Immunofluorescent staining of Polδ and XPA (left) or PCNA and XPA (right) in cells after mock treatment (−HU) or after treatment with siGFP, siRFCp140, or HU and Ara-C (+HU). (E) Relative percentage of visible accumulation of proteins at LUD after treatment with siRNA; LUD marked by XPA accumulation is expressed as a percentage of colocalization with XPA set at 100%. (F) Average intensity of proteins accumulated at site of LUD scored in panel C. Cells were treated and stained simultaneously, pictures were taken with identical exposure times, and the average pixel intensity for each positively scored LUD site (i.e., LUD sites scored negative in panel C were excluded) was calculated by measuring the total signal and area of each LUD site. Subsequently the average intensity was calculated and normalized to that found in nontreated cells. SEM, standard error of the mean.

RFCp140-GFP is localized in the nucleus; however, its distribution changes during the cell cycle. While it is homogeneous in G_1/G_2, it presents a specific, PCNA-like focal pattern during S phase (Fig. 4A). Cotransfection of cells with PCNA-mCherry shows that both proteins colocalize at these foci, which correspond to replication sites (28; also data not shown). After local UV damage infliction in cells expressing RFCp140-GFP, a clear localization to the damaged area could be observed in virtually all cells within a few minutes after irradiation (Fig. 4B, white arrows). RFCp140-GFP colocalized with PCNA-mCherry at the damaged sites, indicative of association of both proteins to NER sites (Fig. 4C, white arrows). These findings further suggest that GFP-tagged RFCp140 is targeted to activity sites (replication and repair) in a manner similar to endogenous RFCp140. Together, these data suggest that the fusion protein is expressed at physiologically relevant levels, is functional in replication and NER, and is a bona fide platform to perform live-cell protein dynamic analysis.

Dynamics of RFCp140-GFP at sites of NER. To measure the dynamic associations of RFCp140-GFP in replication and

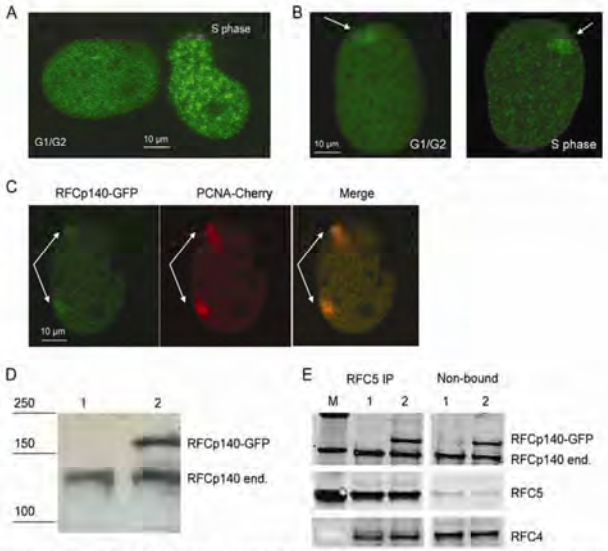

FIG. 4. GFP-RFCp140 colocalizes with PCNA-mCherry to sites of replication and to sites of repair independent of cell cycle. (A) Characteristic nuclear distribution patterns of RFCp140 seen in S-phase and non-S-phase cells. (B) Recruitment of RFCp140-GFP to sites of damage is independent of the cell cycle as it is detectable in G_1/G_2 cells and in S-phase cells. (C) Colocalization of RFCp140-GFP (left) with PCNA-Cherry (middle) at sites of damage; the right panel is the merged image. (D) Immunoblot analysis of MRC5 cells (lane 1) and MRC5 cells expressing RFCp140-GFP (lane 2), probed with anti-RFCp140, showed that the transgene produces a protein of the expected size and that RFCp140-GFP is expressed to a similar level as the endogenous (end) RFCp140. (E) RFCp34 (RFC5) was immunoprecipitated from nuclear extracts of MRC5 (lane 1) and MRC5-RFCp140-GFP (lane 2) cells, and coprecipitating proteins were analyzed by Western blotting. RFCp34 coprecipitates similar amounts of endogenous RFC4 and RFCp140 as well as with GFP-RFCp140, implying that they can form the RFC complex with similar efficiencies.

NER, protein mobility was evaluated by different photobleaching procedures. We designed an adapted FRAP (fluorescence recovery after photobleaching) protocol and combined it with a FLIP (fluorescence loss in photobleaching) protocol by bleaching the GFP fluorescence in half the nucleus and subsequently measuring the fluorescence recovery in the bleached area (recovery or FRAP) and in the nonbleached area (FLIP), as illustrated in Fig. 5A. The time required to reach an equilibrium between FRAP and FLIP is a measure of the overall nuclear mobility of RFCp140-GFP.

We first determined the mobility of RFCp140-GFP in unchallenged G_1/G_2-phase cells (recognizable by the homogenous nuclear distribution) and observed a redistribution time of approximately 120 s (Fig. 5A), significantly slower than GFP-PCNA (50 s for complete fluorescence redistribution) (Fig. 5A). To test whether the slow mobility of RFCp140-GFP is derived from transient macromolecular interactions, a temperature shift of 10°C (from 37°C to 27°C) was applied to the cells. At the lower temperature, the mobility of proteins involved in enzymatic reactions or interactions (protein/protein or protein/DNA) is reduced (19, 42). The mobility of RFCp140-GFP was unchanged, suggesting that RFCp140-GFP is freely diffusing throughout the nucleus during the G_1/G_2 phase of the cell cycle (Fig. 5B), as was previously found for GFP-PCNA (9). The slower mobility observed for RFCp140 is likely due to the larger molecular size of the RFC complex (the RFC complex, including RFCp140 and RFC2-5, has a molecular mass of 289 kDa, while trimeric PCNA-GFP is only 115 kDa) and its different shape, e.g., elongated rather than the compact globular shape of the PCNA trimer. In contrast, the mobility of RFCp140-GFP in S-phase cells (identified by the presence of foci) was sensitive to temperature: at lower temperatures the mobility is retarded. This suggests that RFCp140-GFP is transiently bound to S-phase-specific structures, likely replication foci, in a temperature-dependent fashion. Note that in S-phase cells cultured at 37°C, we do not observe an overall slower mobility than in non-S-phase cells despite the presence of higher concentrations of RFCp140-GFP at replication foci. The transient binding of RFCp140 to replication foci is apparently too short to reveal a significant mobility shift with the applied FRAP procedures unless reaction kinetics or thermodynamic interactions are influenced by a temperature drop.

In order to determine the average residence or binding time of RFCp140-GFP in NER complexes, we bleached the local damage and subsequently monitored the recovery of fluorescence (20)

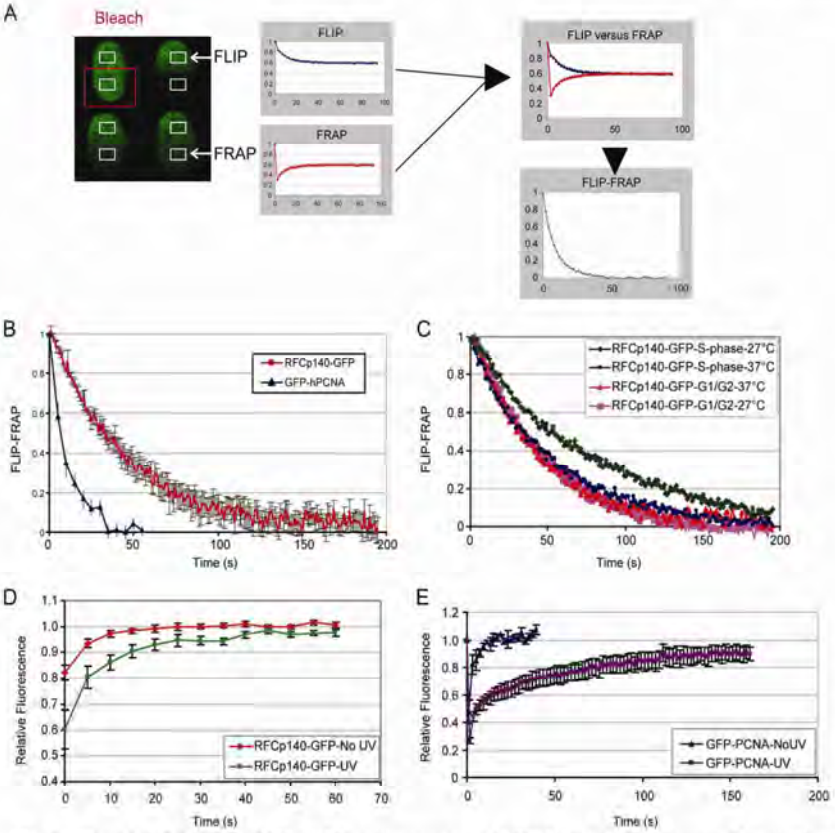

FIG. 5. FRAP analysis of the mobility of RFCp140-GFP in comparison to that of GFP-PCNA. (A) Schematic overview of the combined FLIP-FRAP analysis procedure. Half of the nucleus (indicated by the red box) is bleached by high-intensity laser excitation; the loss of fluorescence (FLIP) in the unbleached part (measured in the upper white box) is measured over time and plotted (upper left graph). The recovery of fluorescence (FRAP) in the bleached part of the cell (lower white box) is also plotted (lower left graph). The difference between FLIP and FRAP (upper right) is normalized to 1 directly after the bleach pulse and plotted over time, indicated in seconds (lower right). (B) Combined FLIP-FRAP analysis of RFCp140-GFP and GFP-PCNA in untreated cells at 37°C. (C) FLIP-FRAP analysis of RFCp140-GFP in G_1/G_2 and S-phase cells at 37°C and 27°C. (D) FRAP in a subnuclear area (similar size as LUD) of RFCp140-GFP in cells without LUD (No-UV) and in LUD (UV) (120 J/m^2); the recovery of fluorescence (expressed as relative fluorescence, where prebleach is set at 1) is plotted against time (in seconds) after bleaching. (E) FRAP of GFP-PCNA in control cells and in LUD, as in panel D.

and compared the recovery time to that of an equally sized subnuclear area of mock-treated cells. In untreated cells it took approximately 25 s for complete recovery while in damaged cells equilibrium was reached after 45 s (Fig. 5C). This rather moderate increase in residence time of RFCp140-GFP in LUD suggests a very short binding at NER sites. Surprisingly, and in contrast to the higher mobility rate of PCNA in unchallenged non-S-phase cells, not all PCNA molecules at LUD sites exchanged even 160 s after bleaching (Fig. 5D) (9). This remarkable difference in association dynamics suggests a scenario in which RFCp140 continuously binds to and dissociates from NER-replication sites as long as gap filling is not completed. The relatively long residence time of PCNA suggests that the loading of PCNA to active sites is much less transient.

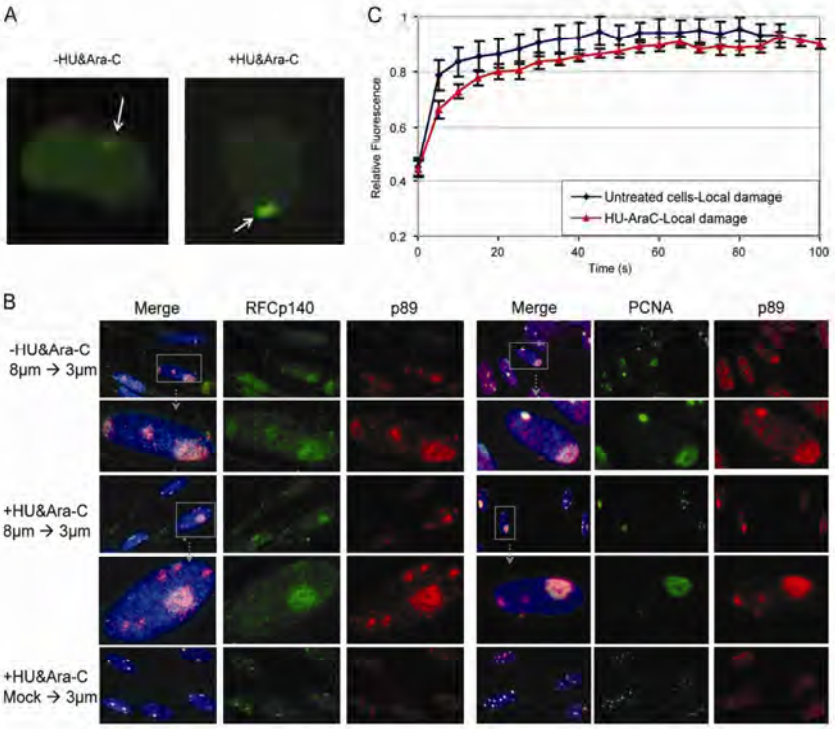

FIG. 6. (A) Confocal images of MRC5 cells expressing RFCp140-GFP after local damage (120 J/m^2), in the absence and presence of HU/Ara-C. (B) Endogenous RFCp140 and PCNA remain associated with the initial site of damage when repair synthesis is inhibited. Cells were locally irradiated through microporous filters, first with 8- and then with 3-μm pores, in the absence or presence of HU and Ara-C. Boxed cells are enlarged in the frame immediately below. (C) FRAP analysis of RFCp140-GFP in LUD in the absence and presence of HU/Ara-C.

Stability of NER complexes in the presence of DNA synthesis inhibitors. To further decipher the function of RFC in NER, we blocked repair synthesis by addition of hydroxyurea (HU) and cytosine-ß-arabinofuranoside (Ara-C). In the presence of these inhibitors a limited number of incisions occur while PCNA and Polδ are still loaded onto DNA at NER sites; however, repair synthesis is severely reduced, repair patches remain unligated, and removal of photolesions is severely impaired (32, 34, 39).

After 30 min of incubation in the presence of these inhibitors, cells expressing RFCp140-GFP were locally irradiated, and 1 h after irradiation they were subjected to imaging, photobleaching, or fixation. Irradiated cells not treated with inhibitors were taken as a control. In the presence of DNA synthesis inhibitors, we observed a much brighter accumulation of RFCp140-GFP at local damage than in the absence of inhibitors (Fig. 6A), suggesting that under these conditions postincision factors are more stably bound to gapped (ssDNA gap-containing) NER intermediates. The higher concentration of RFCp140-GFP at LUD correlates with a higher concentration of substrate, i.e., gapped NER intermediates due to inhibition of DNA synthesis (8), to which this protein has affinity.

The exchange rate of (endogenous) RFC in the NER complex in the presence and absence of inhibitors was further analyzed in a competition experiment by applying a second local damage infliction (with a different pore size) after the first irradiation in quiescent primary human cells. The cells were first irradiated locally with 30 J/m^2 of UVC through 8-μm pores. After 30 min of incubation to allow a maximum accumulation of NER complexes, the cells were again locally irra-

diated but this time through smaller pores (3 μm). Figure 6B (top panel) shows that in the absence of replication inhibitors, both TFIIH (p89) and RFCp140 were able to partially localize to the second LUD (of smaller pore size). However, in the presence of inhibitors, RFC was visible only at the initial damage site, similar to other postincision factors such as PCNA and RPA (Overmeer, unpublished); in contrast, p89 localizes to the second local damage site, similar to other preincision factors (data not shown). These data suggest that DNA synthesis factors remain associated or are continuously targeted to stalled postincision repair complexes. The underlying mechanism is that in the presence of inhibitors, no incisions are made at the second LUD site, and, hence, no substrate is created for these factors to bind to.

To further investigate whether DNA synthesis factors are stably associated or dynamically reassociate to stalled NER repair synthesis complexes, cells were submitted to FRAP analysis in LUD. We noticed that, in living cells (Fig. 6C), RFCp140-GFP exchanges from LUD after DNA synthesis inhibition, though with slower kinetics: ~50 s in untreated cells and ~70s in HU/Ara-C-treated cells for complete exchange at LUD. These data show that RFCp140 (and perhaps other replication factors) dynamically associates with and releases from stalled repair replication complexes. The absence of visible relocalization to the secondary LUD thus corroborates the hypothesis that repair synthesis inhibition prevents incisions at these secondary LUD sites in quiescent cells, preventing the creation of substrate for the postincision factors to bind. We conclude that the proteins are still exchanging and, therefore, behave in a more dynamic way than previously anticipated and that RFCp140 continues to be recruited to repair synthesis sites even after PCNA is loaded. The continued recruitment suggests an additional role beyond loading of the PCNA clamp.

DISCUSSION

Here, we have shown that RFC participates in NER in vivo, involving a highly dynamic association/dissociation cycle with NER intermediates. Previous studies (2, 4) revealed that purified RFC protein supported DNA repair synthesis in vitro employing a reconstituted NER system. The in vitro experiments show that purified RFC stimulates repair synthesis but does not unambiguously identify RFC as the actual clamp loader in vivo. For example, it was long thought that ligase I was the essential NER ligase as it was able to catalyze ligation in in vitro NER assays (2). Although we provided evidence for a role of ligase I in NER in vivo, in fact ligase III appears to be the dominant ligase in NER in living cells (32).

The role of RFC in NER in vivo is manifested by the reduced 6-4PP repair (Fig. 3) and repair synthesis (35) in cells with RFCp140 knockdown. These observations corroborate the previously described findings that impaired gap filling during postincision repair leads to reduced DNA damage removal (32, 34, 39). Moreover, the immunofluorescence analysis of endogenous RFC and the dynamic studies employing GFP-tagged RFCp140 provide direct evidence that RFC is recruited to sites of UV photolesions in an NER-dependent and cell cycle-independent fashion. Finally, the ChIP data show that RFC interacts with other postincision factors in nondividing human cells upon UV irradiation, consistent with its involvement in NER in vivo.

The function of RFC as clamp loader in replicative DNA synthesis is to open the trimeric PCNA ring to allow stable loading of the polymerase clamp at 3′ termini. Our live-cell protein dynamic studies favor such a role of RFC in NER: FRAP analysis of RFCp140-GFP showed that RFCp140-GFP dynamically dissociates and reassociates both with replication foci and LUD and that, on average, RFC molecules are bound to NER complexes for much shorter times than PCNA. These data are in line with a model according to which once RFC has loaded PCNA, the latter remains bound, and RFC leaves. However, other data (Fig. 3D and E) seem to challenge the role of RFC as the principal PCNA clamp-recruiting factor in NER. Most notably, whereas knockdown of RFCp140 reduced the recruitment of Polδ to less than 50% of colocalization, the PCNA recruitment was only mildly affected. These results lead to the unexpected conclusions that RFC is not required for the recruitment PCNA to the postincision NER complex and that the association of PCNA with sites of damage is not sufficient to recruit other postincision factors such as Polδ. An obvious explanation is that PCNA gets recruited to sites of UV damage in an RFC-independent fashion but that this recruitment does not lead to a replication-competent form of PCNA: i.e., RFC is an essential factor required for stable loading of the polymerase clamp, which is necessary to start DNA repair synthesis. Stable loading is likely established by the ATPase activity of RFC that opens the PCNA ring and subsequently allows it to close when it is bound to the 3′ terminus generated by ERCC1-XPF incision (40).

The preincision factor p89 (TFIIH subunit) associates with secondary LUD (induced by sequential UV irradiation) when repair synthesis is inhibited (Fig. 6B). In contrast, endogenous RFC and PCNA are not loaded to secondary LUD sites, suggesting stable binding of the postincision NER factors to the initial LUD. The observed dynamic exchange of RFC on HU- and Ara-C-stalled repair replication (Fig. 6C) seems to contradict the results of immunofluorescence based competition experiments. However, in the immunofluorescence studies the complexes are frozen by the fixation and are thus not suited to reveal dynamic interactions. Stalled postincision repair complexes encompass incised DNA, all postincision factors, RPA, and an incomplete repair patch (34, 39; also Overmeer, unpublished) and obviously form a substrate to which RFC and PCNA dynamically interact with high affinity. We speculate that the RPA-coated 30-nt-long gapped NER intermediate generated by ERCC1-XPF-mediated 5′ incision (40) provides a high-affinity substrate for recruitment of both RFC and PCNA. Next, this intermediate allows preferential binding of RFC to the 3′ terminus and subsequent loading of PCNA. This dynamic mode of RFC association argues further that once PCNA is loaded, RFC dissociates and diffuses away from these sites. However, its localization at LUD long after damage induction, despite inhibition of incision, suggests a model in which RFCp140 continues to be recruited to the initial repair complex even after loading of PCNA. Hence, the dynamic interaction of RFC with sites of NER merely reflects a process of rapid dissociation/association of the complex with the RPA-coated gapped NER intermediate. Together, these data indicate that RFC displays additional functions beyond the clamp-

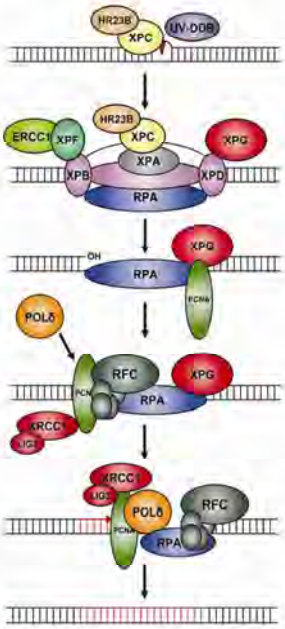

FIG. 7. Model of the NER process. After damage recognition by UV-DDB and/or XPC, the preincision complex is recruited, and the damage is verified. Next, the damage containing oligonucleotide is excised by the XPF and XPG endonucleases, and preincision factors dissociate, with the exception of XPG and RPA. XPG and RPA are involved in the recruitment of PCNA and RFC, respectively, and subsequently PCNA can be loaded by RFC. After loading PCNA, RFC dissociates, and PCNA forms the sliding-clamp template required for the recruitment of other postincision factors. RFC is then able to bind the 5′ phosphate at the other side of the gap through its BRCT domain, where it possibly inhibits Rad17-dependent signaling or facilitates unloading of PCNA after completion of repair.

loading activity, possibly functioning in subsequent binding of Polδ as described for in vitro replication of chromatin (48).

How is PCNA recruited into the postincision NER complex as immunofluorescence studies reveal that RFC is not required? In vitro experiments using reconstituted NER systems implicated XPG in the recruitment of PCNA to incised DNA (30), in line with earlier observations that XPG possesses PCNA binding capacity (12). In addition, impaired recruitment of PCNA is observed in vivo in XPG-deficient cells (9), whereas cells harboring a nuclease-dead mutant of XPG are still able to recruit PCNA (40). As XPF-deficient cells are unable to recruit PCNA, ERCC1-XPF-mediated 5′ incision might be required to allow XPG-dependent recruitment of PCNA. Based on this XPG-PCNA interaction, we propose a model in which PCNA is initially recruited by XPG, but only after incision is it positioned and loaded by RFC, which subsequently enables the recruitment of other postincision factors such as Polδ (Fig. 7) or any of the other DNA polymerases implicated in NER replication (35). Furthermore, our data are consistent with a model in which RFC exchanges dynamically to and from sites of repair even after loading PCNA, in contrast to earlier suggestions that RFC dissociates after PCNA loading to allow Polδ to bind (22, 37). The latter model is based on in vitro studies that employed an N-terminally truncated RFCp140 and therefore lacking a BRCT domain capable of binding 5′ phosphate (3, 26). We therefore speculate that RFC associates with the downstream 5′ phosphate after loading; such interaction would prevent possible signaling events initiated by Rad17 and may assist in unloading of PCNA (26). In model loading/unloading systems, human RFC has been shown to unload PCNA from template-primer DNA in an ATP-dependent reaction (47). Although the Ctf18-like complex is also capable of unloading PCNA (6), this seems more likely to occur during the establishment of sister chromatid cohesion. RFC would therefore represent a good candidate for performing this task in NER.

ACKNOWLEDGMENTS

We gratefully acknowledge B. Stillman and A. E. Tomkinson for kindly providing the anti-RFC p140 antibody and the anti-Lig1 antibody, respectively.

This work was supported by EU FP6 IP DNA Repair (LSHG-CT-2005-512113) and MRTN-CT-2003-503618, ZON-MW projects 912-03-012 and 917-46-364, ALW projects 805.3.42-P and 805.47.190 (MtC), and ESF projects ALW-855.01.074 and 805.47.193.

REFERENCES

1. Abcam. 2010. Nuclear fractionation protocol. Abcam inc., Cambridge, MA. www.abcam.com/ps/pdf/protocols/NuclearFractionation protocol.pdf.
2. Aboussekhra, A., M. Biggerstaff, M. K. K. Shivji, J. A. Vilpo, V. Moncollin, V. N. Podust, M. Protic, U. Hubscher, J. M. Egly, and R. D. Wood. 1995. Mammalian DNA nucleotide excision repair reconstituted with purified protein components. Cell 80:859–868.
3. Allen, B. L., F. Uhlmann, L. K. Gaur, B. A. Mulder, K. L. Posey, L. B. Jones, and S. H. Hardin. 1998. DNA recognition properties of the N-terminal DNA binding domain within the large subunit of replication factor C. Nucleic Acids Res. 26:3877–3882.
4. Araujo, S. J., F. Tirode, F. Coin, H. Pospiech, J. E. Syvaoja, M. Stucki, U. Hubscher, J. M. Egly, and R. D. Wood. 2000. Nucleotide excision repair of DNA with recombinant human proteins: definition of the minimal set of factors, active forms of TFIIH, and modulation by CAK. Genes Dev. 14: 349–359.
5. Bermudez, V. P., L. A. Lindsey-Boltz, A. J. Cesare, Y. Maniwa, J. D. Grif fith, J. Hurwitz, and A. Sancar. 2003. Loading of the human 9-1-1 checkpoint complex onto DNA by the checkpoint clamp loader hRad17-replication factor C complex in vitro. Proc. Natl. Acad. Sci. U. S. A. 100:1633–1638.
6. Bylund, G. O., and P. M. Burgers. 2005. Replication protein A-directed unloading of PCNA by the Ctf18 cohesion establishment complex. Mol. Cell. Biol. 25:5445–5455.
7. Ellison, V., and B. Stillman. 2003. Biochemical characterization of DNA damage checkpoint complexes: Clamp loader and clamp complexes with specificity for 5′ recessed DNA. PLoS Biol. 1:231–243.
8. Erixon, K., and G. Ahnstrom. 1979. Single-strand breaks in DNA during repair of UV-induced damage in normal human and xeroderma pigmentosum cells as determined by alkaline DNA unwinding and hydroxylapatite chromatography: effects of hydroxyurea, 5-fluorodeoxyuridine and 1-beta-D-arabinofuranosylcytosine on the kinetics of repair. Mutat. Res. 59:257–271.
9. Essers, J., A. F. Theil, C. Baldeyron, W. A. van Cappellen, A. B. Houtsmuller, R. Kanaar, and W. Vermeulen. 2005. Nuclear dynamics of PCNA in DNA replication and repair. Mol. Cell. Biol. 25:9350–9359.
10. Fitch, M. E., S. Nakajima, A. Yasui, and J. M. Ford. 2003. In vivo recruitment of XPC to UV-induced cyclobutane pyrimidine dimers by the DDB2 gene product. J. Biol. Chem. 278:46906–46910.
11. Fousteri, M., W. Vermeulen, A. A. van Zeeland, and L. H. F. Mullenders. 2006. Cockayne syndrome A and B proteins differentially regulate recruitment of chromatin remodeling and repair factors to stalled RNA polymerase II in vivo. Mol. Cell 23:471–482.

12. Gary, R., D. L. Ludwig, H. L. Cornelius, M. A. MacInnes, and M. S. Park. 1997. The DNA repair endonuclease XPG binds to proliferating cell nuclear antigen (PCNA) and shares sequence elements with the PCNA binding regions of FEN-1 and cyclin-dependent kinase inhibitor p21. J. Biol. Chem. 272:24522–24529.
13. Gerik, K. J., S. L. Gary, and P. M. Burgers. 1997. Overproduction and affinity purification of Saccharomyces cerevisiae replication factor C. J. Biol. Chem. 272:1256–1262.
14. Gillet, L. C., and O. D. Scharer. 2006. Molecular mechanisms of mammalian global genome nucleotide excision repair. Chem. Rev. 106:253–276.
15. Green, C. M., and G. Almouzni. 2003. Local action of the chromatin assembly factor CAF-1 at sites of nucleotide excision repair in vivo. EMBO J. 22:5163–5174.
16. Hanawalt, P. C., and G. Spivak. 2008. Transcription-coupled DNA repair: two decades of progress and surprises. Nat. Rev. Mol. Cell Biol. 9:958–970.
17. Hashiguchi, K., Y. Matsumoto, and A. Yasui. 2007. Recruitment of DNA repair synthesis machinery to sites of DNA damage/repair in living human cells. Nucleic Acids Res. 35:2913–2923.
18. Hoeijmakers, J. H. 2001. Genome maintenance mechanisms for preventing cancer. Nature 411:366–374.
19. Hoogstraten, D., S. Bergink, J. M. Ng, V. H. Verbiest, M. S. Luijsterburg, B. Geverts, A. Raams, C. Dinant, J. H. Hoeijmakers, W. Vermeulen, and A. B. Houtsmuller. 2008. Versatile DNA damage detection by the global genome nucleotide excision repair protein XPC. J. Cell Sci. 121:2850–2859.
20. Houtsmuller, A. B. 2005. Fluorescence recovery after photobleaching: application to nuclear proteins. Adv. Biochem. Eng. Biotechnol. 95:177–199.
21. Jaharul Haque, S., H. van der Kuip, A. Kumar, W. E. Aulitzky, M. N. Rutherford, C. Huber, T. Fischer, and B. R. Williams. 1996. Overexpression of mouse p140 subunit of replication factor C accelerates cellular proliferation. Cell Growth Differ. 7:319–326.
22. Johnson, A., N. Y. Yao, G. D. Bowman, J. Kuriyan, and M. O'Donnell. 2006. The replication factor C clamp loader requires arginine finger sensors to drive DNA binding and proliferating cell nuclear antigen loading. J. Biol. Chem. 281:35531–35543.
23. Kanellis, P., R. Agyei, and D. Durocher. 2003. Elg1 forms an alternative PCNA-interacting RFC complex required to maintain genome stability. Curr. Biol. 13:1583–1595.
24. Kim, J., and S. A. MacNeill. 2003. Genome stability: a new member of the RFC family. Curr. Biol. 13:R873–R875.
25. Kim, J., K. Robertson, K. J. Mylonas, F. C. Gray, I. Charapitsa, and S. A. MacNeill. 2005. Contrasting effects of Elg1-RFC and Ctf18-RFC inactivation in the absence of fully functional RFC in fission yeast. Nucleic Acids Res. 33:4078–4089.
26. Kobayashi, M., F. Figaroa, N. Meeuwenoord, L. E. T. Jansen, and G. Siegal. 2006. Characterization of the DNA binding and structural properties of the BRCT region of human replication factor C p140 subunit. J. Biol. Chem. 281:4308–4317.
27. Kraemer, K. H., N. J. Patronas, R. Schiffmann, B. P. Brooks, D. Tamura, and J. J. DiGiovanna. 2007. Xeroderma pigmentosum, trichothiodystrophy and Cockayne syndrome: a complex genotype-phenotyperelationship. Neuroscience 145:1388–1396.
28. Leonhardt, H., H. P. Rahn, P. Weinzierl, A. Sporbert, T. Cremer, D. Zink, and M. C. Cardoso. 2000. Dynamics of DNA replication factories in living cells. J. Cell Biol. 149:271–280.
29. Luijsterburg, M. S., B. G. von, A. M. Gourdin, A. Z. Politi, M. J. Mone, D. O. Warmerdam, J. Goedhart, W. Vermeulen, D. R. van, and T. Hofer. 2010. Stochastic and reversible assembly of a multiprotein DNA repair complex ensures accurate target site recognition and efficient repair. J. Cell Biol. 189:445–463.
30. Mocquet, V., J. P. Laine, T. Riedl, Z. Yajin, M. Y. Lee, and J. M. Egly. 2008. Sequential recruitment of the repair factors during NER: the role of XPG in initiating the resynthesis step. EMBO J. 27:155–167.
31. Mone, M. J., M. Volker, O. Nikaido, L. H. F. Mullenders, A. A. van Zeeland, P. J. Verschure, E. M. M. Manders, and R. van Driel. 2001. Local UV induced DNA damage in cell nuclei results in local transcription inhibition. EMBO Rep. 2:1013–1017.
32. Moser, J., H. Kool, I. Giakzidis, K. Caldecott, L. H. F. Mullenders, and M. I. Fousteri. 2007. Sealing of chromosomal DNA nicks during nucleotide excision repair requires XRCC1 and DNA ligase III alpha in a cell-cycle-specific manner. Mol. Cell 27:311–323.
33. Moser, J., M. Volker, H. Kool, S. Alekseev, H. Vrieling, A. Yasui, A. A. van Zeeland, and L. H. F. Mullenders. 2005. The UV-damaged DNA binding protein mediates efficient targeting of the nucleotide excision repair complex to UV-induced photo lesions. DNA Repair (Amst.) 4:571–582.
34. Mullenders, L. H. F., A. C. Vankesterenvanleeuwen, A. A. Vanzeeland, and A. T. Natarajan. 1985. Analysis of the structure and spatial-distribution of ultraviolet-induced DNA repair patches in human cells made in the presence of inhibitors of replicative synthesis. Biochim. Biophys. Acta 826:38–48.
35. Ogi, T., S. Iimsirichaikul, R. M. Overmeer, M. Volker, K. Takenaka, R. Cloney, Y. Nakazawa, A. Niimi, Y. Miki, N. G. Jaspers, L. H. Mullenders, S. Yamashita, M. I. Fousteri, and A. R. Lehmann. 2010. Three DNA polymerases, recruited by different mechanisms, carry out NER repair synthesis in human cells. Mol. Cell 37:714–727.
36. Parrilla-Castellar, E. R., S. J. Arlander, and L. Karnitz. 2004. Dial 9-1-1 for DNA damage: the Rad9-Hus1-Rad1 (9-1-1) clamp complex. DNA Repair (Amst.) 3:1009–1014.
37. Podust, V. N., N. Tiwari, S. Stephan, and E. Fanning. 1998. Replication factor C disengages from proliferating cell nuclear antigen (PCNA) upon sliding clamp formation, and PCNA itself tethers DNA polymerase delta to DNA. J. Biol. Chem. 273:31992–31999.
38. Shiomi, Y., A. Shinozaki, K. Sugimoto, J. Usukura, C. Obuse, and T. Tsurimoto. 2004. The reconstituted human Chl12-RFC complex functions as a second PCNA loader. Genes Cells 9:279–290.
39. Smith, C. A., and D. S. Okumoto. 1984. Nature of DNA repair synthesis resistant to inhibitors of polymerase-alpha in human-cells. Biochemistry 23:1383–1391.
40. Staresincic, L., A. F. Fagbemi, J. H. Enzlin, A. M. Gourdin, N. Wijgers, I. Dunand-Sauthier, G. Giglia-Mari, S. G. Clarkson, W. Vermeulen, and O. D. Scharer. 2009. Coordination of dual incision and repair synthesis in human nucleotide excision repair. EMBO J. 28:1111–1120.
41. Tsurimoto, T., and B. Stillman. 1989. Purification of a cellular replication factor, RF-C, that is required for coordinated synthesis of leading and lagging strands during simian virus 40 DNA replication in vitro. Mol. Cell. Biol. 9:609–619.
42. van den Boom, V., E. Citterio, D. Hoogstraten, A. Zotter, J. M. Egly, W. A. van Cappellen, J. H. Hoeijmakers, A. B. Houtsmuller, and W. Vermeulen. 2004. DNA damage stabilizes interaction of CSB with the transcription elongation machinery. J. Cell Biol. 166:27–36.
43. van der Kuip, H., B. Carius, S. J. Haque, B. R. Williams, C. Huber, and T. Fischer. 1999. The DNA-binding subunit p140 of replication factor C is upregulated in cycling cells and associates with G_1 phase cell cycle regulatory proteins. J. Mol. Med. 77:386–392.
44. van Hoffen, A., J. Venema, R. Meschini, A. A. van Zeeland, and L. H. Mullenders. 1995. Transcription-coupled repair removes both cyclobutane pyrimidine dimers and 6-4 photoproducts with equal efficiency and in a sequential way from transcribed DNA in xeroderma pigmentosum group C fibroblasts. EMBO J. 14:360–367.
45. Volker, M., M. J. Mone, P. Karmakar, A. van Hoffen, W. Schul, W. Vermeulen, J. H. J. Hoeijmakers, R. van Driel, A. A. van Zeeland, and L. H. F. Mullenders. 2001. Sequential assembly of the nucleotide excision repair factors in vivo. Mol. Cell 8:213–224.
46. Waga, S., and B. Stillman. 1998. The DNA replication fork in eukaryotic cells. Annu. Rev. Biochem. 67:721–751.
47. Yao, N., J. Turner, Z. Kelman, P. T. Stukenberg, F. Dean, D. Shechter, Z. Q. Pan, J. Hurwitz, and M. O'Donnell. 1996. Clamp loading, unloading and intrinsic stability of the PCNA, beta and gp45 sliding clamps of human, E. coli and T4 replicases. Genes Cells 1:101–113.
48. Yuzhakov, A., Z. Kelman, J. Hurwitz, and M. O'Donnell. 1999. Multiple competition reactions for RPA order the assembly of the DNA polymerase delta holoenzyme. EMBO J. 18:6189–6199.

Chapter 5

~

Dynamics of replication factors in replication and Nucleotide Excision Repair

Manuscript in preparation

Dynamics of replication factors in replication and Nucleotide Excision Repair

Audrey. M. Gourdin[1], Martijn S. Luijsterburg[2], Loes van Cuijk[1], Alex L. Nigg[3], Guiseppina Giglia-Mari[4], Adriaan B. Houtsmuller[3], Wim Vermeulen[1] and Jurgen A. Marteijn[1].

[1] Department of Genetics, ErasmusMC, Dr. Molewaterplein 50, 3015 GE Rotterdam, the Netherlands.
[2] Department of Cell and Molecular Biology (CMB), Karolinska Institutet, Box 285 / von Eulers väg 3, S-17177Stockholm, Sweden
[3] Department of Pathology, ErasmusMC, Dr. Molewaterplein 50, 3015GE Rotterdam, the Netherlands
[4] CNRS, IPBS (Institut de Pharmacologie et de Biologie Structurale), 205 route de Narbonne, F-31077 Toulouse, France

Nucleotide Excision Repair (NER) allows the removal of UV-induced DNA lesions by the coordinated assembly of pre-and post-incision complexes. The post-incision step of NER includes gap-filling DNA synthesis, carried out by the replication factors Proliferating Cell Nuclear Antigen (PCNA), Replication Protein A (RPA) and Replication Factor C (RFC), as well as a ligation.step By looking at the accumulation kinetics and localization at sites of DNA repair synthesis of these replication factors tagged with GFP in living cells, we demonstrate that these factors have a very different kinetic behavior than the other pre-incision NER factors, since they accumulate at prolonged periods at sites of UV repair. This suggests that the replication factors may have additional functions besides their known functions in repair synthesis. RPA is actually the only factor that is involved both in the pre- and post-incision steps of NER and displays differential dynamic properties

Introduction

Replication Protein A is a single-stranded DNA binding protein that is involved in several processes such as replication, repair, recombination and checkpoint signaling. It consists of three distinct subunits of 70, 32 and 14 kDa and binds ssDNA with a 5' to 3' polarity [Wold, 1997; de Laat et al, 1998]. RPA was initially identified as a crucial replication factor that, together with replication factor C (RFC) and proliferating cell nuclear antigen (PCNA), helps in loading the different catalytic DNA polymerizing enzymes (DNA pols) to chromatin. The complex interplay of these polymerases with DNA as well as the processivity of these enzymes is in part regulated by these replication accessory factors. [Iftode et al, 1999]

Eukaryotic PCNA is a trimeric sliding clamp that gets loaded around the DNA at the 3'- OH end of the nascent DNA in an RPA- and ATP-dependent manner in order to facilitate the tethering and processing of DNA polymerases δ and ε during lagging and leading strand synthesis [Moldovan et al, 2007; Maga et al 2000; Tsurimoto et al, 1990; Tsurimoto et al, 1991]. Loading of PCNA around the DNA is supported by the pentameric complex RFC, also known as clamp loader. The large subunit of RFC, RFCp140, distinguishes it as the specific loader of PCNA during DNA replication and differentiates it from RFC-like complexes that are involved in alternative mechanisms [Majka, Burgers, 2004].

The integrity of the DNA sequence can be impaired by endogenous or exogenous DNA damaging agents that will negatively influence the processivity and fidelity of replicative DNA synthesis. An intricate network of efficient DNA repair pathways, damage tolerance processes and checkpoint mechanisms collectively safeguards genomic integrity. One of the most versatile DNA repair mechanisms is nucleotide excision repair (NER), which is able to remove a broad spectrum of different DNA lesions that destabilize the DNA helix, including the main UV-induced lesions: cyclo-butane pyrimidine dimers (CPD) and 6-4 pyrimidine-pyrimidone dimers (6-4-PP). NER is a "cut and patch" mechanism that involves more than 30 polypeptides which act coordinately to recognize and excise the lesion [Gillet et al, 2006; Friedberg, 2003; de Laat et al, 1999]. The resulting ssDNA gap is filled in by DNA synthesis and sealed. NER can be sub-divided into two pathways that share many similarities but differ by their lesion recognition mechanism. Global Genome NER (GG-NER) detects lesions located anywhere in the genome and initiates the NER reaction by the concerted action of two damage recognizing complexes; XPC/HR23B/ centrin complex for some lesions assisted by the UV-DDB complex [Sugasawa, et al, 1998 and Moser et al, 2005]. Trans-cription Coupled NER (TC-NER) is only active on the transcribed strand of active genes [Venema et al, 1992; Fousteri, and Mullenders, 2008; Bohr et al, 1985] and is

initiated by the stalling of elongating RNA polymerase II on DNA lesions [Fousteri et al, 2006; Laine and Egly, 2006]. Following damage recognition, GG-NER and TC-NER channel into a common mechanism which starts with the local unwinding of the DNA double helix around the lesion by the ten-subunit transcription factor TFIIH [Yokoi et al, 2000; Volker et al, 2001; Giglia-Mari et al, 2006].The unwound DNA is stabilized by XPA and RPA. A 24-32 nucleotide strand is incised in a sequential manner with a first incision made by the ERCC1-XPF complex that incises 5' to the lesion followed by the 3'incision catalyzed by XPG [Bardwell et al, 1994; Sijbers et al, 1996; O'Donovan et al, 1994; Staresincic et al, 2009]. The undamaged strand serves then as a template for further gap-filling DNA synthesis (or repair synthesis) that is carried out by RPA, RFC, PCNA, pol δ (and in some cases pol κ and pol ε) [Ogi et al, 2010], while the gap is sealed by LigaseIII-XRCC1 or Ligase I [Moser et al, 2007].

Several reports have shown that PCNA and RFC are involved in the repair synthesis step of NER *in vitro* and *in vivo* [Nichols and Sancar, 1992; Shivji et al, 1992; Aboussekhra, et al, 1995; Araujo et al, 2000; Green et al, 2003; Essers et al, 2005; Mocquet et al, 2008; Overmeer et al, 2010]. Moreover, RPA displays a dual involvement in NER, since it is implicated both in the pre-incision and the post-incision steps of NER. RPA binds to the undamaged DNA strand and is indispensable for open complex formation. It interacts with several NER proteins (XPA, XPG, ERCC1-XPF) and stimulates the incision activity of both endonucleases [de Laat et al, 1998; He et al, 1995; Matsunaga et al, 1996]. It also plays a crucial role in DNA synthesis [Shivji et al, 1995].

A number of UV lesions however, escape removal by NER before replication starts. This triggers a block in the progression of the replication fork that may, in the worst case, lead to a definitive arrest of replication and cell death. Two damage tolerance mechanisms have evolved in order to avoid replication arrest: Translesion Synthesis (TLS) and recombination-directed damage avoidance. Mono-and poly-ubiquitination of PCNA play a central role in the inter-dependency and regulation of these mechanisms [Hoege, et al, 2002; Kannouche et al, 2004]. TLS consists of the incorporation of nucleotides opposite the damage by a set of specialized TLS DNA polymerases. *In vitro* studies have shown that RFC and RPA are also involved in TLS [Nikolaishvili-Feinberg et al, 2008 and McCulloch, et al, 2007]. Recombination directed damage avoidance consists of a recombinational mechanism to copy genetic information from the undamaged sister duplex into the damaged template in order to restore the lost information. The implication of low-fidelity DNA polymerases in TLS makes this process in principle error-prone, whereas HR-directed replication bypass is considered as error-free. However, this process of HR-directed bypass, mediated by PCNA polyubiquitination, is poorly understood in mammals and it is debated to which extent it occurs. Clearly it is important in uni-cellular eukaryotes such as

S*accharomyces cerevisiae* [Chiu et al, 2006; Langie et al, 2007; Hoege et al, 2002]. In addition, damage induced replication stalling can result in fork collapse and may create DNA double-strand breaks, that are sealed by homologous recombination (HR). In each of these processes the replication factors play a crucial role. In addition, within HR, RPA is pivotal for the nucleo-protein filament formation after end-resection, prior to coating of the single strand DNA by the strand-exchange protein RAD51. Furthermore, it is known that bypass of lesions that occur during S phase can employ recombination-associated processes [Lisby and Rothstein, 2009], implying a potential role for RPA in these events.

Hence, upon UV irradiation, PCNA, RFC and RPA are recruited to the site of damage in order to process the 6-4PPs and CPDs. These factors are not only involved in the repair synthesis step of the NER process that is occurring during G1 and S, but also in the replication associated processes that occur during S-phase. *In vitro* experiments have revealed that RPA remains bound to the DNA substrate after dual incision and initiates the assembly of DNA synthesis factors [Riedl et al, 2003]. On the contrary, additional *in vivo* studies have shown that RPA associates very transiently to sites of NER [Luijsterburg et al, 2010].

In this paper, using immunofluorescence and live cell microscopy of GFP-tagged versions of replication proteins we have analyzed the spatio-temporal distribution of RPA, RFC and PCNA to uncover the dynamic transactions of these factors with the DNA template in the different maintenance processes.

Results

RFCp140, PCNA and RPAp70 are differentially visible at replication foci

To study the spatio-temporal distribution of the DNA replication factors we compared the localization of RPA, RFC and PCNA in living cells. For this purpose the 70 kDa subunit of the heterotrimeric RPA was tagged with GFP on its C-terminus and stably expressed in MRC5 cells, an SV40-transformed human fibroblast cell line. Immunoblot analysis showed that full-length RPAp70-GFP is expressed at physiological levels (Figure 1A). Cell cycle analysis showed that the profile of this cell line was similar to untransfected MRC5 cells, indicating that the construct does neither alter the cell cycle nor affects the S-phase progression (data not shown). RPAp70-GFP localization in living cells was compared to endogenous RPA using immunofluorescence (Figure 1B). In all cells, RPA displayed a quite homogeneous nuclear localization, in addition to regions with lower concentrations coinciding with the nucleoli and a small number of sub-nuclear areas with locally higher concentrations (maximum 10 per cell, previously ascribed to promyelocytic leukemia (PML) bodies [Park et al, 2005

and Groth et al, 2007]). The same nuclear distribution was also observed by immunofluorescence with anti-RPA32 [Groth et al, 2007] (Figure 1B).

Next the sub-cellular localization of RPAp70, RFCp140-GFP and GFP-PCNA in an asynchronous population of living cells was studied by high-resolution confocal scanning imaging (Figure 1C, D, E). In eukaryotes, DNA replication is initiated and propagated from hundreds to thousands of replication sites, called replicons. Several studies have revealed that a number of replication forks cluster into 'replication foci', each containing multiple copies of replication sites and the associated replication factors [Hand 1978; Nakayasu and Berezney, 1989; Nakamura et al, 1986; O'Keefe et al, 1992]. The location, number and size of these replication foci vary throughout S-phase, according to a program that corresponds to the replication of various portions of the genome. Hence, three distinct replication patterns can be distinguished, that correspond to DNA synthesis in early to mid-S phase (small and discrete foci), mid to late S-phase (perinucleolar and perinuclear large foci) and very late S-phase (large foci) (Nakayasu and Berezney, 1989; O'Keefe et al, 1992]. For both GFP-tagged RFCp140 and PCNA we were able to identify in some living cells these different focal patterns and in others, homogenous distributions (Figure 1C), indicative for localization to S-phase foci and G1 or G2, respectively. The focal pattern of PCNA was previously shown in living cells [Leonhardt et al, 2000; Somanathan et al, 2001; Essers et al, 2005], however only recently a similar distribution pattern for RFCp140-GFP was observed [Overmeer et al, 2010] (Figure 1C).

To investigate the cell cycle dependent distribution of RPA70-GFP, mCherry-PCNA was co-expressed to identify cells in S-phase [Soria et al, 2009]. Surprisingly, we do not observe focal accumulation of RPA70-GFP in cells that do present mCherry-PCNA foci (Figure 1D). However, immunofluorescence studies using antibodies directed against endogenous RPA do exhibit foci in S-phase cells [Murti et al, 1996]. These data suggest that RPA, although an important replication factor, is not clustered into replication foci in living cells or that the GFP-tag negatively influences its proper localization. The *in vivo* localization of RPA, using a GFP-tagged version of RPAp34 was previously investigated by Solomon and co-workers who also did not observe focal accumulations of this RPA subunit in S-phase cells [Solomon et al, 2004], in line with our observations. However, in a recent report from the same laboratory [Görisch et al, 2008] the authors do observe limited focal accumulations using the same RPA34-GFP construct, though with low efficiency. When these were analyzed in the presence of the replication inhibitor aphidicolin accumulation of RPA34 was significantly more pronounced, suggesting that under normal conditions the localization of RPA to replication is too transient to clearly visualize in living cells.

To visualize a possible localization of RPA70-GFP in replication foci we attempted to slow down the binding

kinetics of this protein by incubating the cells with the DNA synthesis inhibitors Hydroxyurea and cytosine-β-arabino-furanoside (HU/AraC). After this treatment a large number of cells exhibited S-phase foci (Figure 1E). This observation is in line with previous reports that also showed a focal pattern of RPAp34 upon treatment with the polymerase inhibitor aphidicolin [Görisch et al, 2008; Solomon et al, 2004]. Together these data indicate that either the amount of single-stranded DNA exposed in normal replicating cells is not enough or the residence time of RPAp70 on the ssDNA is too short, to visualize any RPA binding in replication factories.

To test this in more detail, we measured the mobility of RPAp70-GFP by photobleaching in the presence and absence of replication inhibitors. A small square of the cell was bleached and the recovery of fluorescence, i.e. the diffusion rate of RPAp70-GFP, was monitored. Figure 1F shows that inhibition of the replication fork progression by treatment of cells with HU-AraC induces an overall slower mobility in the nucleus. This slower mobility is likely derived from a fraction of proteins that are transiently immobilized at inhibited replication forks. These data are consistent with the idea that in the presence of these inhibitors the DNA polymerases cannot remove RPA from the substrate, which might also account for its longer residence time.

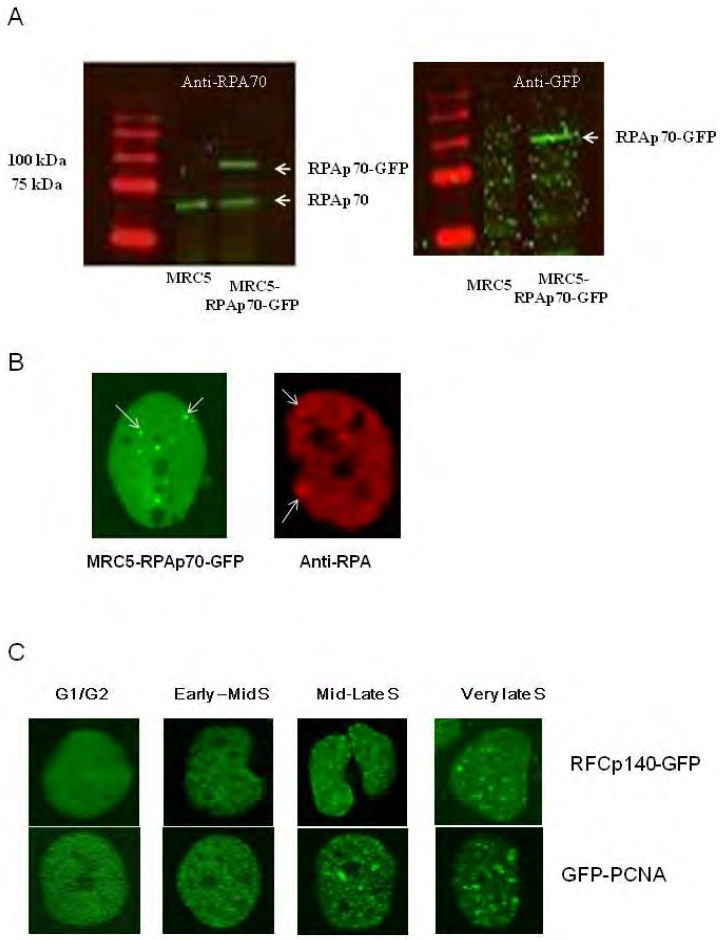

Figure 1: Sub-cellular localization of RFCp140-GFP and RPAp70-GFP.
A. Immunoblot analysis of whole cell extracts of MRC5 and MRC5-RPAp70-GFP cells with anti-RPA anti-GFP antibodies reveal that RPAp70 and RPAp70-GFP at expressed at a 1:1 ratio and that no degradation product is observed. **B**. Localization of RPA into PML bodies observed in living cells expressing RPAp70-GFP (left) and in fixed cells with immunofluorescence with anti-RPAp32 (right) **C.** Confocal images of cycling MRC5 cells expressing RFCp140-GFP and GFP-PCNA. The replication factors display a homogeneous localization in G1/G2 and specific S-phase stage dependent patterns. **D.** Confocal images of cycling MRC5 cells expressing RPAp70-GFP and PCNA-Cherry. RPAp70-GFP displays a homogeneous localization in all cells. **E.** Confocal images of cycling MRC5 cells expressing RPAp70-GFP upon addition of HU/AraC. In the presence of these DNA synthesis inhibitors, RPAp70-GFP localizes to replication foci. **F.** Cells were untreated or treated with HU/AraC for 30mins. A square of the cell was bleached out (FRAP in "local damage") and the recovery of fluorescence monitored over time, showing that in presence of DNA synthesis inhibitors RPAp70-GFP is further immobilized at sites of replication.

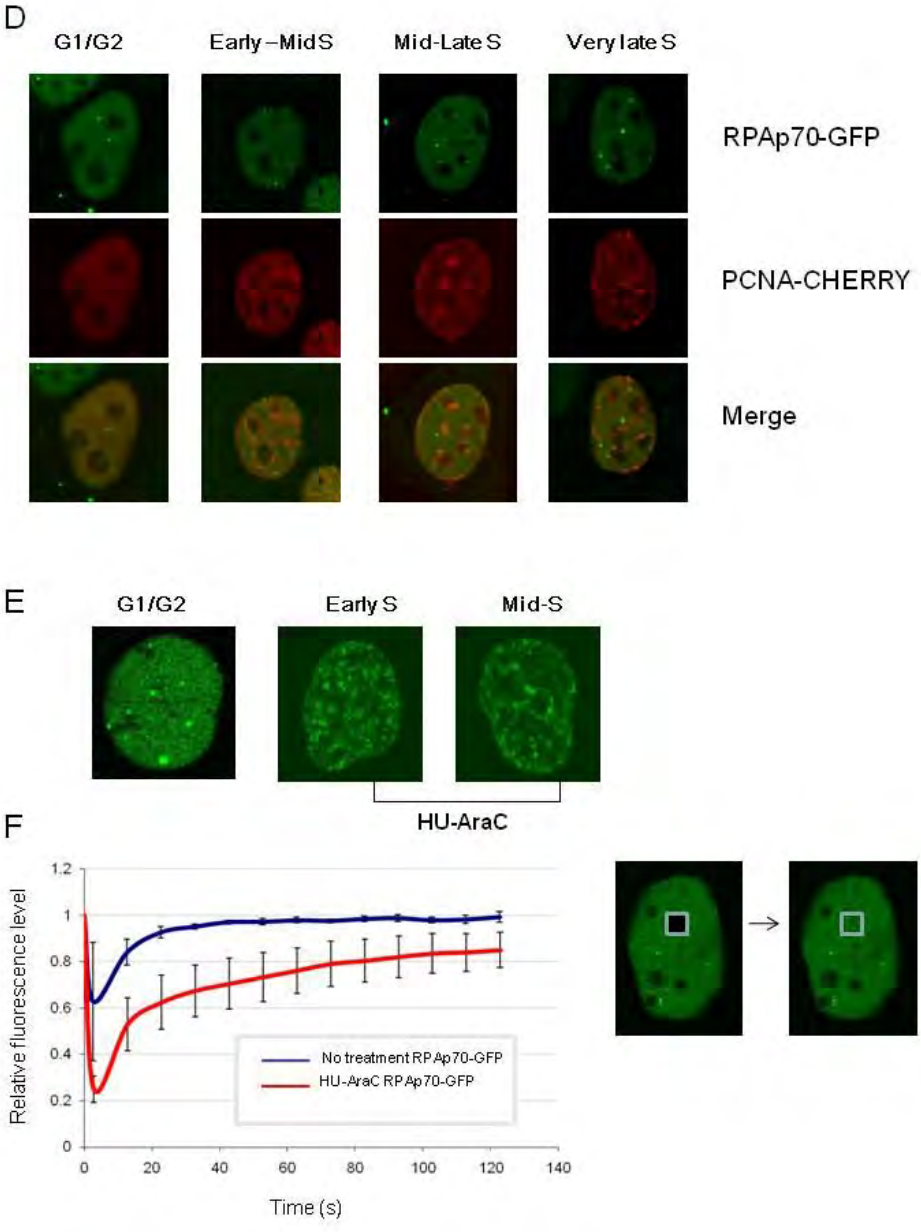
D
G1/G2
Early – Mid S
Mid-Late S
Very late S
RPAp70-GFP
PCNA-CHERRY
Merge
E
G1/G2
Early S
Mid-S
HU-AraC
F
Relative fluorescence level
1.2
1
0.8
0.6
0.4
0.2
0
0
20
40
60
80
100
120
140
Time (s)
No treatment RPAp70-GFP
HU-AraC RPAp70-GFP

.

Comparison of GFP-PCNA, RPAp70-GFP and RFCp140-GFP mobility

In contrast to RPAp70, PCNA and RFCp140 can be clearly identified in replication foci in living cells. Based on the involvement of each of these factors in replication, this apparent discrepancy could be explained by their different binding times, which may in part be influenced by the overall mobility in the nucleus. To determine in more detail the movement of these proteins we applied an adapted FRAP procedure, designated FLIP-FRAP analysis associated to half-nucleus bleaching [Figure 2A; Hoogstraten, 2002; Houtsmuller, 1999; Overmeer et al, 2010]. Previous FRAP studies have shown that in non-S-phase cells the mobility of GFP-PCNA and RFCp140-GFP is mainly determined by free diffusion [Essers et al, 2005; Overmeer et al, 2010]. The mobility curves of GFP-PCNA and RPAp70-GFP were comparable (Figure 2B), with a redistribution time of approximately 50 s. RFCp140-GFP showed a much slower redistribution time of approximately 120s, indicative of a slower diffusion rate, which is likely related to the molecular shape and size of the complex, i.e. almost twice the molecular weight of both the PCNA trimer and the RPA hetero-trimer. Although the mobilities of PCNA and RPA appeared very similar in G1/G2 cells a striking difference was observed in S-phase cells (Figure 2C). S-phase RPAp70-GFP cells were identified by PCNA foci, using co-transfection of PCNA-Cherry which displays a clear S-phase pattern. As expected from earlier studies [Sporbert et al, 2002], GFP-PCNA was highly immobilized in replication factories, with a recovery time of 3 minutes. Interestingly, the dynamics of RPAp70-GFP was similar in G1/G2 phase and in S-phase, with a recovery time of ~25 seconds. The observed differences in mobility of PCNA and RPA in S-phase are likely explained by a very short binding time of RPAp70-GFP molecules with DNA replication substrates and/or factors. Binding times of RFCp140-GFP to replication foci appeared already very short [Overmeer et al, 2010,], though in this case replication foci are visible in live cell imaging. These data suggests that the dwell time of most of the RPA molecules in foci should be extremely short, even shorter than the residence time of the TLS polymerase, pol-eta in replication foci [Sabbioneda et al, 2008], which was also visible in live cell imaging.

RPAp70-GFP accumulates for up to 8 hours at sites of local UV damage

RPA, PCNA and RFC are not involved solely in replication but also in several DNA repair and replication-stress response processes such as NER and Translesion synthesis. In order to obtain a complete overview of replication factor kinetic behavior upon UV damage, we compared the earlier determined kinetic behavior of PCNA and RFC with that of RPA [Overmeer et al, 2010 ; Essers et al, 2005].

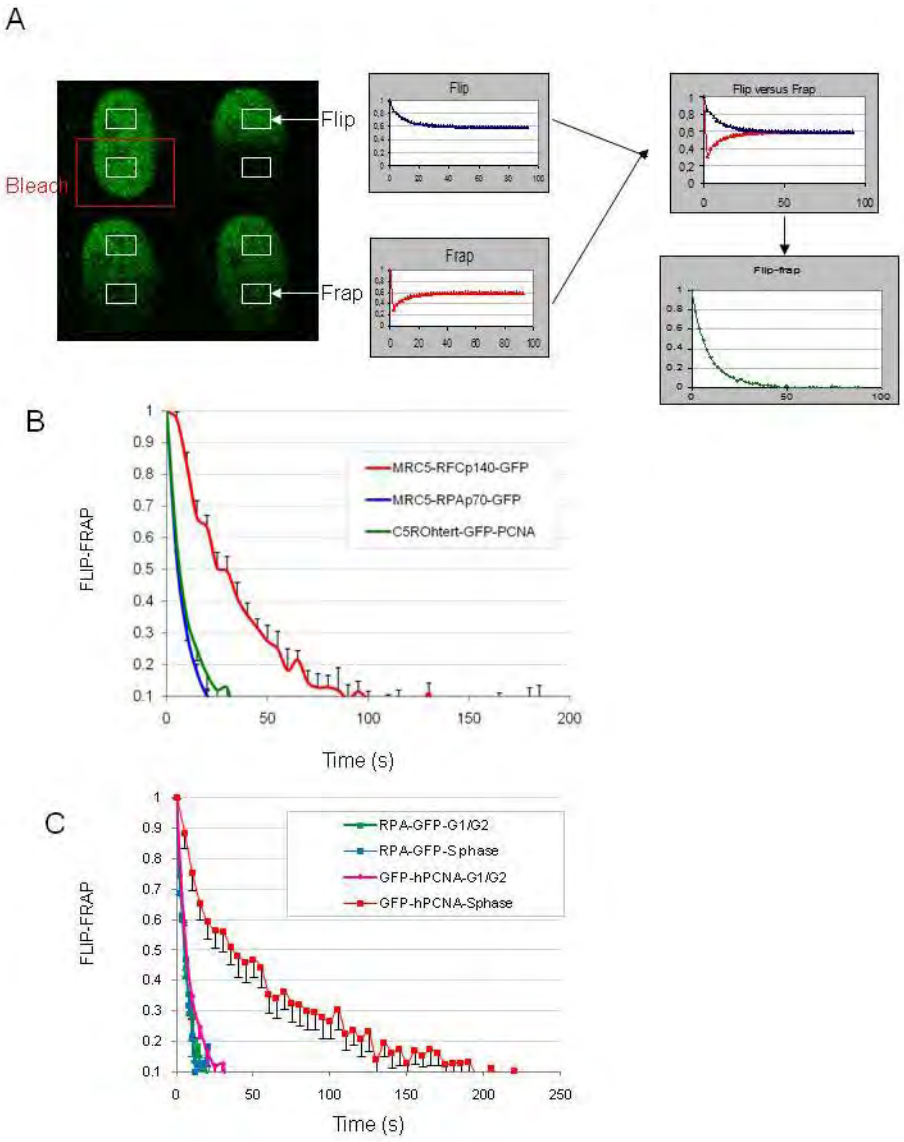

Figure 2: diffusion and dynamics of replication factors at replication foci

A. Half nucleus bleaching associated to FLIP-FRAP procedure and analysis. Half of the nucleus is bleached by high-intensity laser. The loss of fluorescence (FLIP) in the unbleached half is measured over time and plotted against the recovery of fluorescence (FRAP) in the unbleached half of the cell. The difference (FLIP-FRAP) is normalized to 0 after the bleach pulse. **B.** Diffusion curves of RFCp140-GFP, RPAp70-GFP and GFP-PCNA measured by the previous flip-frap procedure show that in untreated cells, RFCp140-GFP diffuses much more slowly than the other replication factors. **C**. FLIP-FRAP in MRC5 cells and C5ROhtert cells respectively expressing RPAp70-GFP and GFP-PCNA show that while GFP-PCNA is immobilized in replication factories, RPA-70-GFP is too transiently immobilized to be detectable.

Hence, accumulation of RPA at sites of damage was first investigated in fixed U2OS cells by immunofluorescence against endogenous RPAp32 (Figure 3A). The population of cells was asynchronous when damage was inflicted. Local UV damage (LUD) was made with a UV-C lamp and 5 μm pore-containing filters, as described previously [Moné et al, 2001]. Cells were fixed at various time points after UV (15 mins, 1, 4 and 8 hours). CPD or XPA staining was used to identify LUD. The lesion recognition factor XPC and the components of the pre-incision complex XPB and XPA start accumulating at LUD shortly after damage infliction (within 15 mins) and disappeared after 4 hours (Figure 3A) [Luijsterburg et al, 2010; Marteijn et al. 2009], when repair of most of the 6/4 photoproducts is completed However, XPA remained visible slightly longer (8 hours), likely due to additional functions of XPA beyond the incision step of NER [Luijsterburg et al, 2010; Marteijn et al, 2009]. On the contrary, only a faint RPA signal could be detected within LUD at the earliest time point (15 mins), while a much stronger staining was visible from one hour after UV on and lasted in some cases even up to 24 hours (Figure 3C). The two major DNA lesions induced by UV irradiation display different repair kinetics: while 6-4PPs are repaired within ~6 hours, CPDs repair is not achieved within 24 hours [Van Hoffen et al, 1995, Marteijn et al, 2009]. In our previous studies, accumulation of NER factors to LUD followed the repair kinetics of 6-4PP [Luijsterburg et al, 2010]. Hence, long-lasting accumulation of RPA at LUD cannot solely be explained by NER of 6-4PP, but suggests additional functions in post-incision events or implication in other replication-associated processes linked with the persistent presence of CPD injury It is thus possible that accumulation in LUD at later time points post-UV may represent replication-stress in cells that where in S-phase at the moment of damage infliction or moved into this phase despite the presence of DNA damage, rather than binding into NER sites. To further dissect these options we developed a four-color immuno-fluorescence procedure to detect RPA and XPA by antibodies, S-phase cells by EdU incorporation [Marteijn, 2009] and nuclei by DAPI (Figure 3B). Accumulation of RPA at LUD one hour after UV is visible in both S-phase and non S-phase cells (Figure 3B), suggesting that RPA accumulation in LUD also marks NER sites.

Interestingly, in quiescent cells where no replication processes occur, RPA localization to LUD was also observed for up to 8 hours after UV, indicating that replication-associated processes are not solely responsible for the observed localization of RPA to LUD (data not shown).

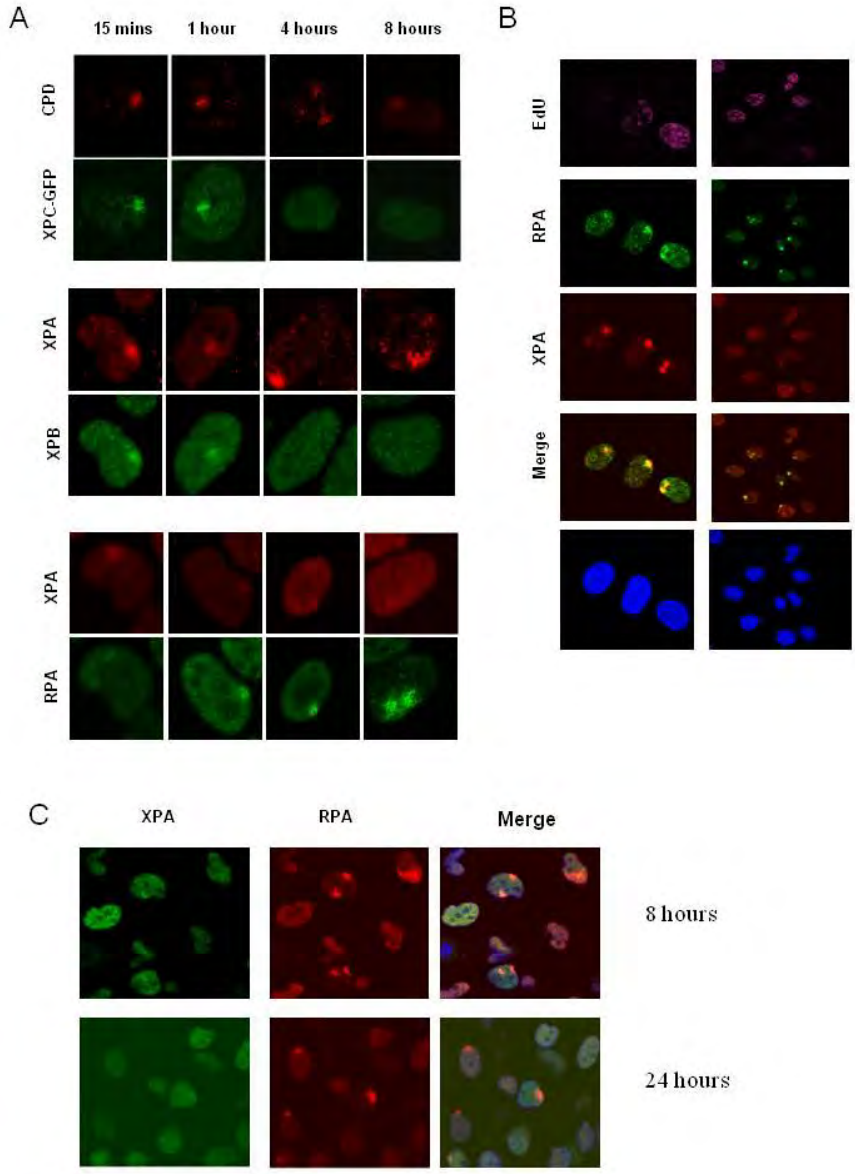

Figure 3: kinetics of accumulation of pre- and post incision factors at sites of local UV damage
A. Representative images of XPB, RPA and XPC-GFP co-localization with a damage marker (either CPD or XPA). Co-localization was determined 15 minutes, 1 hour, 4 hours and 8 hours after Local UV exposure (45 J/M^2). **B.** U2OS cells were exposed to local UV damage and directly after damage incubated for 1 hour in medium containing EDU. Cells that were in S-phase during the 1 hour after the UV exposure stain positive for EDU, visualized by Alexa 647 fluorchrome, XPA was used as a damage marker. RPA accumulates both during S-phase and in cells that were not in S-phase after the UV exposure. **C.** Immunofluorescence of cycling MRC5 cells at several time points after local UV induction through 5µm pore-containing filter, with anti-RPA 32 (red) and anti-XPS (green)

RPA, RFC and PCNA show similar kinetics of accumulation at sites of UV damage

To further investigate the behavior of the replication factors PCNA, RFC and RPA at sites of UV lesions repair, we inflicted local damage in asynchronous living cells expressing the fluorescent versions of the proteins. Irradiation was carried out through 5μm filter pores, with a UV source above the microscope stage and fluorescence levels at LUD was measured over time [Moné et al, 2004] (Figure 4A) and reflects the assembly kinetics of NER factors on lesions. The quantification of the assembly kinetics of GFP-PCNA, RFCp140-GFP and RPAp70-GFP revealed very similar kinetics of accumulation, which is markedly different than those of the pre-incision factors XPC and XPA (Figures 4B and 4C). For the three proteins, binding reached a maximum only after 200 min (more than 3 hours) and did not significantly decrease during the next 3 hours. It is surprising to note that all of the investigated NER-associated replication factors localize at LUD far long after 6-4 P-P removal, which are completely removed at these time points [Van Hoffen et al, 1995] and DNA repair synthesis levels are reduced to background levels (data not shown).

The notion that RPA only becomes visible at LUD at longer time points post-UV than any of the other pre-incision NER factors, although it is absolutely required for the incision [Coverley, et al, 1991; Aboussehkra et al, Cell], suggests that the binding time of RPA in this pre-incision NER step is too short to be visualized by this procedure, similar to the absence in replication foci (Figure 1D). The fact that RPA is present for a long time at sites of local damage, similarly to RFC [Overmeer et al, 2010], in contrast to the pre-incision NER factors, suggests that either RPA is bound longer in repair replication or that a higher number of RPA molecules are bound with higher affinity in these late NER steps.

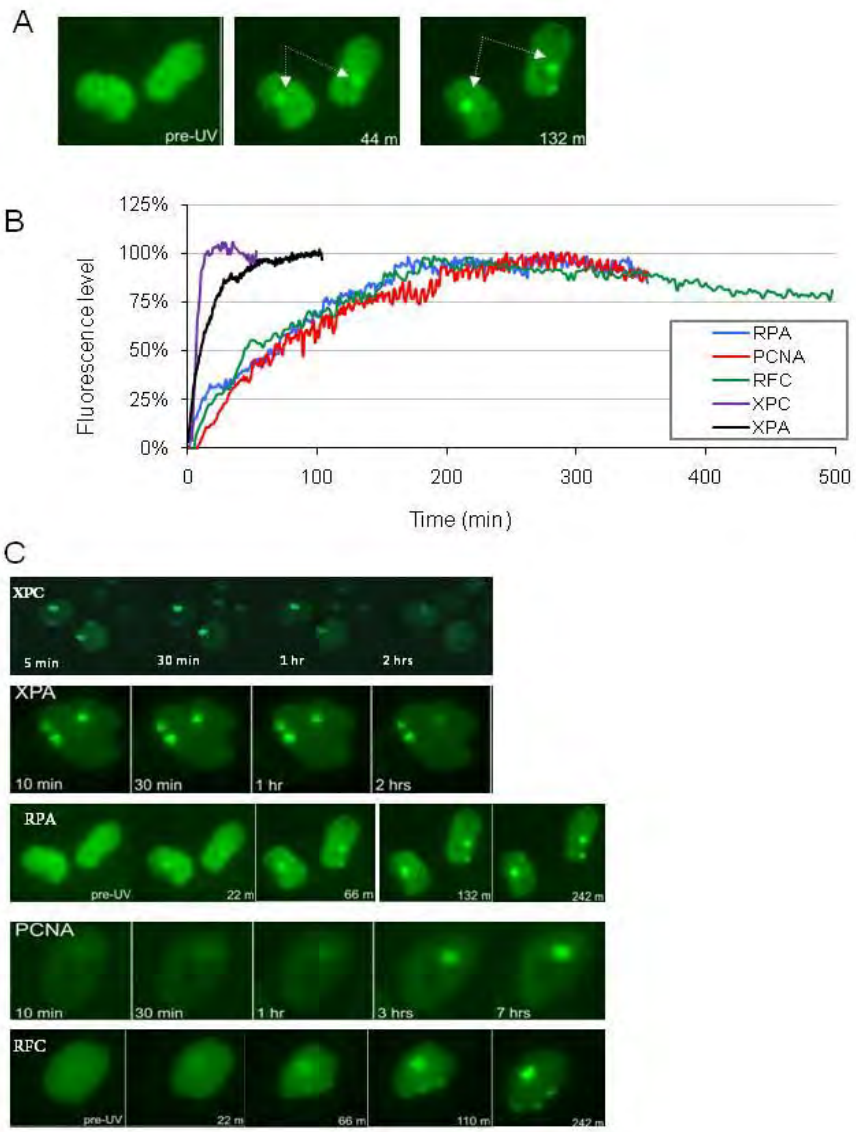

Figure 4: long-lasting accumulation of replication factors at sites of UV-C damage

A. Procedure showing induction of UV local damage and immediate follow-up of accumulation of a protein at the site of damage. **B.** Using this procedure, accumulation of RPAp70-GFP, RFCp140-GFP and GFP-PCNA at sites of UV-C damage was measured over 8 hours and compared to GFP-XPA and XPC-GFP. Accumulation of the replication factors increased during the first 3 hours to reach a plateau and remain constant for up to 8 hours. **C**. Time-lapse imaging of cells displaying various GFP-tagged proteins upon UV-irradiation

Dynamics of RPAp70-GFP at sites of UV- damage upon HU/AraC treatment

To further decipher the mode of action of RPA during the DNA synthesis step of NER, we used the DNA synthesis inhibitors HU/AraC. Upon treatment with HU/AraC, repair synthesis is inhibited, which allows a differentiation between the pre- and post-incision steps of NER [Overmeer et al, 2010]. After mock treatment or treatment of the cells in presence of these inhibitors for 30 mins, cells were locally UV irradiated. In the presence of HU/AraC, much more RPA is found at LUD than in the absence of the inhibitors (data not shown). This could be due, either to an increase of the number of binding places, or to a more stable association of RPA with the substrate. One hour after irradiation, a nuclear volume representing approximately one third of the nuclear volume, located opposite of the LUD, was continuously bleached and the intensity of fluorescence in the local damage was measured (FLIP) [Luijsterburg et al, 2010]. This procedure allows determining of the off-rate of proteins bound in LUD. Figure 5 shows that on average RPAp70-GFP molecules bind longer in the presence of inhibitors as compared to cells with processive replication. If RPA was solely involved in the pre-incision step of NER and if its localization to sites of repair was exclusively rising from this involvement, inhibition of repair synthesis would not trigger any additional immobilization of RPA. Indeed, this experiment confirms that RPA presents differential kinetic properties in pre-incision and in repair synthesis.

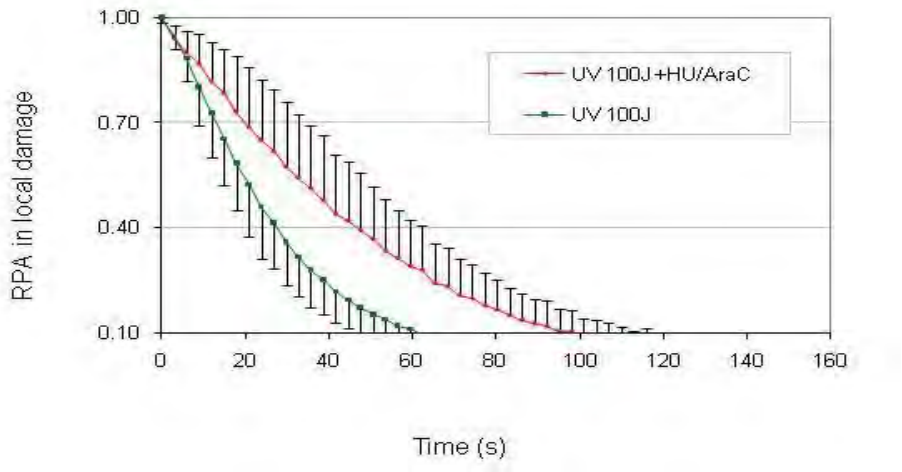

Figure 5: dynamics of RPAp70-GFP at sites of UV-C damage upon HU/AraC

Cells were untreated or treated with HU/AraC for 30mins. All cells were then locally irradiated (100 J/m^2). A nuclear volume away from the damaged region was bleached out while decrease of the signal intensity in the local damage was monitored over time. Additional accumulation of RPAp70-GFP was observed in treated cells.

Focal pattern of the local damage

In contrast to Ionizing-Radiation Induced foci (IRIF) [Bekker-Jensen et al, 2006] in which Homologous Recombination repair factors accumulate after IR, NER proteins do not display such a focal accumulation after UV [Rademakers, 2003; Moné et al, 2004; Giglia-Mari et al, 2006; Zotter, MCB, 2006; Luijsterburg et al, 2007; Alekseev et al, 2008] (Figure 6B).. Remarkably however, RPA displayed a different distribution pattern in LUD (Figure 6A) than XPA (Figure 6B) and the other pre-incision factors. In all cells a very clear focal pattern of RPAp70-GFP was visible within local damage. Although in normal replication RPA appeared not visible in replication foci, this focal pattern might be derived from accumulation of RPA at sites of replication stress, due to the fact that cells might be locally UV-damaged when present in S-phase. It should be noted however that we do observe this focal patter in all LUD inflicted cells, which makes it less likely that all these cells were in S-phase during or shortly after irradiation. Moreover, a similar focal pattern in LUD was observed in cells expressing GFP-PCNA and RFCp140-GFP (Figure 6C and 6D). This was even visible in cells with an overall homogeneous distribution of GFP-PCNA and RFCp140-GFP, indicative for non-S-phase (Figure 6C) and further suggests that this focal pattern is not due to S-phase cells (Figure 6D). These observations could also be explained by the fact that some cells may enter into S-phase at or during the time of imaging. To rule out this option we then tested the accumulation pattern in LUD in cell cycle-arrested primary fibroblasts. To that aim we serum starved a confluent population of C5ROhtert fibroblasts expressing GFP-PCNA, to generate a non-cycling status or G0 phase as tested by the absence of a positive signal for the proliferation marker Ki67 (data not shown). Also in these cells GFP-PCNA was distributed in a focal pattern in LUD (Figure 6E).

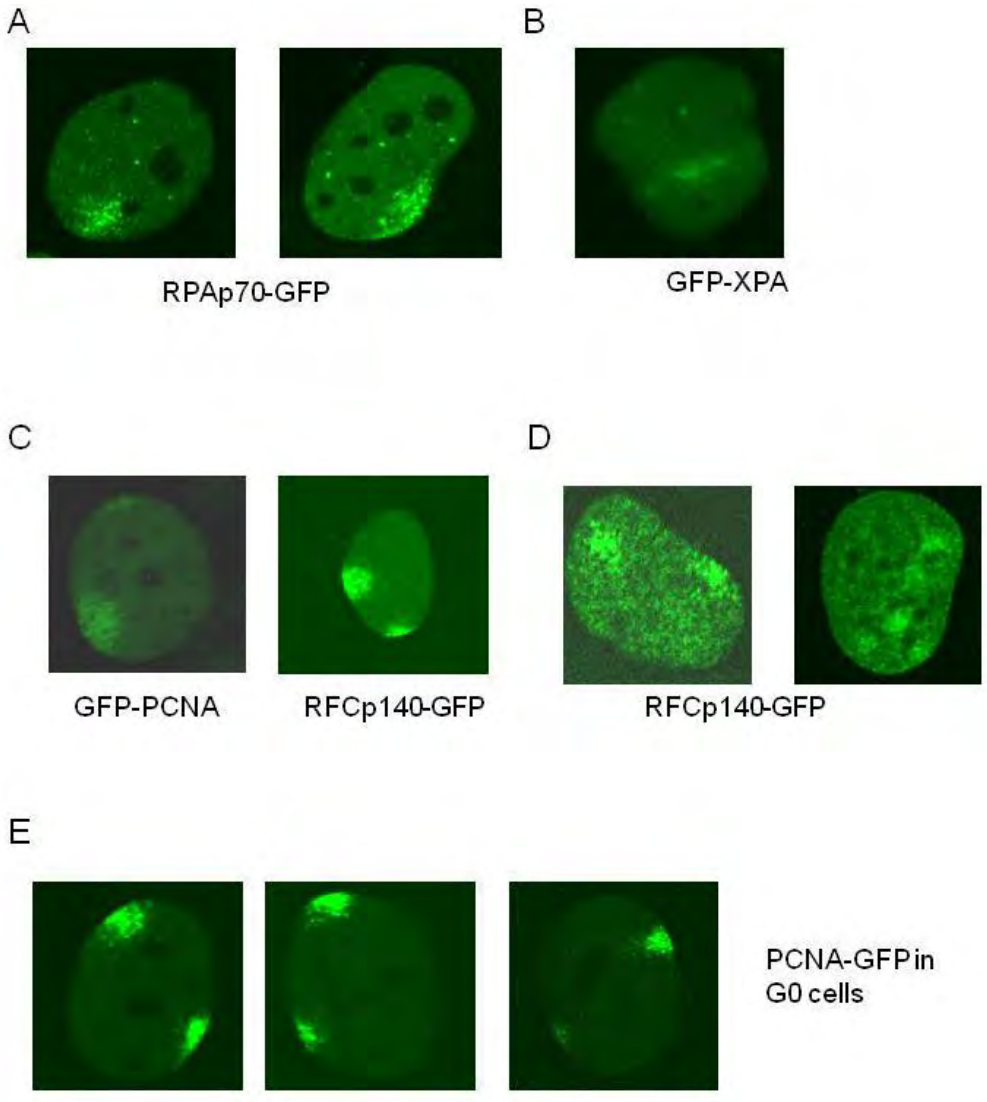

Figure 6: Accumulation of diverse replication factors at sites of local UV-C damage occurs in a focal pattern

Live cells were locally irradiated through 8μm pores (100 J/m2) and confocal pictures were taken**. A.** RPAp70-GFP accumulates focally in all MRC5 cells. **B.** GFP-XPA accumulates homogeneously in all XP2OS (XPA) cells. **C**. GFP-PCNA and RFCp140-GFP accumulates focally in C5ROhtert and MRC5 cells that do not present any S-phase foci. **D.** RFCp140-GFP accumulates focally in S-phase MRC5 cells. **E**. GFP-PCNA accumulates focally in quiescent cells where no replication event is occurring.

Discussion

Transient binding of RPA and RFC at sites of DNA replication

Replication foci or replisomes are "mega-complexes" that contain large amounts of DNA polymerases and other replication factors (PCNA, RPA, DNA polymerases α and ε, DNA Ligase I, CAF 1) [Tubo and Berezney 1987; Cook, 1999] and a growing list of cell cycle control factors (Cdk2/cyclinA, MRE11 etc) and TLS polymerases (DNA polymerases η and ι) [Frouin et al, 2003]. It has been shown that PCNA displays relatively slow exchange kinetics at sites of [Essers et al, 2005; Sporbert et al, 2002]. On the contrary, the clamp loader RFC exhibits a much shorter binding time to replication sites [Overmeer et al, 2010]. This can be explained by the fact that dissociation of RFC from PCNA is necessary for interaction of PCNA with the DNA polymerase [Podust et al, 1998]. The clamp or polymerase platform PCNA remains bound during replication elongation and thus present a much longer residence time. The transient binding of RPA70-GFP (that exchanges in seconds and completely redistributes in 1 min) at replication sites is in line with previous observations by Görisch and co-workers [Görisch et al, 2008; Sporbert et al, 2002]. These observations suggest that although RPA is thought to coat ssDNA it is also swiftly displaced, possibly by the elongating DNA polymerase [Hübscher, Seo, 2001] or as intrinsic property of the protein. Hence, RPA is continuously binding and dissociating from ssDNA patches. In the presence of HU/AraC, the amount of ssDNA patches increases dramatically, thereby increasing also the number of substrates for RPA, which will not be removed the polymerases.

Differential binding of RPA at sites of NER pre-and post-incision

Our results suggest that RPA presents two distinct dynamics of binding at sites of NER: first a very transient binding during pre-incision, after which accumulation of RPA in LUD mainly becomes apparent when pre-incision events are not occurring anymore. This indication is further corroborated by the addition of DNA synthesis inhibitors that showed a more abundant accumulation with longer residence times. On the contrary residence times of other core pre-incision factors such as ERCC1 or XPA are not retarded by the presence of these synthesis inhibitors and in the case of XPA even shorter binding is found [Luijsterburg et al, 2010]. This suggests that the observed localization and dissociation of RPA to and from LUD is mainly derived from its function in repair synthesis. Given its dual role in pre- and post-incision steps of NER, it appears quite surprising that RPA displays such a dynamic behavior and the binding of an RPA molecule to create an incision-competent NER complex is not used for its replication function. It is known that RPA presents two binding modes that come from its intrinsic biochemical properties. Initially, it covers on the 5'side of the lesion a partially unwound structure of 8-10 nucleotides. After this, it elongates towards the 3'

direction and binds ssDNA with a region of around 30 nucleotides. [de Laat et al, 1998; Hermanson-Miller and Turchi, 2002; Kopalschikov et al, 2001]. These differential binding modes may account for different binding affinities of RPA for the ssDNA substrates. Moreover, the amount of substrates should also be taken into account, as well as the interactions between RPA and other repair factors.

RPA, RFC and PCNA accumulate longer than other NER factors at sites of UV-damage

It is striking to see that these three replication factors display very similar behaviors that are, in the same time, very different from other NER factors. While pre-incision factors, accumulate very shortly after UV and disappear within 4 hours, the post-incision factors RPA, RFC and PCNA reach their maximum only after 3 hours and keep accumulating for at least 8 hours. These observations were supported by recent immunofluorescence studies in which accumulation of PCNA, RFC and Ligase I in LUD was shown in quiescent cells for at least 8 hours after irradiation [Overmeer et al, 2010]. Within quiescent cells no replication occurs and the only active repair process following UV-C induction is NER repair synthesis.

A possible explanation could be that these proteins have other roles than their currently known functions in repair synthesis. PCNA, for example, through its interaction with CAF-1 [Rolef Ben-Shahar et al, 2009; Zhang et al, 2000; Gerard et al, 2006; Gaillard et al, et al, 1996; Green et al, 2003], is involved in chromatin remodeling. We have recently shown that RFC is involved in PCNA loading during NER *in vivo* and have also proposed a role for this protein in PCNA unloading [Overmeer et al, 2010]. Similarly, RPA might be ensuring the completion of repair synthesis before it detaches from a repair intermediate that can be potentially hazardous if not completely resolved. Additionally, the persistent localization of these factors at LUD may reflect UV-damages that are difficult to repair by NER due to either their localization or they represent spurious UV-light induced lesions that are not efficiently targeted by NER. Specific chromosomal localization of lesions in e.g. highly condensed chromatin might be refractory to NER-induced repair synthesis. Finally another, perhaps more remote, possibility is that two NER complexes collide during processing of lesions that are in close proximity and that in such an event repair synthesis cannot occur and thus substrate for the replication factors remains present to bind.

Focal pattern

The accumulation of replication factors to sites of repair synthesis into a focal pattern in G1/G2 cells comes across as surprising. Various studies on pre-incision NER factors have shown that these accumulate homogeneously within LUD [Luijsterburg et al, 2010; Zotter et al, 2006; Rademakers et al, 2003]. Several lines of evidence however do support this finding. First of all, focal localization of RPAp34-GFP was observed previously,

following both global UV irradiation and within areas of local UV damage [Solomon et al, 2004]. Others have shown that PCNA localizes to replication foci in fixed quiescent cells following UV irradiation [Celis and Madsen, FEBS Letters 1986; Toschi and Bravo, JCB 1988; Miura et al, Exp Cell Res, 1992; Jackson et al, 1994]. One explanation for these foci could be that several lesions may be inflicted at very proximal sites (as suggested above), although different calculations indicated that the change of closely associated lesions processed simultaneously by NER will not very high [Ogi et al, 2010], however this option should not be totally excluded.

Additionally to this, the TLS polymerase η was recently found to localize to sites of UV repair in G1 cells, although this finding has not been explained yet, it is interesting to note that localization of pol η occurred also in a focal fashion. An interesting model rising from these data is that factors may be recruited to foci of replication and repair without being actively involved in these processes, but rather remaining available, a model known as "be-ready-for".

Hence, another possible explanation for this finding could come from a clustering of repair synthesis sites. Several groups have followed sites of repair synthesis by monitoring incorporation of IdU and biotin-16-dUTP [Jackson et al, 1994; Jackson et al, 1994; Svetlova et al, 1999; Svetlova et al, 2002] and have revealed that sites of UV-dependent repair synthesis display a very clear punctuate pattern.

Understanding of this clustering of repair sites could be based on a comparison with replication factories and replication foci in the case of regular DNA replication. Currently the actual trigger for the formation of the replication focus is unknown. It is possible that foci formation triggers the assembly of replication factories. Early studies on *Xenopus* extracts have revealed that the clustered organization of DNA into foci may be an early replication event which occurs prior to the activation of the kinase activity of Cdk2 at the G1-S transition, also suggesting that this focal formation may correspond to a stable, higher order chromatin state [Newport and Yan, 1996].

Alternatively, the action of the replication process itself at certain loci is fundamental for the formation of these structures. Depositions of proteins at replication initiation sites that have an intrinsic affinity for a number of replication-associated factors are, in this scenario, likely candidates to be fundamental for focus formation. One of these proteins could be PCNA, since a short sequence of homology, called the Replication Factory Targeting Sequence (RFTS), that targets proteins to replication factories, is for a lot of replication factors the binding site for PCNA [Frouin, et al, 2003; Chuang et al, 1997; Montecucco et al, 2001]. Besides, Foci-Forming Activity-1 (FFA-1), a170 kDa protein and orthologue of the human WRN protein (Werner Syndrome), was reported to have a role in foci formation through its interaction with RPA [Yan et al, 1998; Yan et al, 1995]. Moreover, in the case of regular DNA replication, the finding that new replication foci assemble *de novo* at sites

that are located next to the previous cluster of origins rejects a sliding or jumping of the replication machinery to the next origins cluster and argues for an indirect mechanism of origin activation, known as "domino model". Accordingly to this, RPA binding and/or release from NER repair synthesis sites might have a role in further initiation of NER repair.
Finally, specific subsets of lesions that are not properly processed by NER or where repair synthesis is more difficult due to the chromosomal location (e.g. heterochromtin) ssDNA repair-intermediates (created by NER-incision) could be extended by nucleases and lead to long ss-stranded DNA patches that will get covered by many RPA proteins (which therefore are visualized in foci) [Lazzaro et al, 2009].

Materials and methods

Construction of GFP fusion RPA70.

RPA70 was cloned in frame upstream of the eGFP-cDNA in peGFP-N1 (Clontech).
Details of the cloning and primers' sequences will be available on request.

Establishment of a cell line expressing a tagged version of RPAp70 mimicking the expression and behavior of endogenous RPA in replication and repair.

Human RPA70 was tagged at its C-terminus with the green fluorescent protein (GFP), resulting in RPA_{70}-GFP. The fusion cDNA was stably expressed in SV40 transformed human fibroblasts, MRC5 cells. Immunoblot analysis with an anti-RPA70 antibody showed that endogenous RPA70 and RPA70-GFP were expressed at similar levels in the cells. Hybridization with anti-GFP antibody revealed that there was no breakdown product detectable, indicating that all the measured fluorescence in the cells is derived from the full-length protein.

Cell lines and culture conditions

All cells were grown under standard conditions at 37°C and 5% CO_2. U20S, C5RO tert-immortalized, Simian virus 40 (SV40)-immortalized fibroblasts MRC5 (wild type) and C5ROhtert-GFP-hPCNA cells were grown in a 1:1 mixture of Ham's F-10 medium and Dulbecco's modified Eagle's medium (DMEM) supplemented with 10% Fetal Calf serum (FCS) and 1% penicillin-streptomycin (PS). 600 µg/mL G418 was added as selection marker where appropriate. To study quiescent cells, the cells were grown confluent and subsequently incubated for 5 days with medium containing 0.2% FCS.

Global and local UV irradiation

Prior to (confocal) microscopy and immunofluorescence experiments, cells were seeded on 24 mm coverslips (Menzol), rinsed with phosphate-buffered saline (PBS) and irradiated with a UV-C (254 nm) Philips germicidal lamp (predominantly 254 nm). After irradiation cells were incubated with their original medium before being processed for microscopy experiments or immunofluorescence. For local irradiation cells were covered with a micro-porous polycarbonate filter containing 5 µm pores (Millipore) as previously described [Overmeer et al, 2010 and Moné et al, 2001]. For living cell studies, the UV-dose was either 60 or 100 J/m^2 for local irradiation as indicated, with or without HU/AraC treatment and 8 J/m^2 for global irradiation.

DNA synthesis inhibition with HU/AraC

Inhibitors of DNA synthesis were added 30 mins prior to UV irradiation: HU at 100mM and AraC at 10µM [Smith and Okumoto, 1984; Mullenders et al, 1987]

Immunofluorescence

Cells were fixed using 2% paraformaldehyde in the presence of 0.1% Triton X-100. Samples were processed as described previously (Rademakers et al., 2003). Immunofluorescent images were obtained using Zeiss LSM 510 META confocal microscopy equipped with a 63x oil Plan-Apochromar 1.4. NA oil immersion lens (Zeiss). Zeiss LSM image browser version 4.0 acquisition software was used. The following antibodies were used: anti-Ki67 (Abcam), anti-XPB (clone IB3 (Giglia-Mari et al., 2006)), anti-RPA32 (clone 9H8, Abcam), in combination with the corresponding secondary antibodies labeled with ALEXA fluorochromes 488 or 594 as indicated(Molecular Probes and Jackson Laboratory). DNA was stained using DAPI vectashield (Vector Laboratories) As marker for detecting local UV damage anti-hXPA (rabbit polyclonal anti-human XPA), or mouse anti-CPD (TDM-2, MBL) were used, depending on the species where the other used antibody was raised in. Edu incorporation was visualized using Click-iT Alexa Fluor 647 according to manufacturers protocol (Molecular Probes).

Western-blotting

Cell extracts of parental MRC5 and MRC5 cells expressing RPAp70-GFP were generated by sonication, separated by 8% sodium dodecyl sulfate polyacrylamide gel electrophoresis and transferred to nitrocellulose membranes. Expression of RPAp70-GFP was analyzed by immunoblotting with mouse monoclonal anti-RPAp70 antibodiy (B-6/sc-28304, 1:1000, Santa Cruz Biotechnology, Inc) and mouse monoclonal anti-EGFP antibody (1:1000, Roche) followed by a secondary antibody (donkey anti-mouse 800CW, 1:5000; Li-COR Biosciences) and detection using an infrared imaging-scanning system (Odyssey; LI-COR Biosciences)

Confocal microscopy and imaging

(i) Live cell microscopy

Confocal images of the cells were obtained using a Zeiss LSM 510 microscope equipped with a 25mW Ar laser at 488 nm and a 40 X 1.3-numerical aperture oil immersion lens. GFP fluorescence was detected using a dichroic beam splitter (HFT 488), a beam splitter NFT 490 and an additional 505- to 550-nm bandpass emission filter.

(ii) Fixed cells

For images of cells after immunofluorescence, the 25mW Ar laser at 488 nm together with a He/Ne 543 nm laser, and a 40 X 1.3 NA oil immersion lens were used. Alexa-488 was detected using a dichroic beam splitter (HFT 488), and an additional 505- to 530-nm bandpass emission filter. Cy3 was detected using a dichroic beam splitter (HFT 488/543) and a 560- to 615-nm bandpass emission filter.

Photobleaching techniques

(i) Half nucleus bleaching combined with flip-frap:

This protocol was implemented previously [Hoogstraten, 2002; Houtsmuller, 1999; Overmeer et al, 2010 and was as follows: an adapted FRAP (Fluorescence Recovery After Photobleaching) protocol was combined with a FLIP (Fluorescence Loss in Photobleaching) protocol by bleaching the GFP fluorescence in half the nucleus and subsequently measuring the fluorescence recovery in the bleached area (recovery or FRAP) and in the non-bleached area (FLIP). The time required to reach an equilibrium between FRAP and FLIP is a measure for the overall nuclear mobility of the tagged protein. Data analysis was performed in the following way: the FRAP was subtracted from the FLIP. The difference between FLIP and FRAP before bleaching was set as zero and the difference between FLIP and FRAP after bleaching was normalized to 1. The mobility of the protein was determined

as the time necessary for FLIP-FRAP to return to 0.

(ii) Box-frap

An entire square was bleached in 1.2s by two bleaching pulses, and the recovery of fluorescence monitored for 60s by scanning the whole cell every 5s. To overcome the variability in the size and intensity of the damage (i.e. the number of proteins immobilized), the curve was normalized to the overall fluorescence in the cell (including the local damage itself).

(iii) FLIP combined with local damage

FLIP analysis was performed by continuously bleaching a third of a locally-irradiated nucleus opposite to the site of damage at 100% laser intensity (488-nm argon ion laser) as previously described [Hoogstraten et al, 2002; Luijsterburg et al, 2007; Luijsterburg et al, 2010]. Fluorescence in the locally damaged area was monitored with low laser intensity. All values were background corrected.

References

Aboussekhra, A., Biggerstaff, M., Shivji, M.K., Vilpo, J.A., Moncollin, V., Podust, V.N., Protic, M., Hubscher, U., Egly, J.M.,and Wood, R.D. (1995). *Mammalian DNA nucleotide excision repair reconstituted with purified protein components*. Cell **80**(6): 859-68.

Alekseev, S., Luijsterburg, M.S., Pines, A., Geverts, B., Mari, P.O., Giglia-Mari, G., Lans, H., Houtsmuller, A.B., Mullenders, L.H., Hoeijmakers, J.H. and Vermeulen, W.(2008). *Cellular concentrations of DDB2 regulate dynamic binding of DDB1 at UV-induced DNA damage*. Mol Cell Biol **28**(24): 7402-13.

Araujo, S.J.,Tirode, F., Coin, F., Pospiech, H., Syvaoja, J.E., Stucki, M., Hubscher, U., Egly, J.M. and Wood, R.D.(2000). *Nucleotide excision repair of DNA with recombinant human proteins: definition of the minimal set of factors, active forms of TFIIH, and modulation by CAK.* Genes Dev **14**(3): 349-59.

Bardwell, A.J., Bardwell, L., Tomkinson, A.E. and Friedberg, E.C. (1994). *Specific cleavage of model recombination and repair intermediates by the yeast Rad1-Rad10 DNA endonuclease.* Science **265**(5181): 2082-5.

Bekker-Jensen, S., Lukas, C., Kitagawa, R., Melander, F., Kastan, M.B., Bartek, J. and Lukas, J. (2006). *Spatial organization of the mammalian genome surveillance machinery in response to DNA strand breaks*. J Cell Biol **173**(2): 195-206.

Bohr, V.A., Smith, C.A., Okumoto, D.S. and Hanawalt, P.C. (1985). *DNA repair in an active gene: removal of pyrimidine dimers from the DHFR gene of CHO cells is much more efficient than in the genome overall.* Cell **40**(2): 359-69.

Celis, J. E. and Madsen, P. (1986). *Increased nuclear cyclin/PCNA antigen staining of non S-phase transformed human amnion cells engaged in nucleotide excision DNA repair*. FEBS Lett **209**(2): 277-83.

Chiu, R.K., Brun, J., Ramaekers, C., Theys, J., Weng, L., Lambin, P., Gray, D.A. and Wouters, B.G. (2006). *Lysine 63-polyubiquitination guards against translesion synthesis-induced mutations.* PLoS Genet **2**(7): e116.

Chuang, L.S., Ian, H.I., Koh, T.W., Ng, H.H., Xu, G. and Li, B.F. (1997). *Human DNA-(cytosine-5) methyltransferase-PCNA complex as a target for p21WAF1*. Science **277**(5334): 1996-2000.

Cook, P.R. (1999). *The organization of replication and transcription*. Science **284**(5421):1790-5.

Coverley, D., Kenny, M.K., Munn, M., Rupp, W.D., Lane, D.P. and Wood, R.D. (1991). *Requirement for the replication protein SSB in human DNA excision repair.* Nature **349**(6309): 538-41.

de Laat, W.L., Appeldoorn, E., Sugasawa, K., Weterings, E., Jaspers, N.G. and Hoeijmakers, J.H. (1998). *DNA-binding polarity of human replication protein A positions nucleases in nucleotide excision repair*. Genes Dev **12**(16): 2598-609.

de Laat, W. L., Jaspers, N.G. and Hoeijmakers, J.H. (1999). *Molecular mechanism of nucleotide excision repair.* Genes Dev **13**(7): 768-85.

Essers, J., Theil, A.F., Baldeyron, C., van Cappellen, W.A., Houtsmuller, A.B., Kanaar, R. and Vermeulen, W. (2005). *Nuclear dynamics of PCNA in DNA replication and repair.* Mol Cell Biol **25**(21): 9350-9.

Fousteri, M., Vermeulen, W., van Zeeland, A.A. and Mullenders. (2006). *Cockayne syndrome A and B proteins differentially regulate recruitment of chromatin remodelling and repair factors to stalled RNA polymerase II in vivo.* Mol Cell **23**(4): 471-82.

Fousteri, M. and Mullenders, L.H. (2008). *Transcription-coupled nucleotide excision repair in mammalian cells: molecular mechanisms and biological effects.* Cell Res**18**(1):73-84

Friedberg, E.C. (2003). *DNA damage and repair.* Nature **421**(6921): 436-40.

Frouin, I., Montecucco, A., Spadari, S. and Maga, G (2003). *DNA replication: a complex matter*. EMBO Rep **4**(7): 666-70.

Gaillard, P.H., Martini, E.M., Kaufman, P.D., Stillman, B., Moustacchi, E. and Almouzni, G. (1996). *Chromatin assembly coupled to DNA repair: a new role for chromatin assembly factor I.* Cell **86**(6): 887-96.

Giglia-Mari, G., Miquel, C., Theil, A. F., Mari, P.O., Hoogstraten, D., Ng, J.M., Dinant, C., Hoeijmakers, J.H. and Vermeulen, W. (2006). *Dynamic interaction of TTDA with TFIIH is stabilized by nucleotide excision repair in living cells*. PLoS Biol **4**(6): e156

Gillet, L.C. and Scharer, O.D. (2006). *Molecular mechanisms of mammalian global genome nucleotide excision repair*. Chem Rev **106**(2): 253-76.

Gerard, A., Koundrioukoff, S. Ramillon, V., Sergere, J.C., Mailand, N., Quivy, J.P. and Almouzni, G. (2006). *The replication kinase Cdc7-Dbf4 promotes the interaction of the p150 subunit of chromatin assembly factor 1 with proliferating cell nuclear antigen.* EMBO Rep **7**(8): 817-23.

Görisch, S.M., Sporbert, A., Stear, J.H., Grunewald, I., Nowak, D., Warbrick, E., Leonhardt, H. and Cardoso, M.C. (2008). *Uncoupling the replication machinery: replication fork progression in the absence of processive DNA synthesis.*Cell Cycle**7**(13): 1983-90

Green, C.M. and Almouzni, G. (2003). *Local action of the chromatin assembly factor CAF-1 at sites of nucleotide excision repair in vivo*. Embo J **22**(19): 5163-74.

Groth, A., Corpet, A., Cook, A.J., Roche, D., Bartek, J., Lukas, J. and Almouzni, G. (2007). *Regulation of replication fork progression through histone supply and demand.* Science **318**(5858): 1928-31.

Hand, R. (1978). *Eukaryotic DNA: organization of the genome for replication.* Cell **15**(2): 317-25.

Hermanson-Miller, I. L. and Turchi, J.J. (2002). *Strand-specific binding of RPA and XPA to damaged duplex DNA.* Biochemistry **41**(7): 2402-8.

He, Z., Henricksen, L.A. Wold, M.S. and Ingles, C.J.(1995). *RPA involvement in the damage-recognition and incision steps of nucleotide excision repair*. Nature **374**(6522): 566-9

Hoege, C., Pfander, B., Moldovan, G.L., Pyrowolakis, G. and Jentsch, S. (2002). *RAD6-dependent DNA repair is linked to modification of PCNA by ubiquitin and SUMO.* Nature **419**(6903): 135-41.

Hoogstraten, D., Nigg, A. L., Heath, H., Mullenders, L.H., van Driel, R., Hoeijmakers, J.H., Vermeulen, W. and Houtsmuller, A.B. (2002). *Rapid switching of TFIIH between RNA polymerase I and II transcription and DNA repair in vivo.* Mol Cell **10**(5):1163-74

Houtsmuller, A.B., Rademakers, S.,Nigg, A L., Hoogstraten, D., Hoeijmakers, J.H. and Vermeulen, W. (1999*). Action of DNA repair endonuclease ERCC1/XPF in living cells.*Science **284**(5416): 958-61.

Hübscher, U. and Seo, Y.S. (2001). *Replication of the lagging strand: a concert of at least 23 polypeptides.* Mol Cells **12**(2): 149-57.

Iftode, C., Daniely, Y. and Borowiec, J.A. (1999). *Replication protein A (RPA): the eukaryotic SSB. Crit Rev Biochem* Mol Biol **34**(3): 141-80.

Jackson, D.A., Hassan, A.B., Errington, R.J and Cook, P.R. (1994). *Sites in human nuclei damage induced by ultraviolet light is repaired: localization relative to transcription sites and concentrations of proliferating cell nuclear antigen and the tumour suppressor protein, p53.* J Cell Sci **107 (Pt 7)**: 1753-60.

Jackson, D.A., Balajee, A.S., Mullenders, L. and Cook, P.R. (1994*). Sites in human nuclei where DNA damaged by ultraviolet light is repaired: visualization and localization relative to the nucleoskeleton.* J Cell Sci **107 (Pt 7)**: 1745-52.

Kannouche, P. L., Wing, J. and Lehmann, A.R. (2004). *Interaction of human DNA polymerase eta with monoubiquitinated PCNA: a possible mechanism for the polymerase switch in response to DNA damage*. Mol Cell **14**(4): 491-500.

Kolpashchikov, D.M., Khodyreva, S.N., Khlimankov, D.Y., Wold, M.S., Favre, A. and Lavrik, O.I. (2001). *Polarity of human replication protein A binding to DNA.* Nucleic Acids Res **29**(2): 373-9.

Laine, J.P. and Egly, J.M. (2006*). Initiation of DNA repair mediated by a stalled RNA polymerase II*." Embo J **25**(2): 387-97.

Langie, S.A., Knaapen, A.M., Ramaekers, C.H., Theys, J., Brun, J., Godschalk, R.W., van Schooten, F.J., Lambin, P., Gray, D.A., Wouters, B.G. and Chiu, R.K. (2007). *Formation of lysine 63-linked poly-ubiquitin chains protects human lung cells against benzo[a]pyrene-diol-epoxide-induced mutagenicity*. DNA Repair (Amst) **6**(6): 852-62.

Lazzaro, F.. Giannattasio, M., Puddu, F., Granata, M., Pellicioli, A., Plevani, P. and Muzi-Falconi, M. (2009). *Checkpoint mechanisms at the intersection between DNA damage and repair.* DNA Repair (Amst) **8**(9): 1055-67.

Leonhardt, H., Rahn, H.P., Weinzierl, P., Sporbert, A., Cremer, T., Zink, D. and Cardoso, M.C. (2000). *Dynamics of DNA replication factories in living cells.* J Cell Biol **149**(2): 271-80.

Lisby, M. and Rothstein, R. (2009). *Choreography of recombination proteins during the DNA damage response.* DNA Repair (Amst) **8**(9): 1068-76.

Luijsterburg, MS., Goedhart, J., Moser, J., Kool, H., Geverts, B., Houtsmuller, A.B., Mullenders, L.H., Vermeulen, W. and van Driel, R. (2007). *Dynamic in vivo interaction of DDB2 E3 ubiquitin ligase with UV-damaged DNA is independent of damage-recognition protein XPC*. J Cell Sci **120**(Pt 15): 2706-16.

Luijsterburg, M.S., von Bornstaedt, G**.,** Gourdin, A.M., Politi, A.Z., Moné, M.J., Warmerdam, D.O., Goedhart, J., Vermeulen,W., van Driel R., and Höfer, T. (2010). *Stochastic and reversible assembly of a multiprotein DNA repair complex ensures accurate target site recognition and efficient repair.* J Cell Biol **189**(3): 445-63.

Maga, G., Stucki, M. Spadari, S. and Hübscher, U. (2000). *DNA polymerase switching: I. Replication factor C displaces DNA polymerase alpha prior to PCNA loading.* J Mol Biol **295**(4): 791-801.

Majka, J. and Burgers, P.M (2004). *The PCNA-RFC families of DNA clamps and clamp loaders*. Prog Nucleic Acid Res Mol Biol **78**: 227-60.

Marteijn J.A., Bekker-Jensen S., Mailand N., Lans H., Schwertman P., Gourdin A.M., Dantuma N.P, Lukas J., Vermeulen W. (2009). *Nucleotide excision repair-induced H2A ubiquitination is dependent on MDC1 and RNF8 and reveals a universal DNA damage response.* J Cell Biol 186(6): 835-47.

Matsunaga, T., Park, C. H., Bessho, T., Mu, D. and Sancar, A.(1996). *Replication protein A confers structure-specific endonuclease activities to the XPF-ERCC1 and XPG subunits of human DNA repair excision nuclease.* J Biol Chem **271**(19): 11047-50.

McCulloch, S.D., Wood, A., Garg, P., Burgers, P. M. and Kunkel, T.A. (2007). *Effects of accessory proteins on the bypass of a cis-syn thymine-thymine dimer by Saccharomyces cerevisiae DNA polymerase eta.* Biochemistry **46**(30): 8888-96.

Miura, M., Domon, M., Sasaki, T., Kondo, S. and Takasaki, Y.(1992*). Two types of proliferating cell nuclear antigen (PCNA) complex formation in quiescent normal and xeroderma pigmentosum group A fibroblasts following ultraviolet light (uv) irradiation*. Exp Cell Res **201**(2): 541-4.

Mocquet, V., Laine, J.P., Riedl, T., Yajin, Z., Lee, M.Y. and Egly, J.M. (2008). *Sequential recruitment of the repair factors during NER: the role of XPG in initiating the resynthesis step.* Embo J **27**(1): 155-67.

Moldovan, G.L., Pfander, B. and Jentsch, S. (2007). *PCNA, the maestro of the replication fork.*Cell **129**(4): 665-79.

Moné, M.J., Volker, M., Nikaido, O., Mullenders, L.H., van Zeeland, A.A.,Verschure, P.J., Manders, E.M. and van Driel, R. (2001). *Local UV-induced DNA damage in cell nuclei results in local transcription inhibition.* EMBO Rep **2**(11): 1013-7.

Moné, M.J., Bernas, T., Dinant, C., Goedvree, F.A., Manders, E.M., Volker, M., Houtsmuller, A.B., Hoeijmakers, J.H., Vermeulen, W. and van Driel, R. (2004). *In vivo dynamics of chromatin-associated complex formation in mammalian nucleotide excision repair*. Proc Natl Acad Sci U S A **101**(45): 15933-7.

Montecucco, A., Rossi, R., Levin, D.S., Gary, R., Park, M.S., Motycka, T.A., Ciarrocchi, G., Villa, A., Biamonti, G. and Tomkinson, A.E. (1998). *DNA ligase I is recruited to sites of DNA replication by an interaction with proliferating cell nuclear antigen: identification of a common targeting mechanism for the assembly of replication factories* Embo J**17**(13): 3786-95

Moser, J., Volker, M., Kool, H., Alekseev, S., Vrieling, H., Yasui, A., van Zeeland, A.A. and Mullenders, L.H. (2005). *The UV-damaged DNA binding protein mediates efficient targeting of the nucleotide excision repair complex to UV-induced photo lesions*. DNA Repair (Amst) **4**(5): 571-82.

Mullenders, L.H., van Zeeland, A.A. and Natarajan, A.T.(1987). *The localization of ultraviolet-induced excision repair in the nucleus and the distribution of repair events in higher order chromatin loops in mammalian cells* J Cell Sci Suppl**6**: 243-62

Murti, K.G., He, D.C., Brinkley, B.R., Scott, R. And Lee, S.H.(1996). *Dynamics of human replication protein A subunit distribution and partitioning in the cell cycle*. Exp Cell Res **223**(2): 279-89.

Nakamura, H., Morita, T. and Sato, C. (1986). *Structural organizations of replicon domains during DNA synthetic phase in the mammalian nucleus*. Exp Cell Res **165**(2): 291-7.

Nakayasu, H. and Berezney, R. (1989). *Mapping replicational sites in the eucaryotic cell nucleus.* J Cell Biol **108**(1): 1-11.

Newport, J. and Yan, H. (1996). *Organization of DNA into foci during replication*. Curr Opin Cell Biol **8**(3): 365-8.

Nichols, A.F. and Sancar, A. (1992). *Purification of PCNA as a nucleotide excision repair protein.* Nucleic Acids Res **20**(13): 2441-6.

Nikolaishvili-Feinberg, N., Jenkins, G.S., Nevis, K.R., Staus, D.P., Scarlett, C.O., Unsal-Kacmaz, K., Kaufmann, W.K and Cordeiro-Stone, M. (2008). *Ubiquitylation of proliferating cell nuclear antigen and recruitment of human DNA polymerase eta*. Biochemistry **47**(13): 4141-50.

O'Donovan, A., Davies, A.A., Moggs, J.G., West, S.C. and Wood, R.D. (1994). *XPG endonuclease makes the 3' incision in human DNA nucleotide excision repair*. Nature **371**(6496): 432-5.

O'Keefe, R.T., Henderson, S.C. and Spector, D.L. (1992). *Dynamic organization of DNA replication in mammalian cell nuclei: spatially and temporally defined replication of chromosome-specific alpha-satellite DNA sequences*. J Cell Biol **116**(5): 1095-110.

Ogi, T., Limsirichaikul, S., Overmeer, R.M., Volker, M., Takenaka, K., Cloney, R., Nakazawa, Y., Niimi, A., Miki, Y., Jaspers, N. G., Mullenders, L.H., Yamashita, S., Fousteri, M.I. and Lehmann, A.R. (2010) *Three DNA polymerases, recruited by different mechanisms, carry out NER repair synthesis in human cells*. Mol Cell **37**(5): 714-27.

Park, J., Seo, T. Kim, H. and Choe, J. (2005). *Sumoylation of the novel protein hRIP{beta} is involved in replication protein A deposition in PML nuclear bodies*. Mol Cell Biol **25**(18): 8202-14.

Podust, V.N., Tiwari, N., Stephan, S. and Fanning, E. (1998). *Replication factor C disengages from proliferating cell nuclear antigen (PCNA) upon sliding clamp formation, and PCNA itself tethers DNA polymerase delta to DNA*. J Biol Chem **273**(48): 31992-9.

Rademakers, S., Volker, M., Hoogstraten, D., Nigg, A.L., Mone, M.J., Van Zeeland, A.A., Hoeijmakers, J.H., Houtsmuller, A.B. and Vermeulen, W. (2003). *Xeroderma pigmentosum group A protein loads as a separate factor onto DNA lesions*. Mol Cell Biol. **23**:5755-67.

Riedl, T., F. Hanaoka and Egly, J,M. (2003). *The comings and goings of nucleotide excision repair factors on damaged DNA*. Embo J **22**(19): 5293-303.

Rolef Ben-Shahar, T., Castillo, A.G., Osborne, M.J., Borden, K.L., Kornblatt, J. and Verreault, A. (2009). *Two fundamentally distinct PCNA interaction peptides contribute to chromatin assembly factor 1 function*. Mol Cell Biol **29**(24): 6353-65.

Sabbioneda, S., Gourdin, A.M., Green, C.M., Zotter, A., Giglia-Mari, G., Houtsmuller, A., Vermeulen, W. and Lehmann, A.R.(2008). *Effect of proliferating cell nuclear antigen ubiquitination and chromatin structure on the dynamic properties of the Y-family DNA polymerases*. Mol Biol Cell **19**(12): 5193-202.

Shivji, K.K., Kenny, M.K and Wood, R.D. (1992). *Proliferating cell nuclear antigen is required for DNA excision repair.* Cell **69**(2): 367-74.

Shivji, M.K., Podust, V.N., Hubscher, U. and Wood, R.D. (1995). *Nucleotide excision repair DNA synthesis by DNA polymerase epsilon in the presence of PCNA, RFC, and RPA.* Biochemistry **34**(15): 5011-7.

Sijbers, A.M., de Laat, W.L., Ariza, R.R., Biggerstaff, M., Wei, Y.F., Moggs, J.G., Carter, K.C., Shell, B.K., Evans, E., de Jong, M. C., Rademakers, S., de Rooij, J.
Jaspers, N.G., Hoeijmakers, J.H., and Wood, R.D. (1996). *Xeroderma pigmentosum group F caused by a defect in a structure-specific DNA repair endonuclease* Cell **86**(5): 811-22

Smith, C.A. and Okumoto, D.S. (1984). *Nature of DNA repair synthesis resistant to inhibitors of polymerase alpha in human cells.* Biochemistry **23**(7): 1383-91.

Solomon, D.A., Cardoso, M.C and Knudsen, E.S. (2004). *Dynamic targeting of the replication machinery to sites of DNA damage.* J Cell Biol **166**(4): 455-63.

Somanathan, S., Suchyna, T.M., Siegel, A.J. and Berezney, R. (2001). *Targeting of PCNA to sites of DNA replication in the mammalian cell nucleus.*JCell Biochem **81**(1):56- 67

Soria, G., Belluscio, L., van Cappellen, W.A., Kanaar, R., Essers, J. And Gottifredi, V. (2009). *DNA damage induced Pol eta recruitment takes place independently of the cell cycle phase.* Cell Cycle **8**(20): 3340-8.

Sporbert, A., Gahl, A., Ankerhold, R., Leonhardt, H. and Cardoso, M.C. (2002). *DNA polymerase clamp shows little turnover at established replication sites but sequential de novo assembly at adjacent origin clusters*. Mol Cell **10**(6): 1355-65.

Staresincic, L., Fagbemi, A.F., Enzlin, J.H., Gourdin, A.M., Wijgers, N., Dunand, Sauthier, I., Giglia-Mari, G., Clarkson, S.G., Vermeulen, W. and Scharer, O. D. (2009). *Coordination of dual incision and repair synthesis in human nucleotide excision repair.* Embo J **28**(8): 1111-20.

Sugasawa, K., Ng, J.M., Masutani, C., Iwai, S., van der Spek, P.J., Eker, A.P., Hanaoka, F., Bootsma, D. and Hoeijmakers, J.H. (1998). *Xeroderma pigmentosum group C protein complex is the initiator of global genome nucleotide excision repair*. Mol Cell **2**(2): 223-32.

Svetlova, M.P., Solovjeva, L.V., Pleskach, N.A. and Tomilin, N.V.(1999). *Focal sites of DNA repair synthesis in human chromosomes*Biochem Biophys Res Commun **257**(2):378-83

Svetlova, M., Solovjeva, L., Pleskach, N., Yartseva, N., Yakovleva, T., Tomilin, N. and Hanawalt, P. (2002). *Clustered sites of DNA repair synthesis during early nucleotide excision repair in ultraviolet light-irradiated quiescent human fibroblasts*. Exp Cell Res **276**(2): 284-95.

Toschi, L. and Bravo, R. (1988). *Changes in cyclin/proliferating cell nuclear antigen distribution during DNA repair synthesis*. J Cell Biol **107**(5): 1623-8.

Tsurimoto, T., Melendy, T. and Stillman, B. (1990). *Sequential initiation of lagging and leading strand synthesis by two different polymerase complexes at the SV40 DNA replication origin.* Nature **346**(6284): 534-9.

Tsurimoto, T. and B. Stillman (1991). Replication factors required for SV40 DNA replication in vitro. I. *DNA structure-specific recognition of a primer-template junction by eukaryotic DNA polymerases and their accessory proteins*. J Biol Chem **266**(3): 1950-60.

Tubo, R.A. and Berezney, R. (1987). *Pre-replicative association of multiple replicative enzyme activities with the nuclear matrix during rat liver regeneration.* J Biol Chem **262**(3): 1148-54.

van Hoffen, A., Venema, J., Meschini, R., van Zeeland, A.A. and Mullenders, L.H. (1995). *Transcription-coupled repair removes both cyclobutane pyrimidine dimers and 6-4 photoproducts with equal efficiency and in a sequential way from transcribed DNA in xeroderma pigmentosum group C fibroblasts*. Embo J **14**(2): 360-7.

Venema, Bartosova, Z., Natarajan, A.T., van Zeeland, A.A., Mullenders, L.H. (1992). *Transcription affects the rate but not the extent of repair of cyclobutane pyrimidine dimers in the human adenosine deaminase gene*. J Biol Chem **267**(13): 8852-6.

Volker, M., Moné, M.J., Karmakar, P., van Hoffen, A., Schul, W., Vermeulen, W., Hoeijmakers, J.H., van Driel, R., van Zeeland, A.A. and Mullenders, L. H. (2001*). Sequential assembly of the nucleotide excision repair factors in vivo.* Mol Cell **8**(1): 213-24.

Wold, M.S. (1997). *Replication protein A: a heterotrimeric, single-stranded DNA-binding protein required for eukaryotic DNA metabolism*. Annu Rev Biochem **66**: 61-92.

Yan, H. and Newport, J. (1995). *FFA-1, a protein that promotes the formation of replication centers within nuclei.* Science **269**(5232): 1883-5.

Yan, H., Chen,C.Y., Kobayashi, R. and Newport, J. (1998). *Replication focus-forming activity 1 and the Werner syndrome gene product.* Nat Genet **19**(4): 375-8.

Zhang, Z., Shibahara, K. and Stillman, B.(2000). *PCNA connects DNA replication to epigenetic inheritance in yeast.* Nature **408**(6809): 221-5.

Zotter, A., Luijsterburg, M.S., Warmerdam, D.O., Ibrahim, S., Nigg, A., van, Cappellen, W.A., Hoeijmakers, J.H., van Driel, R., Vermeulen, W. and Houtsmuller, A.B. (2006). *Recruitment of the nucleotide excision repair endonuclease XPG to sites of UV-induced dna damage depends on functional TFIIH*. Mol Cell Biol **26**(23): 8868- 79.

Chapter 6

~

Stochastic and reversible assembly of a multiprotein DNA repair complex ensures accurate target site recognition and repair

J Cell Biol (2010), **189** (3)**:** 445-63

Stochastic and reversible assembly of a multiprotein DNA repair complex ensures accurate target site recognition and efficient repair

Martijn S. Luijsterburg,[1,3] Gesa von Bornstaedt,[2,4] Audrey M. Gourdin,[5] Antonio Z. Politi,[6] Martijn J. Moné,[1,3] Daniël O. Warmerdam,[1,5] Joachim Goedhart,[1] Wim Vermeulen,[5] Roel van Driel,[1,3] and Thomas Höfer[2,4]

[1]Swammerdam Institute for Life Sciences, University of Amsterdam, 1098 SM Amsterdam, Netherlands
[2]Research Group Modeling of Biological Systems, German Cancer Research Center, 69120 Heidelberg, Germany
[3]Netherlands Institute for Systems Biology, 1090GE Amsterdam, Netherlands
[4]Bioquant Center, 69120, Heidelberg, Germany
[5]Department of Genetics, Erasmus Medical Center, 3015 GE Rotterdam, Netherlands
[6]Max Delbrück Center for Molecular Medicine, 13092 Berlin-Buch, Germany

To understand how multiprotein complexes assemble and function on chromatin, we combined quantitative analysis of the mammalian nucleotide excision DNA repair (NER) machinery in living cells with computational modeling. We found that individual NER components exchange within tens of seconds between the bound state in repair complexes and the diffusive state in the nucleoplasm, whereas their net accumulation at repair sites evolves over several hours. Based on these in vivo data, we developed a predictive kinetic model for the assembly and function of repair complexes. DNA repair is orchestrated by the interplay of reversible protein-binding events and progressive enzymatic modifications of the chromatin substrate. We demonstrate that faithful recognition of DNA lesions is time consuming, whereas subsequently, repair complexes form rapidly through random and reversible assembly of NER proteins. Our kinetic analysis of the NER system reveals a fundamental conflict between specificity and efficiency of chromatin-associated protein machineries and shows how a trade off is negotiated through reversibility of protein binding.

Introduction

Multiprotein complexes involved in transcription, replication, and DNA repair are assumed to assemble in a sequential and cooperative manner at specific genomic locations (Volker et al., 2001; Black et al., 2006). At the same time, many components of these complexes have been found to exchange rapidly between the chromatin-bound and the freely diffusing protein pools, which has been suggested to serve regulatory functions (Houtsmuller et al., 1999; Dundr et al., 2002; Misteli, 2007; Gorski et al., 2008). We presently do not understand how the ordered formation of chromatin-associated multiprotein machineries can be reconciled with the rapid exchange of their components.

To gain insight into the assembly and functioning of chromatin-associated protein complexes, we have studied the mammalian nucleotide excision repair system, which removes UV-induced DNA damage and other DNA lesions from the genome. Nucleotide excision DNA repair (NER) follows the general organization of chromatin-associated processes, involving: (a) recognition of the target site (e.g., a DNA lesion), (b) assembly of a functional multiprotein complex, and (c) enzymatic action of the machinery on the DNA substrate (Hoeijmakers, 2001; Gillet and Schärer, 2006; Dinant et al., 2009).

M.S. Luijsterburg and G. von Bornstaedt contributed equally to this work.

Correspondence to Roel van Driel: r.vandriel@uva.nl; or Thomas Höfer: t.hoefer@dkfz.de

M.S. Luijsterburg's present address is Dept. of Cell and Molecular Biology, Karolinska Institutet, S-17177 Stockholm, Sweden.

Abbreviations used in this paper: 6-4 PP, 6-4 photoproduct; CPD, cyclobutane pyrimidine dimer; FLIP, fluorescence loss in photobleaching; HU, hydroxyurea; MCMC, Markov chain Monte Carlo; NER, nucleotide excision DNA repair; PCNA, proliferating cell nuclear antigen.

Supplemental Material can be found at:
http://jcb.rupress.org/content/suppl/2010/04/30/jcb.200909175.DC1.html
Original image data can be found at:
http://jcb-dataviewer.rupress.org/jcb/browse/2753

The Rockefeller University Press $30.00
J. Cell Biol. Vol. 189 No. 3 445–463
www.jcb.org/cgi/doi/10.1083/jcb.200909175

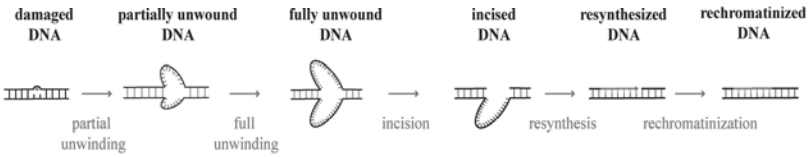

Figure 1. **DNA repair intermediates for NER.** The different states of the DNA substrate during NER (repair intermediates) are interconverted by a series of enzymatic reactions (red arrows).

Damage recognition in global genome NER is performed by the XPC-HR23B protein (Sugasawa et al., 1998; Volker et al., 2001). Binding of XPC to lesions triggers the recruitment of TFIIH, which utilizes its helicase activity to locally unwind the DNA around the lesion (Coin et al., 2007; Sugasawa et al., 2009). The unwound DNA is stabilized and acted upon by further proteins: XPA associates with the DNA lesion, RPA binds to the DNA strand opposite to the damage, and the endonucleases XPG and ERCC1/XPF excise ~30 nucleotides of the unwound DNA strand that contains the lesion (Evans et al., 1997; de Laat et al., 1998; Wakasugi and Sancar, 1999; Park and Choi, 2006; Camenisch et al., 2007). DNA polymerase δ is subsequently loaded by proliferating cell nuclear antigen (PCNA) to fill in the single-stranded gap, which is sealed by the ligase LigIII-XRCCI (Hoeijmakers, 2001; Essers et al., 2005; Moser et al., 2007). Finally, CAF1 assembles new histones on the resynthesized DNA to restore the chromatin structure, completing repair (Green and Almouzni, 2003; Polo et al., 2006).

In vitro studies have been essential in defining the core repair factors and their mode of action but could not account for the dynamic binding of the NER factors to the chromatin substrate (Schaeffer et al., 1993; O'Donovan et al., 1994; Aboussekhra et al., 1995; Sijbers et al., 1996; Riedl et al., 2003; Tapias et al., 2004). In vivo experiments have been crucial in establishing that repair is performed by complexes that are assembled from individual components at the lesion site rather than by binding of a preassembled protein complex (Houtsmuller et al., 1999; Hoogstraten et al., 2002). Together, these studies have led to a conceptual model in which individual NER factors are thought to be incorporated in the chromatin-bound preincision complex in a strict sequential order, followed by the simultaneous dissociation after repair has been completed (Volker et al., 2001; Riedl et al., 2003; Politi et al., 2005). However, previous in vivo studies have focused on the dynamic properties of individual NER proteins and have not addressed the dynamic interplay between NER components during the assembly of the repair complex (Houtsmuller et al., 1999; Hoogstraten et al., 2002; Rademakers et al., 2003; van den Boom et al., 2004; Essers et al., 2005; Zotter et al., 2006; Luijsterburg et al., 2007; Hoogstraten et al., 2008). Thus, a quantitative understanding of how repair complexes assemble in living cells and how the dynamic interactions of NER proteins shape functional properties, such as the rate and specificity of DNA repair, is lacking.

In this study, we present a quantitative analysis of the NER system based on kinetic measurements of seven EGFP-tagged core NER factors in living cells, iterating between experiments and mathematical modeling. We show that all core NER proteins exchange continuously and rapidly on a subminute time scale between chromatin-bound and freely diffusing states. In contrast, the repair factors accumulate at repair sites on a much slower time scale, in the order of hours. This paradox is explained by a kinetic model in which repair proteins assemble stochastically and reversibly to form distinct complexes that catalyze the successive enzymatic steps in the NER process, including DNA unwinding, dual incision, and repair synthesis. Notably, a sequential assembly mechanism is incompatible with the experimental data. Although stochastic assembly and disassembly of NER complexes may seem inefficient at first sight, our theoretical analysis shows that this kinetic design realizes a trade off between the conflicting demands of high rate and specificity of DNA repair. Our results indicate that a major determinant of protein affinity, and thus of the composition of NER complexes, is the state of the DNA substrate. Specificity and rate of damage repair emerge as systems properties that depend on the interplay of repair proteins. Our combined approach of live cell imaging experiments and kinetic modeling provides new fundamental insight into the assembly and functioning of a chromatin-associated multiprotein machinery in vivo.

Results

Long-lasting accumulation of NER proteins on damaged DNA

Previous biochemical and in vivo studies of NER have demonstrated that the repair of a DNA lesion proceeds through a series of distinct repair intermediates: damaged, partially unwound, fully unwound, incised, resynthesized, and rechromatinized DNA (Fig. 1; Shivji et al., 1992; Mu et al., 1996; Evans et al., 1997; Tapias et al., 2004; Polo et al., 2006). The interconversion of repair intermediates requires the action of protein complexes with appropriate enzymatic activities that modify the DNA substrate progressively. It has been suggested that individual NER factors assemble into stable repair complexes through a sequential mechanism (Volker et al., 2001; Politi et al., 2005; Mocquet et al., 2008). In this scenario, the individual proteins remain part of the DNA-bound repair complex during the execution of the enzymatic reactions after which they are released. Alternatively, it is possible that repair factors continuously bind to and dissociate from repair complexes while the enzymatic reactions are being performed. In this scenario, the composition of the repair complexes may change in time, such that a series of transient

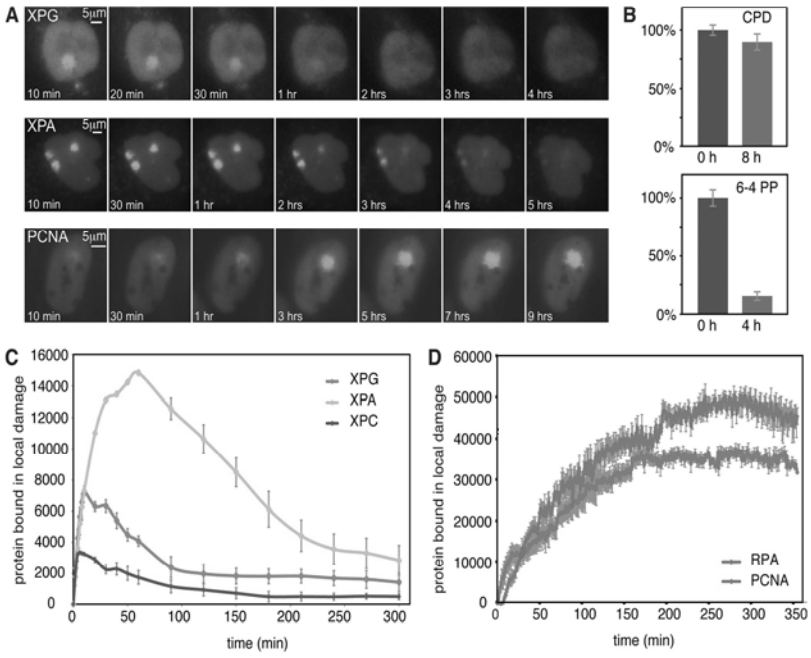

Figure 2. **Long-lasting net accumulation at sites of DNA damage.** (A) Cells stably expressing XPG-EGFP, EGFP-XPA, and EGFP-PCNA shown at various times after local UV-C irradiation (100 J.m^{-2} through 5-μm-diameter pores). (B) Evaluation of the removal of CPDs (top) or 6-4 PPs (bottom) by means of quantitative immunostaining using specific antibodies directly after UV irradiation (0 h) and 4 (for 6-4 PP) or 8 h (for CPD) after UV-C irradiation. Between 50 and 70 cells were analyzed for each time point. (C) Quantification of bound XPC-EGFP (n = 12), XPG-EGFP (n = 5), and EGFP-XPA (n = 7) after UV irradiation. (D) Quantification of bound EGFP-PCNA (n = 5) and RPA-EGFP (n = 5) after UV irradiation. All GFP-tagged repair proteins were stably expressed. (C and D) For consistency, we used only cell nuclei with a single damaged area for quantification. Error bars indicate SEM.

subcomplexes, rather than a single stable complex containing all repair factors, may form at the lesion site.

To analyze the kinetics of the NER process in living cells, we fluorescently tagged seven NER proteins with EGFP and stably expressed the fusion proteins in NER-deficient cells or wild-type cells at physiological levels. The EGFP-tagged NER proteins complement the UV-sensitive phenotype of NER-deficient cells, demonstrating their functionality (see Materials and methods and Fig. S2; Houtsmuller et al., 1999; Hoogstraten et al., 2002, 2008; Rademakers et al., 2003; Essers et al., 2005; Zotter et al., 2006).

We locally irradiated cell nuclei with UV-C light, generating ~60,000 DNA lesions (6-4 photoproducts [6-4 PPs]) per irradiated area (Fig. S1; Moné et al., 2001). Throughout the repair process, we measured the accumulation kinetics of (a) the lesion recognition factor XPC, (b) components of the preincision complex that excise the lesion (TFIIH, XPG, XPA, and ERCC1/XPF), and (c) proteins involved in the repair synthesis of the generated gap (Fig. 2 A; RPA and PCNA). Accounting for the different nuclear concentrations of the proteins (Table I), we found that preincision proteins XPA, XPG (the 3′ endonuclease), and RPA accumulated in the damaged area to higher levels than the lesion recognition protein XPC (Fig. 2, C and D). This finding argues against the recruitment of the preincision proteins into a stable NER complex together with XPC at a 1:1 stoichiometry. Moreover, the proteins reached their maximal accumulation at different times, indicating that the composition of NER complexes changes as repair progresses. The protein accumulation seen in the experiments can be attributed to global genome repair rather than transcription-coupled repair, as no recruitment of repair factors XPA, XPG, and RPA is visible upon local UV irradiation in XPC-deficient cells, which can carry out transcription-coupled repair unhindered but have no global genome repair (Volker et al., 2001; Rademakers et al., 2003).

One of the major DNA lesions induced by UV-C irradiation are the 6-4 PPs, which are repaired considerably faster (within ~5 h) than the cyclobutane pyrimidine dimers (CPDs), which are still present 24 h after UV irradiation (van Hoffen et al., 1995). During the time span of 6-4 PP repair, in which we

Table I. **Values of binding and dissociation rate constants**

Value	XPC	TFIIH	XPG	XPA	XPF/ ERCC1	RPA	PCNA
Concentration (μM)	0.140	0.360	0.440	1.110	0.170	1.110	1.110
Damaged DNA							
k_{on} ($\mu M^{-1}s^{-1}$)	0.008 (0.007; 0.011)	1.6 (0.8; 4.5)	NA	NA	NA	NA	NA
k_{off} (s^{-1})	0.061 (0.007; 0.462)	0.053 (0.004; 0.195)	NA	NA	NA	NA	NA
K_d (μM)	7.8	0.03	NA	NA	NA	NA	NA
Partially unwound DNA							
k_{on} ($\mu M^{-1}s^{-1}$)	0.002 (0.001; 0.003)	0.26 (0.11; 0.27)	0.28 (0.19; 0.31)	0.13 (0.12; 0.16)	1.2 (1.1; 1.6)	0.15 (0.11; 0.22)	NA
k_{off} (s^{-1})	0.007 (0.006; 0.008)	0.012 (0.009; 0.016)	0.015 (0.012; 0.015)	1.04 (0.75; 1.30)	0.01 (0.011; 0.014)	2.6 (1.7; 3.6)	NA
K_d (μM)	3.1	0.05	0.05	7.7	0.01	17	NA
τ = 35 ± 30 min							
Fully unwound DNA							
k_{on} ($\mu M^{-1}s^{-1}$)	0.002 (0.001; 0.003)	0.26 (0.11; 0.27)	0.28 (0.19; 0.31)	0.13 (0.12; 0.16)	1.2 (1.1; 1.6)	0.006 (0.006; 0.007)	NA
k_{off} (s^{-1})	0.007 (0.006; 0.008)	0.012 (0.009; 0.016)	0.015 (0.012; 0.015)	1.04 (0.75; 1.30)	0.01 (0.011; 0.014)	0.021 (0.020; 0.022)	NA
K_d (μM)	3.1	0.05	0.05	7.7	0.01	3.27	NA
τ = 41 ± 36 min							
Incised DNA							
k_{on} ($\mu M^{-1}s^{-1}$)	0.22 (0.13; 0.26)	0.0004 (0.0003; 0.010)	0.001 (0.0004; 0.007)	0.004 (0.004; 0.005)	0.09 (0.07; 0.11)	0.006 (0.006; 0.007)	0.001 (0.001; 0.002)
k_{off} (s^{-1})	0.40 (0.21; 0.48)	0.05 (0.04; 0.07)	0.10 (0.04; 0.11)	0.06 (0.05; 0.07)	0.050 (0.040; 0.101)	0.021 (0.020; 0.022)	0.004 (0.004; 0.004)
K_d (μM)	1.8	137	89	13	0.53	3.27	2.8
τ = 41 ± 36 min							
Resynthesized DNA							
k_{on} ($\mu M^{-1}s^{-1}$)	NA	NA	NA	0.054 (0.054; 0.058)	NA	0.08 (0.05; 0.10)	0.010 (0.007; 0.010)
k_{off} (s^{-1})	NA	NA	NA	0.004 (0.004; 0.005)	NA	0.04 (0.03; 0.05)	0.002 (0.002; 0.002)
K_d (μM)	NA	NA	NA	0.08	NA	0.51	0.19
τ = 2.0 ± 0.7 h							
Rechromatinized DNA							
k_{on} ($\mu M^{-1}s^{-1}$)	NA	NA	NA	NA	NA	0.07 (0.06; 0.07)	0.31 (0.25; 0.34)
k_{off} (s^{-1})	NA	NA	NA	NA	NA	0.04 (0.04; 0.05)	0.05 (0.04; 0.05)
K_d (μM)	NA	NA	NA	NA	NA	0.61	0.16
τ = 2.2 ± 0.7 h							

NA, not applicable. The values for the different repair proteins are arranged in columns for the different DNA repair intermediates to which they bind (rows). The dissociation constants $K_d = k_{off}/k_{on}$ are also given. Reference parameter set and 90% confidence intervals (in parentheses) are shown. Nuclear concentration (in micromolars) of NER factors XPC, XPA, and XPG are based on previously described data (Araújo et al., 2001), whereas RPA and PCNA amounts are estimated to be 250,000 molecules per cell, and TFIIH and ERCC1-XPF were estimated at 65,000 and 50,000 molecules per cell, respectively, based on previous estimates (Houtsmuller et al., 1999; Moné et al., 2004). Concentrations are calculated assuming a nuclear volume of 0.3 pL.

confirmed CPD repair to be negligible (Fig. 2 B), the degree of accumulation of the different NER factors declined at different rates. After reaching a maximum, bound XPC- and XPG-EGFP levels gradually decreased with a $t_{1/2}$ of ∼1 h (Fig. 2 C), which is similar to the decrease in bound ERCC1-GFP (Politi et al., 2005). Bound EGFP-XPA decreased more slowly ($t_{1/2}$ ∼2.5 h; Fig. 2 C), whereas EGFP-PCNA and RPA-EGFP did not decrease within 5 h after UV-C irradiation (Fig. 2 D). For the analysis of RPA and PCNA, we selected cells that were not undergoing S phase to assure that binding of these proteins is not the result of DNA replication. These repair synthesis proteins also accumulated at sites of DNA damage in quiescent cells (unpublished data), further confirming that the binding reflects engagement in DNA repair and not DNA replication.

These results show that NER proteins are engaged in repair for several hours. The mean molecular composition of the NER complexes changes as DNA repair progresses: the damage recognition factor XPC and the two endonucleases XPG and ERCC1/XPF reach their maximal accumulation level early (∼10 min after irradiation), XPA displays intermediate behavior (∼1 h), and the accumulation of PCNA and RPA is considerably slower (maximum at ∼4 h) and lasts longer.

Rapid exchange of NER proteins

Our measurements of the net accumulation kinetics are compatible both with the stable recruitment of repair factors into long-lived complexes and with a scenario in which repair factors associate with and dissociate from repair complexes continuously while repair of a lesion is being performed. To distinguish between these different mechanisms, we measured the dwell times of the NER proteins at sites of DNA damage using fluorescence loss in photobleaching (FLIP; see Materials and methods). In brief, a region distant from the repair site was continuously bleached at 100% laser power, whereas the decrease of fluorescence in the locally damaged area was measured at low laser intensity. We chose experimental conditions in which an EGFP-tagged repair protein that dissociates from sites of DNA damage has a high probability to be bleached before rebinding to a site of damage (see Materials and methods). To determine the contribution of diffusion, we compared the FLIP kinetics of proteins accumulated in the damaged area and of proteins outside the irradiated area at a similar distance from the bleaching area. FLIP kinetics for the latter were at least one order of magnitude faster, implying that binding, but not diffusion, is rate limiting for the dwell time of the NER proteins in the damaged area (unpublished data). Monitoring the loss of accumulated NER factors in the damaged region, we found that all EGFP-tagged preincision proteins dissociated rapidly from repair complexes, with overall half-lives of 20 (RPA), 25 (XPC), 50 (TFIIH, XPG, and ERCC1/XPF), and 80 s (XPA; Fig. 3, A and B). The dissociation kinetics of the repair synthesis factor PCNA were strongly biphasic, with half-lives of 10 and 225 s for the two components (Fig. 3, A and C). Conversely, when monitoring EGFP-tagged histone H4 outside the bleaching area, we did not detect any loss in fluorescence, as would be expected for an immobile component of chromatin (Fig. 3, A and B; Kimura and Cook, 2001). Control experiments showed that cells analyzed by FLIP were still fully capable of repairing UV-induced DNA lesions (Fig. S3), indicating that the FLIP procedure does not affect the repair capacity of a cell.

To verify the FLIP results, we conducted complementary photoconversion experiments using mOrange (Kremers et al., 2009). Monitoring the loss of photoconverted XPC-mOrange or mOrange-XPA in the damaged region confirmed that these NER proteins dissociate rapidly from repair complexes (half-lives of ~25 and 80 s; Fig. 4, A, B, and D). Likewise, bleaching the entire nucleus except for the local accumulation of XPC-mOrange or mOrange-XPA and measuring the loss of fluorescence in the local damage (inverse FRAP; Dundr et al., 2002) gave very similar dissociation curves as FLIP and photoconversion experiments (Fig. 4, C and E). Thus, all measured NER factors exchange rapidly between the freely diffusing and bound states, being part of a repair complex on average for a few tens of seconds. This rapid exchange of individual proteins strongly contrasts with the long overall persistence of repair complexes at UV-damaged sites.

We then perturbed the repair process and measured how this affects the dwell times of NER proteins. When NER was blocked before lesion excision, either by impaired unwinding in cells lacking functional XPB, XPA, or XPG or by impaired excision in cells with compromised ERCC1 or XPF (Evans et al., 1997), XPC dissociation was about fourfold slower than in wild-type cells. This suggests that XPC is bound more stably before dual incision has occurred (irrespective of whether other NER factors can bind or not bind when DNA unwinding is impaired; Fig. 3 D). The observation of prolonged accumulation of XPA during NER prompted us to investigate whether XPA remains bound after dual incision has occurred. To stall NER at the repair synthesis stage, we added hydroxyurea (HU) and AraC (cytosine–β-arabinofuranoside), which are inhibitors of repair synthesis and DNA ligation (Smith and Okumoto, 1984; Mullenders et al., 1987), respectively, ~1 h before local UV-C irradiation. Subsequently, the cells were locally irradiated, and we measured the dwell times of repair factors by FLIP. Blocking repair synthesis and ligation affected the dissociation of XPA and PCNA (Fig. 3, C and E). XPA dissociation was about twofold faster if DNA synthesis and ligation was inhibited, showing that XPA binds to repair synthesis intermediates with high affinity. Dissociation of PCNA was slower in the presence of HU and AraC, indicating its preferential binding to incised DNA (Shivji et al., 1995). The same treatment had no effect on the dissociation kinetics of XPC and ERCC1/XPF (Fig. 3 E). Thus, in contrast to the other preincision proteins, XPA binding becomes stabilized in the process of repair synthesis. These results show that the dwell times of NER proteins change as repair progresses and suggest that the state of the DNA substrate is an important determinant of protein affinity.

Random and rapidly reversible assembly of functional NER complexes

The experiments show kinetics of all proteins involved in NER on two very different time scales. The slow (hours) net accumulation and release of NER proteins at damaged nuclear areas contrasts with their rapid (subminute) exchange between chromatin-bound and unbound states.

To rationalize the experimental findings, we developed a mathematical model of NER. The scaffold of the model is formed by the sequence of enzymatic reaction steps carrying out DNA unwinding, dual incision, and repair synthesis. We assume that DNA adjacent to the lesion is unwound in two steps (Evans et al., 1997) and thus distinguish six DNA repair intermediates (Fig. 1). We have extracted from our work and the work of others the composition of the enzymatically active multiprotein complexes that catalyze the transitions between the repair intermediates (Fig. 5 A and Table S1). Specifically, DNA lesions are recognized by XPC, and the subsequent binding of TFIIH causes unwinding of the DNA around the lesion (Sugasawa et al., 2009). Upon DNA unwinding, all repair proteins can bind to and dissociate from the repair intermediates in any order. Completely sequential and random assembly mechanisms are the extremes of a spectrum of potential assembly mechanisms that the model can describe (Fig. 5 B).

Because the mathematical model distinguishes between enzymatic reactions that interconvert the repair intermediates and the association/dissociation steps of the individual repair proteins, it allows us to scrutinize potential NER complex assembly mechanisms from the in vivo measurements of the core

Published May 3, 2010

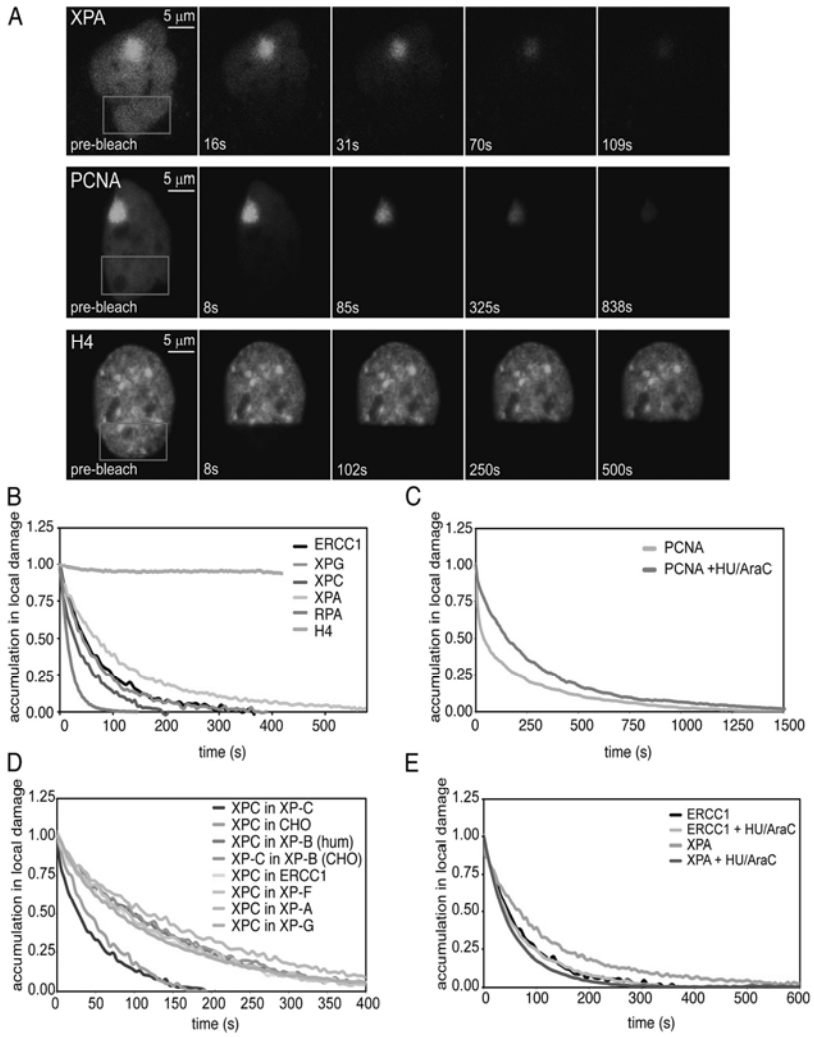

Figure 3. **Rapid exchange of NER proteins at sites of DNA damage.** (A) FLIP measurements in XP2OS cells stably expressing EGFP-XPA (1 h after damage), CHO9 cells stably expressing EGFP-PCNA (2 h after damage), and MRC5 cells transiently expressing EGFP–histone H4. The cells were continuously bleached in the undamaged region (red rectangles), and loss of fluorescence was monitored with low laser intensity in the locally damaged area. (B) Quantification of FLIP experiments on XPC-EGFP in XPC-deficient XP4PA cells, XPG-EGFP in XPG/ERCC5-deficient UV135 cells, EGFP-XPA in XPA-deficient XP2OS cells, RPA-EGFP in MRC5 cells, ERCC1-GFP in ERCC1-deficient 43-3B cells, and EGFP-H4 in MRC5 cells. (C) Quantification of FLIP experiments on EGFP-PCNA in CHO9 cells. All GFP-tagged repair proteins were stably expressed. GFP-H4 was transiently expressed. (D) Quantification of FLIP experiments with perturbations of NER on XPC-mVenus transiently expressed at low levels in various locally irradiated NER-deficient CHO and human cell lines. The following NER mutant cell lines were used: CHO XP-B/ERCC3–deficient 27.1 cells, XPG/ERCC5-deficient UV135 cells and ERCC1-deficient 43-3B cells, and human XPB–deficient XPCS2BA-SV cells (Vermeulen et al., 1994), XPA-deficient XP12RO-SV cells and XPF-deficient XP2YO-SV cells. Additionally, XPC-mVenus was also transiently expressed in wild-type CHO-K1 cells. (E) Quantification of FLIP experiments in the absence or presence of HU and AraC on locally irradiated XP2OS cells expressing stably EGFP-XPA or 43-3B cells stably expressing ERCC1-GFP. The kinetics of EGFP-PCNA in the presence of HU and AraC are shown in C.

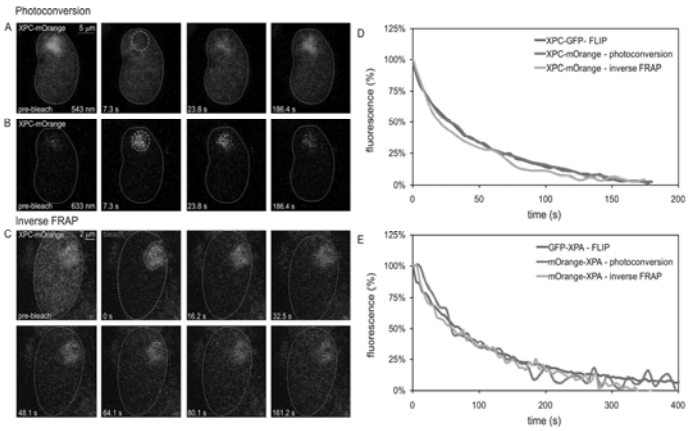

Figure 4. **Photoconversion and inverse FRAP on NER proteins XPC and XPA in the damaged area.** Example of a photoconversion experiment on XP4PA cells transiently expressing low levels of XPC-mOrange. (A and B) Cells were locally irradiated (5 µm; 100 J.m^{-2}) and monitored in the orange channel (A; 543 nm; nonphotoconverted) and the far-red channel (B; 633 nm; photoconverted). 30 min after local UV irradiation, the local accumulation of XPC-mOrange was photoconverted with 488-nm laser light. The levels of nonphotoconverted XPC-mOrange increased at the local damage site (A), whereas the levels of photoconverted XPC-mOrange decreased as a result of the rapid exchange of XPC at the damaged site (B). (B) Example of an inverse FRAP experiment on XP4PA cells transiently expressing low levels of XPC-mOrange. Cells were locally irradiated (5 µm; 100 J.m^{-2}). (C) 30 min after local UV irradiation, the entire nucleus except for the local accumulation of XPC-mOrange at the damaged area was bleached (the bleach region is indicated in red). Cells were monitored in time until the ratio between the fluorescence intensity in the local damage and in the nucleoplasm were restored to the prebleach value. (D) Quantification of the dwell time of XPC-mOrange as measured by photoconversion (red) and inverse FRAP (green). The blue curve, which shows the dwell time of XPC-EGFP measured by FLIP (Fig. 3 B), is shown for comparison. (E) Quantification of the dwell time of mOrange-XPA as measured by photoconversion (red) and inverse FRAP (green). The blue curve, which shows the dwell time of EGFP-XPA as measured by FLIP (Fig. 3 B), is shown for comparison.

NER factors. We found that a strict order of protein binding to the repair intermediates (sequential assembly) would imply the stabilization of early binding proteins by the subsequent proteins incorporated into the complex, resulting in long dwell times of early-binding proteins compared with short dwell times of late-binding proteins. Thus, the recruitment of proteins in a strict order is incompatible with the mutually independent and rapid dissociation of individual NER factors that we observe. In contrast, a random binding and dissociation mechanism of repair proteins can account for both rapid exchange and slow net accumulation of NER proteins at sites of damage, as follows.

We model the formation of multiprotein complexes at the DNA lesions as a predominantly stochastic process in which proteins can associate and dissociate independently of each other and in any order as soon as the DNA becomes partially unwound. When an enzymatically active protein complex is assembled (e.g., the preincision complex with the two endonucleases XPG and ERCC1/XPF), it catalyzes the transition from one DNA repair intermediate to the next (e.g., the excision of the damaged region). Thus, the modeling framework accounts for reversible protein binding as well as irreversible enzymatic reactions that determine the directionality of NER (Fig. 5 A). This model translates into a system of differential equations for the various protein complexes formed at the DNA repair intermediates (Fig. 5 B).

We derived k_{on} and k_{off} values for the binding of the individual proteins to the different repair intermediates and k_{cat} values for the enzymatic reactions by fitting the model to the experimental data (see Materials and methods). For this purpose, we implemented a Markov chain Monte Carlo (MCMC) method to systematically explore the parameter space (ranges for the k_{on}, k_{off}, and k_{cat} values) and obtained a model fit that reproduces all available experimental data simultaneously, including the net accumulation kinetics, the FLIP kinetics for normal NER, and NER blocked at different stages (Fig. 6, A–D). The MCMC algorithm for deriving kinetic parameters from the experimental data also yielded confidence intervals for the estimated parameters (Tables I and II).

Thus, the computational analysis shows that the comprehensive experimental dataset for kinetics of the core NER factors is consistent with a rapidly reversible and predominantly random assembly mechanism of NER complexes.

Lesion recognition is rate limiting for NER

All kinetic parameters extracted from the experimental data fall in biochemically realistic ranges. The in vivo affinities of the NER proteins for the repair intermediates span a considerable range, from micromolar to nanomolar values for the dissociation constants ($K_d = k_{off}/k_{on}$; Fig. 6 E). The model also yields the time evolution of the six DNA repair intermediates (Fig. 6 F). DNA lesions are excised on average 41 ± 36 min after UV irradiation,

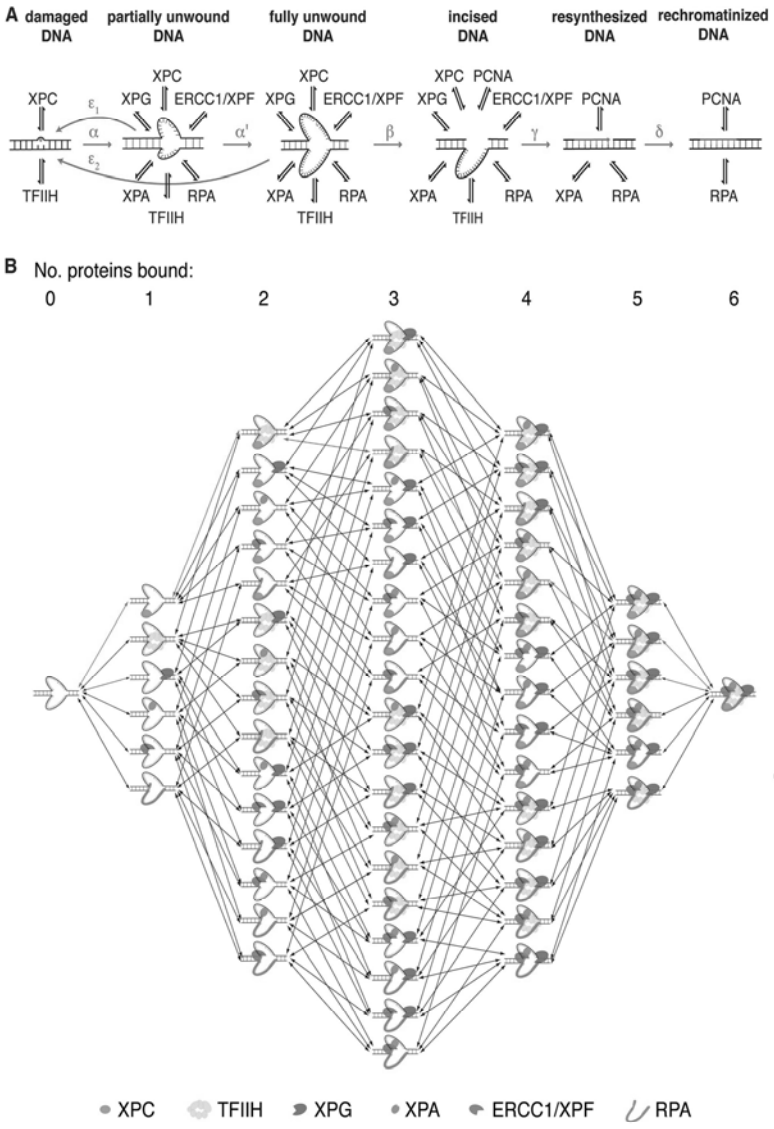

Figure 5. **Kinetic model of NER.** The model distinguishes six DNA repair intermediates, as indicated, that are interconverted by enzymatic steps. Red arrows: α, partial DNA unwinding; α', full unwinding; β, dual incision; γ, resynthesis; δ, rechromatinization; ε_1 and ε_2, reannealing of unwound DNA when it becomes devoid of stabilizing proteins. The indicated NER proteins can bind to the repair intermediates. The binding of TFIIH to the DNA lesion requires the prior binding of XPC. The binding of XPA and ERCC1/XPF is cooperative (Table S1). (B) Possible assembly pathways for the preincision complex on unwound DNA. Random assembly can use all pathways shown, whereas sequential assembly will follow a unique pathway (e.g., the pathway indicated by the red arrows assuming ordered binding of XPC, TFIIH, RPA, XPA, XPG, and ERCC1/XPF).

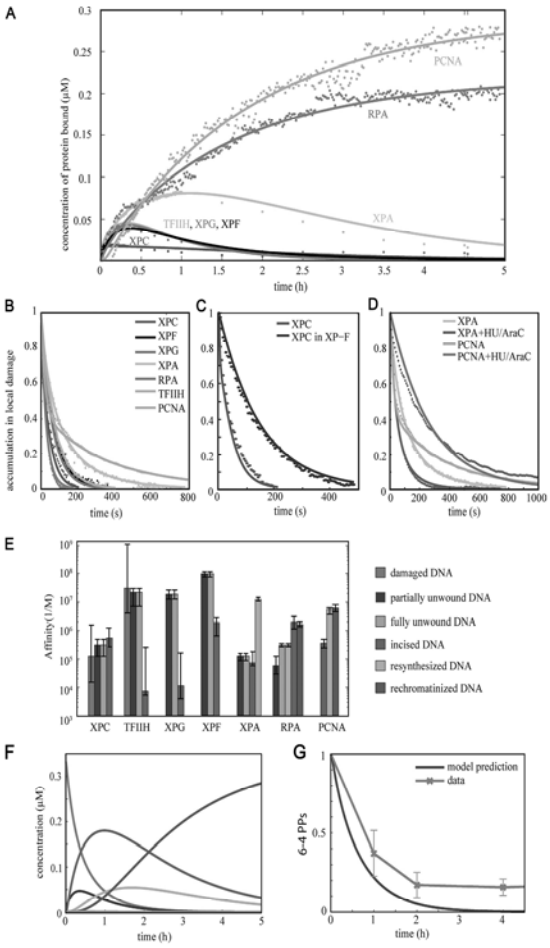

Figure 6. **Random and reversible NER complex assembly accounts both for rapid exchange and prolonged net accumulation of repair proteins.** (A–D) Comparison of model simulations (lines) and experimental data (dots) showing net accumulation kinetics (A) and dissociation kinetics (B) of core NER proteins, dissociation kinetics of XPC in wild-type and XPF-deficient cells unable to perform damage excision (C), and dissociation kinetics of XPA and PCNA in the absence or presence of DNA synthesis/ligation inhibitors HU and AracC (D). (E) Affinity of NER proteins for the repair intermediates ($K_a = k_{on}/k_{off}$). Preincision factors XPG, TFIIH, and ERCC1/XPF lose affinity after lesion excision, whereas the affinities of XPA, PCNA, and RPA increase upon repair synthesis. (F) Computed time courses of the repair intermediates. Note that the color coding of the repair intermediates, as indicated in E, also applies to F. (G) Comparison between the predicted kinetics of the removal of 6-4 PPs (blue) and the measurements on the kinetics of 6-4 PP removal by means of quantitative immunostaining using specific antibodies (red). Between 50 and 70 cells were analyzed for each time point. Error bars indicate SD.

with large stochastic variation from lesion to lesion (see Materials and methods). Damage recognition by XPC and partial unwinding of the DNA by TFIIH takes on average ~35 min, and subsequently, ~6 min are sufficient to fully unwind the DNA and assemble the preincision complex containing XPA, XPG, ERCC1/XPF, RPA, and TFIIH. Thus, the incision time is mainly determined by slow lesion recognition through XPC, after which a functional preincision complex is rapidly formed through random assembly. In agreement, we find that the preincision factors assemble with similar initial rates on chromatin (~15 molecules/s; Fig. 2, C and D; and Fig. S4 A). Indeed, we found that the existence of many different assembly routes in the random mechanisms (Fig. 5 B) outweighs the disadvantage of creating a large number of partially assembled complexes and allows rapid complex assembly (not depicted).

To validate the predicted repair kinetics, we experimentally measured the removal of DNA lesions (6-4 PPs) by quantitative immunostaining (see Materials and methods). The experimentally measured kinetics of lesion excision indeed occurred on the time scale predicted by the model, which was considerably slower (tens of minutes to hours) than the dwell time of individual repair factors (seconds to minutes; Fig. 6 G).

To summarize, the model indicates that recognition of a DNA lesion is time consuming, whereas subsequent preincision

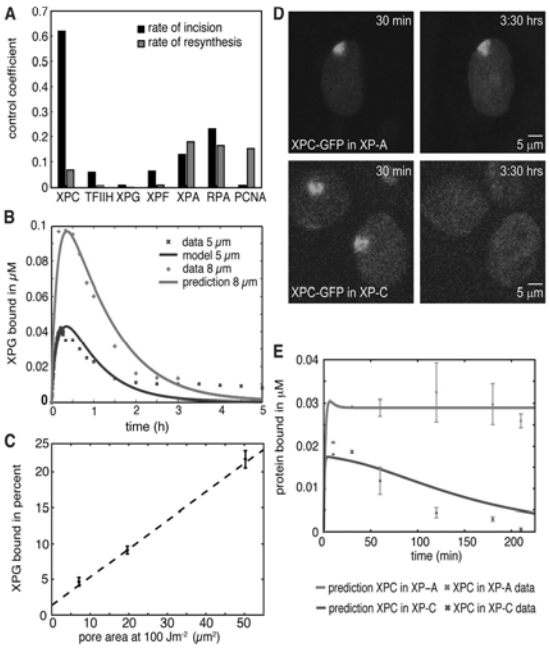

Figure 7. **Capacity of NER.** (A) Control of NER proteins on the rate of incision (black) and rate of DNA resynthesis (gray). Control coefficients were calculated with the following equation:

$$C_i^{\tau} = \frac{X_i}{\tau^{-1}} \frac{\partial \tau^{-1}}{\partial X},$$

where τ denotes the mean time (for incision or repair synthesis) and X_i the total concentration of protein i. (B) The model correctly predicts the kinetics of XPG binding when the amount of initial DNA damage is increased ~2.6-fold (+, experimental data for irradiation through 8-μm pores; red line, model simulation) as compared with reference conditions (x, experimental data; blue line, model). (C) Maximally bound XPG-EGFP after local UV-C irradiation of differently sized areas (100 J.m^{-2} through 3-, 5-, and 8-μm pores). (D) The model correctly predicts the kinetics (amplitude and shape of the curve) of XPC-EGFP binding in XPA-deficient cells (red line, model prediction; red crosses, experimental data). The predicted curve and the measured kinetics of XPC-EGFP binding in (complemented) XPC-deficient cells are shown in blue for comparison. Error bars indicate SD.

complexes are formed rapidly by reversible binding of the individual components. The theoretically predicted time scale of lesion removal has been confirmed experimentally.

High capacity for parallel processing of DNA lesions

To determine the control of each NER protein on the rates of incision and repair synthesis, we calculated the control coefficients that quantify how a change in the concentration of an individual protein affects these rates (Materials and methods). Most proteins have an appreciable impact, showing that the rate of NER is a systems property rather than being determined by a single protein (Fig. 7 A). However, XPC has the dominant control on the rate of incision, whereas RPA, XPA, and PCNA control the rate of repair synthesis.

To quantify the dependence of the rate (v) of NER on the amount of DNA lesions (D), we approximated the repair rate by the Michaelis–Menten equation $v = v_{max} D/(K_M + D)$. From our data, we estimated the maximal rate v_{max} = 6,000 lesions min^{-1} (see Materials and methods), which agrees with previous measurements (Kaufmann and Wilson, 1990; Ye et al., 1999). The estimated half-saturation at K_M = 216,000 lesions indicates that NER is not saturated under our experimental conditions (~60,000 DNA lesions at $t = 0$). In fact, the model predicts that an increase in the number of DNA lesions would not change the net accumulation kinetics of a repair factor. Rather, it would increase the number of repair proteins engaged in DNA repair (Fig. 7 B, red line), and this increase in engaged DNA repair proteins is predicted to be approximately proportional to the number of DNA lesions.

To address experimentally whether NER is indeed unsaturated, we inflicted different amounts of DNA damage per nucleus and monitored the accumulation of the preincision protein XPG. The experimental curves for the measured amplitude and kinetics of XPG accumulation for increased DNA damage matched the predicted curves generated by the model (Fig. 7 B, red crosses). Nearly twice the number of XPG molecules was engaged in DNA repair when the number of DNA lesions was doubled, without changes in the long-term accumulation of XPG, which fully agreed with the model prediction (Fig. 7 B). Further supporting the prediction that NER is far from saturation, we observed an essentially linear relationship between XPG accumulation and the number of DNA lesions (Fig. 7 C and Fig. S4 B). Thus, NER has a high capacity to process DNA lesions in parallel.

As global genome NER is strictly dependent on damage recognition by XPC (Volker et al., 2001), we further tested to what extent XPC (~0.14 μM) can become bound to DNA damage (6-4 PP; ~0.33 μM). When the repair of the DNA lesions is prevented, the model predicts only a moderate increase in XPC net accumulation because of the rather low XPC affinity (Fig. 7 E, red line, compare with blue line for predicted XPC

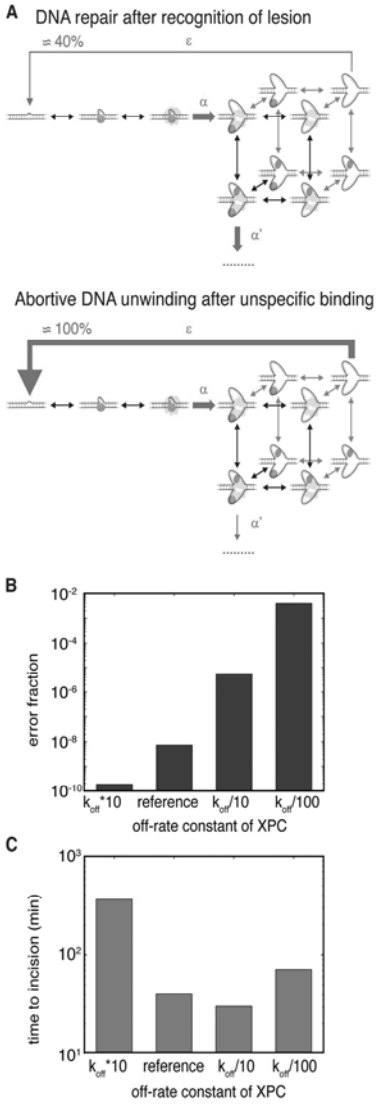

Figure 8. **Specificity of NER.** (A) Damage recognition, DNA unwinding, and kinetic proofreading by XPC, TFIIH, and XPA. We estimated that in ~40% of the unwinding events after the recognition of a true lesion, the DNA will reanneal, and the repair process must start again. After unspecific binding, this number increases to almost 100%. For simplicity, only binding of XPC, TFIIH, and XPA to the DNA lesion is shown, using the same symbols as in Fig. 4 B. (B) Error fractions in the model for different dissociation rates of XPC. The affinity ratio for damaged versus undamaged DNA is always 100. The error fraction was calculated as the ratio of mean times to dual excision for a true lesion (τ_t) and an incidental incision on undamaged DNA (τ_U): $f = \tau_t / \tau_U$. High specificity would result in large τ_t (incidental incisions are extremely rare) and thus small f. (C) Mean time to incision for different dissociation rates of XPC.

accumulation when repair takes place). To test this prediction, we expressed XPC-EGFP in repair-deficient XP-A cells and measured its binding kinetics after localized UV irradiation (Fig. 7 D). The net accumulation of XPC-EGFP on DNA damage in XPA-deficient cells was indeed only slightly increased compared with its accumulation in repair-proficient cells and closely matched the amplitude predicted by the model (Fig. 7 E, red crosses and red line, respectively). Unlike the decreasing XPC accumulation in repair-proficient cells (Fig. 7, D and E, blue crosses), XPC accumulation in the repair-deficient cells remained at a plateau level in further agreement with the model prediction. Remarkably, this plateau is at ~10% of the estimated total DNA damages (6-4 PPs). This finding corroborates the prediction of low XPC affinity and indicates that the unsaturated nature of NER is, at least in part, due to the comparatively weak XPC binding.

Reversible binding of repair proteins can ensure accurate damage recognition

The NER machinery must recognize DNA lesions with high specificity to avoid accidental repair of nondamaged DNA, which is potentially mutagenic. The lesion recognition factor XPC binds to DNA damage with only ~100-fold higher affinity than to undamaged DNA (Hey et al., 2002; Hoogstraten et al., 2008). About 10^5 incisions on nondamaged sites per hour would occur if the specificity of NER were determined by XPC alone (see Materials and methods). Obviously, much higher damage specificity is required to prevent erroneous DNA incisions by the NER machinery. The model demonstrates that specificity can be increased by several orders of magnitude through a kinetic proofreading mechanism based on the reversibility of DNA unwinding. Using model simulations, we estimate that most DNA unwinding events around a true lesion immediately lead to incision (~60%). In the remaining cases, DNA reanneals before a preincision complex is formed and NER starts again by XPC binding to the lesion. In contrast, XPC and other NER factors bind so weakly in the absence of a lesion that undamaged DNA will reanneal with near 100% efficiency if it has accidentally been unwound after unspecific binding of XPC and TFIIH (Fig. 8 A).

XPA and possibly TFIIH can also discriminate between lesions and undamaged DNA (Villani and Tanguy Le Gac, 2000; Dip et al., 2004; Camenisch et al., 2006; Giglia-Mari et al., 2006). These factors may contribute significantly to kinetic proofreading. We estimated the specificity of the NER system by assuming a 100-fold selectivity of XPC, TFIIH, and XPA for damaged over nondamaged DNA. This results in an error fraction of $f < 10^{-8}$ (erroneous incisions per correctly excised damage), which compares with the error rate in DNA

replication ($\sim 10^{-9}$; Kunkel and Bebenek, 2000). Importantly, when suppressing DNA reannealing in the model (by setting $\varepsilon_{1,2} = 0$), we observed a large increase in the error fraction to $f > 10^{-4}$. Thus, kinetic proofreading enhances molecular discrimination between damaged and nondamaged sites by several orders of magnitude. These results outline a potential proofreading mechanism that utilizes reversible DNA unwinding for achieving the exquisite discriminative power of the NER system.

The model shows that rapidly exchanging proteins are a prerequisite for high specificity. Stably bound proteins would prevent proofreading by stabilizing the unwound DNA repair intermediate; for example, if the XPC dwell time increased 100-fold, the error fraction would increase by six orders of magnitude to $f \sim 10^2$ (Fig. 8 B). However, the rate of NER will be compromised if XPC binds too weakly (Fig. 8 C). Thus, specificity and efficiency of the NER system cannot be maximized simultaneously, and the kinetic design of the NER system must realize a trade-off between these two objectives. The model predicts that a comparatively low XPC affinity, with readily reversible binding of XPC and other repair proteins, results in high specificity and efficiency.

Discussion

We have used a combination of live cell imaging and kinetic modeling to study the formation of DNA repair complexes on the chromatin fiber. Based on extensive kinetic measurements of the binding and dissociation of individual components of the NER machinery, we have computationally reconstructed the assembly dynamics of the multiprotein complexes that catalyze the successive steps of repair. Our results show that the recognition of DNA lesions is strongly rate limiting for repair, whereas after the subsequent DNA unwinding, NER proteins assemble rapidly, randomly, and reversibly into multiprotein complexes. This model reconciles the slow net accumulation kinetics of NER factors at repair sites with their continuous rapid exchange between bound and unbound states (Figs. 2–4). The model makes testable predictions on the rate and capacity of the repair process that have been verified experimentally (Figs. 6 and 7). Moreover, our analysis suggests a kinetic proofreading mechanism for achieving high specificity in lesion recognition that utilizes reversible DNA unwinding and rapidly reversible protein binding (Fig. 8). The model has implications for the kinetic organization of other chromatin-associated processes, including transcription regulation and DNA replication.

Comparison with previous models of protein complex formation on DNA

Our approach differs from previous experimentally based mathematical models that described the kinetic behavior of individual proteins binding to chromatin based on FRAP data (Dundr et al., 2002; Darzacq and Singer, 2008; Gorski et al., 2008; Karpova et al., 2008). In this study, we quantified the formation of multiprotein complexes that are the active units of the DNA repair process. To this end, we developed an integrated kinetic model that simultaneously accounts for the kinetic behavior of seven core NER proteins. Fitting the model to the experimental data yields biochemically plausible estimates for the kinetic parameters of the individual molecular interactions in vivo that account for both the long-term accumulation and the rapid exchange of the NER factors (Fig. 6 and Table I). The model provides a versatile and testable framework for understanding the repair process on the systems level of its interacting factors. At present, techniques for measuring on- and off-rate constants as well as affinities directly in vivo are limited (Michelman-Ribeiro et al., 2009), as are techniques for measuring repair intermediates in vivo. The development of such experimental methods would provide additional tools to further scrutinize and refine the model.

Our results show that the NER system becomes saturated at a remarkably high number of DNA lesions, with an estimated half-saturation at 216,000 lesions per nucleus. For comparison, sunlight is thought to induce up to 30,000 DNA lesions per hour in each skin cell. The maximal rate of repair is estimated at 6,000 lesions per minute, which is consistent with direct measurements of the rate of incision (Kaufmann and Wilson, 1990; Ye et al., 1999). Previous estimates of the time taken to incise a single lesion ($\sim$4 min) were based on the dissociation rates of individual repair factors from damaged DNA in vivo (Houtsmuller et al., 1999; Rademakers et al., 2003; Zotter et al., 2006). These dissociation rates reflect the k_{off} of individual repair proteins but may not provide information about the time it takes to repair DNA lesions. Indeed, our results imply that repair factors can bind to and dissociate from the same lesion multiple times before it is excised, reconciling the rapid exchange of repair factors and their long-term accumulation at damaged sites. Thus, the mean time to remove a lesion is predicted to be much larger than previous estimates suggested, on average $\sim$40 min (Table I). Moreover, there is high stochastic variability in excision time between lesions. At the same time, the NER system has the capacity to process a large number of lesions in parallel, such that the mean time to incise a single lesion or several thousands of them is rather similar. The processing capacity appears to be further regulated by the DDB2 complex that seems to stimulate the recognition of 6-4 PPs by XPC when the concentration of DNA lesions is relatively low. This may be brought about by priming UV-damaged chromatin for the binding of XPC. At higher lesion concentrations, however, DDB2 does not further accelerate the repair of 6-4 PPs (Moser et al., 2005; Nishi et al., 2009).

Experimental testing of model predictions

To validate the predicted kinetics of lesion excision, we monitored the time course over which 6-4 PPs are excised and found good agreement between experiment and model (Fig. 6 G). In view of the fact that no experimental information on the kinetics of DNA repair intermediates was used to parameterize the model, this result attests to the predictive capability of the model. Additional experimental tests have provided further validation of the model. First, the linear dependence of XPG accumulation on the amount of DNA lesions confirms the model prediction that NER is far from saturation under our experimental conditions (Fig. 7, B and C). Second, the relatively low accumulation of XPC in repair-deficient mutants matches the model simulations quite precisely and confirms

the prediction of a comparatively low in vivo affinity of XPC for DNA lesions (Fig. 7 E). Thus, the model has correctly predicted both the time scale of repair and the magnitude of accumulation of NER factors under different experimental conditions.

Efficiency and specificity of NER

The low XPC affinity for damaged DNA and fast reversibility of binding are advantageous for both specificity and efficiency of NER (Fig. 8). The model shows that two distinct mechanisms together can render the error fraction in the recognition of lesions compared with nondamaged DNA as low as $<10^{-8}$: (a) the involvement of multiple factors in damage recognition (XPA and possibly TFIIH) and (b) kinetic proofreading (Hopfield, 1974). These mechanisms greatly increase the specificity of the NER system beyond the poor specificity of XPC (for XPC alone $f_{min} \sim 10^{-2}$; Hey et al., 2002; Hoogstraten et al., 2008). Thus, proofreading may strongly reduce "accidental" repair on nondamaged DNA, which is potentially mutagenic. Kinetic proofreading is naturally realized in our model as a result of the reversibility of the DNA-unwinding steps, which require the binding of NER factors to prevent reannealing. If one or several of these factors bind with higher affinity to a lesion than to undamaged DNA, the specificity is greatly amplified by the proofreading mechanism. Both specificity-enhancing mechanisms are particularly effective when the recognition factors cannot readily be saturated with DNA lesions. Indeed, we have estimated for XPC and XPA rather low affinities for damaged DNA (K_d of 7–8 µM; Table I). A too-low affinity of XPC, however, would strongly slow down repair. Our results suggest that the observed low XPC affinity mediates an appropriate trade off between specificity and efficiency of NER. In addition, the model indicates that the reversibility of protein binding is beneficial because it prevents the trapping of NER proteins in incomplete (and thus unproductive) repair complexes. Specifically, this explains that the repair rate is maximal at an intermediate k_{off} value for XPC (Fig. 8 C).

General implications of the model for chromatin-associated processes

This study provides a systems-level framework for dissecting the assembly and function of multiprotein machineries acting on chromatin. Our results show that repair factors bind reversibly and assemble mainly stochastically to form enzymatically active protein complexes. In particular, the in vivo data presented in this study and previously (Volker et al., 2001; Rademakers et al., 2003) argue against alternative models that propose irreversible and sequential binding of NER factors (Politi et al., 2005) or NER initiation by proteins other than XPC (Kesseler et al., 2007). In contrast to these earlier models, our results explain the sequentiality of the NER process in a natural manner by the stepwise enzymatic modifications of the DNA substrate at which the proteins assemble. Our model also accommodates cooperative protein–protein interactions, as shown for XPC and TFIIH in the initial unwinding of DNA near a DNA lesion (Yokoi et al., 2000; Sugasawa et al., 2009), and for XPA and ERCC1/XPF (Volker et al., 2001; Tsodikov et al., 2007). Thus, the assembly of NER complexes at chromatin appears to be governed primarily by protein–DNA interactions and, to a lesser extent, by stable protein–protein interactions. Long-term stability of protein complexes is not necessary because enzymatically active complexes need only be stable for a time interval required to carry out their function (such as DNA unwinding, dual incision, etc.). On the contrary, we find that reversibility of protein binding is beneficial for NER by ensuring high specificity of lesion recognition without compromising efficiency. Our analysis demonstrates the enormous potential of kinetic proofreading for specific damage recognition.

Many proteins involved in transcription and DNA replication have enzymatic activities that may affect histones and other proteins determining chromatin accessibility (van Attikum and Gasser, 2009). Therefore, the formation of chromatin-associated machineries may be orchestrated in time primarily by progressive enzymatic modifications of the chromatin substrate, leaving considerable freedom for the binding mode of individual proteins. Like the components of the NER complex, many transcription factors and RNA polymerases exchange rapidly in the transcription initiation complex, which has been considered inefficient (Dundr et al., 2002; Darzacq et al., 2007; Gorski et al., 2008). However, our analysis suggests that such conclusion may need to be reevaluated when the functioning of multiprotein complexes in terms of specificity and efficiency is taken into account. Our results suggest that proofreading based on reversible protein binding and DNA unwinding, as described for NER, may also support specific target site recognition in transcription. The conflict between specificity and efficiency uncovered in this study is likely a general design principle for chromatin-associated machineries.

Materials and methods

DNA constructs

The XPC cDNA (Hoogstraten et al., 2008) was ligated in frame with mVenus and mOrange (Shaner et al., 2004; Kremers et al., 2006), resulting in XPC-mVenus and XPC-mOrange. In addition, XPA cDNA (Rademakers et al., 2003) was ligated in frame with mOrange, yielding mOrange-XPA. Constructs were transiently transfected in several NER mutant cell lines at low levels using Lipofectamine 2000 (Invitrogen) according to the manufacturer's instructions. RPA70 cDNA (Henricksen et al., 1994) was cloned in frame with EGFP in pEGFP-N1 (Takara Bio Inc.) and stably expressed in SV40-transformed MRC5 human fibroblasts. The EGFP–histone H4 plasmid was provided by S. Diekmann (Leibniz Institute for Age Research, Jena, Germany).

Cell lines

Cell lines stably expressing EGFP-tagged NER proteins used in this study were human fibroblasts XPC-deficient XP4PA-SV– expressing XPC-EGFP (Hoogstraten et al., 2008), XPA-deficient XP2OS-SV–expressing EGFP-XPA (Rademakers et al., 2003), XPB-deficient XPCS2BA-SV–expressing XPB-EGFP (Hoogstraten et al., 2002), and wild-type MRC5-SV–expressing RPA70-EGFP. The following CHO cells were used: XPG/ERCC5-deficient UV135–expressing XPG-EGFP (Zotter et al., 2006), ERCC1-deficient 43-3B–expressing ERCC1-GFP (Houtsmuller et al., 1999), wild-type CHO9-expressing EGFP-PCNA (Essers et al., 2005), and CHO K1. The expression level of all EGFP-tagged repair proteins is comparable with the level of endogenous proteins as shown by Western blot analysis (Houtsmuller et al., 1999; Hoogstraten et al., 2002, 2008; Rademakers et al., 2003; Essers et al., 2005; Zotter et al., 2006). The following NER mutant cell lines were used: human XP-B (XPCS2BA-SV; Vermeulen et al., 1994), XP-A (XP12RO-SV; Satokata et al., 1992), XP-F (XP2YO-SV; Yagi et al., 1991), CHO XP-B/ERCC3 (27.1; Hall et al., 2006), XP-G/ERCC5

(UV135; MacInnes et al., 1993), and ERCC1 (43-3B; van Duin et al., 1986). All cell lines expressing EGFP-tagged NER proteins were cultured in a 1:1 mixture of DME/Ham's F10 medium. All media contained glutamine (Invitrogen) supplemented with antibiotics and 10% FCS, and all cells were cultured at 37°C in an atmosphere of 5% CO_2.

Western blotting

Cell extracts of parental MRC5 cells and MRC5 cells expressing RPA70-EGFP were generated by sonication, separated by 8% sodium dodecyl sulfate polyacrylamide gel electrophoresis, and transferred to nitrocellulose membranes. Expression of RPA70-EGFP was analyzed by immunoblotting with mouse monoclonal anti-RPA70 antibodies (B-6/sc-28304; 1:1,000; Santa Cruz Biotechnology, Inc.) and mouse monoclonal anti-EGFP antibodies (1:1,000; Roche) followed by a secondary antibody (donkey anti–mouse 800CW; 1:5,000; LI-COR Biosciences) and detection using an infrared imaging-scanning system (Odyssey; LI-COR Biosciences).

UV irradiation

For all experiments, cells were irradiated with a UV source containing four UV lamps (9-W TUV PL-S; Philips) above the microscope stage. The UV dose rate was measured to be 3 W/m^{-2} at 254 nm. For induction of local UV damage, cells were UV irradiated through a polycarbonate mask (Millipore) with pores of 5 µm and subsequently irradiated for 39 s (100 $J.m^{-2}$; Moné et al., 2004; Luijsterburg et al., 2007).

Microscopic analysis

Binding kinetics were measured on a widefield fluorescence microscope (Axiovert 200M; Carl Zeiss, Inc.) equipped with a 100× Plan Apochromat 1.4 NA oil immersion lens (Carl Zeiss, Inc.) and a xenon arc lamp with monochromator (Cairn Research Ltd.). Images were recorded with a cooled charge-coupled device camera (CoolSNAP HQ; Roper Industries) using MetaMorph imaging software (version 6.1; MDS Analytical Technologies). FLIP, inverse FRAP, and photoconversion experiments were performed on a confocal microscope (LSM 510 META; Carl Zeiss, Inc.) equipped with a 63× Plan A 1.4 NA oil immersion lens (Carl Zeiss, Inc.), a 60-mW argon laser (488 and 514 nm), a 5-mW helium neon 1 (543 nm) laser, a 15-mW helium neon 2 (633 nm) laser, two photomultiplier tubes, and a META detector. Images were recorded using imaging software (LSM; Carl Zeiss, Inc.). Both microscopes were equipped with an objective heater and a climate chamber. Cells were examined in microscopy medium (137 mM NaCl, 5.4 mM KCl, 1.8 mM $CaCl_2$, 0.8 mM $MgSO_4$, 20 mM D-glucose, and 20 mM Hepes) at 37°C.

Binding kinetics

Cells were grown in glass-bottom dishes (MatTek) and locally UV irradiated as described previously (Moné et al., 2004; Luijsterburg et al., 2007). Individual cells were subsequently monitored for up to 6 h. Accumulation of EGFP-tagged repair proteins after local irradiation was quantified with Objective Image software. Time courses were normalized with respect to the plateau level. Start of the UV irradiation was defined as t = 0. The bound fraction of EGFP-tagged NER proteins in the local damage was calculated by the following equation: bound percent = $(I_{spot} - I_{outspot}) \times pixels_{spot}/(I_{nucleus} - I_{background}) \times pixels_{nucleus}$; where I_{spot} and $I_{outspot}$ are the mean pixel intensities inside the damaged spot and outside the spot, respectively. $I_{nucleus}$ is the mean pixel intensity of the nucleus, including the spot, and $I_{background}$ is the mean pixel intensity outside of the cell.

FLIP

FLIP analysis was performed by continuously bleaching a third of a locally UV-irradiated nucleus opposite to the site of damage at 100% laser intensity (488-nm argon ion laser) as previously described (Hoogstraten et al., 2002; Luijsterburg et al., 2007). A 60-mW argon ion laser was used for excitation at 488 nm, passed onto the sample by a 490-nm dichroic mirror, and emission light was filtered by a 505–550-nm emission filter. Fluorescence in the locally damaged area was monitored with low laser intensity. All values were background corrected. We chose experimental conditions (extended bleaching area and high bleaching frequency) in which an EGFP-tagged repair protein that dissociates from sites of DNA damage will likely be bleached before rebinding to sites of damage. For example, a protein with a fast on rate of 10^5 $M^{-1}s^{-1}$ would take of the order of 30 s to rebind to DNA damage occurring at a concentration of 0.35 µM (as in the experiments reported in this study). By comparison, diffusion over the typical nuclear dimension of 5 µm to hit the bleaching area with a comparatively low diffusion coefficient of 10 μm^2 s^{-1} (as measured for TFIIH; Hoogstraten et al., 2002; Luijsterburg et al., 2007) would require on average only 1.25 s.

FLIP experiments with pertubation of NER

To stall NER at the repair synthesis stage, we added inhibitors of repair synthesis and DNA ligation, i.e., HU at 100 mM and AraC at 10 µM (Smith and Okumoto, 1984; Mullenders et al., 1987) ∼1 h before local UV-C irradiation. Subsequently, the cells were locally irradiated, and we determined the dissociation kinetics of NER factors by FLIP when the maximal amount of bound proteins was reached.

Photoconversion experiments

XP4PA cells transiently expressing low levels of XPC-mOrange were locally irradiated with UV-C light. Cells were monitored in multitrack mode. A 5-mW helium neon laser was used for excitation at 543 nm, passed onto the sample by a 543-nm dichroic mirror, and emission light was filtered by a 560–615-nm emission filter. Simultaneously, a 15-mW helium neon laser was used for excitation at 633 nm, passed onto the sample by a 633-nm dichroic mirror, and emission light was filtered by a 650-nm long-pass emission filter. Images of 512 × 512 pixels were acquired with a scan time of 1.97 s (two means per line) at zoom 5 in the 543 and 633 channels. After three images, a region of 90 × 90 pixels containing the damaged area was photoconverted (15 iterations) with maximal 488-nm laser intensity (AOTF 100%; Kremers et al., 2009). Fluorescence in the locally damaged area was monitored with low laser intensity for at least 25 images with a 5-s time interval between images in the 543 and 633 channels. The loss of fluorescence at the locally damaged in the 633 channel (FLIP; caused by dissociation of photoconverted molecules) and the recovery of fluorescence in the 543 channel (FRAP; caused by association of nonphotoconverted molecules) were quantified. Curves represent the FLIP from which the FRAP has been subtracted, which is a measure for the dissociation kinetics.

Inverse FRAP

XP4PA cells transiently expressing low levels of XPC-mOrange were locally irradiated with UV-C light. After three images, the entire nucleus except for the locally damaged area was bleached (15 iterations) with maximal 488-nm laser intensity (AOTF 100%). The reequilibration of bleached and nonbleached molecules was monitored with low laser intensity for at least 25 images with an 8-s time interval between images in the 543 channel. The loss of fluorescence at the locally damaged was quantified (ImageJ; National Institutes of Health), which is a measure for the dissociation kinetics.

Immunofluorescent labeling of 6-4 PP and CPD

XP4PA cells expressing XPC-EGFP were seeded on poly-D-lysine–coated coverslips, irradiated through 5-µm pores at 100 $J.m^{-2}$, and fixed at different time points after UV irradiation (directly after UV and 1, 2, 4, and 8 h after UV). Control cells were mock treated (i.e., not irradiated) and fixed. Cells were fixed with 4% formaldehyde in PBS for 15 min at 4°C, permeabilized in 0.5% Triton X-100 (Serva) in PBS for 5 min, and incubated with 100 mM glycine in PBS for 10 min to block unreacted aldehyde groups. Subsequently, DNA was denatured with 0.1 M HCl for 10 min at 37°C, and cells were blocked in 10% BSA in PB for 15 min. Cells were rinsed with PB (130 mM KCl, 10 mM Na_2HPO_4, and 2.5 mM $MgCl_2$, pH 7.4) and equilibrated in WB (PB containing 0.5% BSA, 0.2% gelatin, and 0.05% Tween 20; Sigma-Aldrich). Antibody steps and washes were performed in WB. The primary antibodies mouse anti-CPD (1:400; Nordic Biosite) and mouse anti–6-4 PP (1:500; Nordic Biosite) were incubated overnight. Detection was performed using donkey anti–mouse Ig coupled to Alexa Fluor 546 (1:1,000; Jackson ImmunoResearch Laboratories, Inc.). Samples were mounted in Mowiol, and images were acquired on a confocal microscope (LSM 510; see Microscopic analysis). The fluoresence intensity of at least 50 local UV spots was measured using ImageJ software. The measured intensities were background corrected (using nonirradiated control images) and normalized to 1 (using cells that were fixed immediately after local UV irradiation; i.e., 0-h time point).

Estimation of the amount of locally inflicted lesions

To estimate the concentration of 6-4 PPs inflicted using local UV-C irradiation at 100 $J.m^{-2}$ through 5-mm pores of a polycarbonate mask, we used available measurements of the absolute amounts of 6-4 PPs and CPDs inflicted upon UV-C irradiation of CHO cells (Perdiz et al., 2000). These data demonstrate that the number of inflicted 6-4 PPs and CPDs does not increase linearly with increasing UV dose. By extrapolating the data of Perdiz et al. (2000), we estimate that global UV-C irradiation at 100 $J.m^{-2}$ produces ∼6 ×10^5 6-4 PPs genome wide (Fig. S1 A). However, by irradiating cells locally through 5-µm pores, we irradiate ∼10% of the nuclear volume and thus produce ∼6 × 10^4 6-4 PPs in the locally damaged area,

which translates to a nuclear concentration of 0.3 μM (assuming a nuclear volume of 0.3 pL). For comparison, global UV-C irradiation at 16 J.m^{-2}, a dose often used to saturate NER, produces 3 × 10^5 6-4 PPs genome wide. In agreement with the nonlinear increase of 6-4 PPs at increasing UV-C fluencies, we show that the amount of immobilized XPG-EGFP does not increase beyond ~10% of the protein pool when the UV-C dose is increased beyond 100 J.m^{-2} (Fig. S1 B). However, when we increase the amount of inflicted 6-4 PPs by irradiating a larger nuclear area (by using pores with 3, 5, and 8 μm, respectively), we obtain a linear increase in the amount of immobilized XPG-EGFP up to 22% of the protein pool (Fig. 7 C). These results show that (a) the used UV-C dose is not a quantitative measure for the amount of inflicted DNA lesions and (b) the lesion concentration upon local irradiation at 100 J.m^{-2} (5-μm pores) is only about twofold higher than the concentration after global irradiation at 16 J.m^{-2}, whereas the absolute amount of damages is about fivefold lower (~60,000 6-4 PPs). Thus, we estimated that our standard local UV-C irradiation introduces ~60,000 6-4 PPs, corresponding to a nuclear concentration of 0.3 μM.

Mathematical model

The model structure translates into 214 nonlinear differential equations for the various protein complexes that can be formed at the DNA repair intermediates and the free concentrations of the repair proteins. Nucleoplasmic diffusion of NER factors is not considered explicitly, as it is much faster than the characteristic times for binding and release at damage sites (Houtsmuller et al., 1999; Rademakers et al., 2003; Zotter et al., 2006).

The concentration of any possible state (repair intermediate with bound proteins) is indicated by y^R_π. The superscript index, R, refers to the repair intermediate that is defined by the modification of the DNA substrate (damaged DNA I, partially unwound DNA II, fully unwound DNA III, incised DNA IV, resynthesized DNA V, and chromatinized DNA VI). The presence of the individual proteins is encoded in a binary way in the tuple, π. The tuple π consists of seven elements: one for each protein $p \in \{C, T, G, A, F, R, \text{and } P\}$. Each protein variable $\pi(p) \in \{1, 0\}$ reveals if the protein is bound, $\pi(p) = 1$, or not, $\pi(p) = 0$. If the protein cannot bind to the given repair intermediate R, $\pi(p) = 0$ by definition.

In principle, each repair intermediate can have 2^N possible states, depending on which proteins are bound, where N is the number of proteins that can bind to the given DNA substrate. However, in two cases, we restrict the number of states as follows. First, to damaged DNA (repair intermediate I), XPC must bind first before TFIIH can bind so that the tuple with $C = 0$, $T = 1$ is excluded, and consequently, $2^{2-1} = 3$ states exist for repair intermediate I. Second, XPF/ERCC1 (F) can only bind if XPA (A) is already bound (Table S1), so that any tuple with $A = 0$ and $F = 1$ is excluded. In repair intermediates II and III, where six proteins can bind, this results in $2^6 - 2^4 = 48$ possible states. For repair intermediate IV, we have $2^7 - 2^5 = 96$ possible states. Repair intermediate V has $2^3 = 8$ states, and repair intermediate VI has 4 states for the binding of PCNA and RPA only. The time evolution of the 207 states of repair intermediates is governed by following system of differential equation:

$$\frac{d}{dt} y^R_\pi = \sum_{p \text{ in } R} \underbrace{(-1)^{\pi(p)} l^R_p \, y^R_\pi \big|_{\pi(p)=1}}_{\text{protein dissociation}} + \underbrace{(-1)^{1+\pi(p)} k^R_p C_p(t) \, y^R_\pi \big|_{\pi(p)=0}}_{\text{protein binding}} + \underbrace{E\left(y^R_\pi\right)}_{\text{enzymatic reactions}}, \tag{1}$$

where for each R = I,...,VI all allowed tuples π are to be considered.

The on-rate constant of protein p for a certain repair intermediate R is given by k^R_p and the corresponding off-rate constant by l^R_p. The time-dependent concentrations of free protein C_p are determined by Eq. 2.

The enzymatic reactions are denoted by $E(y^R_\pi)$ if a state has no in- or outgoing enzymatic reaction, $E = 0$. For damaged DNA (R = I), we have

$$E\left(y^{\mathrm{I}}_{00}\right) = \varepsilon_1 y^{\mathrm{II}}_{000000} + \varepsilon_2 y^{\mathrm{III}}_{000000} \quad \text{and} \quad E\left(y^{\mathrm{I}}_{11}\right) = -\alpha y^{\mathrm{I}}_{11}.$$

For partially unwound DNA (R = II),

$$E\left(y^{\mathrm{II}}_{000000}\right) = -\varepsilon_1 y^{\mathrm{II}}_{000000}, \quad E\left(y^{\mathrm{II}}_{110000}\right) = \alpha y^{\mathrm{I}}_{11},$$

$$E\left(y^{\mathrm{II}}_{111101}\right) = -\alpha' y^{\mathrm{II}}_{111101}, \text{ and } \quad E\left(y^{\mathrm{II}}_{111111}\right) = \alpha' y^{\mathrm{II}}_{111111}.$$

For fully unwound DNA (R = III),

$$E\left(y^{\mathrm{III}}_{000000}\right) = -\varepsilon_2 y^{\mathrm{II}}_{000000}, \quad E\left(y^{\mathrm{III}}_{011111}\right) = -\beta y^{\mathrm{III}}_{011111},$$

$$E\left(y^{\mathrm{III}}_{111101}\right) = \alpha' y^{\mathrm{II}}_{111101}, \text{ and } \quad E\left(y^{\mathrm{III}}_{111111}\right) = -\beta y^{\mathrm{III}}_{111111} + \alpha' y^{\mathrm{II}}_{111111}.$$

For incised (R = IV) and resynthesized DNA (R = V),

$$E\left(y^{\mathrm{IV}}_{111111}\right) = \beta y^{\mathrm{III}}_{111111} \quad \text{and} \quad E\left(y^{\mathrm{V}}_{011}\right) = \gamma y^{\mathrm{IV}}_{0001011} - \delta y^{\mathrm{V}}_{011}.$$

Finally, for rechromatinized DNA (R = VI),

$$E\left(y^{\mathrm{VI}}_{011}\right) = \delta y^{\mathrm{V}}_{011}.$$

The time evolution of the free concentrations of the C_p of the proteins $p \in \{C, T, G, A, F, R, \text{and } P\}$ is governed by the following seven differential equations:

$$\frac{d}{dt} C_p = \sum_{R=1}^{\mathrm{VI}} \sum_{\pi} \delta_{p1} \, l^R_p \, y^R_\pi - \delta_{p0} \, k^R_p C_p \, y^R_\pi. \tag{2}$$

The second sum runs over all allowed index tuples π for the given repair intermediate R. The Kronecker δ,

$$\delta_{ij} = \begin{cases} = 1 & \text{if } i = j \\ = 0 & \text{if } i \neq j \end{cases},$$

ensures that proteins only bind to complexes not containing the protein yet and only leave complexes containing them.

The accumulation curves of the core proteins XPC, TFIIH, XPG, XPA, ERCC1/XPF, RPA, and PCNA are generated by summing over the concentration of all states that contain the respective protein. The initial conditions of Eqs. 1 and 2 for simulating protein accumulation after UV damage are given by the free concentrations of all proteins equal to the total concentrations and the value for the initial damage concentration of y^{I}_{00} (0.33 μM); all other states empty. For simulating the FLIP curves of a given protein, its on-rate constants are set to zero (corresponding to the simplifying assumption that any unbound fluorescent molecule is bleached before it rebinds). The initial conditions are given by the state of the system during the response to UV damage at the time point at which the FLIP experiment was started (i.e., 600s for XPC and ERCC1/XPF, 900s for XPG and TFIIH, 2,000s for XPA, and 7,200s for PCNA).

Fit of the model to the data

The FLIP measurements indicate that most repair proteins bind to DNA lesions without noticeable binding cooperativity with other proteins (except for strictly sequential binding of XPC and TFIIH and strong cooperativity between ERCC1/XPF and XPA). Rather, a sequence of binding events appears to be established by the enzymatic action of protein complexes on the chromatin (e.g., through unwinding of the DNA and excision of the lesion, etc.) that changes the affinity of the repair proteins for the chromatin substrate. Random protein binding may create a large number of protein complex species (most of them being partially assembled complexes), and the question arises as to which kind of measurements need to be conducted to quantify their assembly dynamics.

As a simple case, consider the formation of a multiprotein complex from N reversibly binding components on a single repair intermediate of constant (or slowly varying) concentration, B. If the proteins bind independently of one another and their free concentrations are sufficiently large, the kinetic equations for the concentrations of the various complexes y_π (compare with Eq.1) can be integrated to yield

$$y_\pi = B \underbrace{\prod_i \frac{k_i'}{k_i' + l_i} \left(1 - \exp\left\{-(k_i' + l_i')t\right\}\right)}_{\text{proteins } i \text{ present}} \underbrace{\prod_j \frac{k_j' \exp\left\{-(k_j' + l_j')t\right\} + l_j}{k_j' + l_j}}_{\text{proteins } j \text{ absent}},$$

where the indices i and j stand for the protein species that must bind and dissociate, respectively, to form the complex; i.e., $\pi(i) = 1$ and $\pi(j) = 0$.

As unbound proteins are in excess, we have assumed their concentrations as constant and defined the first-order binding rate constants $k_i' = k_i C_i$.

The term

$$B\frac{k_i'}{k_i'+l_i'}\left(1-\exp\left\{-(k_i'+l_i')t\right\}\right)$$

is the net accumulation curve of protein i (and the terms with index j are the corresponding complements). Therefore, the composition of any protein complex formed from independently binding proteins can be inferred when the accumulation curves of all individual proteins are known.

From experimentally measured accumulation curves, we can determine the amplitude,

$$A_i = B\frac{k_i'}{k_i'+l_i'}, \tag{3}$$

and the characteristic time of accumulation,

$$t_{\mathrm{acc},i} = \frac{1}{k_i'+l_i'}, \tag{4}$$

allowing us to separately identify the on- and off-rate constants k_i' and l_i, provided that the total amount of binding sites B (i.e., the number of DNA lesions) is known. FLIP measurements provide an estimate of the characteristic dwell times of the repair protein in the complexes

$$t_{\mathrm{dwell},i} = \frac{1}{l_i'}. \tag{5}$$

Having joint measurements of A_i and $t_{\mathrm{acc},i}$ (from the accumulation curves) and $t_{\mathrm{dwell},i}$ (from the FLIP experiments), we can estimate all three parameters on the right-hand sides of Eqs. 3–5: k_i', l_i, and B; note that an independent estimate of B is no longer needed (but nevertheless exists in our data and proves useful for the fit of the full model). Thus, the simplified model of protein complexes assembling on a single kind of DNA repair intermediate is completely identifiable with two types of measurement: (1) accumulation kinetics of all individual proteins (in absolute concentration scale) and (2) dwell times of all proteins.

We have checked numerically on surrogate data that this property also holds when a particular protein complex has enzymatic activity that decreases the concentration of the binding substrate (to be specific, we chose the multiprotein complex in which all components are bound). B becomes a function of time, $B = B_0\, f(t; k_i', l_i, \alpha)$. The additional parameter, the enzymatic rate constant α, can also be estimated from the given data as long as it is not much faster than k_i'. If α is much faster than the k_i', the reaction is limited by protein binding. Then, α has negligible control on the kinetics so that its actual value is of little interest.

In the full model, we have several DNA repair intermediates, and protein complexes of appropriate composition have enzymatic activities that convert one repair intermediate into another. This model has no explicit solution; therefore, its identifiably can not be determined analytically. However, guided by the aforementioned considerations, we have found that the following experimental data yielded reliable estimates of the model parameters: accumulation kinetics of all proteins in the model, dwell times of all proteins for unperturbed NER, total amounts of repair proteins in the nucleus and inflicted lesions together with dwell of XPC, XPA, PCNA, and ERCC1/XPF in various settings of stalled NER, and a few appropriate restrictions on the parameter space.

In particular, the FLIP experiments for NER stalled at various repair intermediates help to discriminate the dwell times of the proteins at different repair intermediates. To constrain the model, we included several experimental observations and simplifications as follows.

Because RPA binds to long stretches of single-stranded DNA more strongly than to short stretches, we constrained the RPA affinity to fully unwound DNA (repair intermediate III) to be at least five times as large as to partially unwound DNA (repair intermediate II; Blackwell and Borowiec, 1994). However, RPA should have the same affinity for fully unwound DNA (repair intermediate III) and incised DNA (repair intermediate IV) because the single-stranded–binding partner stays the same. All proteins except RPA (i.e., XPC, TFIIH, XPG, XPA, and ERCC1/XPF) have the same affinity for partially unwound (repair intermediate II) and fully unwound DNA (repair intermediate III). For XPC, this is implied by the FLIP data, which show that the XPC dissociation rate changes only after formation of the full preincision complex (and likely after dual incision). For the other proteins, we make the same assumption because their binding does not appear to require large-scale DNA unwinding. These assumptions reduce the number of distinct binding and dissociation rate constants. The binding of TFIIH is dependent on the binding of the damage recognition factor XPC to the DNA lesion (i.e., repair intermediate I), and the dimer XPF/ERCC1 can only bind if XPA is present (Volker et al., 2001).

Table II. **Values of the enzymatic rate constants**

Enzymatic rate	k_{cat}
	s^{-1}
Partial unwinding α	0.08 (0.06; 0.11)
Full unwinding α'	0.74 (0.59; 0.74)
Incision β	4.1 (3.8; 6.0)
Resynthesis γ	0.05 (0.04; 0.06)
Rechromatinization δ	0.012 (0.012; 0.013)
Reannealing ε_1	3.1 (2.5; 24.1)
Reannealing ε_2	11.0 (4.9; 11.1)

Reference parameter set and 90% confidence intervals (in parentheses) are shown.

To systematically explore the parameter space of the model, we used an MCMC method (Press et al., 2007) for minimizing the residual sum of squares (χ^2) between the data shown in Fig. 5 (A–D) and the corresponding model simulations. This procedure yielded a distribution of the best-fit values for each parameter. Tables I and II show the best-fit values (smallest χ^2) and 90% confidence intervals (given by the parameter distributions) for the 47 parameters, 20 pairs of k_{on} (k) and k_{off} (l) values, five catalytic rate constants, k_{cat} (α, α', β, γ, and δ), and two reannealing rate constants (ε_1 and ε_2). The confidence intervals are comparably small for all parameters except for the reannealing rate constants ε_1 and ε_2. However, the reannealing of a ~30-nucleotide stretch of DNA is very fast, and we found that the precise values do not matter as long as the characteristic times for the reannealing are in the subsecond range (as shown in Table II). In this case, the reannealing of the DNA is limited by the dissociation rates of the proteins stabilizing the unwound state, as one can reasonably expect. In addition, the dissociation constants $K_D = k_{off}/k_{on}$ were calculated; characteristic times for enzymatic reactions are given by $1/k_{cat}$. The mean times to produce repair intermediates τ are also listed (see following paragraph).

Characteristic times

The characteristic time τ (y^R_π) of the state $y^R(t)$ is defined by the first moment of the distribution divided by the zeroth moment. With the m^{th} moment defined by

$$\mu^{(m)} = \int t^m\, y^R_\pi(t)\, dt,$$

where the characteristic time is

$$\tau = \frac{\mu^{(1)}}{\mu^{(0)}},$$

and the standard deviation is

$$\sigma = \sqrt{\frac{\mu^{(2)}}{\mu^{(0)}} - \tau^2}. \tag{6}$$

The characteristic times to partial unwinding (τ_{par}; i.e., $R = \mathrm{I}$), to full unwinding (τ_{full}; i.e., $R = \mathrm{II}$), and to incision (τ_{inc}; i.e., $R = \mathrm{III}$) are given by

$$\tau_R = \frac{\int_0^\infty t \sum_{x=1}^{R} \sum_\pi y^x_\pi(t)\, dt}{\int_0^\infty \sum_{x=1}^{R} \sum_\pi y^x_\pi(t)\, dt}.$$

The first sum runs over all repair intermediates proceeding and the repair intermediate itself. The second sum runs over all tuple π and is thereby

summing over the concentrations of all states within a given repair intermediate. To ensure convergence of the integrals, the time to resynthesis is calculated by tracking all repair intermediates before resynthesis using the equation

$$\tau_{syn}=\frac{\int_0^\infty t\left(y_{00}^{I}(0)-\left(\sum_\pi y_\pi^{IV}(t)+\sum_\pi y_\pi^{I}(t)\right)\right)dt}{\int_0^\infty y_{00}^{I}(0)-\left(\sum_\pi y_\pi^{IV}(t)+\sum_\pi y_\pi^{I}(t)\right)dt}.$$

The time to chromatinize is calculated analogously:

$$\tau_{chrom}=\frac{\int_0^\infty t\left(y_{00}^{I}(0)-\sum_\pi y_\pi^{V}(t)\right)dt}{\int_0^\infty \left(y_{00}^{I}(0)-\sum_\pi y_\pi^{V}(t)\right)dt}. \quad (7)$$

The corresponding standard deviations are calculated in the same manner, according to Eq. 6. With the reference parameter set, these definitions yield for partially unwound DNA (τ_{part} = 35 ± 30 min), fully unwound DNA (τ_{full} = 41 ± 36 min), incised DNA (τ_{inc} = 41 ± 36 min), resynthesized DNA (τ_{syn} = 2.0 ± 0.7 h), and rechromatinized DNA (τ_{chrom} = 2.2 ± 0.7 h). The high standard deviations indicate that there are considerable stochastic variations in timing from lesion to lesion.

Michaelis–Menten approximation

As a phenomenological approximation for the dependence of the incision rate v on the amount of initial damage D, consider the Michaelis–Menten equation

$$v(t)=v_{max}\frac{D(t)}{K_M+D(t)}.$$

We approximate the time-dependent change of the total damage by

$$\frac{dD}{dt}=-v(t),$$

and separation of variables by

$$v_{max}\,dt=-\frac{K_m+D(t)}{D(t)}dD,$$

To obtain the characteristic time for repair,

$$\tau=\frac{1}{D(0)}\int_0^\infty D(t)dt=\frac{1}{2}\frac{D(0)}{v_{excision}}+\frac{K_M}{v_{max}}.$$

Eq. 7 predicts that the time to incision will rise as a linear function of initial damage $D(0)$ (compare with Fig. S4 B). Therefore, we approximated the initial part of the τ_{inc} curve in Fig. S4 B as the characteristic time to incision versus the initial amount of damage by a straight line, yielding a slope of approximately

$$\frac{1}{2}\frac{1}{v_{max}}=\frac{5\,\text{min}}{60{,}000\,\text{lesions}},$$

and consequently, the maximal rate of repair (of 6-4 PPs) per cell nucleus is v_{max} = 6,000 lesions/min. The interpolated intersection with the ordinate is approximately at K_M/v_{max} = 36 min, yielding a half-saturation constant of K_M = 216,000 lesions. Thus, there is very considerable capability for the parallel processing of DNA lesions by the NER system.

Specificity of NER

In this study, we assess the specificity of NER when it would be determined by the binding of XPC only. We assume that binding of XPC may trigger DNA unwinding and the assembly of the NER complex regardless of whether it binds to DNA lesions. Measurements indicate that a DNA-bound XPC molecule occupies 20–30 base pairs of DNA (Sugasawa et al., 1998; Min and Pavletich, 2007). Given that a diploid human cell has 6.4 10^9 base pairs, we estimate approximately between 2 and 3× 10^8 unspecific binding sites (B) for XPC and thus the NER complex. This translates to a nuclear concentration of 1.21–1.77 mM (assuming a nuclear volume of 0.3 pL). The affinity of XPC for unspecific binding is 100-fold lower than for DNA lesions (Hey et al., 2002; Hoogstraten et al., 2008), which is 0.78 mM for our model parameters. On average, the concentration of XPC bound to undamaged sites will be

$$[\text{XPC}-\text{B}]=\frac{[\text{XPC}]_{free}[\text{B}]_{free}}{K_D},\ \text{where}$$

$$[\text{XPC}-\text{B}]_{total}=[\text{XPC}]_{free}+[\text{XPC-B}]\ \text{and}$$

$$[\text{B}]_{total}=[\text{B}]_{free}+[\text{XPC-B}].$$

The solution indicates that between 61 and 69% of the XPC molecules (15,000–18,000 molecules) are nonspecifically bound at any given time. This number agrees with recent measurements on XPC-GFP in vivo, where 50% of the XPC pool was shown to be transiently bound to chromatin at all times (Hoogstraten et al., 2008). From our model, we estimate that it takes between 6 and 10 min to incision if XPC is already bound; consequently, there should be ≈10^4–10^5 incisions/h at undamaged sites of the genome if no further mechanisms were in place to prevent such erroneous incisions. However, our model naturally accounts for a kinetic proofreading mechanism that, under certain conditions, can strongly enhance the specificity of NER. In kinetic proofreading, an enzyme–substrate complex is taken through a series of high energy intermediates at the expense of metabolic energy before the final committing reaction step can take place. In the passage through these intermediate states, the stability of the complex is tested several times, thus leading to a more faithful discrimination between the true substrate and close analogues than could be achieved by a single binding step (Hopfield, 1974). In our model, kinetic proofreading naturally occurs through reversible unwinding of the DNA around a lesion. As the DNA will reanneal spontaneously when the stabilizing preincision proteins (stochastically) dissociate, the binding of these proteins is subjected to a stringent stability test.

The affinities of XPC and XPA for DNA depend on the distorted helical structure and the presence of the lesion, respectively (Camenisch et al., 2006; Maillard et al., 2007). Moreover, the subunit composition of TFIIH is different when binding to a DNA lesion as compared with its engagement in transcription (Giglia-Mari et al., 2006) so that it may also bind with different affinities to damaged and nondamaged DNA (Villani and Tanguy Le Gac, 2000; Dip et al., 2004). Additionally, XPA preferentially binds to kinks in the helical DNA structure that are induced by DNA lesions and therefore can also contribute to the discrimination between damaged and nondamaged DNA (Camenisch et al., 2006).

The affinities of XPC and XPA for DNA depend on the distorted helical structure and the presence of the lesion, respectively (Camenisch et al., 2006; Maillard et al., 2007). Moreover, the subunit composition of TFIIH is different when binding to a DNA lesion as compared with its engagement in transcription (Giglia-Mari et al., 2006) so that it may also bind with different affinities to damaged and nondamaged DNA (Villani and Tanguy Le Gac, 2000; Dip et al., 2004). Additionally, XPA preferentially binds to kinks in the helical DNA structure that are induced by DNA lesions and therefore can also contribute to the discrimination between damaged and nondamaged DNA (Camenisch et al., 2006).

Online supplemental material

Fig. S1 shows locally inflicted lesions. Fig. S2 shows immunoblot analysis of RPA70-EGFP cells. Fig. S3 shows that cells analyzed by FLIP remain repair competent. Fig. S4 shows the rate of NER. Table S1 shows model assumptions. Online supplemental material is available at http://www.jcb.org/cgi/content/full/jcb.200909175/DC1.

We acknowledge Drs. K. Rippe, R.T. Dame, and F.A. Salomons for critical reading of the manuscript and Dr. Nico Dantuma for the opportunity to finish this work in his laboratory.

This work was supported by ZonMW (grant 912-03-012 to R. van Driel and W. Vermeulen), the Netherlands Organization for Scientific Research (NWO; grant 2007/09198/ALW/825.07.042 to MSL), and the Initiative and Networking Fund of the Helmholtz Association within the Helmholtz Alliance on Systems Biology/SBCancer (grant to T. Höfer).

Submitted: 30 September 2009
Accepted: 2 April 2010

References

Aboussekhra, A., M. Biggerstaff, M.K. Shivji, J.A. Vilpo, V. Moncollin, V.N. Podust, M. Protić, U. Hübscher, J.M. Egly, and R.D. Wood. 1995. Mammalian DNA nucleotide excision repair reconstituted with purified protein components. *Cell.* 80:859–868. doi:10.1016/0092-8674(95)90289-9

Araújo, S.J., E.A. Nigg, and R.D. Wood. 2001. Strong functional interactions of TFIIH with XPC and XPG in human DNA nucleotide excision repair, without a preassembled repairosome. *Mol. Cell. Biol.* 21:2281–2291. doi:10.1128/MCB.21.7.2281-2291.2001

Black, J.C., J.E. Choi, S.R. Lombardo, and M. Carey. 2006. A mechanism for coordinating chromatin modification and preinitiation complex assembly. *Mol. Cell.* 23:809–818. doi:10.1016/j.molcel.2006.07.018

Blackwell, L.J., and J.A. Borowiec. 1994. Human replication protein A binds single-stranded DNA in two distinct complexes. *Mol. Cell. Biol.* 14:3993–4001.

Camenisch, U., R. Dip, S.B. Schumacher, B. Schuler, and H. Naegeli. 2006. Recognition of helical kinks by *xeroderma pigmentosum* group A protein triggers DNA excision repair. *Nat. Struct. Mol. Biol.* 13:278–284. doi:10.1038/nsmb1061

Camenisch, U., R. Dip, M. Vitanescu, and H. Naegeli. 2007. *Xeroderma pigmentosum* complementation group A protein is driven to nucleotide excision repair sites by the electrostatic potential of distorted DNA. *DNA Repair (Amst.).* 6:1819–1828. doi:10.1016/j.dnarep.2007.07.011

Coin, F., V. Oksenych, and J.M. Egly. 2007. Distinct roles for the XPB/p52 and XPD/p44 subcomplexes of TFIIH in damaged DNA opening during nucleotide excision repair. *Mol. Cell.* 26:245–256. doi:10.1016/j.molcel.2007.03.009

Darzacq, X., and R.H. Singer. 2008. The dynamic range of transcription. *Mol. Cell.* 30:545–546. doi:10.1016/j.molcel.2008.05.009

Darzacq, X., Y. Shav-Tal, V. de Turris, Y. Brody, S.M. Shenoy, R.D. Phair, and R.H. Singer. 2007. In vivo dynamics of RNA polymerase II transcription. *Nat. Struct. Mol. Biol.* 14:796–806. doi:10.1038/nsmb1280

de Laat, W.L., E. Appeldoorn, K. Sugasawa, E. Weterings, N.G. Jaspers, and J.H. Hoeijmakers. 1998. DNA-binding polarity of human replication protein A positions nucleases in nucleotide excision repair. *Genes Dev.* 12:2598–2609. doi:10.1101/gad.12.16.2598

Dinant, C., M.S. Luijsterburg, T. Höfer, G. von Bornstaedt, W. Vermeulen, A.B. Houtsmuller, and R. van Driel. 2009. Assembly of multiprotein complexes that control genome function. *J. Cell Biol.* 185:21–26. doi:10.1083/jcb.200811080

Dip, R., U. Camenisch, and H. Naegeli. 2004. Mechanisms of DNA damage recognition and strand discrimination in human nucleotide excision repair. *DNA Repair (Amst.).* 3:1409–1423. doi:10.1016/j.dnarep.2004.05.005

Dundr, M., U. Hoffmann-Rohrer, Q. Hu, I. Grummt, L.I. Rothblum, R.D. Phair, and T. Misteli. 2002. A kinetic framework for a mammalian RNA polymerase in vivo. *Science.* 298:1623–1626. doi:10.1126/science.1076164

Essers, J., A.F. Theil, C. Baldeyron, W.A. van Cappellen, A.B. Houtsmuller, R. Kanaar, and W. Vermeulen. 2005. Nuclear dynamics of PCNA in DNA replication and repair. *Mol. Cell. Biol.* 25:9350–9359. doi:10.1128/MCB.25.21.9350-9359.2005

Evans, E., J.G. Moggs, J.R. Hwang, J.M. Egly, and R.D. Wood. 1997. Mechanism of open complex and dual incision formation by human nucleotide excision repair factors. *EMBO J.* 16:6559–6573. doi:10.1093/emboj/16.21.6559

Giglia-Mari, G., C. Miquel, A.F. Theil, P.O. Mari, D. Hoogstraten, J.M. Ng, C. Dinant, J.H. Hoeijmakers, and W. Vermeulen. 2006. Dynamic interaction of TTDA with TFIIH is stabilized by nucleotide excision repair in living cells. *PLoS Biol.* 4:e156. doi:10.1371/journal.pbio.0040156

Gillet, L.C., and O.D. Schärer. 2006. Molecular mechanisms of mammalian global genome nucleotide excision repair. *Chem. Rev.* 106:253–276. doi:10.1021/cr040483f

Gorski, S.A., S.K. Snyder, S. John, I. Grummt, and T. Misteli. 2008. Modulation of RNA polymerase assembly dynamics in transcriptional regulation. *Mol. Cell.* 30:486–497. doi:10.1016/j.molcel.2008.04.021

Green, C.M., and G. Almouzni. 2003. Local action of the chromatin assembly factor CAF-1 at sites of nucleotide excision repair in vivo. *EMBO J.* 22:5163–5174. doi:10.1093/emboj/cdg478

Hall, H., J. Gurský, A. Nicodemou, I. Rybanská, E. Kimlíčková, and M. Pirsel. 2006. Characterization of ERCC3 mutations in the Chinese hamster ovary 27-1, UV24 and MMC-2 cell lines. *Mutat. Res.* 593:177–186.

Henricksen, L.A., C.B. Umbricht, and M.S. Wold. 1994. Recombinant replication protein A: expression, complex formation, and functional characterization. *J. Biol. Chem.* 269:11121–11132.

Hey, T., G. Lipps, K. Sugasawa, S. Iwai, F. Hanaoka, and G. Krauss. 2002. The XPC-HR23B complex displays high affinity and specificity for damaged DNA in a true-equilibrium fluorescence assay. *Biochemistry.* 41:6583–6587. doi:10.1021/bi012202t

Hoeijmakers, J.H. 2001. Genome maintenance mechanisms for preventing cancer. *Nature.* 411:366–374. doi:10.1038/35077232

Hoogstraten, D., A.L. Nigg, H. Heath, L.H. Mullenders, R. van Driel, J.H. Hoeijmakers, W. Vermeulen, and A.B. Houtsmuller. 2002. Rapid switching of TFIIH between RNA polymerase I and II transcription and DNA repair in vivo. *Mol. Cell.* 10:1163–1174. doi:10.1016/S1097-2765(02)00709-8

Hoogstraten, D., S. Bergink, J.M. Ng, V.H. Verbiest, M.S. Luijsterburg, B. Geverts, A. Raams, C. Dinant, J.H. Hoeijmakers, W. Vermeulen, and A.B. Houtsmuller. 2008. Versatile DNA damage detection by the global genome nucleotide excision repair protein XPC. *J. Cell Sci.* 121:2850–2859. doi:10.1242/jcs.031708

Hopfield, J.J. 1974. Kinetic proofreading: a new mechanism for reducing errors in biosynthetic processes requiring high specificity. *Proc. Natl. Acad. Sci. USA.* 71:4135–4139. doi:10.1073/pnas.71.10.4135

Houtsmuller, A.B., S. Rademakers, A.L. Nigg, D. Hoogstraten, J.H. Hoeijmakers, and W. Vermeulen. 1999. Action of DNA repair endonuclease ERCC1/XPF in living cells. *Science.* 284:958–961. doi:10.1126/science.284.5416.958

Karpova, T.S., M.J. Kim, C. Spriet, K. Nalley, T.J. Stasevich, Z. Kherrouche, L. Heliot, and J.G. McNally. 2008. Concurrent fast and slow cycling of a transcriptional activator at an endogenous promoter. *Science.* 319:466–469. doi:10.1126/science.1150559

Kaufmann, W.K., and S.J. Wilson. 1990. DNA repair endonuclease activity during synchronous growth of diploid human fibroblasts. *Mutat. Res.* 236:107–117.

Kesseler, K.J., W.K. Kaufmann, J.T. Reardon, T.C. Elston, and A. Sancar. 2007. A mathematical model for human nucleotide excision repair: damage recognition by random order assembly and kinetic proofreading. *J. Theor. Biol.* 249:361–375. doi:10.1016/j.jtbi.2007.07.025

Kimura, H., and P.R. Cook. 2001. Kinetics of core histones in living human cells: little exchange of H3 and H4 and some rapid exchange of H2B. *J. Cell Biol.* 153:1341–1353. doi:10.1083/jcb.153.7.1341

Kremers, G.J., J. Goedhart, E.B. van Munster, and T.W. Gadella Jr. 2006. Cyan and yellow super fluorescent proteins with improved brightness, protein folding, and FRET Förster radius. *Biochemistry.* 45:6570–6580. doi:10.1021/bi0516273

Kremers, G.J., K.L. Hazelwood, C.S. Murphy, M.W. Davidson, and D.W. Piston. 2009. Photoconversion in orange and red fluorescent proteins. *Nat. Methods.* 6:355–358. doi:10.1038/nmeth.1319

Kunkel, T.A., and K. Bebenek. 2000. DNA replication fidelity. *Annu. Rev. Biochem.* 69:497–529. doi:10.1146/annurev.biochem.69.1.497

Luijsterburg, M.S., J. Goedhart, J. Moser, H. Kool, B. Geverts, A.B. Houtsmuller, L.H. Mullenders, W. Vermeulen, and R. van Driel. 2007. Dynamic in vivo interaction of DDB2 E3 ubiquitin ligase with UV-damaged DNA is independent of damage-recognition protein XPC. *J. Cell Sci.* 120:2706–2716. doi:10.1242/jcs.008367

MacInnes, M.A., J.A. Dickson, R.R. Hernandez, D. Learmonth, G.Y. Lin, J.S. Mudgett, M.S. Park, S. Schauer, R.J. Reynolds, G.F. Strniste, et al. 1993. Human ERCC5 cDNA-cosmid complementation for excision repair and bipartite amino acid domains conserved with RAD proteins of *Saccharomyces cerevisiae* and *Schizosaccharomyces pombe*. *Mol. Cell. Biol.* 13:6393–6402.

Maillard, O., S. Solyom, and H. Naegeli. 2007. An aromatic sensor with aversion to damaged strands confers versatility to DNA repair. *PLoS Biol.* 5:e79. doi:10.1371/journal.pbio.0050079

Michelman-Ribeiro, A., D. Mazza, T. Rosales, T.J. Stasevich, H. Boukari, V. Rishi, C. Vinson, J.R. Knutson, and J.G. McNally. 2009. Direct measurement of association and dissociation rates of DNA binding in live cells by fluorescence correlation spectroscopy. *Biophys. J.* 97:337–346. doi:10.1016/j.bpj.2009.04.027

Min, J.H., and N.P. Pavletich. 2007. Recognition of DNA damage by the Rad4 nucleotide excision repair protein. *Nature.* 449:570–575. doi:10.1038/nature06155

Misteli, T. 2007. Beyond the sequence: cellular organization of genome function. *Cell.* 128:787–800. doi:10.1016/j.cell.2007.01.028

Mocquet, V., J.P. Lainé, T. Riedl, Z. Yajin, M.Y. Lee, and J.M. Egly. 2008. Sequential recruitment of the repair factors during NER: the role of XPG in initiating the resynthesis step. *EMBO J.* 27:155–167. doi:10.1038/sj.emboj.7601948

Moné, M.J., M. Volker, O. Nikaido, L.H. Mullenders, A.A. van Zeeland, P.J. Verschure, E.M. Manders, and R. van Driel. 2001. Local UV-induced DNA damage in cell nuclei results in local transcription inhibition. *EMBO Rep.* 2:1013–1017. doi:10.1093/embo-reports/kve224

Moné, M.J., T. Bernas, C. Dinant, F.A. Goedvree, E.M. Manders, M. Volker, A.B. Houtsmuller, J.H. Hoeijmakers, W. Vermeulen, and R. van Driel. 2004. In vivo dynamics of chromatin-associated complex formation in mammalian nucleotide excision repair. *Proc. Natl. Acad. Sci. USA.* 101:15933–15937. doi:10.1073/pnas.0403664101

Moser, J., M. Volker, H. Kool, S. Alekseev, H. Vrieling, A. Yasui, A.A. van Zeeland, and L.H. Mullenders. 2005. The UV-damaged DNA binding protein mediates efficient targeting of the nucleotide excision repair complex to UV-induced photo lesions. *DNA Repair (Amst.).* 4:571–582. doi:10.1016/j.dnarep.2005.01.001

Moser, J., H. Kool, I. Giakzidis, K. Caldecott, L.H. Mullenders, and M.I. Fousteri. 2007. Sealing of chromosomal DNA nicks during nucleotide excision repair requires XRCC1 and DNA ligase III alpha in a cell-cycle-specific manner. *Mol. Cell.* 27:311–323. doi:10.1016/j.molcel.2007.06.014

Mu, D., D.S. Hsu, and A. Sancar. 1996. Reaction mechanism of human DNA repair excision nuclease. *J. Biol. Chem.* 271:8285–8294. doi:10.1074/jbc.271.32.19451

Mullenders, L.H., A.A. van Zeeland, and A.T. Natarajan. 1987. The localization of ultraviolet-induced excision repair in the nucleus and the distribution of repair events in higher order chromatin loops in mammalian cells. *J. Cell Sci. Suppl.* 6:243–262.

Nishi, R., S. Alekseev, C. Dinant, D. Hoogstraten, A.B. Houtsmuller, J.H. Hoeijmakers, W. Vermeulen, F. Hanaoka, and K. Sugasawa. 2009. UV-DDB-dependent regulation of nucleotide excision repair kinetics in living cells. *DNA Repair (Amst.).* 8:767–776. doi:10.1016/j.dnarep.2009.02.004

O'Donovan, A., A.A. Davies, J.G. Moggs, S.C. West, and R.D. Wood. 1994. XPG endonuclease makes the 3′ incision in human DNA nucleotide excision repair. *Nature.* 371:432–435. doi:10.1038/371432a0

Park, C.J., and B.S. Choi. 2006. The protein shuffle. Sequential interactions among components of the human nucleotide excision repair pathway. *FEBS J.* 273:1600–1608. doi:10.1111/j.1742-4658.2006.05189.x

Perdiz, D., P. Grof, M. Mezzina, O. Nikaido, E. Moustacchi, and E. Sage. 2000. Distribution and repair of bipyrimidine photoproducts in solar UV-irradiated mammalian cells. Possible role of Dewar photoproducts in solar mutagenesis. *J. Biol. Chem.* 275:26732–26742.

Politi, A., M.J. Moné, A.B. Houtsmuller, D. Hoogstraten, W. Vermeulen, R. Heinrich, and R. van Driel. 2005. Mathematical modeling of nucleotide excision repair reveals efficiency of sequential assembly strategies. *Mol. Cell.* 19:679–690. doi:10.1016/j.molcel.2005.06.036

Polo, S.E., D. Roche, and G. Almouzni. 2006. New histone incorporation marks sites of UV repair in human cells. *Cell.* 127:481–493. doi:10.1016/j.cell.2006.08.049

Press, W., S. Teukolsky, W. Vetterling, and B. Flannery. 2007. Numerical Recipes: The Art of Scientific Computing. Third edition. Cambridge University Press, Cambridge/New York. 1235 pp.

Rademakers, S., M. Volker, D. Hoogstraten, A.L. Nigg, M.J. Moné, A.A. Van Zeeland, J.H. Hoeijmakers, A.B. Houtsmuller, and W. Vermeulen. 2003. *Xeroderma pigmentosum* group A protein loads as a separate factor onto DNA lesions. *Mol. Cell. Biol.* 23:5755–5767. doi:10.1128/MCB.23.16.5755-5767.2003

Riedl, T., F. Hanaoka, and J.M. Egly. 2003. The comings and goings of nucleotide excision repair factors on damaged DNA. *EMBO J.* 22:5293–5303. doi:10.1093/emboj/cdg489

Satokata, I., K. Tanaka, N. Miura, M. Narita, T. Mimaki, Y. Satoh, S. Kondo, and Y. Okada. 1992. Three nonsense mutations responsible for group A *xeroderma pigmentosum. Mutat. Res.* 273:193–202.

Schaeffer, L., R. Roy, S. Humbert, V. Moncollin, W. Vermeulen, J.H. Hoeijmakers, P. Chambon, and J.M. Egly. 1993. DNA repair helicase: a component of BTF2 (TFIIH) basic transcription factor. *Science.* 260:58–63. doi:10.1126/science.8465201

Shaner, N.C., R.E. Campbell, P.A. Steinbach, B.N. Giepmans, A.E. Palmer, and R.Y. Tsien. 2004. Improved monomeric red, orange and yellow fluorescent proteins derived from *Discosoma sp.* red fluorescent protein. *Nat. Biotechnol.* 22:1567–1572. doi:10.1038/nbt1037

Shivji, K.K., M.K. Kenny, and R.D. Wood. 1992. Proliferating cell nuclear antigen is required for DNA excision repair. *Cell.* 69:367–374. doi:10.1016/0092-8674(92)90416-A

Shivji, M.K., V.N. Podust, U. Hübscher, and R.D. Wood. 1995. Nucleotide excision repair DNA synthesis by DNA polymerase epsilon in the presence of PCNA, RFC, and RPA. *Biochemistry.* 34:5011–5017. doi:10.1021/bi00015a012

Sijbers, A.M., W.L. de Laat, R.R. Ariza, M. Biggerstaff, Y.F. Wei, J.G. Moggs, K.C. Carter, B.K. Shell, E. Evans, M.C. de Jong, et al. 1996. *Xeroderma pigmentosum* group F caused by a defect in a structure-specific DNA repair endonuclease. *Cell.* 86:811–822. doi:10.1016/S0092-8674(00)80155-5

Smith, C.A., and D.S. Okumoto. 1984. Nature of DNA repair synthesis resistant to inhibitors of polymerase alpha in human cells. *Biochemistry.* 23:1383–1391. doi:10.1021/bi00302a008

Sugasawa, K., J.M. Ng, C. Masutani, S. Iwai, P.J. van der Spek, A.P. Eker, F. Hanaoka, D. Bootsma, and J.H. Hoeijmakers. 1998. *Xeroderma pigmentosum* group C protein complex is the initiator of global genome nucleotide excision repair. *Mol. Cell.* 2:223–232. doi:10.1016/S1097-2765(00)80132-X

Sugasawa, K., J. Akagi, R. Nishi, S. Iwai, and F. Hanaoka. 2009. Two-step recognition of DNA damage for mammalian nucleotide excision repair: Directional binding of the XPC complex and DNA strand scanning. *Mol. Cell.* 36:642–653. doi:10.1016/j.molcel.2009.09.035

Tapias, A., J. Auriol, D. Forget, J.H. Enzlin, O.D. Schärer, F. Coin, B. Coulombe, and J.M. Egly. 2004. Ordered conformational changes in damaged DNA induced by nucleotide excision repair factors. *J. Biol. Chem.* 279:19074–19083. doi:10.1074/jbc.M312611200

Tsodikov, O.V., D. Ivanov, B. Orelli, L. Staresincic, I. Shoshani, R. Oberman, O.D. Schärer, G. Wagner, and T. Ellenberger. 2007. Structural basis for the recruitment of ERCC1-XPF to nucleotide excision repair complexes by XPA. *EMBO J.* 26:4768–4776. doi:10.1038/sj.emboj.7601894

van Attikum, H., and S.M. Gasser. 2009. Crosstalk between histone modifications during the DNA damage response. *Trends Cell Biol.* 19:207–217. doi:10.1016/j.tcb.2009.03.001

van den Boom, V., E. Citterio, D. Hoogstraten, A. Zotter, J.M. Egly, W.A. van Cappellen, J.H. Hoeijmakers, A.B. Houtsmuller, and W. Vermeulen. 2004. DNA damage stabilizes interaction of CSB with the transcription elongation machinery. *J. Cell Biol.* 166:27–36. doi:10.1083/jcb.200401056

van Duin, M., J. de Wit, H. Odijk, A. Westerveld, A. Yasui, M.H. Koken, J.H. Hoeijmakers, and D. Bootsma. 1986. Molecular characterization of the human excision repair gene ERCC-1: cDNA cloning and amino acid homology with the yeast DNA repair gene RAD10. *Cell.* 44:913–923. doi:10.1016/0092-8674(86)90014-0

van Hoffen, A., J. Venema, R. Meschini, A.A. van Zeeland, and L.H. Mullenders. 1995. Transcription-coupled repair removes both cyclobutane pyrimidine dimers and 6-4 photoproducts with equal efficiency and in a sequential way from transcribed DNA in *xeroderma pigmentosum* group C fibroblasts. *EMBO J.* 14:360–367.

Vermeulen, W., R.J. Scott, S. Rodgers, H.J. Müller, J. Cole, C.F. Arlett, W.J. Kleijer, D. Bootsma, J.H. Hoeijmakers, and G. Weeda. 1994. Clinical heterogeneity within *xeroderma pigmentosum* associated with mutations in the DNA repair and transcription gene ERCC3. *Am. J. Hum. Genet.* 54:191–200.

Villani, G., and N. Tanguy Le Gac. 2000. Interactions of DNA helicases with damaged DNA: possible biological consequences. *J. Biol. Chem.* 275:33185–33188. doi:10.1074/jbc.R000011200

Volker, M., M.J. Moné, P. Karmakar, A. van Hoffen, W. Schul, W. Vermeulen, J.H. Hoeijmakers, R. van Driel, A.A. van Zeeland, and L.H. Mullenders. 2001. Sequential assembly of the nucleotide excision repair factors in vivo. *Mol. Cell.* 8:213–224. doi:10.1016/S1097-2765(01)00281-7

Wakasugi, M., and A. Sancar. 1999. Order of assembly of human DNA repair excision nuclease. *J. Biol. Chem.* 274:18759–18768. doi:10.1074/jbc.274.26.18759

Yagi, T., J. Tatsumi-Miyajima, M. Sato, K.H. Kraemer, and H. Takebe. 1991. Analysis of point mutations in an ultraviolet-irradiated shuttle vector plasmid propagated in cells from Japanese *xeroderma pigmentosum* patients in complementation groups A and F. *Cancer Res.* 51:3177–3182.

Ye, N., M.S. Bianchi, N.O. Bianchi, and G.P. Holmquist. 1999. Adaptive enhancement and kinetics of nucleotide excision repair in humans. *Mutat. Res.* 435:43–61.

Yokoi, M., C. Masutani, T. Maekawa, K. Sugasawa, Y. Ohkuma, and F. Hanaoka. 2000. The *xeroderma pigmentosum* group C protein complex XPC-HR23B plays an important role in the recruitment of transcription factor IIH to damaged DNA. *J. Biol. Chem.* 275:9870–9875. doi:10.1074/jbc.275.13.9870

Zotter, A., M.S. Luijsterburg, D.O. Warmerdam, S. Ibrahim, A. Nigg, W.A. van Cappellen, J.H. Hoeijmakers, R. van Driel, W. Vermeulen, and A.B. Houtsmuller. 2006. Recruitment of the nucleotide excision repair endonuclease XPG to sites of UV-induced dna damage depends on functional TFIIH. *Mol. Cell. Biol.* 26:8868–8879. doi:10.1128/MCB.00695-06

Supplemental material JCB

Luijsterburg et al., http://www.jcb.org/cgi/content/full/jcb.200909175/DC1

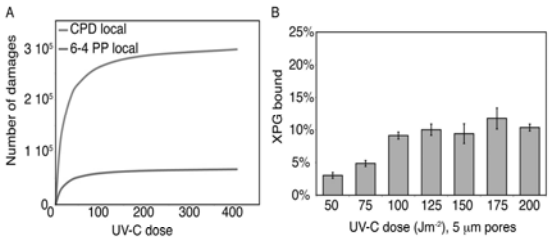

Figure S1. **Locally inflicted lesions.** (A) Estimate of the amount of 6-4 PPs produced at different UV fluencies (including experimental conditions used in this study) based on extrapolation of previous data by Perdiz et al. (2000). (B) UV-C dose ($J.m^{-2}$) response curve (measured in percentage of protein bound in the locally irradiated area) of UV135 cells expressing XPG-EGFP locally irradiated through 5 μm irradiated at UV-C fluencies ranging from 50 to 200 $J.m^{-2}$.

Published May 3, 2010

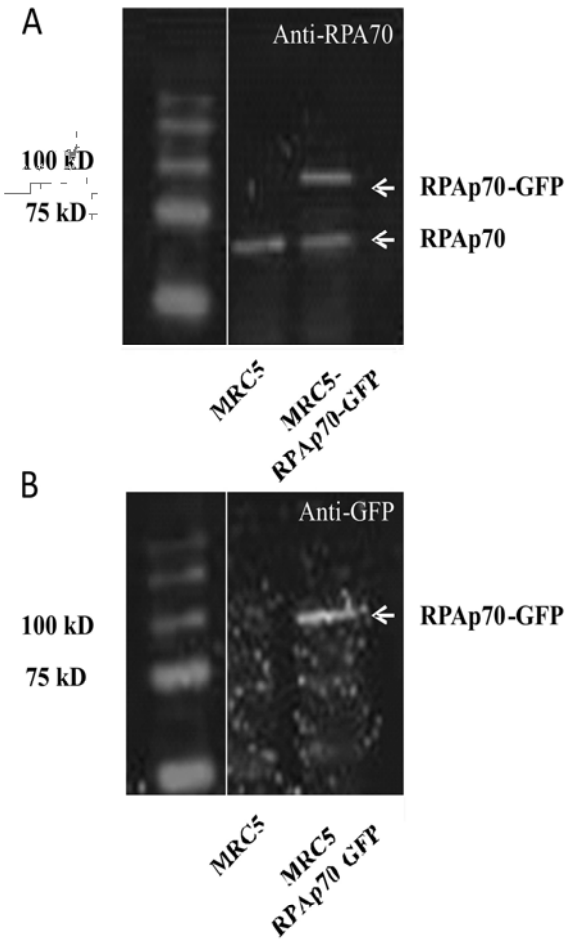

Figure S2. **Immunoblot analysis of RPA70-EGFP cells.** (A and B) Immunoblot probed with monoclonal anti-RPA antibodies (A) and monoclonal anti-GFP antibodies (B) of whole cell extracts from untransfected MRC5 cells and MRC5 cells stably expressing EGFP-tagged RPA70. The molecular mass of protein markers is indicated in kilodaltons. (A) EGFP-tagged RPA70 migrates slower than endogenous RPA (arrows), as detected by anti-RPA antibodies. This allows for a direct comparison between the expression level of RPA70-GFP relative to the levels of endogenous RPA, which shows that endogenous RPA70 and RPA70-EGFP are expressed at a 1:1 ratio. (B) Anti-EGFP antibodies specifically detect RPA70-EGFP at the size expected for the full-length fusion protein. Detection was performed using an infrared imaging system.

Published May 3, 2010

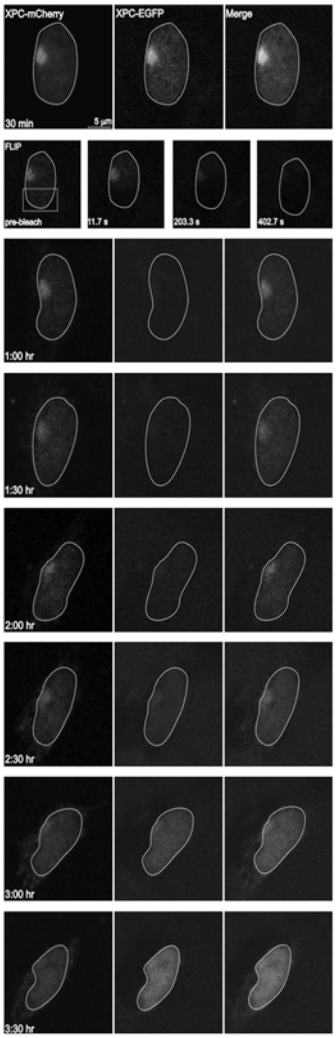

Figure S3. **Cells analyzed by FLIP remain repair competent.** XP4PA cells stably expressing XPC-GFP and transiently expressing XPC-mCherry were locally irradiated (5 µm; 100 J.m^{-2}). 30 min after local UV irradiation, cells were analyzed by FLIP as described in Fig. 3 and Material and methods. The FLIP experiment resulted in the loss of the XPC-GFP signal (as a result of bleaching) but not of the XPC-mCherry signal. The same cells that were analyzed by FLIP were subsequently monitored for several hours after UV irradiation until binding of XPC mCherry could no longer be detected, indicating successful repair of 6-4 PPs. Note that the signal in the green channel gradually increases several hours after FLIP as a result of synthesis of new XPC-GFP. This experiment was performed three times with similar results. Red rectangle indicates the area of photobleaching.

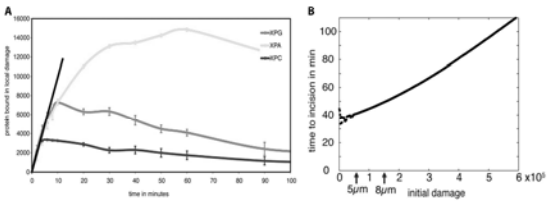

Figure S4. **NER rate.** (A) Cells expressing XPC-EGFP, XPG-EGFP, and EGFP-XPA were locally irradiated (5-µm pores; 100 J.m^{-2}) as described in Materials and methods. The binding curve shows the first 100 min of the binding curve shown in Fig. 2 B. The assembly rates of these NER proteins can be estimated from the initial slope of the binding curves. The tangent shows an immobilization of ~3.6%, ~1.1%, and ~0.5% of the total protein pool per minute for XPC, XPG, and XPA, respectively. Given that the concentrations of XPC (about three 10^4 molecules/cell), XPG (about eight 10^4 molecules/cell), and XPA (about two 10^5 molecules/cell) are different (Araújo et al., 2001), this tangent translates to assembly rates of ~900 molecules/min or ~15 molecules/s for XPC, XPG, and XPA. (B) Computation of the mean time to incision in the model versus the initial amount of DNA damage (6-4 PPs). The arrows indicate the amounts of damage estimated for the experimental setup with UV-permeable pores of 5- and 8-µm diameter.

Table S1. **Model assumptions**

Repair intermediate	Binding proteins	Catalyzed process required proteins	Remarks	References
Damaged DNA with helical distortion	XPC, TFIIH (3 states)	Partial unwinding (reaction α) XPC and TFIIH	Initiation by binding of XPC and subsequent recruitment of TFIIH	Evans et al., 1997; Rademakers et al., 2003; Riedl et al., 2003; Volker et al., 2001; Yokoi et al., 2000
Partially unwound DNA	XPC, TFIIH, XPG, XPA, ERCC1/XPF, RPA (48 states)	Full unwinding (reaction α') XPC, TFIIH, XPG, XPA, RPA	ERCC1/XPF only binds to repair complexes that contain XPA; if the DNA becomes devoid of any protein, it will reanneal to repair intermediate I (reaction ε_1)	Evans et al., 1997; Mu et al., 1997; Volker et al., 2001
Fully unwound DNA	XPC, TFIIH, XPG, XPA, XPF-ERCC1, RPA (48 states)	Dual incision (reaction β) TFIIH, XPG, XPA, ERCC1-XPF, RPA	If the DNA becomes devoid of any protein, it will reanneal (reaction ε_2); dual incision requires the endonucleases XPG and ERCC1-XPF and is stimulated by TFIIH, XPA, RPA, and possibly XPC	Evans et al., 1997; Winkler et al., 2001; O'Donovan et al., 1994; de Laat et al., 1998; Sijbers et al., 1996
Incised DNA	XPC, TFIIH, XPG, XPA, ERCC1/XPF, RPA, PCNA (96 states)	Repair synthesis (reaction γ) XPA, RPA, PCNA	PCNA binds to the free 3′-OH group generated by the ERCC1-XPF incision. DNA polymerase is also required (not measured)	Evans et al., 1997; Winkler et al., 2001
Resynthesized DNA	XPA, RPA, PCNA (9 states)	Rechromatinization (reaction δ) RPA, PCNA	Accumulation and FLIP data imply that XPA binds to repaired DNA, whereas the preincision proteins do not (Figs. 2 and 3)	Moser et al., 2007; Shivji et al., 1995; This study
Rechromatinized DNA	RPA, PCNA (4 states)	ND	RPA and PCNA associate with repair intermediate VI, as levels of bound EGFP-PCNA and EGFP-RPA are high up to at least 4 h after UV irradiation, whereas other repair proteins are no longer bound	Riedl et al., 2003; This study

References

Araújo, S.J., E.A. Nigg, and R.D. Wood. 2001. Strong functional interactions of TFIIH with XPC and XPG in human DNA nucleotide excision repair, without a preassembled repairosome. *Mol. Cell. Biol.* 21:2281–2291. doi:10.1128/MCB.21.7.2281-2291.2001

de Laat, W.L., E. Appeldoorn, K. Sugasawa, E. Weterings, N.G. Jaspers, and J.H. Hoeijmakers. 1998. DNA-binding polarity of human replication protein A positions nucleases in nucleotide excision repair. *Genes Dev.* 12:2598–2609. doi:10.1101/gad.12.16.2598

Evans, E., J.G. Moggs, J.R. Hwang, J.M. Egly, and R.D. Wood. 1997. Mechanism of open complex and dual incision formation by human nucleotide excision repair factors. *EMBO J.* 16:6559–6573. doi:10.1093/emboj/16.21.6559

Moser, J., H. Kool, I. Giakzidis, K. Caldecott, L.H. Mullenders, and M.I. Fousteri. 2007. Sealing of chromosomal DNA nicks during nucleotide excision repair requires XRCC1 and DNA ligase III alpha in a cell-cycle-specific manner. *Mol. Cell.* 27:311–323. doi:10.1016/j.molcel.2007.06.014

Mu, D., M. Wakasugi, D.S. Hsu, and A. Sancar. 1997. Characterization of reaction intermediates of human excision repair nuclease. *J. Biol. Chem.* 272:28971–28979. doi:10.1074/jbc.272.46.28971

O'Donovan, A., A.A. Davies, J.G. Moggs, S.C. West, and R.D. Wood. 1994. XPG endonuclease makes the 3′ incision in human DNA nucleotide excision repair. *Nature.* 371:432–435. doi:10.1038/371432a0

Perdiz, D., P. Grof, M. Mezzina, O. Nikaido, E. Moustacchi, and E. Sage. 2000. Distribution and repair of bipyrimidine photoproducts in solar UV-irradiated mammalian cells. Possible role of Dewar photoproducts in solar mutagenesis. *J. Biol. Chem.* 275:26732–26742.

Rademakers, S., M. Volker, D. Hoogstraten, A.L. Nigg, M.J. Moné, A.A. Van Zeeland, J.H. Hoeijmakers, A.B. Houtsmuller, and W. Vermeulen. 2003. Xeroderma pigmentosum group A protein loads as a separate factor onto DNA lesions. *Mol. Cell. Biol.* 23:5755–5767. doi:10.1128/MCB.23.16.5755-5767.2003

Riedl, T., F. Hanaoka, and J.M. Egly. 2003. The comings and goings of nucleotide excision repair factors on damaged DNA. *EMBO J.* 22:5293–5303. doi:10.1093/emboj/cdg489

Shivji, M.K., V.N. Podust, U. Hübscher, and R.D. Wood. 1995. Nucleotide excision repair DNA synthesis by DNA polymerase epsilon in the presence of PCNA, RFC, and RPA. *Biochemistry.* 34:5011–5017. doi:10.1021/bi00015a012

Sijbers, A.M., W.L. de Laat, R.R. Ariza, M. Biggerstaff, Y.F. Wei, J.G. Moggs, K.C. Carter, B.K. Shell, E. Evans, M.C. de Jong, et al. 1996. Xeroderma pigmentosum group F caused by a defect in a structure-specific DNA repair endonuclease. *Cell.* 86:811–822. doi:10.1016/S0092-8674(00)80155-5

Winkler, G.S., K. Sugasawa, A.P. Eker, W.L. de Laat, and J.H. Hoeijmakers. 2001. Novel functional interactions between nucleotide excision DNA repair proteins influencing the enzymatic activities of TFIIH, XPG, and ERCC1-XPF. *Biochemistry.* 40:160–165. doi:10.1021/bi002021b

Yokoi, M., C. Masutani, T. Maekawa, K. Sugasawa, Y. Ohkuma, and F. Hanaoka. 2000. The xeroderma pigmentosum group C protein complex XPC-HR23B plays an important role in the recruitment of transcription factor IIH to damaged DNA. *J. Biol. Chem.* 275:9870–9875. doi:10.1074/jbc.275.13.9870

Volker, M., M.J. Moné, P. Karmakar, A. van Hoffen, W. Schul, W. Vermeulen, J.H. Hoeijmakers, R. van Driel, A.A. van Zeeland, and L.H. Mullenders. 2001. Sequential assembly of the nucleotide excision repair factors in vivo. *Mol. Cell.* 8:213–224. doi:10.1016/S1097-2765(01)00281-7

Chapter 7

~

Influence on the live cell DNA marker DRAQ5 on chromatin-associated processes

DNA Repair (Amst) (2010), **9** (7)**:** 848-55

DNA Repair 9 (2010) 848–855

Contents lists available at ScienceDirect

DNA Repair

journal homepage: www.elsevier.com/locate/dnarepair

Brief report

Influence of the live cell DNA marker DRAQ5 on chromatin-associated processes

Pierre-Olivier Mari[a,b,c,1], Vincent Verbiest[a,1], Simone Sabbioneda[d], Audrey M. Gourdin[a], Nils Wijgers[a], Christoffel Dinant[a,2], Alan R. Lehmann[d], Wim Vermeulen[a,*], Giuseppina Giglia-Mari[a,b,c,**]

[a] Department of Genetics, Erasmus MC, Dr Molewaterplein 50, 3015 GE Rotterdam, The Netherlands
[b] CNRS, IPBS (Institut de Pharmacologie et de Biologie Structurale), 205 route de Narbonne, F-31077 Toulouse, France
[c] Université de Toulouse, UPS, IPBS, F-31077 Toulouse, France
[d] Genome Damage and Stability Centre, University of Sussex, Falmer, Brighton BN1 9RQ, UK

ARTICLE INFO

Article history:
Received 8 March 2010
Accepted 6 April 2010
Available online 2 May 2010

Keywords:
TFIIH
XPB
RPA
TLS polymerases
NER
PCNA
Histones

ABSTRACT

In the last decade, live cell fluorescence microscopy experiments have revolutionized cellular and molecular biology, enabling the localization of proteins within cellular compartments to be analysed and to determine kinetic parameters of enzymatic reactions in living nuclei to be measured. Recently, *in vivo* DNA labelling by DNA-stains such as DRAQ5, has provided the opportunity to measure kinetic reactions of GFP-fused proteins in targeted areas of the nucleus with different chromatin compaction levels. To verify the suitability of combining DRAQ5-staining with protein dynamic measurements, we have tested the cellular consequences of DRAQ5 DNA intercalation. We show that DRAQ5 intercalation rapidly modifies both the localization and the mobility properties of several DNA-binding proteins such as histones, DNA repair, replication and transcription factors, by stimulating a release of these proteins from their substrate. Most importantly, the effect of DRAQ5 on the mobility of essential cellular enzymes results in a potent inhibition of the corresponding cellular functions. From these observations, we suggest that great caution must be used when interpreting live cell data obtained using DRAQ5.

1. Introduction

Recently, tools have become available that allow the analysis of molecular mechanisms within living cells. Next to technical developments in microscopy these studies are mainly boosted by the availability of a still increasing set of fluorescent markers, including (genetic) tagging of proteins with green fluorescent protein (GFP) and its many spectral variants and fluorescent probes that target specific sub-cellular components or structures. These tools have enabled the study of *in vivo* cellular localization, dynamic behaviour and interactions of proteins with their partners [1–8]. Particularly, spatio-temporal dynamics studies on DNA-related processes, such as replication, transcription and DNA repair would be greatly aided by viable stains that would differentiate chromatin compaction, since regulation of these processes is tightly linked to chromatin condensation and DNA conformation [9]. The anthraquinone derivate DRAQ5 [10,11] has been recently introduced as a new way to label and visualize DNA and chromatin. This new DNA-probe possesses several advantages for visualizing DNA in living cells [12] compared to other DNA dyes such as 4′,6-diamidino-2-phenylindole (DAPI) and Hoechst 33258, mainly because its deep red $Ex_{\lambda\ max}/Em_{\lambda\ max}$ ($Ex_{\lambda\ max}$ 646 nm; $Em_{\lambda\ max}$ 681; $Em_{\lambda\ range}$ 665 → 800 nm) does not interfere with other fluorescent species used for tagging proteins and at the same time avoids the use of toxic UV irradiation as excitation source [13,14]. Additionally, DRAQ5 penetrates very quickly into the nucleus and stains the DNA stochiometrically without apparent severe cytotoxic effects [13,15]. Finally, DRAQ5 is not bleached under standard imaging conditions and is still clearly detectable 24 h after its addition to cells [12]. These properties make DRAQ5 a suitable DNA dye to be used in live cell imaging and could potentially be coupled to kinetic measurements of cellular activities. However, because DRAQ5 intercalates into the DNA-helix and thereby possibly distorts the helical structure of it, we have investigated the effect of DRAQ5 on DNA/chromatin bound proteins and nuclear processes. Our study shows that DRAQ5 alters the chromatin structure and influences the interaction of a large spectrum of DNA-binding proteins, leading to inhibition of different DNA-dependent processes such as transcription, replication and nucleotide excision repair (NER).

* Corresponding author.
Tel.: +31 10 70 43 194; fax: +31 10 70 44 468.
** Corresponding author at: CNRS, IPBS (Institut de Pharmacologie et de Biologie Structurale), 205 route de Narbonne, F-31077 Toulouse, France.
Tel.: +33 5 61 17 58 54; fax: +33 5 61 17 59 94.
E-mail addresses: w.vermeulen@erasmusmc.nl (W. Vermeulen), ambra.mari@ipbs.fr (G. Giglia-Mari).
[1] These authors contributed equally.
[2] Present address: Institute of Cancer Biology and Centre for Genotoxic Stress Research, Danish Cancer Society, Strandboulevarden 49, DK-2100 Copenhagen, Denmark.

1568-7864/$ – see front matter © 2010 Elsevier B.V. All rights reserved.
doi:10.1016/j.dnarep.2010.04.001

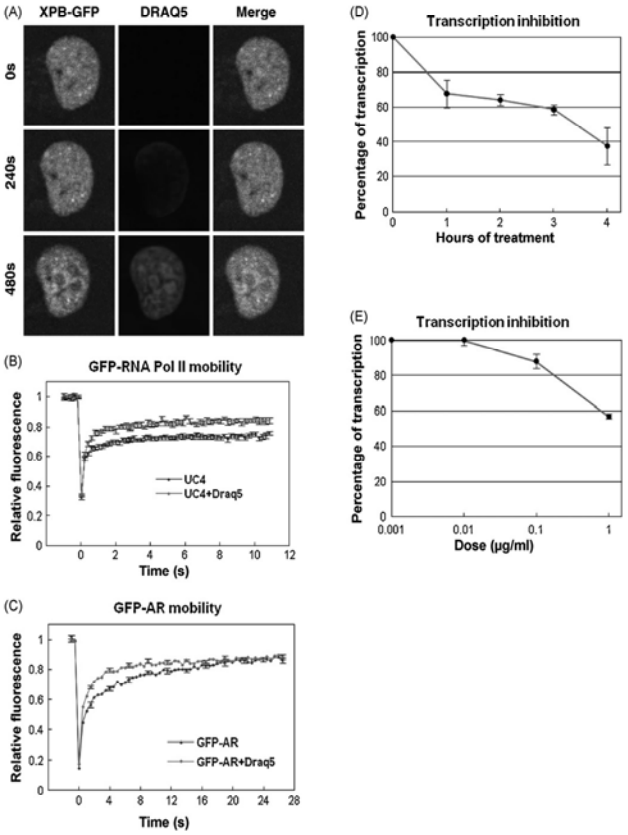

Fig. 1. DRAQ5 DNA intercalation inhibits transcription. (A) Confocal imaging of XPB-GFP expressing fibroblasts after DRAQ5 treatment. Localization of XPB (GFP signal in green) is altered when DRAQ5 (red) is intercalated into the DNA. (B) FRAP analysis of GFP-RNA Pol II in the nucleus of cells incubated (red filled squares) or not (empty blue circle) with DRAQ5 for 1 h. (C) FRAP analysis of GFP-AR in the nucleus of cells incubated (red filled squares) or not (empty blue circle) with DRAQ5 for 1 h. (D) MRC5SV40 transformed human fibroblasts treated with DRAQ5 (5 μM) for different times. Transcription is detected by [^{3}H]uridine incorporation as described in Section 4. (E) Transcription inhibition assay. MRC5SV40 transformed human fibroblasts treated with three different concentrations of DRAQ5 for 3 h. Transcription is detected by [^{3}H]uridine incorporation as described in Section 4.

2. Results and discussion

2.1. Effect of DRAQ5 DNA intercalation on transcription

We tested the effect of DRAQ5 DNA intercalation on cellular transcription by studying differences in localization and/or mobility of the basal transcription factor, TFIIH [16], RNA polymerase II [17] and a specific transcription activator, the androgen receptor [18].

TFIIH is a heterodecameric complex involved in both transcription and nucleotide excision repair. Mutations in some of the subunits can give rise to the genetic disorder xeroderma pigmentosum (XP) and related conditions. TFIIH dynamically interacts with both RNA polymerases I (RNAPI) and II (RNAPII) transcription sites and its dynamic properties as well as its sub-nuclear distribution are greatly influenced by transcription interfering molecules [16]. To investigate whether DRAQ5 has an effect on the interaction of TFIIH with DNA, we used a cell line that stably expresses a biological functional GFP-tagged XPB protein [16] (details on cell line used and expression are in M & M's or simply referred). XPB encodes the largest subunit of the transcription/DNA repair complex TFIIH.

Imaging of untreated cells showed that XPB-GFP is homogenously distributed in the nuclear compartment [16,19]. However, rapidly after treatment with DRAQ5, the sub-cellular localization of TFIIH is substantially changed (Fig. 1A): as DRAQ5 DNA intercalation progressed, TFIIH became more heterogeneously distributed and progressively excluded from the nucleoli.

This result prompted us to test whether this change in localization of a transcription initiation factor would affect the kinetic behaviour of elongation factors as well. Therefore, we

performed photo-bleaching experiments on cells expressing a fluorescent alpha-amanitin resistant form of the largest subunit (RPB1) of RNAPII (GFP-RPB1$^{\alpha\text{-amaR}}$) [20,21] (UC4 in Fig. 1B). This alpha-amanitin resistant fluorescent form was expressed in cells which expressed also the endogenous non-fluorescent alpha-amanitin sensitive RNAPII, however, when exposed to alpha-amanitin, cells expressing these two forms will exclusively use the transcriptionally active fluorescent alpha-amanitin resistant form. Human SV40-immortalised fibroblasts (MRC5SV) were first transfected with GFP-RPB1$^{\alpha\text{-amaR}}$ and selected with 20 μg/ml of alpha-amanitin for 16 h prior to FRAP (fluorescence recovery after photo-bleaching) experiments. As previously shown [17], two distinct kinetic populations of RNAPII exist: a free pool diffusing in the nucleus and a second pool (approx 30% of the population) that is immobile and represents RNAPII engaged in transcription (Fig. 1B). FRAP measurements, performed 1 h after treatment with DRAQ5, show a marked reduction of the RNAPII immobile fraction (Fig. 1B). The release of the polymerase is comparable to the one observed with another potent transcription inhibitor, 5,6-dichloro-1-β-D-ribofuranosylbenzimidazole (DRB) [17,22], and suggests that the intercalation of DRAQ5 in DNA disrupts the interaction of RNAPII with transcribed genes.

To further investigate the effect of DRAQ5 on specific DNA-binding proteins involved in transcription, we measured the effect of DRAQ5 intercalation on a specific transcription activator, the androgen receptor (AR). A fluorescent form of this transcription factor was previously described [23] and shown to bind Hormone Response Elements sequences [18] after addition of steroid hormones in a transcription-dependent fashion. A stable cell line expressing GFP-AR [18] was cultured in the presence of steroid hormones and the mobility of the fluorescent transcription factor was monitored by FRAP with and without exposure to DRAQ5 (Fig. 1C). After 1 h of treatment with DRAQ5, we measured a clear increase in the speed of fluorescence recovery, compatible with a strong reduction of the GFP-AR binding pool (Fig. 1C, red curve). To verify that the reduced binding of these different transcription factors is a specific effect of DRAQ5 on DNA-binding proteins, we measured the mobility of free GFP as a protein that does not show any DNA-binding capability. As expected, GFP mobility is not altered after incubation with DRAQ5 (Figure S1A), supporting the idea that DRAQ5 mainly affects the mobility of chromatin-associated proteins implicated in transcription such as AR and RNAPII and suggests that DRAQ5 interferes with binding of these factors to their DNA substrates.

The impact of DRAQ5 on transcription factor localization and dynamic behaviour suggests that this DNA dye could interfere with normal transcription. We therefore investigated the transcription capacity in human transformed fibroblasts by determining the incorporation of [^{3}H]uridine in cells incubated with 1 μM DRAQ5 (recommended dose by the manufacturer for live cell imaging) and mock treated cells. Already after 1 h of treatment, transcriptional activity dropped below 70% (Fig. 1D), declining to 40% after 4 h of DRAQ5 incubation. Under these conditions, DRAQ5 is a more potent transcription inhibitor than alpha-amanitin (data not shown), which is one of the most common drugs used to inhibit RNAPII transcription. Surprisingly, even at a concentration of DRAQ5 tenfold lower than recommended by the manufacturer we observed a slight but consistent inhibition of the transcriptional activity (Fig. 1E). Taken together, these data suggest that labelling DNA with DRAQ5 inhibits transcription, most likely by releasing the transcriptional machinery from its template.

2.2. Effect of DRAQ5 on DNA replication

In view of the inhibitory effect of DRAQ5 on transcription, we wondered whether other cellular functions involving DNA-binding activity, such as DNA replication and DNA repair, could also be affected by DRAQ5 DNA intercalation. To investigate the effect of DRAQ5 on DNA replication, we analysed the localization and mobility of the Proliferating Cell Nuclear Antigen (PCNA; a processivity factor for DNA polymerase) after DRAQ5 intercalation. For this purpose we used a CHO9 cell line stably expressing a GFP-tagged PCNA (GFP-PCNA) [24] was treated with DRAQ5. Within untreated cells, we observed the PCNA focal distributions characteristic of early-, mid-, and late-S-phase replication sites [24]. However, time-lapse confocal imaging revealed that during DRAQ5 intake PCNA foci progressively faded and the localization of GFP-PCNA became more diffuse (Fig. 2A). Once DRAQ5 was fully incorporated into the cells (Fig. 2B, white arrows, 10 min time point), most of the replication foci were no longer discernable suggesting that PCNA is released from the replication foci.

To verify that, after DRAQ5 intercalation, PCNA has a reduced binding capacity to DNA, we measured the mobility of this factor in presence of DRAQ5. We bleached half the nucleus of replicative GFP-PCNA expressing cells and monitored the recovery of fluorescence in the bleached area (half-nucleus FRAP: HN-FRAP) (Fig. 2B, bottom row). In order to perform the experiment exclusively in S-phase cells even in the presence of DRAQ5, we marked the position of cells with replication foci prior the treatment with the DNA dye (Fig. 2B, white arrows). The HN-FRAP data obtained before and 10 min after treatment indicates that DRAQ5 DNA intercalation increases the mobility of GFP-PCNA (Fig. 2C), probably by interfering with the stable formation of PCNA ring-structures on replication forks.

Akin to our approach of the transcription reaction, we hypothesized that impeded binding of essential replication factors to their substrate would influence their normal functioning. We therefore tested the effect of DRAQ5 on DNA replication by determining the DNA synthesis both in the presence and absence of DRAQ5 by measuring the incorporation of ^{3}H-thymidine using autoradiography (Fig. 2D). In untreated cells, we could clearly identify cells undergoing replication and distinguish early- from late-S-phase cells (Fig. 2D, arrows 1 and 2 respectively). Conversely, replication was severely inhibited under DRAQ5 treatment since no DNA synthesis could be detected (absence of autoradiographic grains). These data demonstrate that intercalation of DRAQ5 in DNA inhibits not only transcription but also replication by preventing the loading of proteins onto DNA and/or by reducing the DNA-binding affinity of proteins engaged in replication.

2.3. Effect of DRAQ5 on DNA repair

We have observed striking effects of DRAQ5 on both transcription and replication. The fact that both TFIIH and PCNA also play a central role in nucleotide excision repair (NER), raised the question of whether DRAQ5 could have an effect on DNA repair activity. NER, is a versatile multi-protein DNA repair mechanism able to remove a large variety of DNA lesions, including UV-induced DNA lesions. We examined the mobility of one of the NER initiating factors: the xeroderma pigmentosum group C protein (XPC). XPC is involved in the recognition of a wide range of DNA-helix distorting lesions [25] by its increased affinity for these injuries. In addition, XPC has a high affinity for undamaged DNA, as is apparent from its remarkably slow mobility caused by a continuous binding and dissociation from DNA, even in the absence of UV-induced DNA lesions [26]. After DRAQ5 treatment, FRAP measurements on XPC-GFP revealed a faster and more complete recovery of fluorescence (Fig. 3A). This increase in XPC mobility probably results from a reduced DNA-binding affinity of XPC for DRAQ5 containing DNA. After recognition of UV-induced DNA lesions, the basal transcription/repair factor TFIIH loads at the site of the damage to unwind the DNA-helix containing the UV-lesion. TFIIH assembly

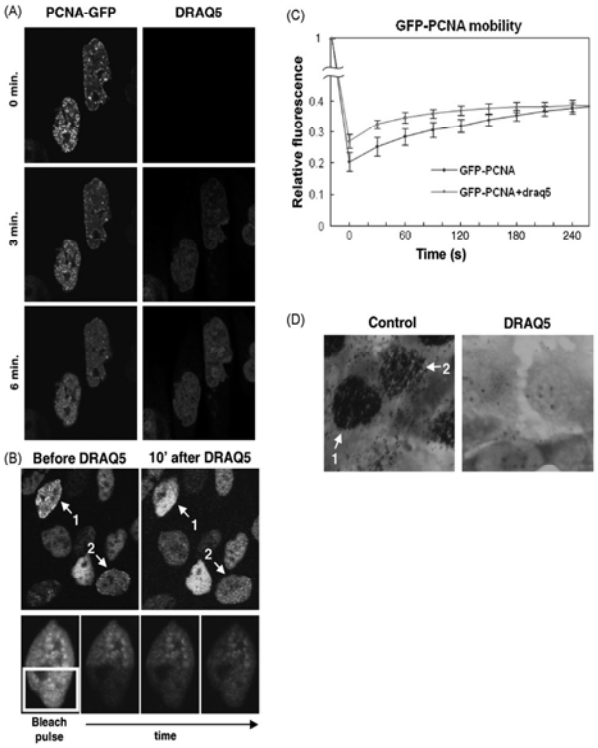

Fig. 2. Intercalation of DRAQ5 in DNA modifies localization and dynamics of GFP-PCNA and inhibits DNA synthesis. (A) Time-lapse confocal imaging of PCNA-GFP expressing cells during DRAQ5 intercalation. PCNA-GFP (green) and DRAQ5 (red). (B) Scheme of the half-nucleus FRAP procedure. Prior to DRAQ5 treatment, position of S-phase cells was marked (arrows). 10 min after DRAQ5 incubation, half the nucleus of S-phase cells was bleached and recovery of fluorescence was monitored in the bleached area. (C) Half-nucleus FRAP analysis of PCNA-GFP of untreated cells (empty blue circle) compared with cells incubated with DRAQ5 for 10 min. (D) DNA synthesis measure by autoradiography of cells incubated with 1 μM of DRAQ5 for 1 h or not (control) and subsequently pulse-labelled for 3 h with [^{3}H-1′,2′]-thymidine.

during NER can be visualized by the accumulation of this factor in an area of locally damaged DNA [27]. To determine whether DRAQ5 might have an effect on the binding capacity of TFIIH to DNA lesion bound NER-complexes, the disassembly kinetics of XPB-GFP (one of the ten TFIIH components) from locally UV-induced DNA damage was monitored in living cells. XPB-GFP expressing cells were locally irradiated with a UVC lamp through a porous filter [28] in the absence of DRAQ5, to allow accumulation of XPC and TFIIH at the locally damaged areas. Shortly after local damage induction, we started to monitor the progressive disappearance of the locally accumulated XPB-GFP by time-lapse imaging. In untreated cells, XPB-GFP accumulation at the locally damaged area diminished during the first hour after irradiation, due to the ongoing repair process with its corresponding decline in total number of DNA lesions (Fig. 3B, blue curve). However, XPB-GFP accumulation in locally damaged areas diminished more quickly in the presence of DRAQ5 (Fig. 3B), demonstrating that XPB is delocalized from the repair reaction when DRAQ5 intercalates in the DNA.

To determine the effect of DRAQ5 on the repair activity of cells, we quantified the DNA repair synthesis (or unscheduled DNA synthesis; UDS) in UV-irradiated wild-type (NER-proficient) human fibroblasts (MRC5SV) by ^{3}H-thymidine labelling. Labelled nucleotides, incorporated during the repair synthesis step of NER, were visualized by autoradiography as dispersed small grains above cell nuclei (Fig. 3C, arrow head). After 1 h of incubation with DRAQ5, an almost complete absence of autoradiographic grains was observed, indicating a dramatic reduction in repair synthesis, hence that DNA repair is severely affected by DRAQ5.

2.4. Effect of DRAQ5 on nuclear organization and DNA structure

Among the different DNA dyes available, it has been shown that DRAQ5 presents the best co-localization with the histone H2B [12], thus positioning it as a valid indicator of chromatin density in living cells. However, in view of our findings on the effect of DRAQ5 DNA intercalation on chromatin/DNA interacting proteins and in view of previous work showing that DRAQ5 can have a deleterious effect on higher order chromatin structure [29], we decided to examine *in vivo* both the localization and binding kinetics of the core histone H2A (labelled with GFP), in response to DRAQ5 exposure. Similarly

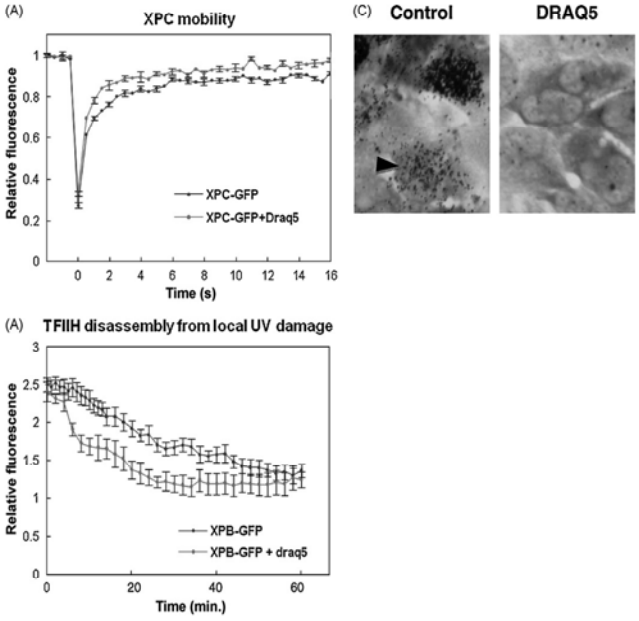

Fig. 3. Intercalation of DRAQ5 in DNA alters the mobility of proteins involved in NER and the efficiency of repair.
(A) FRAP analysis on the nucleus of XPC-GFP expressing cells incubated (red filled squares) or not (empty blue circle) with DRAQ5 for 1 h. (B) Disassembly rate of XPB-GFP from the local damage. Curves correspond to the ratio of the fluorescence intensity in the damaged area and the rest of the nucleus. Results present the average of ten analysed cells. (C) Unscheduled DNA synthesis measured by autoradiography of cells globally irradiated with 16 J/m^2 of UVC and incubated for 1 h with (DRAQ5) or without (control). Cells were pulse-labelled for 3 h with [^{3}H-1′,2′]-thymidine, fixed and developed as described in Section 4.

to H2B-GFP [12], GFP-H2A dense regions co-localized with high DRAQ5 concentrations (supplementary Figures S1B and S1C). However, using a previously described square-FRAP method [30] we observed an acceleration in the exchange kinetics of GFP-H2A after DRAQ5 treatment (Fig. 4A and B). Approximately 15% of the GFP-H2A signal was recovered 2 min after photo-bleaching, whereas practically no recovery was seen in untreated cells within this time scale (Fig. 4B). This result shows that the slow apparent mobility resulting from the tight association of GFP-H2A to chromatin is altered when cells are exposed to DRAQ5, suggesting that DRAQ5 DNA intercalation affects the normal histone dynamics and may alter the structure of the chromatin.

The mobility analysis of proteins involved in different nuclear processes described above indicates that labelling of DNA by DRAQ5 mostly leads to a reduced binding of these proteins to DNA. Surprisingly, the opposite effect was observed when we analysed another DNA-binding protein, the DNA polymerase Delta (Pol δ) [31]. FRAP measurements were performed in non-S-phase cells expressing a GFP-tagged version of the p66 subunit of this replicative polymerase (S-phase cells display typical replicative focal distributions of the protein). In non-treated cells, the non-engaged Pol δ shows a fast recovery in the bleached area (Fig. 4C, blue). However, the mobility of GFP-Pol δ is drastically decreased in cells incubated with DRAQ5 as seen by the higher (40%) immobile fraction (Fig. 4C, red). These data suggest that modifications in the DNA structure after DRAQ5 intercalation increase the binding affinity of Pol δ for DNA. Because DNA polymerases have a strong affinity for single-stranded DNA, we tested whether DRAQ5 could locally unwind double-stranded DNA by studying the mobility of the Replication Protein A (RPA) in undamaged DNA after exposure to DRAQ5. RPA is a single strand DNA-binding protein that protects single-stranded stretches from nucleases and prevents hairpin formation during replication, repair and recombination [32–34]. Strip-FRAP experiments performed (in presence or absence of DRAQ5) within the nucleus of cells expressing a GFP-tagged version of RPA show that the mobility of the fluorescent protein remains unchanged (Figure S1D), indicating that intercalation of DRAQ5 does not generate single-stranded stretches of DNA.

2.5. DNA labelling by DRAQ5 does not activate the cellular stress response

Since DRAQ5 modifies the DNA-binding activity of a number of proteins, most likely via a structural change of the DNA macromolecule, which in turn may also affect chromatin integrity, we explored the potential of this DNA dye to trigger the genotoxic stress response. Because most types of DNA damage activate the kinases ATM and ATR [35,36] and subsequently phosphorylate their effectors Chk1 and Chk2 [36] that regulate cell cycle progression, we tested whether DRAQ5 intercalation would induce checkpoint phosphorylation. In contrast to the UV-induced Chk1 phosphorylation (Fig. 4D), incubation with DRAQ5 did not induce Chk1 and Chk2 phosphorylation (Fig. 4D).

In addition, the specific damage-induced PCNA ubiquitination at lysine 164 [37] was also tested. This post-translational modification of PCNA is involved in translesion synthesis (TLS) by facilitating the

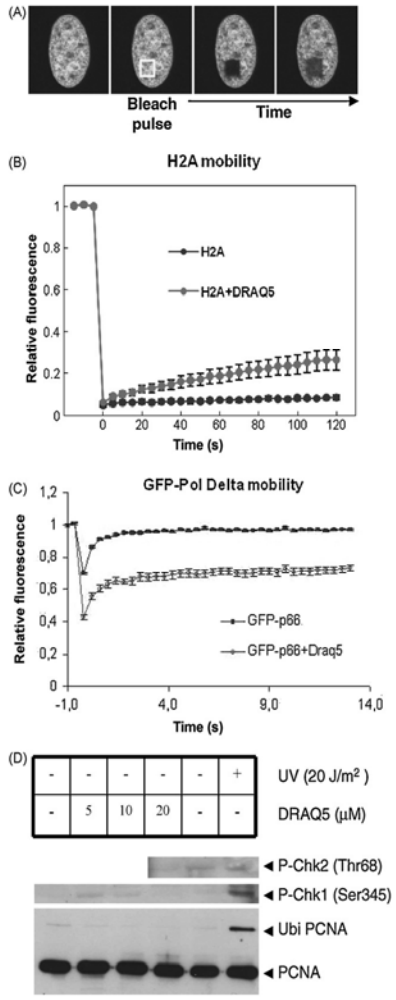

Fig. 4. Effects of DRAQ5 on nuclear organization and DNA structure. (A) Scheme of the square-FRAP procedure. (B) Square-FRAP graph presenting the mobility of GFP-H2A measured in cells incubated (red) or not (blue) with DRAQ5 for 10 min. (C) FRAP analysis of GFP-Pol Delta in the nucleus of cells presenting no focal accumulation and incubated (red) or not (blue) with DRAQ5 for 20 min. (D) Analysis of cellular response to DNA labelling by DRAQ5. MRC5V1 cells were treated with the indicated DRAQ5 concentration for 20 min or irradiated 30 J/m^2 UV and incubated for 6 h. PCNA ubiquitination and Chk phosphorylation were analysed by western blotting using αPCNA (PC10, CRUK), αP-Chk1 (Ser345) and αP-Chk2 (Thr68).

switch of DNA polymerases at blocked replication sites [37]. While after UVC irradiation, we detected this damage-specific PCNA ubiquitination (Fig. 4D), we did not detect monoubiquitination of PCNA after incubation of cells with DRAQ5 (Fig. 4D). Taken together, these data indicate that, unlike another study reports [38], intercalation of DRAQ5 into the DNA does not activate cellular stress responses, even though DRAQ5 alters the structure of the DNA molecule and possibly its organization in the nucleus.

3. Conclusion

The DNA intercalating molecule DRAQ5 is shown to be a highly useful molecule to stain DNA in living cells. The far-red fluorescence that can be emitted during intercalation with the DNA allows simultaneous analysis of GFP-fused proteins, permitting the co-visualization of DNA and proteins in the same live cell. Previous studies suggested that DRAQ5 treatment did not induce cellular toxicity [12], suggesting that it could be used in studying the mobility of DNA-binding proteins in different chromatin domains (dense *versus* decondensed areas). However, using time-lapse imaging and live cell photo-bleaching techniques we have revealed that DRAQ5 intercalation interferes with both the localization and the mobility of DNA-binding proteins, such as histones, polymerases, repair proteins and transcription factors, while non-DNA-binding factors, such as non-fused GFP, are not affected. Without causing DNA damage signalling, and without unwinding the double-helix, DRAQ5 may likely modify the structure of chromatin, resulting in a generally reduced binding of several DNA-binding proteins. One exception we found is the DNA polymerase Delta (this study and [39]), which on the contrary became tightly bound to the DRAQ5 DNA substrate. However, this substrate is not an open fork since no single-stranded DNA stretches could be detected. More generally, we have shown that DRAQ5 induced changes in localization and DNA-binding capacity of DNA-binding proteins and concomitantly affects cellular functions as transcription, DNA replication and DNA repair.

4. Materials and methods

4.1. Cell lines and specific treatments

Human wild-type SV40 transformed fibroblasts (MRC5SV), and NER-deficient SV40 transformed fibroblasts stably expressing XPB-GFP [16,26] or XPC-GFP were cultured in DMEM-F10 supplemented with 10% serum and 1% antibiotics. Chinese Hamster Ovary (CHO9) cells stably expressing PCNA-GFP or non-fused GFP [24] were cultured in DMEM supplemented with 10% serum and 1% antibiotics. The human hepatoma Hep3B cell line stably expressing GFP-AR [18] was cultured in α-MEM supplemented with antibiotics and 5% serum. All cells were cultured under standard conditions at 37 °C in 5% CO_2. Cell lines stably expressing GFP-RPB1$^{\alpha\text{-amaR}}$ was generated by transfection of MRC5SV with 1 μg of pAT7h1$^{\alpha\text{-amaR}}$ [40] using FuGEN6 (Roche Diagnostics, Mannheim, Germany). One day after transfection, cells expressing GFP-RPB1$^{\alpha\text{-amaR}}$ were selected by overnight incubation with 20 μg/ml of alpha-amanitin. Two stable cell lines expressing respectively eGFP-tagged p66 [31] and eGFP-tagged RPA_{70}, resulting from the cloning of the human RPA70 subunit in peGFP-N1 (clonetech), were established by transfecting the DNA's coding for the chimeric proteins in MRC5SV. Stable clones were selected after 2 weeks of culture in medium containing G418 (1.2 mg/ml) and screened for the presence of eGFP expression. The presence of free GFP was excluded for each cell line by western blot analysis. eGFP-p66 in the stable cell line had the expected nuclear localization [31]. Functionality of eGFP-p66 was confirmed by its ability to immunoprecipitate endogenous p125, the major

subunit of Pol δ (data not shown). Except where otherwise indicated, DRAQ5 (Biostatus) was always diluted directly in the culture medium at 1 μM as recommended by the manufacturer.

4.2. Imaging and FRAP analysis on confocal microscopy

For each FRAP experiment, cells were seeded onto 24-mm-diameter coverslips 2 days before analysis. Imaging and FRAP were performed on a Zeiss LSM 510 meta confocal laser scanning microscope (Zeiss, Oberkochen, Germany) with a argon laser (458, 477, 488, 514 nm) GFP and a HeNe to excite respectively GFP and DRAQ5. Strip-FRAP analysis was performed at high time resolution. Briefly, a strip spanning the nucleus was photo-bleached for 20 ms at 100% laser intensity (laser current set at 6.1 A). Recovery of fluorescence in the strip was monitored either every 100 ms or every 200 ms for different time laps at 0.5% of laser intensity. Average values from 10 independent measurements were used for every mobility curve. Mobility curves are plotted as relative fluorescence (fluorescence post-bleach divided by fluorescence pre-bleach) measured against time. For square and half-nucleus FRAP analysis, a region corresponding to a square in the nucleus or half the nucleus was bleached and recovery of fluorescence was monitored by imaging the entire nucleus every 5 s for 2 min in the case of square FRAP and every 30 s for 7 min in the case of half-nucleus FRAP. For local damage induction cells were grown on coverslips 2 days before treatment, washed with PBS, covered with a polycarbonate filter (5 μm pore size; Millipore), irradiated with 60 J/m^2 (overall dose) and incubated in standard growth medium for 10 min. Disassembly of the complex from the locally damaged areas was measured by imaging every minute for 14 min and then every 2 min for 46 min and was quantified as the ratio of the fluorescence intensity in the damaged area and the rest of the nucleus. Curves present the average of 10 analysed cells.

4.3. RNA synthesis assay

Before [^{3}H]uridine incorporation, exponentially growing cells were prelabelled with [^{14}C]thymidine (0.02 μCi/ml; spec. act. 56 mCi/mmol; Amersham) for a day to uniformly label the DNA. RNA synthesis was measured after pulse-labelling with [^{3}H]uridine (10 μCi/ml; specific activity, 50 Ci/mmol, Amersham) as previously described [41]. Cells were cultured for different times with 1 μM DRAQ5 or with different concentrations of DRAQ5 for 1 h.

4.4. DNA synthesis assay

Cellular replication activity was detected by incubation for 3 h in medium containing 10 μCi/MI [^{3}H-1′,2′]-thymidine (120 Ci/mmol; Amersham). For global genome NER activity, unscheduled DNA synthesis [42] was measured by exposure of cells to 16 J/m^2 of UV light and subsequent incubation in the same medium as described above [42]. Cells were fixed, coverslips were dipped in Ilford K2 photographic emulsion, and slides were developed after 3 days of exposure and were stained with Giemsa. Nuclear silver grains were counted in 50 cells.

4.5. Western blots

MRC5V1 cells were treated with the indicated DRAQ5 concentration for 20 min. Cells irradiated with 20 J/m^2 UV and incubated for 6 h were used as positive control for PCNA ubiquitination and Chk1 activation. Extract were run on a 10% SDS-PAGE gel, transferred, blocked in 5% milk and probed respectively with αPCNA (PC10, CRUK), αP-Chk1 (Ser345) and αP-Chk2 (Thr68) (Cell Signalling).

Conflict of interest statement

Authors have no conflict of interest.

Acknowledgments

We thank Drs. A.B. Houtsmuller and W.A. van Cappellen (applied Optical Image Center, Erasmus MC, Rotterdam) for providing the confocal live cell-imaging facility, Dr. Houtsmuller for providing the GFP-AR expressing cell line and Cornelia Poitelea for assistance in the analysis of the cell line expressing GFP-p66. This work was supported by an Erasmus University fellowship, an Association for International Cancer Research (grant nr: 07-0129), ZonMW (Dutch Science Organisation for Medical Sciences grant nr: 917-46-364) the ESF Eurodyna program, the UK Medical Research Council, and EU FP6 grants, Research Training Network integrated project on DNA Repair (grants MRTN-CT-2003-503618 and LSHG-CT-2005-512113), the Centre national de la Recherche Scientifique (CNRS contract nr. 039438) and the Institut National du Cancer (InCa contract nr: 2009-001).

Sponsors had no involvement in study design; collection, analysis and interpretation of data; the writing of the manuscript; the decision to submit the manuscript for publication.

Appendix A. Supplementary data

Supplementary data associated with this article can be found, in the online version, at doi:10.1016/j.dnarep.2010.04.001.

References

[1] P.A. Bubulya, D.L. Spector, "On the move" ments of nuclear components in living cells, Exp. Cell Res. 296 (1) (2004) 4–11.
[2] K.A. Giuliano, D.L. Taylor, Measurement and manipulation of cytoskeletal dynamics in living cells, Curr. Opin. Cell Biol. 7 (1) (1995) 4–12.
[3] A.B. Houtsmuller, W. Vermeulen, Macromolecular dynamics in living cell nuclei revealed by fluorescence redistribution after photobleaching, Histochem. Cell Biol. 115 (1) (2001) 13–21.
[4] E.A. Jares-Erijman, T.M. Jovin, Imaging molecular interactions in living cells by FRET microscopy, Curr. Opin. Chem. Biol. 10 (5) (2006) 409–416.
[5] J. Lippincott-Schwartz, G.H. Patterson, Development and use of fluorescent protein markers in living cells, Science 300 (5616) (2003) 87–91.
[6] E.A. Reits, J.J. Neefjes, From fixed to FRAP: measuring protein mobility and activity in living cells, Nat. Cell Biol. 3 (6) (2001) E145–E147.
[7] Y. Shav-Tal, R.H. Singer, X. Darzacq, Imaging gene expression in single living cells, Nat. Rev. Mol. Cell Biol. 5 (10) (2004) 855–861.
[8] D. Zink, T. Cremer, Cell nucleus: chromosome dynamics in nuclei of living cells, Curr. Biol. 8 (9) (1998) R321–R324.
[9] A.E. Ehrenhofer-Murray, Chromatin dynamics at DNA replication, transcription and repair, Eur. J. Biochem. 271 (12) (2004) 2335–2349.
[10] P.J. Smith, N. Blunt, M. Wiltshire, T. Hoy, P. Teesdale-Spittle, M.R. Craven, J.V. Watson, W.B. Amos, R.J. Errington, L.H. Patterson, Characteristics of a novel deep red/infrared fluorescent cell-permeant DNA probe, DRAQ5, in intact human cells analyzed by flow cytometry, confocal and multiphoton microscopy, Cytometry 40 (4) (2000) 280–291.
[11] P.J. Smith, M. Wiltshire, S. Davies, L.H. Patterson, T. Hoy, A novel cell permeant and far red-fluorescing DNA probe, DRAQ5, for blood cell discrimination by flow cytometry, J. Immunol. Methods 229 (1–2) (1999) 131–139.
[12] R.M. Martin, H. Leonhardt, M.C. Cardoso, DNA labeling in living cells, Cytometry A 67 (1) (2005) 45–52.
[13] S.K. Davis, C.J. Bardeen, Cross-linking of histone proteins to DNA by UV illumination of chromatin stained with Hoechst 33342, Photochem. Photobiol. 77 (6) (2003) 675–679.
[14] R.E. Durand, P.L. Olive, Cytotoxicity, mutagenicity and DNA damage by Hoechst 33342, J. Histochem. Cytochem. 30 (2) (1982) 111–116.
[15] R. Edward, Use of DNA-specific anthraquinone dyes to directly reveal cytoplasmic and nuclear boundaries in live and fixed cells, Mol. Cells 27 (4) (2009) 391–396.
[16] D. Hoogstraten, A.L. Nigg, H. Heath, L.H. Mullenders, R. van Driel, J.H. Hoeijmakers, W. Vermeulen, A.B. Houtsmuller, Rapid switching of TFIIH between RNA polymerase I and II transcription and DNA repair in vivo, Mol. Cells 10 (5) (2002) 1163–1174.
[17] H. Kimura, K. Sugaya, P.R. Cook, The transcription cycle of RNA polymerase II in living cells, J. Cell Biol. 159 (5) (2002) 777–782.

[18] P. Farla, R. Hersmus, J. Trapman, A.B. Houtsmuller, Antiandrogens prevent stable DNA-binding of the androgen receptor, J. Cell Sci. 118 (Pt 18) (2005) 4187–4198.
[19] S. Iben, H. Tschochner, M. Bier, D. Hoogstraten, P. Hozak, J.M. Egly, I. Grummt, TFIIH plays an essential role in RNA polymerase I transcription, Cell 109 (3) (2002) 297–306.
[20] M.S. Bartolomei, J.L. Corden, Localization of an alpha-amanitin resistance mutation in the gene encoding the largest subunit of mouse RNA polymerase II, Mol. Cell. Biol. 7 (2) (1987) 586–594.
[21] K. Sugaya, M. Vigneron, P.R. Cook, Mammalian cell lines expressing functional RNA polymerase II tagged with the green fluorescent protein, J. Cell Sci. 113 (Pt 15) (2000) 2679–2683.
[22] M. Hieda, H. Winstanley, P. Maini, F.J. Iborra, P.R. Cook, Different populations of RNA polymerase II in living mammalian cells, Chromosome Res. 13 (2) (2005) 135–144.
[23] V. Georget, J.M. Lobaccaro, B. Terouanne, P. Mangeat, J.C. Nicolas, C. Sultan, Trafficking of the androgen receptor in living cells with fused green fluorescent protein-androgen receptor, Mol. Cell. Endocrinol. 129 (1) (1997) 17–26.
[24] J. Essers, A.F. Theil, C. Baldeyron, W.A. van Cappellen, A.B. Houtsmuller, R. Kanaar, W. Vermeulen, Nuclear dynamics of PCNA in DNA replication and repair, Mol. Cell. Biol. 25 (21) (2005) 9350–9359.
[25] K. Sugasawa, J.M. Ng, C. Masutani, S. Iwai, P.J. van der Spek, A.P. Eker, F. Hanaoka, D. Bootsma, J.H. Hoeijmakers, Xeroderma pigmentosum group C protein complex is the initiator of global genome nucleotide excision repair, Mol. Cell 2 (2) (1998) 223–232.
[26] D. Hoogstraten, S. Bergink, J.M. Ng, V.H. Verbiest, M.S. Luijsterburg, B. Geverts, A. Raams, C. Dinant, J.H. Hoeijmakers, W. Vermeulen, et al., Versatile DNA damage detection by the global genome nucleotide excision repair protein XPC, J. Cell Sci. 121 (Pt 17) (2008) 2850–2859.
[27] M. Volker, M.J. Mone, P. Karmakar, A. van Hoffen, W. Schul, W. Vermeulen, J.H. Hoeijmakers, R. van Driel, A.A. van Zeeland, L.H. Mullenders, Sequential assembly of the nucleotide excision repair factors in vivo, Mol. Cell 8 (1) (2001) 213–224.
[28] M.J. Mone, M. Volker, O. Nikaido, L.H. Mullenders, A.A. van Zeeland, P.J. Verschure, E.M. Manders, R. van Driel, Local UV-induced DNA damage in cell nuclei results in local transcription inhibition, EMBO Rep. 2 (11) (2001) 1013–1017.
[29] K. Wojcik, J.W. Dobrucki, Interaction of a DNA intercalator DRAQ5, and a minor groove binder SYTO17, with chromatin in live cells—influence on chromatin organization and histone–DNA interactions, Cytometry A 73 (6) (2008) 555–562.
[30] T. Higashi, S. Matsunaga, K. Isobe, A. Morimoto, T. Shimada, S. Kataoka, W. Watanabe, S. Uchiyama, K. Itoh, K. Fukui, Histone H2A mobility is regulated by its tails and acetylation of core histone tails, Biochem. Biophys. Res. Commun. 357 (3) (2007) 627–632.
[31] J.R. Pohler, M. Otterlei, E. Warbrick, An in vivo analysis of the localisation and interactions of human p66 DNA polymerase delta subunit, BMC Mol. Biol. 6 (2005) 17.
[32] C. Braet, H. Stephan, I.M. Dobbie, D.M. Togashi, A.G. Ryder, Z. Foldes-Papp, N. Lowndes, H.P. Nasheuer, Mobility and distribution of replication protein A in living cells using fluorescence correlation spectroscopy, Exp. Mol. Pathol. 82 (2) (2007) 156–162.
[33] C. Iftode, Y. Daniely, J.A. Borowiec, Replication protein A (RPA): the eukaryotic SSB, Crit. Rev. Biochem. Mol. Biol. 34 (3) (1999) 141–180.
[34] M.S. Wold, Replication protein A: a heterotrimeric, single-stranded DNA-binding protein required for eukaryotic DNA metabolism, Annu. Rev. Biochem. 66 (1997) 61–92.
[35] C.J. Bakkenist, M.B. Kastan, Initiating cellular stress responses, Cell 118 (1) (2004) 9–17.
[36] J. Yang, Y. Yu, H.E. Hamrick, P.J. Duerksen-Hughes, ATM, ATR and DNA-PK: initiators of the cellular genotoxic stress responses, Carcinogenesis 24 (10) (2003) 1571–1580.
[37] P.L. Kannouche, J. Wing, A.R. Lehmann, Interaction of human DNA polymerase eta with monoubiquitinated PCNA: a possible mechanism for the polymerase switch in response to DNA damage, Mol. Cell 14 (4) (2004) 491–500.
[38] H. Zhao, F. Traganos, J. Dobrucki, D. Wlodkowic, Z. Darzynkiewicz, Induction of DNA damage response by the supravital probes of nucleic acids, Cytometry A 75A (6) (2009) 510–519.
[39] S. Sabbioneda, A.M. Gourdin, C.M. Green, A. Zotter, G. Giglia-Mari, A. Houtsmuller, W. Vermeulen, A.R. Lehmann, Effect of proliferating cell nuclear antigen ubiquitination and chromatin structure on the dynamic properties of the Y-family DNA polymerases, Mol. Biol. Cell 19 (12) (2008) 5193–5202.
[40] V.T. Nguyen, F. Giannoni, M.F. Dubois, S.J. Seo, M. Vigneron, C. Kedinger, O. Bensaude, In vivo degradation of RNA polymerase II largest subunit triggered by alpha-amanitin, Nucleic Acids Res. 24 (15) (1996) 2924–2929.
[41] L.V. Mayne, A.R. Lehmann, Failure of RNA synthesis to recover after UV irradiation: an early defect in cells from individuals with Cockayne's syndrome and xeroderma pigmentosum, Cancer Res. 42 (4) (1982) 1473–1478.
[42] L. Roza, W. Vermeulen, J.B. Bergen Henegouwen, A.P. Eker, N.G. Jaspers, P.H. Lohman, J.H. Hoeijmakers, Effects of microinjected photoreactivating enzyme on thymine dimer removal and DNA repair synthesis in normal human and xeroderma pigmentosum fibroblasts, Cancer Res. 50 (6) (1990) 1905–1910.

Chapter 8

~

Effect of PCNA ubiquitination and chromatin structure on the dynamic properties of the Y-family DNA polymerases

Mol Biol Cell (2008), **19** (12)**:** 5193-202

Molecular Biology of the Cell
Vol. 19, 5193–5202, December 2008

Effect of Proliferating Cell Nuclear Antigen Ubiquitination and Chromatin Structure on the Dynamic Properties of the Y-family DNA Polymerases

Simone Sabbioneda,* Audrey M. Gourdin,† Catherine M. Green,*‡ Angelika Zotter,† Giuseppina Giglia-Mari,† Adriaan Houtsmuller,§ Wim Vermeulen,† and Alan R. Lehmann*

*Genome Damage and Stability Centre, University of Sussex, Falmer, Brighton BN1 9RQ, United Kingdom; and †MGC Department of Genetics and Cell Biology and §Department of Pathology, Erasmus Medical Center, 3000 DR Rotterdam, The Netherlands

Submitted July 15, 2008; Revised August 19, 2008; Accepted September 8, 2008
Monitoring Editor: Orna Cohen-Fix

Y-family DNA polymerases carry out translesion synthesis past damaged DNA. DNA polymerases (pol) η and ι are usually uniformly distributed through the nucleus but accumulate in replication foci during S phase. DNA-damaging treatments result in an increase in S phase cells containing polymerase foci. Using photobleaching techniques, we show that polη is highly mobile in human fibroblasts. Even when localized in replication foci, it is only transiently immobilized. Although ubiquitination of proliferating cell nuclear antigen (PCNA) is not required for the localization of polη in foci, it results in an increased residence time in foci. polι is even more mobile than polη, both when uniformly distributed and when localized in foci. Kinetic modeling suggests that both polη and polι diffuse through the cell but that they are transiently immobilized for ~150 ms, with a larger proportion of polη than polι immobilized at any time. Treatment of cells with DRAQ5, which results in temporary opening of the chromatin structure, causes a dramatic immobilization of polη but not polι. Our data are consistent with a model in which the polymerases are transiently probing the DNA/chromatin. When DNA is exposed at replication forks, the polymerase residence times increase, and this is further facilitated by the ubiquitination of PCNA.

INTRODUCTION

Most types of damage in cellular DNA block the progress of the replication fork because the highly stringent replicative DNA polymerases (pols) δ and ε are unable to accommodate the damaged bases in their active sites. An important mechanism for bypassing these replication blocks is by translesion synthesis (TLS), in which a low-stringency specialized polymerase is able to substitute for the blocked replicative polymerase (Friedberg *et al.*, 2005). Most of these specialized TLS polymerases belong to the Y-family, whose members have a much more open structure than the B-family replicative polymerases (Yang and Woodgate, 2007). This enables them to accommodate damaged bases in their active sites, each Y-family polymerase having a different specificity for different types of altered bases. For example, polη can accommodate both bases of a cyclobutane pyrimidine dimer (CPD) in its active site and is able to replicate past a CPD with similar efficiency to an undamaged base (McCulloch *et al.*, 2004). Moreover, in most cases it inserts the "correct" bases opposite the CPD (Masutani *et al.*, 2000). Mutations in the *POLH* gene result in the variant form of xeroderma pigmentosum (XP-V) (Masutani *et al.*, 1999; Johnson *et al.*, 1999a). The high incidence of sunlight-induced skin cancer associated with this disorder probably results from a less efficient polymerase substituting for polη in its absence. When this substituting polymerase carries out TLS past UV photoproducts, it is presumed to be more error-prone than polη, resulting in a higher UV-induced mutation frequency, as seen in XP-V cells (Maher *et al.*, 1976).

Polη and its paralogue polι are uniformly distributed throughout the cell nucleus in G2-M-G1 phases of the cell cycle. During S phase, both pols are localized in microscopically visible bright foci, representing replication factories (Kannouche *et al.*, 2001, 2003). Treatments like UV and the inhibitor hydroxyurea (HU) result in an accumulation of cells in which polη and ι are localized in foci (Kannouche *et al.*, 2001, 2003). These treatments reduce or block the progression of replication forks, slow down the passage through S phase and result in an increase in the proportion of S phase nuclei in the cell population. This accounts at least partially for the increased number of cells with polymerase foci.

The actual engagement of pol η and ι at the sites of stalled replication forks is mediated by the homotrimeric sliding clamp accessory protein PCNA. When the replication fork stalls, exposed single-stranded regions of DNA at the stalled forks activate the E3 ubiquitin ligase Rad18. Together with its E2 partner Rad6, Rad18 mono-ubiquitinates PCNA at the stalled fork on lysine-164 (Hoege *et al.*, 2002; Kannouche *et al.*, 2004; Watanabe *et al.*, 2004). As well as having "PIP box" PCNA-binding motifs (Kannouche *et al.*, 2001; Vidal *et al.*,

This article was published online ahead of print in *MBC in Press* (http://www.molbiolcell.org/cgi/doi/10.1091/mbc.E08–07–0724) on September 17, 2008.

‡ Present address: Department of Zoology, University of Cambridge, Cambridge CB2 3EJ, United Kingdom.

Address correspondence to: Alan R. Lehmann (a.r.lehmann@sussex.ac.uk).

2004), polη and ι both have ubiquitin-binding motifs in the C-terminal parts of the proteins (Bienko *et al.*, 2005). Thus, when PCNA is ubiquitinated, its affinity for these polymerases is increased by virtue of these motifs, and this facilitates their binding to the stalled forks. This mechanism, deduced from in vivo studies, has recently been demonstrated for polη in a reconstituted in vitro system (Zhuang *et al.*, 2008).

The microscopically visible replication foci presumably represent subnuclear structures at which replication-associated factors are concentrated. However, little is known about the nature of these structures or about the dynamics of the different factors that are localized in them. We have used high-resolution confocal microscopy and fluorescence recovery after photobleaching (FRAP) together with biochemical fractionation to give further insight into the relationship of polη and polι to the replication foci. Both polymerases were highly mobile within the nucleus, and interacted with immobile elements (most likely DNA) very transiently, with characteristic binding times of the order of 100–200 ms. Remarkably, we find that even when localized in foci, they remained highly mobile, with half-lives of <1 s. The foci thus represent dynamic "work stations" with polymerases entering and exiting continually, remaining in the foci for fractions of a second. We demonstrate that the two polymerases act independently, and we show that ubiquitination of PCNA facilitates but is not essential for accumulation of polη into the foci.

MATERIALS AND METHODS

Cell Lines and Culture Conditions

XP30RO SV40 transformed fibroblasts were transfected with enhanced green fluorescent protein (eGFP)-polη and eGFP-polη-pol-dead plasmids, and stable clones expressing the respective alleles of polη were isolated. All cell lines described in this article were grown in Eagle's minimal essential medium supplemented with 15% fetal calf serum. Cell lines were generated as described previously (Kannouche *et al.*, 2001).

For global UV-irradiation, the cells were treated essentially as described previously (Kannouche *et al.*, 2001) and irradiated, unless otherwise stated, with 15 Jm^{-2} UV-C before a further incubation for 7 h. For local UV-irradiation, cells were UV-irradiated with 120 Jm^{-2} through 5-μm pores of a polycarbonate filter. For HU treatment, the cells were incubated in 1 mM HU for 24 h. To inhibit the proteasome, the cells were preincubated for 1 h with 0.1 μM epoxomicin before UV-irradiation and incubated for a further 6 h in epoxomicin-containing medium after irradiation. DRAQ5 (Biostatus Limited, Leicestershire, United Kingdom) was used at the concentration of 10 μM and incubated with the cells for the duration of the experiment. Detectable DNA staining was visible already after a 3-min incubation.

Transfections and Plasmids

Plasmids were transfected into simian virus 40 (SV40)-transformed fibroblasts by using FuGENE 6 as described previously (Kannouche *et al.*, 2001). eGFPpolη, eGFPpolι, eGFP-H2B, hRad18, and hRad18C28F were constructed in peGFP-C3 or pCDNA3.1 plasmids (Kannouche *et al.*, 2004). eGFP-PCNA was subcloned in pCDNA3.1 by cutting a 1.6-kb fragment with XbaI and BamHI from pENeGFP-PPCNAL2 (a kind gift of Cristina Cardoso, Max Delbrück Center for Molecular Medicine, Berlin, Germany). To analyze the effect of Rad18 expression the cells were simultaneously cotransfected with monomeric red fluorescent protein (mRFP)-α-tubulin (a kind gift from Sally Wheatley) as a marker for transfected cells.

To generate the polη pol-dead mutant, amino acids D115 and E116 were mutated to alanine using the QuikChange kit (Stratagene, La Jolla, CA). The full coding region of polη was then sequenced to check for mutations.

For small interfering RNA (siRNA) knockdown, ONTARGET+ Smartpools (Dharmacon RNA Technologies, Lafayette, CO) containing four siRNAs against USP1 were used at 5 nM final concentration. The negative control (NTC) represents a pool of four siRNAs designed to have at least four mismatches for all the sequences present in the human genome. The cells were transfected in a 3-cm dish with siRNA by using Hiperfect (QIAGEN, Hilden, Germany) according to manufacturer's instructions using the fast forward procedure, and incubated for 48 h before analysis.

In Vivo Cell Imaging

Cells were plated at 5×10^5 cells/3-cm dish (MatTek, Ashland, MA) for at least 48 h before imaging. The cells were monitored under the microscope in a temperature-controlled chamber in 5% CO_2 atmosphere.

All the FRAP analysis was performed on an LSM510 confocal microscope (Carl Zeiss, Jena, Germany) by using a 40× numerical aperture 1.3 differential interference contrast oil objective. Except otherwise stated, a region of 1.44 μm^2 was monitored for 3 s (100 scans taken every 30 ms) before being bleached (1 iteration), and recovery of fluorescence was subsequently monitored for another 16.5 s (550 scans every 30 ms) using bidirectional scans. For the strip-FRAP, the monitored region was changed to a 2-μm strip positioned in the middle and spanning the whole nucleus. Using monodirectional scans, the cell was followed for 4 s before bleaching (200 scans every 20 ms, monodirectional) and 22 s after bleaching (1100 scans every 20 ms).

To avoid monitor bleaching, the laser was set to a power of 700 nW except during the bleaching iterations (140 μW). Raw fluorescence data were then background subtracted and normalized as described previously (Houtsmuller and Vermeulen, 2001). Briefly, the relative fluorescence was calculated as I_t/I_0, where I_t represents the fluorescence intensity at time t, and I_0 represents the average intensity of 20 points just before bleaching. Average measurements of at least 30 cells were used for each FRAP curve. The $t_{0.5}$ was calculated by interpolation on the FRAP curves as the time required to reach half-fluorescence recovery ($I_{0.5} = 0.5(I_{end} + I_{bleach})$, where I_{end} is the average fluorescence of the last 20 points, and I_{bleach} is the fluorescence recorded immediately after the bleaching). The long-lasting immobile fraction is calculated as $(1 - I_{end})/(1 - I_{bleach})$.

Half-Nucleus Bleaching Combined with Fluorescence Loss in Photobleaching (FLIP)-FRAP

For FLIP-FRAP, half of the nucleus was bleached for 2.4 s (4 iterations), after which the whole cell was imaged every 2 s for 50 s. To analyze the data, the FRAP (intensity of fluorescence in the whole of the bleached half-nucleus) was subtracted from the FLIP (intensity of fluorescence in the whole of the unbleached half-nucleus). The difference between FLIP and FRAP after bleaching was normalized to 1. The results are presented on a log scale, and the mobility of the protein is presented as the time necessary for the FRAP value to reach 90% of the prebleach value. Errors bars represent the SEs of the mean.

FRAP in Local Damage

The entire local damage was bleached in 0.7 s with two bleaching pulses, and the recovery of fluorescence monitored for by scanning the whole cell every second. The intensity of fluorescence in the local damage before bleaching was normalized to 1. Errors bars represent the SEs of the mean.

FRAP Data Modeling

For the model-based analysis of the FRAP data, raw FRAP curves were normalized to prebleach values and the best fitting curve (by ordinary least squares) was picked from a large set of computer simulated FRAP curves in which three parameters representing mobility properties were varied: diffusion rate (ranging from 0.04–25 $\mu m^2/s$), immobile fraction (ranging from 0 to 90%), and time spent in immobile state (ranging from 0.1 to 300 s).

The Monte Carlo computer simulations used to generate FRAP curves for the fit were based on a model that simulates diffusion of molecules and binding to immobile elements in an ellipsoidal volume. The laser bleach pulse was simulated based on experimentally derived three-dimensional (3D) laser intensity profiles, which were used to determine the probability for each molecule to get bleached, considering their 3D position. The simulation of the FRAP curve was then run using discrete time steps corresponding to the experimental scan interval of 21 ms. Diffusion was simulated at each new time step $t + \Delta t$ by deriving the new positions ($x_{t+\Delta t}$, $y_{t+\Delta t}$, $z_{t+\Delta t}$) of all mobile molecules from their current positions (x_t, y_t, z_t) by $x_{t+\Delta t} = x_t + G(r_1)$, $y_{t+\Delta t} = y_t + G(r_2)$, and $z_{t+\Delta t} = z_t + G(r_3)$, where r_i is a random number ($0 \leq r_i \leq 1$) chosen from a uniform distribution, and $G(r_i)$ is an inversed cumulative Gaussian distribution with $\mu = 0$ and $\sigma^2 = 6D\Delta t$, where D is the diffusion coefficient. Immobilization was derived from simple binding kinetics described by $k_{on}/k_{off} = F_{imm}/(1 - F_{imm})$, where F_{imm} is the relative number of immobile molecules. The probability for each particle to become immobilized is defined as $P_{immobilize} = k_{on} = k_{off} \cdot F_{imm}/(1 - F_{imm})$, where $k_{off} = 1/T_{imm}$, and T_{imm} is the average time spent in the immobile state. The probability to be released is given by $P_{mobilize} = k_{off} = 1/T_{imm}$. In simulations of two immobile fractions with different kinetics, two immobilization/mobilization probabilities were evaluated at each unit time step. Simulations of the FRAP curve were performed at every unit time step by counting the number of unbleached molecules in the bleached region after simulations of diffusion and binding during that time step.

In all simulations, the size of the ellipsoid was based on the size of the nuclei, and the region used in the measurements determined the size of the simulated bleach region. The laser intensity profile using the simulation of the bleaching step was derived from confocal images stacks of chemically fixed nuclei containing green fluorescent protein (GFP) that were exposed to a stationary

laser beam at various intensities and varying exposure times. The unit time step Δt corresponded to the experimental sample rate of 21 ms. The number of molecules in the simulations was 10^6, which was empirically determined by producing curves that closely approximate the data with comparable fluctuations.

Epifluorescence and Triton Extraction

Cells were seeded directly on a coverslip and irradiated the next day with 15 J/m^2 before incubation for 7 h. Cells were then washed twice with phosphate-buffered saline (PBS) and fixed in 2% paraformaldehyde for 30 min before further washing in PBS and then mounted in VECTASHIELD (Vector Laboratories, Burlingame, CA) + 4,6-diamidino-2-phenylindole (DAPI). To extract the soluble proteins before fixation, the coverslips were washed in 0.2% Triton X as described previously (Kannouche and Lehmann, 2006).

Size Exclusion Chromatography

Cells were harvested from a 10-cm dish and lysed in 75 μl of buffer A20 (20 mM HEPES, pH 7.5, 20 mM NaCl, 1 mM $MgCl_2$, 0.5% Triton X-100, and 1 μl/ml Benzonase [Sigma Chemical. Poole, Dorset, United Kingdom]). The extracts were incubated for 30 min on ice to allow DNA digestion by Benzonase. After incubation the extract was diluted in an equal volume of buffer A500 (same as buffer A20 but with 500 mM NaCl, 0.4 mM EDTA and 1 mM dithiothreitol). The extract was then spun down at 10,000 × *g* and filtered through a 0.2-μm pore Ultrafree Micro (Whatman, Maidstone, United Kingdom) before loading onto a 2.4-ml Superdex200 size exclusion column on a SMART system (GE Healthcare, Little Chalfont, Buckinghamshire, United Kingdom). By using standards of known Stokes radii run on the same column, the respective values for polη and polι were calculated by interpolation.

Glycerol Gradient

Cell extracts prepared as for the gel filtration were loaded on a 5-ml 15–35% glycerol gradient in buffer A260 (as described above but containing 260 mM NaCl). The gradient was centrifuged for 16 h in an AH650 swing-out rotor (Sorvall, Newton, CT) at 42,500 rpm, and finally 200 μl fractions were collected from the top. By using standards of known sedimentation coefficient alongside the extract, the respective values for polη and polι were calculated. The molecular weight (MW) was calculated as follows: $MW = (6\pi\eta NaS)/(1 - \nu\rho)$, where η is the viscosity of the medium, N is Avogadro's number, a is the Stokes radius, S is the sedimentation coefficient, ν is the partial specific volume of the protein, and ρ is the density of the medium.

Western Blot

Western blotting was performed on nitrocellulose and probed using the following antibodies: clones 7.1 and 13.1 (Roche Diagnostics, Mannheim, Germany) against GFP and PC10 (CRUK) against PCNA. Antibodies against full-length polη (Kannouche *et al.*, 2001), against the C-terminal peptide of polι (a kind gift from Roger Woodgate, National Institutes of Health, Bethesda, MD; Kannouche *et al.*, 2003), and against the N-terminal part of USP1 (a kind gift from Tony Huang, New York University, New York, NY; Huang *et al.*, 2006) have been described previously.

RESULTS

To measure the dynamics of polη in human cells, we used a cell line in which N-terminally tagged eGFP-polη was expressed in XP30RO cells (Kannouche *et al.*, 2001). These cells contain a truncation mutation in the *POLH* gene close to the N terminus (Johnson *et al.*, 1999a) and can be considered as polη null mutants. We previously showed that the eGFP-polη expressed in this cell line was able to correct the typical sensitivity of XP30RO to UV followed by treatment with caffeine (Kannouche *et al.*, 2001). Using fluorescence-activated cell sorting, we selected a subpopulation of the cells in which the level of eGFP-polη was similar to that of endogenous polη in normal MRC5 cells. Figure 1A shows a Western blot of polη in this cell line, compared with that in the normal cell line MRC5. Polη expression levels remained stable over several weeks. There was no evidence, either by Western blotting or by the appearance of cytoplasmic autofluorescence, for any free eGFP protein (data not shown). We conclude that the quantitative fluorescence measurements described in the following sections were derived from cells that express full-length and biologically active GFP-tagged polη.

In previous work, we showed that eGFP-polη transfected into human fibroblasts was uniformly distributed throughout the nucleus outside S phase but that it accumulated in bright foci representing replication factories in S phase cells. In cells treated with 15 Jm^{-2} UV-irradiation and incubated for 7 h or with 1 mM HU for 24 h, the number of cells in which polη was located in foci increased substantially, partly or wholly because of the accumulation of S phase cells after these treatments (Kannouche *et al.*, 2001). Supplemental Figure S1 shows stills from a confocal time-lapse series in which the stable cell line was UV-irradiated through a micropore filter to generate localized damage within the nucleus (Volker *et al.*, 2001). Using this procedure, proteins involved in processing of DNA damage accumulate at the sites of the localized irradiation. We found that, throughout S phase, eGFP-polη accumulated at the sites of local damage. Within the damaged area polη accumulated in a focal pattern because of the stalling of replication forks (Kannouche *et al.*, 2001). In contrast, in G2 the eGFP-polη neither accumulated at the local damage nor was it in bright foci, but it became uniformly distributed through the nucleus. These data confirm the S phase-specific function of polη.

We have used FRAP to measure the mobility of polη under different conditions. We photobleached a small square of the nucleus and measured the rate of recovery of fluorescence within the square. Polη that was uniformly distributed in the nucleus (i.e., in G1 or G2 cells) relocalized into the bleached area extremely rapidly with a $t_{0.5}$ of 0.15 s (Figure 1B, polη untreated-diffuse), indicating that it is highly mobile within the nucleus.

We next photobleached the eGFP-polη within a focus in an S phase nucleus by aligning the square over a visible focus in S phase cells (Box-FRAP). We used a square as small as possible so that the focus filled almost the whole area of the square. In this situation, the recovery rate was reduced about two-fold (Figure 1B). The $t_{0.5}$ was still very short, 0.33 s. The mobility of polη in foci generated in cells irradiated with UV-irradiation or following HU treatment was indistinguishable from that in an unperturbed S phase (Figure 1B). Thus, surprisingly, even when associated with microscopically visible structures, the majority of the polη molecules within the focus remained highly mobile. Examination of the curves in Figure 1B at later times (up to 15 s; see inset) suggests that at most only 7% of the molecules were immobilized for a long period (see *Materials and Methods* for definitions of $t_{0.5}$ and immobile fraction). In contrast to the highly dynamic association of eGFP-polη, we observed a relatively large (~60%) fraction of eGFP-PCNA (Figure 1C), in which proteins were significantly immobilized for long periods (see *Materials and Methods* for calculation of long-lasting immobile fractions), in line with previous studies (Sporbert *et al.*, 2002; Essers *et al.*, 2005).This demonstrates that our system was capable of detecting immobilized proteins.

To determine whether the catalytic activity of polη might affect its mobility, we generated an XP30RO cell line expressing eGFP-polη in which amino acids (aa) D115 and E116, shown to be vital for catalytic activity (Johnson *et al.*, 1999b), were mutated to alanines. This mutation allows the incoming dNTP to bind but cannot support the formation of the phosphodiester bond (Li *et al.*, 1998). The mobility of this "pol dead" polη mutant, when distributed uniformly in the nucleus, was identical to that of wild-type polη (data not shown), but interestingly, its mobility in foci was about twofold lower than that of wild-type polη, with a $t_{0.5}$ of ~0.67 s and a long-lasting immobile fraction of 15% (Figure 1C).

As an alternative methodology, we have also used FLIP-FRAP in which we bleached half the nucleus. We then

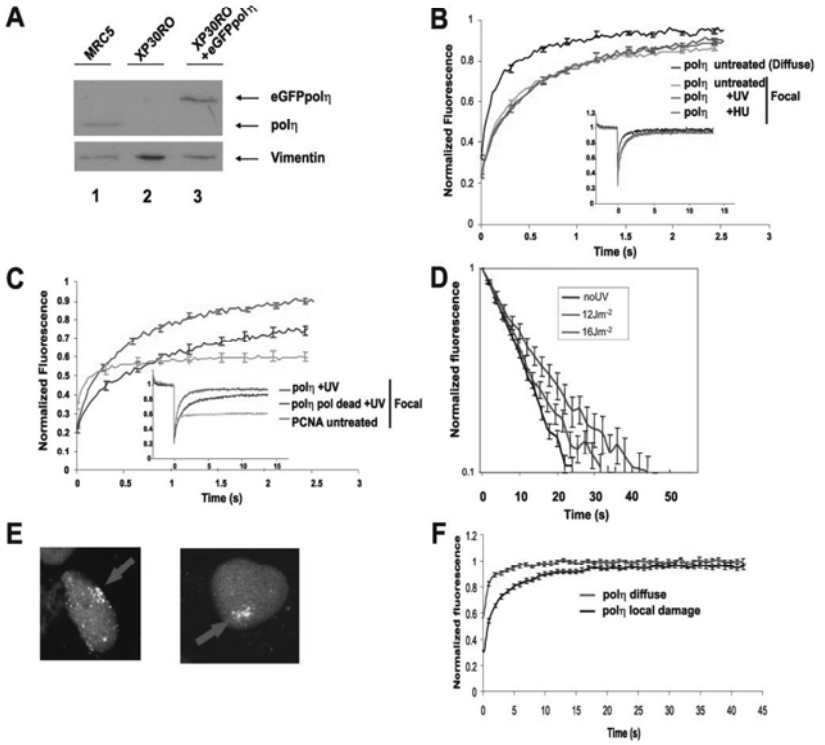

Figure 1. Dynamics of eGFP-polη in living cells. (A) Western blot of the XP30RO-eGFP-polη cell line used in this study (lane 3), compared with MRC5 (lane 1) and XP30RO (lane 2). (B) Comparison of FRAP curves (relative fluorescence recovery plotted against time) of eGFP-polη uniformly distributed in untreated XP30RO-eGFP-polη cells and in foci in S phase cells from untreated, UV-treated, and HU-treated cells. (C) Fluorescence recovery of "pol-dead" mutant (blue) and wild-type polη (red) in foci (7 h after 15 Jm^{-2} UV-C). Also shown is the FRAP curve for eGFP-PCNA in foci (orange), showing large immobile fraction. (D) FLIP-FRAP analysis of eGFP-polη. Cells were not irradiated (no UV, mean of 63 cells) or globally irradiated with 12 (mean of 50 cells) and 16 Jm^{-2} (mean of 27 cells). Five hours later, half-nucleus bleaching associated with FLIP-FRAP analysis was performed. The data were normalized as described in *Materials and Methods*. The error bars represent the SE of the mean. (E) eGFP-polη accumulated at site of local irradiation. (F) Five hours after local irradiation, the area of local damage was entirely bleached, the recovery of fluorescence was measured in the bleached area and normalized to the level of fluorescence in the whole nucleus. Control cells represent cells in which no local damage was inflicted, but in which a square of the same size as irradiated cells was bleached.

measured both the rate of reduction in fluorescence intensity of the unbleached half (FLIP) and the rate of recovery in the bleached half of the nucleus (FRAP). With this technique, we are able to analyze the overall mobility in the whole of the nucleus, providing the collective mobility of polη in a large number of foci, in contrast to the mobility within a single focus in the experiments described above. As with bleaching of a small square, we observed rapid redistribution of polη. The difference between FLIP and FRAP immediately after bleaching was normalized to 1, and, in Figure 1D, at different times after bleaching, the normalized difference between the FLIP and FRAP is presented on a log scale. With nuclei in which polη was uniformly distributed, polη had returned to 90% of the prebleach distribution (i.e., normalized fluorescence = 0.1) in 25 s (Figure 1D). Using this FLIP-FRAP analysis, we have examined the effect of different doses of UV on the mobility of polη in nuclei containing focal polη. We compared polη mobility in these cells with its mobility when diffusely distributed in untreated cells. A UV dose response was observed, with increasing delay in polη redistribution due to transient immobilization to subnuclear structures (Figure 1D). Higher UV doses resulted in a more pronounced delay in redistribution, reaching a maximum after irradiation with 16 Jm^{-2}, with a redistribution time of about 45 s, compared with ~25 s in untreated cells not exhibiting foci. This approximate doubling of the redistribution time agrees well with the approximately two-fold decrease in mobility in the Box-FRAP data presented in Figure

1B. These data suggest that with increasing UV-doses, as expected, more substrate sites (i.e., stalled forks) were created that transiently bind a larger pool of the resident polη molecules but that the average binding time within a single focus is not affected by an increasing number replication blocks.

In a further variation, we UV-irradiated cells through a micropore filter to produce localized damage in the nucleus (Volker *et al.*, 2001). Five hours after irradiation, we selected cells in which polη had accumulated in foci at the sites of local damage (examples shown in Figure 1E), and we bleached the entire site of local damage. As control, we bleached an identical area in a nucleus in which no local damage had been inflicted. Relocalization into the bleached damaged site was again approximately two-fold slower than into undamaged areas (Figure 1F). We conclude from these different photobleaching studies that polη is highly mobile within the nucleus and that its mobility is only slightly reduced within replication foci.

Role of PCNA-Ubiquitination

Polη has a PIP box binding motif for interaction with PCNA (Haracska *et al.*, 2001; Kannouche *et al.*, 2001), and it is likely that PCNA plays a role in assisting polη to find its substrate. After exposure of cells to UV-irradiation or other agents that block progression of the replication fork, PCNA becomes mono-ubiquitinated on lysine-164 at the sites of stalled forks, a reaction mediated by the Rad6–Rad18 ubiquitination system (Hoege *et al.*, 2002; Kannouche *et al.*, 2004; Watanabe *et al.*, 2004). It is widely assumed, but without direct evidence, that ubiquitination of PCNA is required for localization of polη in replication foci. Dantuma *et al.* (2006) reported that treatment of cells with the general proteasome inhibitor MG132 induced a depletion of the free ubiquitin pool and a concomitant reduction of mono-ubiquitinated target proteins such as ubiquitinated histones. We observed similar effects on UV-irradiation–induced PCNA mono-ubiquitination when cells were treated with either MG132 (data not shown) or with another proteasome inhibitor epoxomicin (Figure 2A). Remarkably, polη accumulated in foci to a similar extent in UV-irradiated MRC5 cells treated with or without epoxomicin (Figure 2B), indicating that ubiquitination of PCNA is not essential for polη foci formation.

These findings do not however rule out the possibility that ubiquitination of PCNA affects the dynamics of polη in foci. Because inhibition of the proteasome is likely to have many pleiotropic effects, it would be difficult to interpret dynamic experiments making use of this inhibitor. An alternative way of preventing PCNA ubiquitination is by depletion of Rad18, by using siRNA (Kannouche *et al.*, 2004). However, Rad18 interacts physically with polη and is required for the accumulation of polη in foci, independently from its role in PCNA ubiquitination (Watanabe *et al.*, 2004); so, this approach also could not be used. Instead, we looked at the effect of overexpressing Rad18 in our eGFP-polη–expressing cells and measured the mobility of polη, both uniformly distributed and in foci. Overexpression of Rad18 has been reported to cause increased PCNA ubiquitination (Huang *et al.*, 2006; Davies *et al.*, 2008). To test whether this was also the case in our experimental system, we contransfected His-PCNA and Rad18. The use of His-PCNA was needed because the low transfection efficiency of our cell lines made it impossible to detect any changes in endogenous PCNA. In the overexpressing cells, there was an increase in the level of ubiquitination of His-tagged PCNA, especially after UV-irradiation (Figure 2C, compare lanes 4 and 2).

Overexpression of Rad18 (together with mRFP-α-tubulin, used as transfection marker) had no effect on the mobility of uniformly distributed polη (Figure 2D). In contrast, there was a decrease in the mobility of polη in foci (Figure 2D). To determine whether this effect of Rad18 was mediated by ubiquitination of PCNA or by binding to polη, we mutated the RING finger motif of Rad18 that is required for its ubiquitin ligase activity and the ubiquitination of PCNA but is not involved in direct interaction of Rad18 with polη (Watanabe *et al.*, 2004). Using the Rad18-C28F mutation (Tateishi *et al.*, 2000), in which the E3 ubiquitin ligase activity is inactivated, levels of ubiquitinated PCNA were the same as in mock-transfected cells (Figure 2C, lane 6), and the reduction in mobility of focal polη was abolished (Figure 2D).

USP1 is a deubiquitinating enzyme (DUB), which removes the ubiquitin from ubiquitinated PCNA (Huang *et al.*, 2006). Depletion of USP1 by using siRNA results in increased levels of ubiquitinated PCNA in undamaged cells (Huang *et al.*, 2006; Figure 2E, bottom, lane 3). In these USP1-depleted cells, the mobility of uniformly distributed GFP-polη was slightly reduced; in foci in HU-treated cells, it was reduced to a similar level to that in the cells overexpressing Rad18 (Figure 2F). (Note that we could not use UV in these experiments as UV-irradiation results in disappearance of USP1 from the cell. This is not seen after HU treatment; Huang *et al.*, 2006 and our unpublished data.) Together, these results suggest that although ubiquitination of PCNA is not required for accumulation of polη into replication factories, it results in an increased residence time of polη in the factories.

Mobility of polι

Polι is a paralogue of polη (Tissier *et al.*, 2000), but its precise function remains to be established. In previous work, we showed that polη could physically interact with polι, although we could not demonstrate such an interaction in human cell lysates (Kannouche *et al.*, 2003). Polι accumulates in replication foci in an identical manner to polη, and this accumulation is substantially dependent on the presence of polη, because it was greatly reduced in XP-V cells (Kannouche *et al.*, 2003). To investigate the intracellular relationship between polη and ι further, we established stable MRC5 and XP-V XP30RO cell lines expressing eGFP-polι. The levels of polι expression are shown in Figure 3A and are approximately 4 times the endogenous level (see Supplemental Figure S3 for calculation). This is the minimum level of expression that enables us to visualize the eGFP-polι foci. However, by comparing cells expressing different levels of eGFP-polι, we ascertained that the mobility of polι was independent of its expression level. We compared the mobility of polι with that of polη. We found that polι was even more mobile than polη, with a $t_{0.5}$ of only 90 ms when uniformly distributed, this mobility being similar in MRC5 and XP30RO cells and therefore independent of the presence of polη (Figure 3B). As with polη, the mobility of polι was somewhat decreased in replication foci ($t_{0.5}$ of 200 ms), but it remained more mobile than polη (Figure 3C). These data do not support the idea that the two polymerases exist in the same complex within the cell (although they do not rule out the possibility that a small subfraction might be associated).

Because polη and ι have very similar molecular weights, if they exist in the cell as freely diffusible monomers, their redistribution kinetics should be very similar. There are two possible explanations for the different kinetics. The first possibility is that when uniformly distributed, both polymerases are components of protein complexes that are freely diffusible within the cell and the polη complex is larger than the polι complex. Alternatively, the polymerases spend a

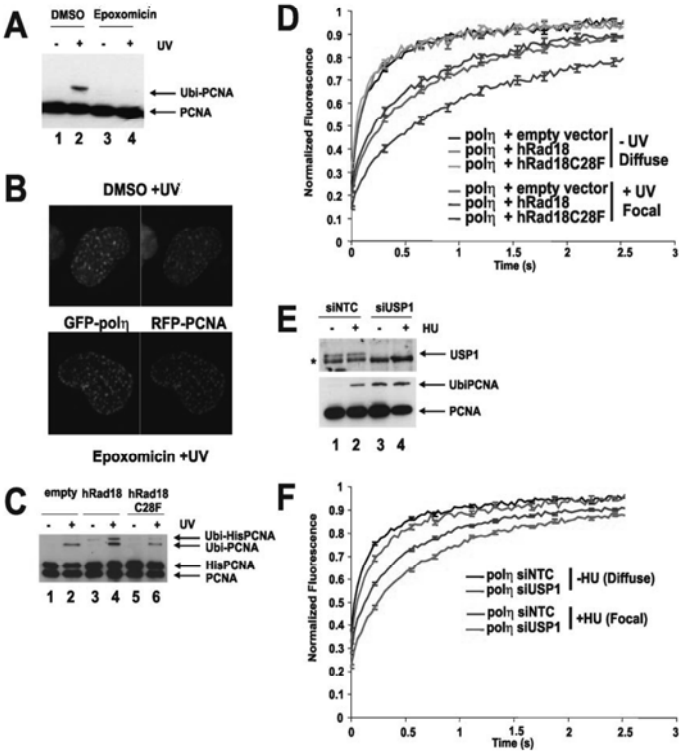

Figure 2. Ubiquitination of PCNA and polη mobility. (A) MRC5 cells were UV-irradiated (15 Jm^{-2}) and incubated for 6 h with epoxomicin. PCNA was analyzed by Western blotting. (B) MRC5 cells transfected with eGFP-polη and mRFP-PCNA were UV irradiated and incubated either in the presence or absence of epoxomicin. Six hours later, the cells were fixed and analyzed by autofluorescence. (C) MRC5 cells were transfected with empty vector, wild-type Rad18, or C28F mutant together with His-tagged PCNA, treated with or without UV, and then incubated for 6 h before analysis by Western blotting. (D) XP30RO-eGFP-polη cells were cotransfected with either wild-type or C28F mutant Rad18 together with mRFP-tubulin to identify the transfected cells. The following day, they were unirradiated or UV irradiated, and the mobility of eGFP-polη was measured using FRAP. (E) Western blot showing increased ubiquitination of PCNA in XP30RO-eGFP-polη cells in which USP1 was depleted by siRNA (lanes 3 and 4). Nontargeting control (siNTC, lanes 1 and 2). (F) Effect of siUSP1 on mobility of eGFP-polη in foci in HU-treated cells.

proportion of their time transiently immobilized. To distinguish between these alternatives, we have applied Monte Carlo simulations to the redistribution kinetics of uniformly distributed polη and ι. The best fits to the data are shown in Supplemental Figure S2 and Table 1, and they are derived from a model in which both polymerases diffuse through the cell but are transiently immobilized. As shown in Table 1, the diffusion coefficients of the two polymerases inside the cell are quite similar, but it is the proportion of transiently immobilized polη (48%) that is much greater than that of polι (17.5%) and accounts for the slower redistribution of polη than polι. The immobilization time is ~150 ms for both.

To explore further the relationship between polη and polι inside cells, we have fractionated cell lysates by both gel filtration and glycerol gradient centrifugation and analyzed the fractions for the polymerases by immunoblotting. Gel filtration separates proteins on the basis of their size and shape, whereas glycerol gradient fractionates on the basis of sedimentation coefficient, which is determined by mass, size, and shape (see *Materials and Methods*). Using gel filtration (Figure 4A), we found that polη and polι were associated with complexes of different Stokes radii, and interestingly the exclusion of polη increased following UV-irradiation. On the glycerol gradients (Figure 4B), both polymerases sedimented at approximately the same rate and this was independent of UV-irradiation. Putting these data together (Figure 4C) suggests that polη and ι are in complexes of 112 and 130 kDa, respectively, somewhat greater than the molecular weights of the polymerases themselves (78 kDa).

Combining the biochemical with the cell biological data, we conclude that the majority of polη and ι molecules diffuse independently in the cell, possibly complexed with

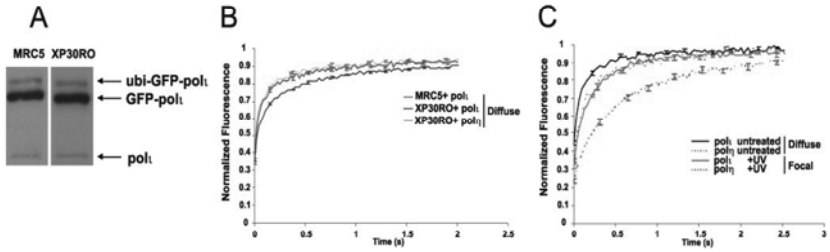

Figure 3. Polι is more mobile than polη. (A) Western blot with anti-polι of lysates from stable cell lines expressing eGFP-polι. (Note that the slow mobility band is the previously reported ubiquitinated form of polι; Bienko *et al.*, 2005.) (B) Comparison of mobilities of eGFP-polι in stable cell lines of MRC5 and XP30RO expressing GFP-polι. (C) Comparison of mobilities of polι distributed uniformly in unirradiated cells and in foci in irradiated cells. Data for polη from Figure 1B are also shown (as dotted curves) for comparison.

other proteins, but the major difference in their mobilities results from the larger fraction of transiently immobilized polη than polι.

Effect of Chromatin Structure on Mobility of Polymerases

To gain further insight into factors affecting the intracellular mobilities of the polymerases, we looked for ways of disrupting chromatin structure to expose the DNA. We made use of the intercalating agent DRAQ5, which binds to DNA with selectivity for A-T base pairs (Njoh *et al.*, 2006). DRAQ5 has recently been shown to disrupt chromatin structure (Wojcik and Dobrucki, 2008), and we have shown that the immobile fraction of transcription factor TFIIH becomes mobilized on treatment of cells with DRAQ5 (Giglia-Mari and Vermeulen, unpublished data). We measured the effect of DRAQ5 on the mobility of the core histone H2B. Histones are normally completely immobile in chromatin, but remarkably, 20% of H2B became mobile within minutes of DRAQ5 treatment (Figure 5A). This result is consistent with findings of Wojcik and Dobrucki (2008). After 1 h in DRAQ5, the original immobility was restored (data not shown). These data suggest that DRAQ5 causes a temporary opening up of the chromatin structure. We next exposed cells to DRAQ5 and measured the effects on the mobilities of polη and ι. Strikingly, we found that treatment of cells in which polη is uniformly distributed resulted in a long-lasting immobilization of 25% of the total polη population within 3 min (Figure 5A). In contrast, the effect on the mobility of polι was much smaller (Figure 5A), with just a slightly reduced mobility and <5% increase in the long-lasting immobile fraction. The effect of DRAQ5 on polη was temporary, and normal mobility was restored within 1 h (data not shown), consistent with the reimmobilization of H2B. We interpret these data as follows: DRAQ5 loosens chromatin structure resulting in release of histones and exposure of the DNA to nucleoplasmic proteins. Polη is then able to bind to DNA and becomes immobilized for a long time (in contrast to the very transient immobilization seen under normal conditions). We can exclude the possibility that DRAQ5 generates a DNA damage response that somehow accounts for the observed changes in mobility, because DRAQ5 treatment does not result in either ubiquitination of PCNA or activation of a DNA damage checkpoint (Verbiest, Mari, Gourdin, Sabbioneda, Wijgers, Dinant, Lehmann, Vermeulen, and Giglia-Mari, unpublished data).

Polι has a lower affinity for DNA than polη and remains mobile. Consistent with the idea that polι is more loosely associated with nuclear structures than polη, we confirmed our earlier findings (Kannouche and Lehmann, 2004) that polη localized in foci was resistant to extraction with triton, whereas polι was quantitatively extracted under identical conditions (Figure 5B).

Table 1. Mobility parameters of polη and i

	Diffusion coefficient	Immobile fraction	Binding time
Polη	7.4 ± 1.6	0.48 ± 0.11	0.15 ± 0.07
Polι	8.9 ± 1.4	0.175 ± 0.11	0.14 ± 0.08

These parameters were based on modeling the raw FRAP data as described in *Materials and Methods*.

DISCUSSION

Our data show that 1) Polη is highly mobile in nuclei of human fibroblasts; 2) even when localized in replication factories, it remains very mobile, albeit somewhat less so than when uniformly distributed in the nuclei, and this mobility in foci is similar during a normal S phase or in cells treated with UV light or hydroxyurea; 3) although ubiquitination of PCNA is not required for the localization of polη in replication foci, it results in an increased residence time in foci; 4) polι is even more mobile than polη, both when uniformly distributed and when localized in factories; and 5) treatment of cells with DRAQ5, which seems to result in the transient opening of the chromatin structure, causes a dramatic immobilization of polη but not polι.

The high mobility of polη in human cells, both uniformly distributed and in foci, agrees with the observations of Solovjeva *et al.* (2005) using Chinese hamster cells, and emphasizes that even though visible in fluorescent replication structures, proteins may still interact there very transiently. Our biochemical data suggest that polη may be associated with another protein in a complex of total molecular mass of 112 kDa. Rad18 has been shown to interact with polη both in cell lysates and as recombinant proteins (Watanabe *et al.*, 2004; Yuasa *et al.*, 2006). However in cells depleted of Rad18 the mobility of diffusely localized polη is hardly affected (data not shown), ruling out the possibility that binding to

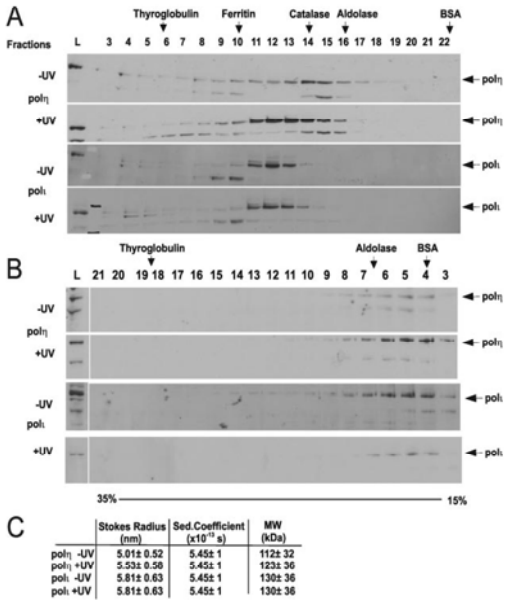

Figure 4. Fractionation of polη and polι from cell lysates. (A) Lysates from unirradiated or UV-irradiated MRC5 cells were fractionated on a Superdex 200 gel filtration column, and fractions were analyzed by immunoblotting for polη and polι. L, load. (B) Equivalent lysates were centrifuged on glycerol gradients. (C) Molecular weight calculations from data obtained in A and B.

Rad18 is responsible for the reduced mobility of polη inside cells.

Our modeling shows that the principal factor responsible for the reduced mobility of polη relative to polι is the greater proportion of transiently immobilized polη molecules. We hypothesize that this immobilization represents polη transiently probing either the DNA itself or proteins associated with the DNA. Our data are consistent with a model in which polη has a weak affinity for DNA (Kusumoto *et al.*, 2004) and is continually probing the chromatin. Outside S phase, the DNA is almost inaccessible inside chromatin, so polη is only retarded very briefly. During S phase, DNA is exposed at the replication forks, polη probes the exposed DNA for suitable substrates and its residence in the foci is increased by binding to the exposed DNA and by interaction with PCNA, especially when PCNA is ubiquitinated. However even under these circumstances, binding is weak and the polymerase remains at the fork for <1 s. Only when the fork is blocked is a substrate available for polη to engage and carry out TLS. This is likely to render the engaged polη molecule immobile for a relatively long period (compared with the transient immobilization discussed above). We have calculated that there are ~80,000 molecules of polη in MRC5 cells (and a similar number of polι molecules) (Sup-

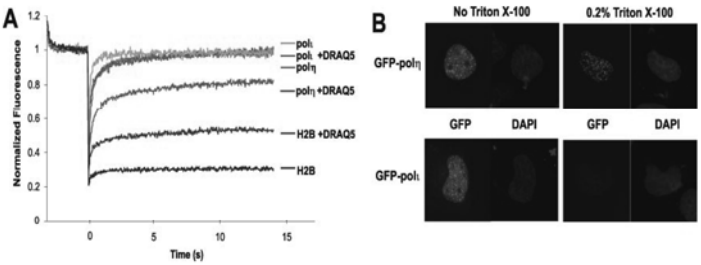

Figure 5. Effects of DRAQ5 on the mobilities of polη and ι. (A) Effect of DRAQ5 on the mobility of eGFP-histone H2B, eGFP-pol η, and eGFP-polι. Cells were treated with or without DRAQ5 for 3 min and then subjected to FRAP analysis. (B) MRC5 cells transfected with either eGFP-polη or eGFP-polι were UV irradiated, incubated for 6 h, and either fixed immediately or extracted with Triton X-100 before analysis by epifluorescence.

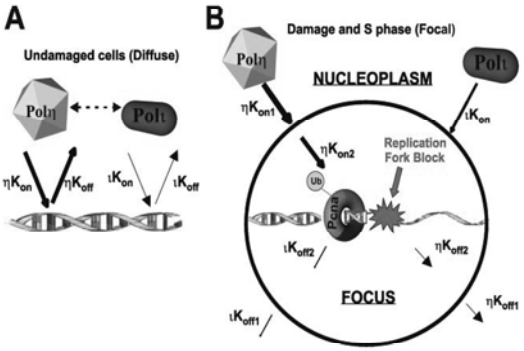

Figure 6. Model for dynamics of polη and ι. (A) In undamaged cells, polη and polι probe the chromatin, but the residence time of polη is greater than that of polι, implying either a higher K_{on} or lower K_{off} rate. The double-headed arrow signifies weak interaction between the two polymerases. (B) In damaged S phase cells, where there is a replication fork blocked by damage and resulting ubiquitination of PCNA, there are two dynamic processes, transport into the focus and association with the blocked fork.

plemental Figure S3), and it is likely that only a small fraction of these are engaged in TLS at any one time. This explains why we detect only a small long-lasting immobile fraction, even in UV-irradiated cells. In the pol dead mutant, we interpret the increased long-lasting immobile fraction as indicating that on engagement, the polymerase becomes temporarily trapped with substrate in its active site.

Relationship between polη and polι

In a previous study, we showed that polη and ι colocalize in replication foci and that the localization of polι in foci is dependent on polη. The two polymerases are able to interact physically, as demonstrated by Far Western blotting, yeast two-hybrid analysis, and coimmunoprecipitation in insect cells (Kannouche *et al.*, 2003). However, three observations suggest that polι binds less strongly to chromatin than polη inside cells. First, our modeling data suggest that less polι is transiently immobile (Table 1). Second, polι is less tightly bound in replication foci than polη (Figure 5B). And third, polη is temporarily immobilized after treatment with DRAQ5, whereas polι is not (Figure 5A). Taking our previous and present observations together, we conclude that interactions between polη and ι must be transient or unstable, that polη helps polι to accumulate in foci, but that polι dissociates from foci more rapidly than polη. Our finding of polη and ι in different complexes on gel filtration also suggests that interactions between them are likely to be transient.

Ubiquitination of PCNA and Localization of polη in Foci

Our finding that PCNA ubiquitination is not required for polη to localize in foci is at first sight surprising, because focal localization is dependent on the UBZ ubiquitin-binding motif of polη (Bienko *et al.*, 2005). However, polη localization in undamaged S phase cells is also dependent on the UBZ motif, even though there seems to be minimal ubiquitination of PCNA under these conditions. We conclude that ubiquitinated PCNA is not the only ubiquitinated target that drives polη into foci. However, once localized in foci, our data are consistent with the idea that ubiquitinated PCNA increases the residence time of polη, presumably by binding to polη via its UBZ motif at sites of stalled replication forks.

A schematic diagram to account for our data is indicated in Figure 6. Outside of S phase, the polymerases are probing the chromatin with K_{on}/K_{off} for polη greater than that for polι. In S phase cells exposed to HU or DNA damage, there are two steps, namely, accumulation into foci and binding at the fork. For the first step, accumulation of polη in foci (K_{on1}) is independent of PCNA ubiqitination. The second step is facilitated by PCNA ubiquitination, which stabilizes the presence of polη and polι at the stalled replication fork. This results in an increase in the overall K_{on}/K_{off} for both polymerases with consequent decreased mobility.

ACKNOWLEDGMENTS

We are grateful to Roger Woodgate, Tony Huang, Cristina Cardoso, and Sally Wheatley for reagents, and to Roger Phillips for assistance with the microscopy. This work was supported by grants from ESF Eurodyna program, the UK Medical Research Council, the Dutch Science organization (NWO) for medical Sciences (ZonMW) VIDI grants, NWO Molecule to Cell program, and an European Union research training network and integrated project on DNA Repair.

REFERENCES

Bienko, M., Green, C. M., Crosetto, N., Rudolf, F., Zapart, G., Coull, B., Kannouche, P., Wider, G., Peter, M., Lehmann, A. R., Hofmann, K., and Dikic, I. (2005). Ubiquitin-binding domains in translesion synthesis polymerases. Science *310*, 1821–1824.

Dantuma, N. P., Groothuis, T. A., Salomons, F. A., and Neefjes, J. (2006). A dynamic ubiquitin equilibrium couples proteasomal activity to chromatin remodeling. J. Cell Biol. *173*, 19–26.

Davies, A. A., Huttner, D., Daigaku, Y., Chen, S., and Ulrich, H. D. (2008). Activation of ubiquitin-dependent DNA damage bypass is mediated by replication protein A. Mol. Cell *29*, 625–636.

Essers, J., Theil, A. F., Baldeyron, C., van Cappellen, W. A., Houtsmuller, A. B., Kanaar, R., and Vermeulen, W. (2005). Nuclear dynamics of PCNA in DNA replication and repair. Mol. Cell. Biol. *25*, 9350–9359.

Friedberg, E. C., Lehmann, A. R., and Fuchs, R. P. (2005). Trading places: how do DNA polymerases switch during translesion DNA synthesis? Mol. Cell *18*, 499–505.

Haracska, L., Johnson, R. E., Unk, I., Phillips, B., Hurwitz, J., Prakash, L., and Prakash, S. (2001). Physical and functional interactions of human DNA polymerase η with PCNA. Mol. Cell. Biol. *21*, 7199–7206.

Hoege, C., Pfander, B., Moldovan, G.-L., Pyrowolakis, G., and Jentsch, S. (2002). RAD6-dependent DNA repair is linked to modification of PCNA by ubiquitin and SUMO. Nature *419*, 135–141.

Houtsmuller, A. B., and Vermeulen, W. (2001). Macromolecular dynamics in living cell nuclei revealed by fluorescence redistribution after photobleaching. Histochem. Cell Biol. *115*, 13–21.

Huang, T. T., Nijman, S. M., Mirchandani, K. D., Galardy, P. J., Cohn, M. A., Haas, W., Gygi, S. P., Ploegh, H. L., Bernards, R., and D'Andrea, A. D. (2006). Regulation of monoubiquitinated PCNA by DUB autocleavage. Nat. Cell Biol. *8*, 341–347.

Johnson, R. E., Kondratick, C. M., Prakash, S., and Prakash, L. (1999a). hRAD30 mutations in the variant form of xeroderma pigmentosum. Science *285*, 263–265.

Johnson, R. E., Prakash, S., and Prakash, L. (1999b). Requirement of DNA polymerase activity of yeast Rad30 protein for its biological function. J. Biol. Chem. *274*, 15975–15977.

Kannouche, P., Broughton, B. C., Volker, M., Hanaoka, F., Mullenders, L.H.F., and Lehmann, A. R. (2001). Domain structure, localization and function of DNA polymerase η, defective in xeroderma pigmentosum variant cells. Genes Dev. *15*, 158–172.

Kannouche, P., Fernandez de Henestrosa, A. R., Coull, B., Vidal, A. E., Gray, C., Zicha, D., Woodgate, R., and Lehmann, A. R. (2003). Localization of DNA polymerases η and ι to the replication machinery is tightly co-ordinated in human cells. EMBO J. *22*, 1223–1233.

Kannouche, P., and Lehmann, A. (2006). Localization of Y-family polymerases and the DNA polymerase switch in mammalian cells. Methods Enzymol. *408*, 407–415.

Kannouche, P. L., and Lehmann, A. R. (2004). Ubiquitination of PCNA and the polymerase switch in human cells. Cell Cycle *3*, 1011–1013.

Kannouche, P. L., Wing, J., and Lehmann, A. R. (2004). Interaction of human DNA polymerase η with monoubiquitinated PCNA; A possible mechanism for the polymerase switch in response to DNA damage. Mol. Cell *14*, 491–500.

Kusumoto, R., Masutani, C., Shimmyo, S., Iwai, S., and Hanaoka, F. (2004). DNA binding properties of human DNA polymerase eta: implications for fidelity and polymerase switching of translesion synthesis. Genes Cells *9*, 1139–1150.

Li, Y., Korolev, S., and Waksman, G. (1998). Crystal structures of open and closed forms of binary and ternary complexes of the large fragment of Thermus aquaticus DNA polymerase I: structural basis for nucleotide incorporation. EMBO J. *17*, 7514–7525.

Maher, V. M., Ouellette, L. M., Curren, R. D., and McCormick, J. J. (1976). Frequency of ultraviolet light-induced mutations is higher in xeroderma pigmentosum variant cells than in normal human cells. Nature *261*, 593–595.

Masutani, C., Araki, M., Yamada, A., Kusumoto, R., Nogimori, T., Maekawa, T., Iwai, S., and Hanaoka, F. (1999). Xeroderma pigmentosum variant (XP-V) correcting protein from HeLa cells has a thymine dimer bypass DNA polymerase activity. EMBO J. *18*, 3491–3501.

Masutani, C., Kusumoto, R., Iwai, S., and Hanaoka, F. (2000). Accurate translesion synthesis by human DNA polymerase η. EMBO J. *19*, 3100–3109.

McCulloch, S. D., Kokoska, R. J., Masutani, C., Iwai, S., Hanaoka, F., and Kunkel, T. A. (2004). Preferential cis-syn thymine dimer bypass by DNA polymerase η occurs with biased fidelity. Nature *428*, 97–100.

Njoh, K. L. *et al.* (2006). Spectral analysis of the DNA targeting bisalkylaminoanthraquinone DRAQ5 in intact living cells. Cytometry A *69*, 805–814.

Solovjeva, L., Svetlova, M., Sasina, L., Tanaka, K., Saijo, M., Nazarov, I., Bradbury, M., and Tomilin, N. (2005). High mobility of flap endonuclease 1 and DNA polymerase eta associated with replication foci in mammalian S-phase nucleus. Mol. Biol. Cell *16*, 2518–2528.

Sporbert, A., Gahl, A., Ankerhold, R., Leonhardt, H., and Cardoso, M. C. (2002). DNA polymerase clamp shows little turnover at established replication sites but sequential de novo assembly at adjacent origin clusters. Mol. Cell *10*, 1355–1365.

Tateishi, S., Sakuraba, Y., Masuyama, S., Inoue, H., and Yamaizumi, M. (2000). Dysfunction of human Rad18 results in defective postreplication repair and hypersensitivity to multiple mutagens. Proc. Natl. Acad. Sci. USA *97*, 7927–7932.

Tissier, A., McDonald, J. P., Frank, E. G., and Woodgate, R. (2000). Polι, a remarkably error-prone human DNA polymerase. Genes Dev. *14*, 1642–1650.

Vidal, A. E., Kannouche, P. P., Podust, V. N., Yang, W., Lehmann, A. R., and Woodgate, R. (2004). PCNA-dependent coordination of the biological functions of human DNA polymerase ι. J. Biol. Chem. *279*, 48360–48368.

Volker, M., Mone, M. J., Karmakar, P., van Hoffen, A., Schul, W., Vermeulen, W., Hoeijmakers, J. H., van Driel, R., van Zeeland, A. A., and Mullenders, L. H. (2001). Sequential assembly of the nucleotide excision repair factors in vivo. Mol. Cell *8*, 213–224.

Watanabe, K., Tateishi, S., Kawasuji, M., Tsurimoto, T., Inoue, H., and Yamaizumi, M. (2004). Rad18 guides poleta to replication stalling sites through physical interaction and PCNA monoubiquitination. EMBO J. *23*, 3886–3896.

Wojcik, K., and Dobrucki, J. W. (2008). Interaction of a DNA intercalator DRAQ5, and a minor groove binder SYTO17, with chromatin in live cells–influence on chromatin organization and histone-DNA interactions. Cytometry A *73*, 555–562.

Yang, W., and Woodgate, R. (2007). What a difference a decade makes: insights into translesion DNA synthesis. Proc. Natl. Acad. Sci. USA *104*, 15591–15598.

Yuasa, M. S., Masutani, C., Hirano, A., Cohn, M. A., Yamaizumi, M., Nakatani, Y., and Hanaoka, F. (2006). A human DNA polymerase eta complex containing Rad18, Rad6 and Rev1; proteomic analysis and targeting of the complex to the chromatin-bound fraction of cells undergoing replication fork arrest. Genes Cells *11*, 731–744.

Zhuang, Z., Johnson, R. E., Haracska, L., Prakash, L., Prakash, S., and Benkovic, S. J. (2008). Regulation of polymerase exchange between Poleta and Poldelta by monoubiquitination of PCNA and the movement of DNA polymerase holoenzyme. Proc. Natl. Acad. Sci. USA *105*, 5361–5366.

Chapter 9

~

Focus on foci:

DNA damage foci,

a structure without a function ?

Cell Cycle (2009), **8** (23)**:** 3812-3

Focus on foci: DNA damage foci, structures without a function?

Audrey M. Gourdin and Wim Vermeulen

News and Views, Cell Cycle 8:23, 3809-3815; December 1, 2009
Comment on: Soria G, et al. Cell Cycle 2009; 8:3340-8

Sub-nuclear foci are a focal point in DNA damage response (DDR) research. In a recent *Cell Cycle* paper, the Soria et al. report on the surprising focal distribution of the TLS-polymerase η at sites of UV-induced DNA damage in non-S phase cells. This unexpected observation raises questions on the structural-functional link of these sub-nuclear structures.

Exposure to genotoxic agents triggers a complex DNA damage response (DDR), involving damage removal pathways, cell cycle checkpoint activation and damage bypass replication. When lesions that block replication fork progression are present during S phase a specialized set of translesion synthesis (TLS) polymerases is called on action to bypass these roadblocks. Amongst them, the Y-family polymerase η (Polη) is crucial to accurately bypass the poorly repaired UV-light induced cyclo-butane-pyrimidine dimers (CPDs). Its significance is clearly illustrated by the cancer-prone phenotype of inherited mutations in Polη as in XP-variant patients[1].

Previously it was thought that a focal accumulation of Polη exclusively occurred in S phase at the so-called replication foci[1] considering its function in TLS, which by virtue of its nature is in DNA replication. However, recent studies revealed a focal pattern of Polη at sites of UV damage also in non-S phase cells[2]. This was independently confirmed and further investigated by Soria et al.[3] Soria and co-workers use several procedures, i.e., GFP-Polη expression in cells arrested in G1 by transient over expression of p21 and co-expression with the (cell cycle marker) mCherry-PCNA, to select for or identify non-S-phase cells. Elegant, time resolved microscopic studies applying different procedures to locally inflict DNA lesions, clearly demonstrated that Polη accumulated in a focal pattern at sites of UV-damage in S phase as well as G1 cells.

This surprising notion raises several questions concerning the potential role(s) of Polη outside TLS: what is the mechanism triggering this non-replication associated focal pattern? What is the functional relevance of this localization? Interestingly, recent studies suggested a more promiscuous functioning of the Y-family polymerases outside

TLS, such as a function for Polη in homologous recombination (HR)[4] and a role for polymerase κ in gap-filling synthesis during nucleotide excision repair (NER)[5].The procedures Soria applied to locally induce UV-damage will introduce high local concent-rations of lesions and may cause DNA double-strand breaks (DSBs). Thus activation of DSB repair mechanisms cannot be ruled out. However, participation in HR could not explain the G1 focal accumulation, as this pathway does not function in this stage of the cell cycle. Although the other DSB repair process; non-homologous end joining (NHEJ) is functional in G1 cells, participation of Polη in this process is not likely as this process mainly utilizes X-family of polymerases[6]. However, a function in this versatile and flexible repair system (in terms of alternative utilization of key enzymatic functions[6]) cannot be ruled out and should be further investigated.

A likely explanation, as the authors indicated, for the observed Polη rearrangement, is that it is recruited to UV-damaged sites by the NER machinery, analogous to the NER-induced gap-filling synthesis function of polymerase κ[5]. Although Polη does not play a dominant role in NER, as XP-V cells have a proficient NER, a stimulatory or redundant function in this process seems likely. This option is particularly attractive as it was recently shown that PCNA mono-ubiquitination (PCNA-Ub), known to facilitate TLS polymerases recruitment to (stalled) replication sites[1], also occurs or at least persists outside S phase[7]. Strikingly however, focal reorganization of Polη in G1 cells after UV also occurred in several NER-deficient cells derived from XP patients (groups A, F and G) to the same extent as in wild type cells. As these XP cells are deficient in dual incision, no gap-filling synthesis will be initiated, suggesting that functional NER is not required for Polη recruitment.

The most confusing finding is perhaps the fact that binding of PCNA (shown by the absence of PCNA binding in NER-deficient cells) seems not to precede Polη recruitment. Even more astonishing is the notion that the PCNA-binding domain of Polη (PIP-box) is required for efficient loading, whereas PCNA itself is not required. This apparent paradox could only be explained either when this mutation disrupts the structure of the protein or if the PIP-box is required to load to another as yet undefined structure or DDR intermediate. An obvious question linked to these observations is of course: What is the substrate or the signal that causes this structural reorganization? A few options are left: (1) binding to UV-damage recognition factors (i.e., the NER initiating factors UV-DDB and/or the XPC-complex); (2) recruitment by other Y-family polymerases, such as Rev1 that was also found to accumulate in foci at UV-damaged sites outside S

phase[8] and known to interact with Polη; (3) direct binding of UV-lesions or damaged chromatin. The latter option can be investigated by biochemical approaches. Future genetic experiments could be performed to investigate options (1) and (2). However, an important challenge for the investigation on the biological significance of Polη function in DDR outside TLS (e.g., mutation prevention) will be confounded by its important role in TLS.

As in many cases however, this research triggered more questions than it provided answers. Having excluded the most plausible mechanisms for recruiting Polη to damaged sites in non-replicating cells (replication-stress, HR and NER) and suggesting a further extension of the already pleiotropic functions of this polymerase in DDR, the manuscript by Soria et al. does not provide an answer for a possible function and mechanism of this sub-nuclear distribution of Polη in response to UV in non-replicating cells. The authors do however postulate the possibility that the focal organization is not a reflection of activity but rather provides a structural basis for DDR factors to accumulate that may be called into action when necessary, a model dubbed as "be ready for." This scenario is analogous to ionizing radiation induced foci (IRIF)[9] that also harbor a large number of DDR factors of which it was suggested[10] that these structures may serve as a "tool-belt" to locate activities for "just in case" action[11]. The TLS factor-containing foci are then a by-product of an unknown DDR signal. Suggestions implying that these structures do not have any functional significance should be taken with caution, as it is unlikely that a simple by-product of genomic catastrophe will survive evolution.

References

1. Kannouche P, et al. Genes Dev 2001; 15:158.
2. Akagi J, et al. DNA Repair 2009; 8:585.
3. Soria G, et al. Cell Cycle 2009; 8:3340-8.
4. Kawamoto T, et al. Mol Cell 2005; 20:793.
5. Ogi T, et al. Nat Cell Biol 2006; 8:640.
6. Lieber MR. J Biol Chem 2008; 283:1.
7. Niimi A, et al. PNAS 2008;105:16125.
8. Murakumo Y, et al. Genes Cells 2006; 11:193
9. Bekker-Jensen S, et al. JCB 2006; 173:195.
10. Harper JW, et al. Mol Cell 2007; 28:739.
11. Essers J, et al. Curr Opin Cell Biol 2006; 18:240.

Summary

Though genetic changes, or mutations, might account for the long term survival of a species (creating genetic variations), the crucial factor for the survival of an organism resides in genetic stability. In fact the integrity of the DNA sequence, that carries out and regulates genetic information, can be impaired by inaccurate maintenance processes, endogenous metabolites or exogenous agents. DNA lesions, by disturbing DNA replication and transcription, induce degenerative and mutagenic changes as well as aberrations that lead to ageing and carcinogenesis. Therefore, a sophisticated network of efficient DNA damage response mechanisms, including DNA repair and checkpoint mechanisms, are dedicated to remove most of these genomic insults. Additionally when lesions are not completely removed before replication occurs, specialized pathways, called damage tolerance processes, get activated in order to bypass the lesions, without repairing them, at stalled replication forks. The significance of this multi-protein DDR response is illustrated by the severe clinical symptoms associated with inherited defects in DDR factors. Live cell spatio-temporal dynamics studies represent a precious tool for a better characterization of these DDR factors. In **Chapter 1** different DNA lesions, the specific repair pathways, checkpoint mechanisms, damage tolerance processes and DDR-associated diseases are summarized as well as the most appropriate technical approach to study the different DDR factors. The focus of this chapter is on the versatile nucleotide excision repair (NER) mechanism as this is the main study focus described in this thesis.

Genetic stability also requires a very accurate DNA replication mechanism that involves the tightly regulated interplay of numerous replication factors. Moreover, replication factors also play an important role in most of the DDR processes described in Chapter 1. **Chapter 2** provides an overview on replication and DDR-associated DNA synthesis mechanisms. In this chapter a description of the properties of crucial factors (PCNA, RFC and RPA) in both normal replication and damage-associated replication is also included, as these are studied extensively in this thesis.

In **Chapter 3** the coordination between incision and the start of DNA repair synthesis within NER is described. Using catalytically inactive mutants of the NER-specific endonucleases XPG (that incises 3' to the lesion) and ERCC1-XPF (responsible for the 5'incision), we showed that incision by ERCC1-XPF depends on the presence, but not the catalytic activity of XPG, while 3' incision by XPG requires the catalytic activity of ERCC1-XPF. In cells expressing catalytically inactive XPG, but not in cells expressing catalytically inactive XPF, partial DNA synthesis is detectable *in vitro* and *in vivo*. Post-incision NER factors, (PCNA, pol δ, CAF-1) are recruited to sites of local UV damage in the catalytic-dead XPG mutants and UDS proceeds at intermediate levels. This suggests a "cut-patch-cut-patch" mechanism whereby following 5' cleavage by ERCC1-XPF, the repair synthesis machinery is recruited and repair synthesis is initiated prior to 3'cleavage by XPG. This

latter cleavage appears to occur subsequently, may be induced upon stalling of the polymerase and allows the completion of repair synthesis.

The tethering of DNA polymerases for further repair synthesis is carried out by PCNA, a sliding ring-shaped clamp that needs to be opened and loaded around the DNA by a clamp loader. In regular DNA replication, this function is carried out by the RFCp140 (or RFC1)-containing Replication Factor C complex. Different RFC-like complexes exist, that include, besides the core proteins (RFC2-5), an alternative RFC1 subunit such as Rad 17, Elg1, or Ctf18. In **Chapter 4**, using a combination of immunofluorescence, live cell microscopy techniques (using a GFP tagged version of RFC), Chromatin immuno- precipitation (ChIP) and repair synthesis inhibition by HU/AraC, we showed that RFC localizes *in vivo* to sites of local UV damage for a long period post-UV, though in a very dynamic fashion. These data suggest that RFC has other functions in repair replication besides loading of PCNA during NER repair synthesis. Surprisingly, RFC does not seem to be required for recruiting PCNA to NER sites but appears to be crucial for loading PCNA, in order to confer it into a replication-competent status that allows the recruitment of pol δ and initiation of repair synthesis.

In chapter 5, by looking at the accumulation kinetics and localization in living cells of GFP-tagged replication factors RPA, PCNA and RFC at sites of NER repair synthesis, we demonstrate that these factors have a very different kinetic behavior than the other pre-incision NER factors, since they accumulate at prolonged periods at sites of UV repair. This suggests that these factors may have additional functions besides their known functions in repair synthesis. RPA is actually the only factor that is involved both in the pre- and post-incision steps of NER and displays differential dynamic properties.

In vivo dynamic studies using GFP-tagged proteins have been crucial to understand the dynamic interplay between NER components during the assembly of the repair complex. In **Chapter 6** of this thesis, we have focused on a more quantitative understanding of how repair complexes assemble in living cells and how the dynamic interactions of NER proteins shape functional properties, such as the rate and specificity of DNA repair. This analysis is based on kinetic measurements of seven GFP-tagged core NER factors and mathematical modeling. This study shows that all core NER proteins exchange continuously and rapidly between chromatin-bound and freely diffusing states, however they do accumulate in a slower time scale (in the order of hours), revealing that assembly of NER factors is not sequential but rather stochastic and reversible. A major component of protein affinity is the state of the DNA substrate.

Tagged proteins play a central role in determining the spatio-temporal distribution of vital processes such as replication, transcription and DNA repair. However, many additional tools, like *in vivo* DNA labeling by DNA-stains such as the anthraquinone derivate Draq5,

are also important to visualize the interaction of GFP-fused proteins with the target substrate and to determine different chromatin compaction levels. In the technique-orientated **Chapter 7**, the suitability of combining Draq5 staining with protein dynamic measurements is verified. Draq5 intercalation modifies the localization and dynamic behavior of several chromatin-binding proteins by either stimulating release or binding of these proteins to their substrate. Moreover, this results in an inhibition of the corresponding cellular functions of these factors. This study indicates that caution should be taken to implement so-called viable DNA stains in live cell studies as they may perturb the analysis.

Not all UV lesions are repaired by NER before the cell enters S-phase, this can therefore seriously hamper replication elongation. In this case, upon stalling of the classical polymerase on the lesion, alternative sets of polymerases are recruited, which are able to bypass the lesion. The main polymerase that can bypass CPDs (the most abundant UV-lesion) in an error-free fashion is pol η, which co-localizes with pol ι at replication foci induced by UV irradiation. **Chapter 8** focuses on the interactions between these polymerases and their recruitment to sites of damage. Using tagged versions of these polymerases, we show that the two polymerases are highly mobile, with pol ι being even more mobile than pol η. Moreover PCNA ubiquitination facilitates but is not essential for accumulation of pol η into the foci. Finally, the polymerases seem to be continuously but transiently probing the DNA/chromatin.

Interestingly, a report of 2009 by Soria et al in Cell Cycle has shown that pol η localizes not only to TLS sites during S phase, but also to UV-damaged sites in G1 cells in a focal pattern. In **Chapter 9** we discuss these data and try to interpret the meaning of this surprising finding in view of recent reports which indicate that the TLS polymerases may have additional functions beyond TLS, such as NER repair synthesis for pol κ or Rev1 and HR for pol η. Hence pol η might also be implicated in NER or another repair pathway. Alternatively the localization of pol η to foci may support a model known as "be-ready-for", in which several DDR factors accumulate in high local concentrations (foci) near the damage, in order to be available if necessary. The facts that the PIP-binding domain of pol η, but not the presence of PCNA, are required for the recruitment of pol η into these foci, suggest that an unknown intermediate may be necessary to signal the relocalization of the protein into sites of repair and could support this last hypothesis.

Samenvatting

Ook al kunnen genetische veranderingen, of mutaties, verantwoordelijk zijn voor de lange termijn overleving van een species (waardoor genetische variaties onstaan), de meest cruciale factor voor overleving van een organisme ligt in genetische stabiliteit. De integriteit van de DNA sequentie, welke de genetische informatie bevat en reguleert, kan worden verstoord door onnauwkeurig onderhoud, endogene metabolieten of exogene stoffen. Lesies in het DNA, door het verstoren van transcriptie en DNA replicatie, induceren degeneratieve en mutagene veranderingen en aberraties welke leiden tot veroudering en tot carcinogenese. Daarom is een goed ontwikkeld netwerk van efficiënte DNA schade respons mechanismen aanwezig om de meeste van deze veranderingen in het genoom te verwijderen. Daarnaast worden speciale biologische routes ('damage tolerance processes') geactiveerd wanneer bepaalde lesies niet volledig zijn verwijderd voordat replicatie optreedt. Deze "biologische routes" kunnen lesies zo omzeilen zonder deze te herstellen op vastgelopen replicatie vorken. De betekenis van deze multi-eiwit DDR respons (DNA schade respons) wordt geïllustreerd door de ernstige klinische symptomen die geassocieerd zijn met de erfelijke defecten in DDR factoren. Studies naar de spatiotemporale dynamiek van deze DDR factoren in een levende cel zijn hierbij een belangrijk instrument voor een betere karakterisering van deze eiwitten. In **Hoofdstuk 1** worden DNA lesies, de specifieke reparatie mechanismen, 'checkpoint' mechanismen, schade tolerantie processen en DDR-geassocieerde ziekten beschreven. Daarnaast worden de meest geschikte technische methoden om de verschillende DDR factoren te bestuderen, beschreven. De nadruk in dit hoofdstuk ligt op het veelzijdige 'nucleotide excision repair' (NER) mechanisme, het voornaamste onderwerp van deze studie, zoals beschreven in dit proefschrift.

Genetische stabiliteit vereist een zeer nauwkeurig DNA replicatie mechanisme waarbij een precies gereguleerd samenspel van een groot aantal replicatie factoren nodig is. Daarnaast spelen deze replicatie factoren een belangrijke rol in de meeste DDR processen, zoals beschreven in **Hoofdstuk 1**. **Hoofstuk 2** geeft een overzicht over de replicatie en de DDR-geassocieerde DNA synthese mechanismen. In dit hoofdstuk worden eigenschappen van de cruciale factoren (PCNA, RFC en RPA) in meer detail bestudeerd en beschreven in zowel de normale replicatie als de schade-geassocieerde replicatie.

In **Hoofdstuk 3** wordt de coördinatie tussen incisie en de start van DNA repair synthese tijdens NER beschreven. Door een enzymatische inactieve mutant van de NER-specifieke endonuclease XPG te gebruiken, dat leidt tot incisie van 3' in de lesie, tonen we aan dat 5' incisie door ERCC1-XPF afhankelijk is van de aanwezigheid, maar niet de katalytische activiteit van XPG, terwijl het gebruik van een katalytische inactieve variant van XPF aantoont dat de incisie door XPG de katalytische activiteit van ERCC1-XPF nodig heeft. In cellen die katalytisch inactieve XPG, maar niet die katalytisch inactieve XPF tot expressie brengen, is gedeeltelijke DNA synthese detecteerbaar *in vitro* en *in vivo*. Post-incisie NER

factoren (PCNA, pol ∂, CAF-1) verzamelen zich op de plaatsen van UV schade in de katalytisch-dode XPG mutanten en de DNA schade herstel synthese gaat door op een lager niveau**.** Dit suggereert een 'knip-plak-knip-plak' mechanisme waarbij het DNA schade herstel synthese mechanisme activeert en repair synthese wordt geïniteerd voorafgaand aan 3' splitsing door XPG en na 5' splitsing door ERCC1-XPF. De 3' splitsing treedt later op en wordt waarschijnlijk geïnduceerd wanneer polymerases vastlopen en maakt voltooiing van DNA schade herstel synthese mogelijk.

Het PCNA eiwit zorgt voor binding van DNA polymerasen voor verdere DNA schade herstel synthese. PCNA is een glijdende ringvormige klem welke geopend en geladen dient te worden om het DNA door een 'klemlader'. Tijdens normale DNA replicatie wordt deze functie vervuld door het RFCp140 (of RFC1)- bevattende Replication Factor C complex. Er bestaan verschillende RFC-achtige complexen, welke naast de kern RFC2, RFC3, RFC4 en RFC5 eiwitten een alternatieve RFC1 subeenheid bevatten: Rad17, Elg1 of Ctfl18. In **Hoofdstuk 4** tonen we aan dat RFC zich *in vivo* op plaatsen van lokale UV schade begeeft gedurende een langere periode post-UV; in een zeer dynamische wijze. Dit is aangetoond door gebruik van een combinatie van immunofluorescentie, levende cel microscopie technieken (m.b.v. een GFP gelabelde versie van RFC), chromatine immunoprecipitatie en inhibitie van DNA schade herstel synthese Deze data suggereren dat RFC andere functies in de repair replicatie heeft naast het laden van PCNA gedurende NER geinduceerde DNA schade herstel synthese. Verrassend is dat RFC niet nodig lijkt te zijn voor het groeperen van PCNA naar plaatsen waar NER actief is, maar dat het cruciaal is voor het laden van PCNA en het veranderen hiervan naar een replicatie-competente status, waardoor recrutering van pol δ en de initiatie van DNA schade herstel synthese mogelijk zijn.

In **Hoofdstuk 5** tonen we aan dat, door bestudering van de accumulatie kinetiek en lokalisatie van GFP-labelede replicatie factoren RPA, PCNA en RFC op plaatsen van NER schade herstel synthese in levende cellen, deze factoren sterk verschillende kinetische kenmerken hebben dan de andere pre-incisie NER factoren, aangezien deze ophopen gedurende langdurige perioden op plaatsen van UV schade. Deze bevindingen doen vermoeden dat deze factoren additionele functies hebben naast hun bekende functies in DNA schade herstel synthese. RPA is de enige factor die zowel betrokken is bij pre- en post-incisie stappen van NER en RPA vertoont onderscheidende dynamische eigenschappen.

In vivo dynamische studies waarbij GFP-gelabelde eiwitten worden gebruikt, zijn cruciaal geweest in het begrijpen van het dynamische samenspel tussen NER componenten gedurende de verzameling van het DNA schade herstel complex**.** In **Hoofdstuk 6** leggen we de nadruk op een meer kwantitatief begrip van hoe DNA schade herstel complexen zich verzamelen in levende cellen en hoe dynamische interacties van NER eiwitten functionelen eigenschappen bepalen, zoals de snelheid en specificiteit van DNA repair. Deze analyse is gebaseerd op de kinetische metingen van zeven belangrijke GFP-gelabelde NER factoren en

op mathematische modellen. De studie toont aan dat alle kern NER eiwitten continu en snel wisselen tussen chromatine-gebonden en vrij diffunderende toestand, hoewel deze niet ophopen in een tragere tijdschaal (in de grootte van uren). Dit toont aan dat het opbouwen van het NER complex niet sequentieel maar eerder **s**tochastisch en reversibel is.

Gelabelde eiwitten spelen een centrale rol in het bepalen van de spatiotemporale verdeling van vitale processen, zoals replicatie, transcriptie en DNA schade herstel. Vele aanvullende technieken, zoals *in vivo* DNA labeling met DNA-kleuringen zoals het anthraquinone derivaat Draq5, zijn ook van belang voor visualisering van interactie tussen GFP-gefuseerde eiwitten met het doel-substraat en om verschillende chromatine compactie niveau's te bepalen. In het techniek georiënteerde **Hoofdstuk 7** controleren we de geschiktheid van het combineren van Draq5 kleuring met eiwit dynamische metingen. Draq5 intercalatie verandert de lokalisatie en het dynamische gedrag van verschillende chromatine bindende eiwitten. Dit leidt vervolgens tot inhibitie van gerelateerde cellulaire functies van deze factoren. Deze studie wijst er op dat men voorzichtig dient te zijn bij implementatie van deze DNA kleuring in levende cellen aangezien deze de analyse kunnen verstoren.

Niet alle UV lesies worden gerepareerd door NER voordat de cel de S-fase ingaat. Dit zal echter wel de DNA replicatie verhinderen. In dat geval worden, op moment van plaatsing van de klassieke polymerase op de lesie, alternatieve sets van polymerases gegroepeerd, die de lesie kunnen omzeilen. De voornaamste polymerase, die de CPD's kan omzeilen (de meest voorkomende UV lesie) op een foutloze manier is pol η, welke zich ook bevindt op dezelfde plaats als pol ι op de foci van replicatie, geïnduceerd door UV straling. **Hoofdstuk 8** beschrijft met name de interacties tussen deze polymerases en hun groepering naar de plaatsen van schade. We tonen d.m.v. gelabelde versie van de polymerases aan dat deze twee polymerases sterk mobiel zijn, waarbij pol ι zelfs mobieler is dan pol η. Verder tonen we aan dat PCNA ubiquitinatie niet essentieel is, maar faciliteert, ophoping van pol η in de foci,

In 2009 een rapport door Soria et al in Cell Cycle, aantoont dat pol η zich niet alleen naar TLS plaatsen begeeft gedurende de S-fase, maar ook naar UV-beschadigde plaatsen in G1 cellen in een focaal patroon. In **Hoofdstuk 9** gaan we hier op in, waarbij we de betekenis van deze verrassende bevindingen proberen te interpreteren in het licht van de recente ontdekking dat TLS polymerases een additionele functie buiten TLS hebben, zoals NER schade herstel synthese voor pol κ of Rev1 en HR voor pol η. Pol η kan dus ook een rol hebben bij NER of andere DNA herstel mechanismen. Anderzijds, kan lokalisatie van de foci een model, bekend als 'be-ready-for', ondersteunen, waarin verschillende DDR factoren zich ophopen in hoge lokale concentraties (foci) vlakbij de schade en gebruikt kunnen worden indien nodig. Het feit dat het PIP-binding domein van pol η, maar niet de aanwezigheid van PCNA nodig is voor groepering van pol η op deze plaatsen, doet vermoeden dat een onbekende intermediaire stof wellicht nodig is om relokalisatie van het eiwit naar plaatsen van repair te signaleren. Dit zou de laatste hypothese ondersteunen.

Curriculum vitae

Name	Audrey Marie Gourdin
Birth date	15th of August 1979
Birth place	PONTOISE, France

Education and Research

2004-2009	**PhD student** at the Department of Cell Biology and Genetics. *Erasmus Medical Center*, ROTTERDAM (the Netherlands) Promotor : Jan Hoeijmakers, Co-promotor: Wim Vermeulen
2002	**Masters of Engineering in Life Sciences,** option "Biotechnologies and Plant Engineering" **Masters of Science in Life Sciences** *Ecole Nationale Superieure d'Agronomie et des Industries Alimentaires (ENSAIA),* NANCY
2001	**Training period and research project** *AgResearch,* HAMILTON (New Zealand)
1999	**Preparatory Classes** to Engineering School (Maths Sup Biologie and Maths Spé Biologie (BCPST) Preparatory school "*Lycée Hoche",* VERSAILLES
1997	**Scientific « baccalauréat »,** option Mathematics Secondary School "*Lycée Kastler"*, CERGY

PhD Portfolio

Name PhD student:	A. Gourdin
PhD period:	Feb 2004-June 2009
Erasmus MC department:	Cell Biology and Genetics
Promotor:	Prof.dr. J.H.J Hoeijmakers
Supervisor:	Dr. W. Vermeulen
Research school:	MGC

Research skills
Working in the C-lab
Confocal microscopy course

In depth-course (e.g. Research school, medical training)
Experimental approach to Molecular and Cell Biology

Presentations
EC Marie Curie (Marseille, 2007 and Strasbourg, 2008)

International conference

Noordwijkerhout	2006
3R- Giens	2007
EC-Marie Curie	2004-2008

Seminars and workshops

MGC Promovendi worskshop	2005-2008
Organizing committee	2006

Teaching
Supervision of 2 bachelor students
Confocal microscopy workshop

List of Publications

Overmeer R.*, **Gourdin A.M.*,** Fousteri M.I., Giglia-Mari G., Siegal G., Mullenders L.H. and Vermeulen, W. (**2010**).
RFC is required for recruitment of polδ to sites of NER by loading but not recruitment of PCNA Mol Cell Biol, in press.
*A.M. Gourdin and R. Overmeer contributed equally to this work

Mari P.O.*, Verbiest, V.*, Sabbioneda S., **Gourdin A.M.**, Wijgers N., Dinant C., Lehmann A.R., Vermeulen W. and Giglia-Mari G. (**2010**).
Influence of the live cell DNA marker DRAQ5 on chromatin-associated processes.
DNA Repair (Amst) **9**(7): 848-55.
*P.O. Mari and V. Verbiest contributed equally to this work.

Luijsterburg M.S.*, von Bornstaedt G*., **Gourdin A.M.**, Politi A.Z., Moné M.J., Warmerdam D.O., Goedhart J., Vermeulen W., van Driel R. and Höfer T. (**2010**).
Stochastic and reversible assembly of a multiprotein DNA repair complex ensures accurate target site recognition and efficient repair. J Cell Biol **189**(3): 445-63.
*MS. Luijsterburg and G. Von Bornstaedt contributed equally to this work.

Gourdin, A. M. and Vermeulen, W. (**2009**).
Focus on foci: DNA damage foci, structures without a function? Cell Cycle **8**(23): 3812-3.

Staresincic L., Fagbemi A.F., Enzlin J.H., **Gourdin A.M.**, Wijgers N., Dunand-Sauthier I., Giglia-Mari G., Clarkson S.G., Vermeulen W. and Schärer O.D. (**2009**).
Coordination of dual incision and repair synthesis in human nucleotide excision repair. Embo J **28**(8): 1111-20.

Marteijn J.A., Bekker-Jensen S., Mailand N., Lans H., Schwertman P., **Gourdin A.M.**, Dantuma N.P, Lukas J., and Vermeulen W. (**2009**).
Nucleotide excision repair-induced H2A ubiquitination is dependent on MDC1 and RNF8 and reveals a universal DNA damage response. J Cell Biol **186**(6): 835-47.

Sabbioneda, S., **Gourdin, A.M**., Green, C.M., Zotter, A., Giglia-Mari, G., Houtsmuller, A., Vermeulen, W. and Lehmann, A.R. (**2008**).
Effect of proliferating cell nuclear antigen ubiquitination and chromatin structure on the dynamic properties of the Y-family DNA polymerases. Mol Biol Cell **19**(12): 5193-202.

Gourdin, A.M., Luijsterburg, M.S., van Cuijk, L.**,** Nigg, A.L, Giglia-Mari, G., Houtsmuller, A.B., Vermeulen, W. and Marteijn, J.A.
Dynamics of replication factors in replication and Nucleotide Excision Repair. Manuscript in preparation.

Acknowledgements

A lot of people say that writing a thesis is a little like giving birth to a child. Having not given birth to any child so far, I would nevertheless like to say that achieving a PhD and writing a thesis constitute a difficult and tremendous task. However, if I had to do it again, I would not think about it twice, I would go for it right away (even if I might then delocalize the EMC and the people who work in it into another city…). The reason for this is that despite the difficulties inherent to a PhD and to life as an expatriate in a tough city, I have had a great time, have learnt a lot, scientifically and personally, and have met a lot of special people that I would like to thank, since without you I would not be writing these lines.

First of all, I would like to thank my promoter: Jan, thank you for your trust and for letting me achieve this PhD in the department. I really appreciated all the very pertinent and constructive remarks that you have made about my work throughout these 5 years. I have learnt a lot from you and from your incredible knowledge. I also would like to thank you for your availability (even in the busiest of times you always found some time to discuss my thesis) and your kindness.

To my co-promotor, Wim: it will be very tough to summarize in one paragraph these five years of being your PhD student! I guess the main words that will come to my mind are: thank you!!! Firstly, for the fact that you have trusted me from the first day to the very last. Also, you have always been very supportive, kind, open-minded and concerned, especially during the difficult times I went through. Thank you also for having been so helpful in the last stages of the thesis writing. I have learnt an incredible amount of things from you, scientifically speaking of course, but also as far as working ethics and diplomacy are concerned. And I did also enjoy a lot our multiple conversations and jokes (I really do appreciate your fantastic sense of humor!!). I truly wish you a splendid scientific career and personal life of course with your great family.

I would like to thank Leon for the great collaboration, your ever-constructive and friendly remarks and for correcting my thesis as a member of the reading committee. I also want to thank Adriaan for your interesting remarks and availability to discuss any microscopy issue, as well as for accepting to be in the reading committee. Alan, this collaboration with you has been very productive; it has been a real pleasure to work in your lab and to learn from your unbelievable knowledge. I also would like to thank you for your kindness and for coming all the way down from the UK to sit in my jury. Niels, we had a great conversation on the thesis, thank you so much for having read it so cautiously and for your numerous interesting remarks. Gert, thanks for your ever-patience with the confocal microscope and for accepting to be a jury member. Ambra, we have had a lot of good times in the lab and I have learnt soooo much from you, thanks for your patience! And of course I appreciate a lot that you accepted to come all the way up from Toulouse to sit in my jury! I wish you a brilliant scientific career and I hope we will have many occasions to see each other again.

Life as a PhD student is not always easy and it is therefore very important to work in a nice atmosphere. I must say I have been very lucky since this has been the case all throughout these five years. Therefore, there are a lot of people that I would like to acknowledge for having been such nice, cooperative and fun labmates!
I would like to start with the people who have been here from the beginning, Arjan and Nils. Arjan, you deserve your french nickname as "Argent" (=silver): you are an extraordinary guy, sweet, funny, pro in your work. We had a lot of fun! Thank you also for supporting me when I needed it and for being my paranimf. Nils, it was fun having you around, I wish you all the best. To the people who were in the lab when I started, and then who left…Vincent, it was so nice having you around, all the best with your nice family. PO, I enjoyed a lot our great conversations about many things. I benefited a lot from your great expertise of microscopy and mathematics, thanks for your patience. Angelika, I enjoyed your presence in the lab and wish you all the best, you really deserve it. Chris, I also would like to thank you for your infinite patience in answering all my questions. We had fun! Ana, Steven, Deborah, PO, Raoul, Astrid, Catherine, Wendy….and many more people from the start, I really had some great times with all of you and I will always remember fondly our post-lab beer-drinking chatting sessions!
To some colleagues who unfortunately did not stay around long enough…but enough to become very good friends! Lidija of course: it was great working with you, we had the time of our lives with climbing and chatting and I hope we will see each other more often!! Maartje, it was nice having you around, I really hope we will stay in touch. Kiki, it was great to work together with you and to see each other in Zurich! Charlene, we had great conversations. I wish you all the best with your scientific career. Alexandre, we had really some nice times and I hope we'll keep in touch now that you are back in France.
I would like of course to acknowledge Marieke, Jurgen, Hannes, Petra, Hervé, Joris, Mickael, Özge, Charlie, Sophie, Erik, Arifa, Humaira…good luck to all of you and thanks for the nice conversations we had. A special thanks to Jurgen for the collaboration on the paper and for correcting my samenvatting.

Then, there is my whole bunch of colleagues who work on the 7th floor, in the department or in the building. With some of you I have become really good friends, with some others I only had a couple of conversations (science-orientated or not), but one thing is for sure, the presence of each of you in this building has lighted up the dark sky of Rotterdam and these hours of long conversations or small chit-chats, in or outside of the lab, will always remain very special to me. Eugin (good luck for your PhD. I wish you could have coached me a bit more with poker), Filippo (thanks for all the nice conversations, we will definitely keep in touch and play poker again), Tiago (we had so many nice conversations!), Karl (good luck for your PhD and the growing family), Gosia, Eva, Alex N., Roel, Sander, Monika, Antonio, Sanja, Umut, Stavros, Raymond, Sahar, Tobias, Rejane, Cintia, Ricardo (thanks to the three of you for bringing the beautiful sun of Brasil here), Eskeww, Ekim, Oanh, Harald, Frank S., Hanny, Anja, Jeroen, Cecile, Nicole, Flavia, Berina (thanks for your precious pieces of advice for the printing), Jan de Wit (Jean le Blanc !), Koos (you always gave me good pieces

of advice and I am amazed by your culture, both scientific and general), Frank G. (thanks for the very nice conversations), Charlotte (I really enjoyed chatting with you and hope to keep in touch with you, Eric and Oronte back in Paris) and many more….I sincerely wish you all a splendid personal life and a great scientific career.

There is a room next to my lab with five people that I could definitely rename "angels"; they are also known as…"computer guys"! Pim, Ton, Leo, Sjozef, Mario: thank you so much for your infinite patience and efficiency in sorting out my computer issues, from hard disk dropping (!) to all kinds of problems (and I have been pretty creative!). A special thought for Pim, we had great laughs and conversations, I hope I can once listen to your saxophone playing in a concert hall (I am doing a bit of advertisement for you here…!)

Jasperina, Marieke, Bep, Corianna, thank you so much for everything! You are just super efficient and always available. Any kind of question and after five seconds there you came with the piece of information I needed! I wish you all the best…
Thank you also to Melle, Arthur, Nuran (all the best to you and I hope we keep in touch), Riet, Koos and our precious cell culture ladies (Jopie, Fatima, Joke…), all of you have helped me throughout this PhD in one way or another, whether for administrative purposes, for making sure we could culture our cells with clean and sterile material or just for nice chit-chats!

To the people with whom I collaborated: Simone: thanks for your kindness and patience. I learnt a lot of things in Sussex. A big thought also to all the people from the GDSC in Sussex (Tomoo, Akari, Richard, Steph, Sharada…. I had a fantastic time there). Martijn, I'm still amazed by your rapidity in understanding, working and providing results! It was really great working with you. We had fun too! Gregg, Rene, I learnt a lot of things from collaborating with you, it was a nice experience and I enjoyed our work discussions.

Of course there are my close friends, whom I have met in EMC: you truly have been here throughout the best and the worst of times, by listening, advising, supporting, laughing, chatting, or sometimes by just being here…..In a nutshell, by being true friends: Debbie of course (thanks also for being my paranimf!), Sonha (I wish you a lot of happiness with your lovely family) and Michael (thank you so much for everything, including for letting me stay in your flat).

To my friends from Rotterdam and the Netherlands, who made life easier and so much nicer: Claire (thank you so much for your incredible charisma and beautiful friendship but also for letting me stay in your house, and for the samenvatting translation), Joelle, Marie-Laure, Philippe and Christine, Louis and Marianne, Lorena and Rafael…

To my very precious family and friends in France: Stéphanie et Matthieu, Raoudhette, Francine, Laure, Grégory, Ana ainsi que Solange et Jean-Marie, et beaucoup d'autres… Merci pour votre soutien infaillible, pour les longues conversations téléphoniques, pour vos

visites aux Pays-Bas, pour m'avoir accueillie lors de mes WE parisiens…Un merci particulier à Nicole, je me souviendrai toujours de nos interminables et si apaisantes conversations téléphoniques ! Caroline, merci de m'avoir tant soutenue et d'être venue si souvent me rendre visite. A toutes et tous, je suis heureuse d'être de retour en France et de profiter de votre présence. Un grand merci à Jean-Marie pour la belle couverture de thèse, ainsi qu'à SAR (je peux maintenant dé-feng-shuiser mon appartement de la conformation thèse…).
Et bien sûr, un grand, grand merci à Vincent, pour l'aide au formatage bien évidemment, mais aussi pour tout le reste, que je ne développerai pas ici…

And at last, to my ever-friend Véronique. Simply speaking, I would not have made it to the end without your friendship, your support, your sense of humor, your fantastic way of seeing people and life…Our looooong phone conversations have helped me through so much, in these moments when I felt desperate and when you were the only person whom I could talk to and "hang to". One says that only a true friend knows the darkest part of you, well…..during this stay in Rotterdam, where sometimes I was just losing myself, you simply helped me remember who I am and where I am going.

Again, thanks to all of you and I hope we will stay in touch….

~

Audrey M. Gourdin, 2010

No man is a failure who has friends (Frank Capra, It's a wonderful life)